Host proteins involved in *Turnip mosaic virus* life cycle

Karine Thivierge, Ph.D.

A thesis submitted to the Faculty of Graduate Studies and Research in partial fulfillment of the requirements for the degree of Doctor of Philosophy.

Department of Plant Science
McGill University
Montreal, Quebec, Canada.

October, 2009

Karine Thivierge©, 2009

TABLE OF CONTENTS

LIST OF TABLES AND FIGURES

Chapter 2:

Chapter 3:

Chapter 4:

Chapter 5:

Chapter 6:

ABSTRACT

All viruses are gene poor relative to their host, thus, most steps in virus infection involve interactions between viral components and host factors. Identification of these factors represents one of the major frontiers in current virus research. In this study, protein-protein interaction methodologies were used to find host interactors of *Turnip mosaic virus* (TuMV) RNA-dependent RNA polymerase (RdRP), VPg-protease (VPg-Pro) and P3 protein.

First, eukaryotic elongation factor 1A (eEF1A) was shown to interact with TuMV RdRp and VPg-Pro using tandem affinity purification in *Arabidopsis thaliana* and/or *in vitro* assays. Interaction of eEF1A with both viral proteins was shown to take place within 6K-VPg-Pro-induced vesicles. The same vesicles were also shown to contain poly(A)-binding (PABP) and heat shock cognate 70-3 proteins (Hsc70), two previously identified RdRp interactors. To further characterize the content of these vesicles upon TuMV infection, a fluorescently labeled 6K-GFP TuMV infectious clone was constructed and used in confocal microscopy experiments. The inclusion of eEF1A, PABP, Hsc70, eukaryotic initiation factor (iso)4E and VPg-Pro in TuMV-induced vesicles was demonstrated. It is well establish that positive-strand RNA viruses assemble their RNA replication complexes on intracellular membranes, usually in association with vesicle formation. For TuMV, our data suggest that it is the 6K-induced vesicles that house the viral replication complex (VRC). Moreover, the presence of replication and translation elements in these vesicles indicates that both processes might be coupled in TuMV VRC.

Secondly, the yeast two-hybrid system was used to identify plant P3-interacting proteins in a cDNA library from *A. thaliana*. A lipase was recovered

from the screen and shown to interact with P3 *in vitro*. Both proteins were also demonstrated to partially co-localize in the cytoplasm of the cell. Given that lipases play important roles in the plant response to biotic stress, this interaction reinforce the role of TuMV P3 in plant resistance and/or pathogenesis.

RÉSUMÉ

Les virus ont de petits génomes qui codent pour un nombre limité de protéines et dépendent conséquemment des facteurs de l'hôte pour compléter leur cycle de réplication. Dans ce projet, nous avons utilisé différentes méthodes pour identifier des partenaires protéiques de la polymérase virale à ARN (RdRp), de la VPg-Pro et de la protéine P3 du virus de la mosaïque du navet (TuMV).

Premièrement, nous avons trouvé que le facteur eucaryote d'élongation de la traduction 1A (eEF1A) interagit avec la RdRp et la VPg-Pro en utilisant une stratégie de purification en tandem in planta et/ou des essais *in vitro*. Nous avons montré que ces interactions se produisent en association avec les membranes du réticulum endoplasmique, plus précisément dans les vésicules induites par le polypeptide 6K-VPg-Pro. Nous avons aussi démontré que ces mêmes vésicules contiennent les protéines Hsc70-3 et PABP, deux partenaires connus de la RdRp. Afin de poursuivre la caractérisation du contenu de ces vésicules, nous avons créé un vecteur infectieux du TuMV permettant d'étiqueter les vésicules avec la GFP et d'être utilisé en microscopie confocale. À l'aide de ce vecteur, nous avons observé la présence du facteur eEF1a, de la PABP, de la Hsc70, du facteur eucaryote d'initiation de la traduction (iso) 4E et de la VPg-Pro dans les vésicules induites par le TuMV. Il est bien établit que le complexe de réplication des virus à ARN positif est associé aux membranes cytoplasmiques, généralement sous forme de vésicules. Pour le TuMV, nos données semblent indiquer que les vésicules induites par la protéine 6K contiennent le complexe de réplication viral (VRC). De plus, la présence d'éléments participants à la réplication ainsi qu'à la

traduction dans ces vésicules suggère que ces deux processus sont possiblement couplés dans le VRC du TuMV.

Deuxièmement, le système du double-hybride en levure a été utilisé pour rechercher des partenaires protéiques de P3. Le criblage de P3 contre une banque d'ADNc d'*Arabidopsis thaliana* a révélé une interaction entre P3 et une lipase. Lorsque exprimées ensembles dans *Nicotiana benthamiana*, les deux protéines co-localisent au cytoplasme. Étant donné le rôle des lipases dans les réponses des plantes aux attaques pathogènes, cette interaction renforce le rôle suggéré de la protéine P3 dans la pathogenèse et les mécanismes de résistance des plantes.

ACKNOWLEDGMENTS

Through the course of my doctoral studies, I was extremely fortunate to have been encouraged, supported and guided by many people who have enriched me both as a researcher and as a person.

I would first like to thank Dr. Jean-François Laliberté and Dr. Suha Jabaji, my co-supervisors, who each in their own complementary ways have provided guidance throughout my studies. To Dr. Laliberté I owe a constant support and encouragement which helped me forge ahead when I appeared to be lost at sea. I appreciate his knowledge and skills in many areas, and his assistance in writing papers and reports from which I preciously benefited. His understanding, positivism and patience added considerably to my graduate experience. I acknowledge Dr. Suha Jabaji for her help in writing this thesis and for her assistance in the last miles of this project. I must also thank Dr. Fortin for its support during the first years of this project. I also would like to extent special thanks to Drs. Eliane Ubalijoro and Laura Silva-Rosales who provided much appreciated support at a critical point during my studies.

I would like to thank the members of my committee, Drs. Jacqueline Bede and Philippe Séguin for the assistance they provided at all levels of the research project.

Many thanks to the administrative assistants of the Department of Plant Science for their time and patience: Carolyn Bowes, Louise Mineau, Meline Chatoyan and Roselyn James. I am particularly grateful to Carolyn for her devotion in always finding me an office every time I was asked to move. I must also thank Guy Rimmer, Department of Plant Science senior technician, for all his technical assistance.

Many thanks go to all my labmates, Christine Ide, Vicky Muise, Geneviève Morin, Julie Beaulieu, Patrick Cournoyer, Sophie Cotton, Philippe Dufresne and Dan Kiambi whose support greatly helped throughout these years. Particular mention goes to my fellow Ph.D. colleagues Sophie, Philippe and Chantal Beauchemin for their constant friendship and precious collaborations on many manuscripts. Many thanks to Christine Ide for her assistance in many of my experiments conducted in the laboratory.

I must also acknowledge the IBVM team at INRA Bordeaux in France for their hospitality during my internship: Drs. Sylvie German-Retana, Thierry Michon, Olivier Legall, as well as all the interns for their generosity.

I thank Dr. Fernando Ponz for the clone of TuMV, Dr. Michael Fromm for pNTAPi and pNTAPi-GFP vectors, Dr. Michel E. Hardy for pGEX-4T1 NV GST-VPg vector, Dr. Valerian Dolja for plasma membrane marker, and Dr. Karen S. Browning for rabbit polyclonal anti-wheat eEF1A antibodies. I must also thank Dr. Hélène Sanfaçon for critical reading of chapter III and IV of my thesis.

I recognize that this research would not have been possible without financial assistance of FQRNT, the Department of Plant Science (teaching assistantships), the Centre SEVE (travel awards), the Faculty of Agriculture and Environmental Research (travel awards), McGill University (Alma Matter travel grants) and McGill Graduate fellowships, and express my gratitude to these agencies. I am also very grateful to Dr. Marc G. Fortin, who always supported me financially from his research grants during nearly seven-years of graduated studies.

Last but not least, I would like to thank my husband, Félix Harvey. I would never have finished this thesis without his love, presence and encouragement.

CONTRIBUTION OF AUTHORS TO MANUSCRIPTS

This thesis is written in the form of manuscripts according to the "Guidelines Concerning Thesis Preparation". The thesis contains three chapters (III to V) representing three different manuscripts, all of which have been published (chapter III and IV) or in preparation (chapter V). Each co-author is mentioned, along with his/her corresponding address, at the beginning of each chapter. Below is a general description of the contribution of every-co-author. A detailed description of the contribution of each co-author can also be found in the connecting statements preceding each chapter.

My role in chapters III and V was to design and conduct all of the work involved in all experiments including data analysis, data mining and preparation of the first draft of the two manuscripts. Chapter IV is the result of an equal contribution between my-self, Dr. Philippe Dufresne, and Sophie Cotton. We equally designed the experimental set-up, conducted the experiments, and wrote the manuscript. Dr. M. G. Fortin provided funds throughout this research. He made available technical assistance for chapters IV and V. Dr. J.-F. Laliberté provided valuable suggestions in the design of most experiments related to chapter III, and corrected several versions of the manuscript found in this chapter. He also provided operating funds for chapters III and V. Isabelle Mathieu and Chantal Beauchemin constructed several binary vectors used in chapters III. Christine Ide assisted in the construction of many vectors used in chapters III and IV, and in the two-hybrid assay described in chapter V. My

supervisor, Dr. S. Jabaji provided supervision through the writing of my Ph.D. thesis.

LIST OF ABBREVIATIONS

(+) ssRNA:	positive-sense single-stranded RNA
$2A^{pro}$:	2A viral protease
3CD:	poliovirus 3CD protein
$3C^{Pro}$:	3C viral protease
$3D^{pol}$:	poliovirus 3D polymerase
3-AT:	3-aminotriazole
$6K_1$:	6 kDa protein 1
$6K_2$:	6 kDa protein 2 (also referred to as 6K)
AAE:	acetylajmalan esterase
aa-tRNA:	aminoacyl-Trna
AD:	activation domain
ANOVA:	analysis of variance
ATP:	adenosine triphosphate
BLAST:	basic local alignment search tool
BMV:	*Brome mosaic virus*
BSA:	bovine serum albumin
BVDV:	Bovine viral diarrhea virus
CaMV:	*Cauliflower mosaic virus*
CBP:	calmodulin-binding protein
ClYVV:	*Clover yellow mosaic virus*
CPIP:	capsid protein interacting protein
cDNA:	complementary DNA
CI:	cylindrical inclusion
CNV:	*Cucumber necrosis virus*
CP:	viral capsid or coat protein
CTP:	cytidine triphosphate
DBD:	DNA binding domain
DNA:	deoxyribonucleic acid
DNase:	Deoxyribonuclease
dNTP:	deoxynucleotide triphosphate
Dpi	days post-infection
dsDNA:	double-stranded DNA
DTT:	Dithiothreitol
EDTA:	ethylene diamine tetraacetic acid
eEF:	eukaryotic elongation factor
EF-Tu:	elongation factor thermo unstable
EGTA:	ethylene glycol tetraacetic acid
eIF:	eukaryotic translation initiation factor
ELISA:	enzyme-linked immunosorbent assay
ER:	endoplasmic reticulum
FCV:	Feline calicivirus
GFP:	green fluorescent protein
GST:	glutathione-S-transferase

GTP:	guanadine triphosphate
HC-Pro:	helper component-protease
HEPES:	N-2-hydroxyethylpiperazine-N´-2-ethanesulfonic acid
HR:	hypersensitive response
HRP:	horse radish peroxidase
Hsc70:	heat shock cognate 70 kDa protein
HSP:	heat shock protein
Hsp70:	heat shock 70 kDa protein
IgG:	immunoglobulin G
IPTG:	isopropyl-β-D-galactopyranoside
IRES:	internal ribosomal entry site
kb:	kilobase (s)
kDa:	Kilodalton
LB:	luria broth
LSD:	least significant difference
m^7GTP:	methyl-7-guanidine cap
MeJa:	methyl jasmonate
MES:	2-(*N*-morpholino)ethanesulfonic acid
mRNA:	messenger RNA
NIa:	nuclear inclusion a
NIb:	nuclear inclusion b
NLS:	nuclear localization signal
nm:	Nanometer
NSm:	non-structural movement protein
NSP3:	rotavirus non-structural protein 3
NTP:	nucleoside triphosphate
NV:	Norwalk virus
OD:	optical density (absorbance)
OPD:	o-phenylenediamine dihydrochloride
ORF:	open reading frame
P1:	TuMV protein 1
P3:	TuMV protein 3
PABPN:	nuclear PABP
PABP:	poly(A)-binding protein
Paip2:	PABP-interacting protein 2
PBS:	phosphate-buffered saline solution
pmol:	Picomole
PCBP:	poly(rC)-binding protein
PCR:	polymerase chain reaction
PLA2:	phospholipase A2
PM:	plasma membrane
Poly(A):	polyadenylate
PR:	pathogenesis-related proteins
Pro:	Protease
PSbMV:	*Pea seed borne mosaic virus*

PV:	Poliovirus
PVA:	*Potato virus A*
PVY:	*Potato virus Y*
RCBD:	randomized complete block design
RdRp:	RNA-dependent RNA polymerase
RLU:	relative light units
RNA:	ribonucleic acid
RNase:	Ribonuclease
RRM:	RNA recognition motif
RRL:	rabbit reticulocyte lysate
rRNA:	ribosomal RNA
RT-PCR:	reverse-transcriptase PCR
SA:	salicylic acid
SAR:	systemic acquired resistance
SEM:	standard error of the mean
SDS:	sodium dodecyl sulfate
SDS-PAGE:	SDS-polyacrylamide electrophoresis
SSC:	saline-sodium citrate
TAP:	tandem affinity purification
TBE:	tris/Borate/EDTA
TBS:	tris-buffered saline
TBSV:	*Tomato bushy stunt virus*
T-DNA:	transferred DNA
TEV:	*Tobacco etch virus*
TLS:	tRNA-like structure
TMV:	*Tobacco mosaic virus*
ToMV:	*Tomato mosaic virus*
Tris:	tris-hydroxymethyl aminomethane
tRNA:	transfer RNA
$tRNA^{met}$:	methionine transfer RNA
TSWV:	*Tomato spotted wilt virus*
TuMV:	*Turnip mosaic virus*
TVMV:	*Tobacco vein mottling virus*
TYMV:	*Turnip yellow mosaic virus*
UTP:	uridine-5'-triphosphate
UTR:	untranslated region
VPg:	viral protein genome-linked
VRC:	viral replication complex
VSV:	Vesicular stomatitis virus
WGE:	wheat germ extract
WNV:	West Nile virus
YTHS:	yeast two-hybrid system
VPg-Pro:	VPg fused to a protease domain in C terminus
ZYMV:	*Zucchini yellow mosaic virus*

CHAPTER I

INTRODUCTION

1.1. General introduction

The family *Potyviridae,* which includes *Turnip mosaic virus* (TuMV), comprises more than 30% of known plant virus species (Fauquet et al., 2005). Potyviruses have a worldwide distribution and are of major economical significance as they infect a large variety of field-grown vegetables (Walsh and Jenner, 2002). Despite the prevalence and economic impact of potyviruses, little is known about their replication within plant cells and the molecular events leading to the alteration of host metabolism.

One crucial aspect for potyvirus multiplication is the involvement of host factors in most steps of their replication cycle. In fact, all viruses are gene poor relative to their hosts; thus, interactions between viral and cellular factors play important roles in viral infection. Whereas recent studies show the importance of host factors, identifying these factors and their specific roles in viral infection remain a challenge (Nagy, 2008). The recent significant progress in this research area is based on development of powerful *in vivo* and *in vitro* approaches, including intracellular localization studies, reverse genetic approaches, protein-protein interaction methodologies, and the use of novel viral and plant model systems. TuMV is an excellent model to study plant-virus interactions. Its ability to infect *Arabidopsis thaliana*, the availability of an infectious clone and its known full-length genome sequence are tools of enormous potential to study the molecular genetics of TuMV (Walsh and Jenner, 2002). Its similarities, in genome organization and replication strategies, to the well-studied animal viruses of the *Picornaviridae* family, are

also of interest when it comes to gain insight into the functions of potyvirus proteins (Thivierge et al., 2005).

For potyviruses, emerging results indicate that eukaryotic translation initiation factors (eIFs) are an important class of host factors that are critical for infection. Firstly, eIF4E and eIF4G are known to interact with the protein genome-linked (VPg) or its precursor VPg-Pro (Léonard et al., 2004; Plante et al., 2004; Wittmann et al., 1997). The disruption of eIF4E and eIF4G translation initiation factors *in planta* results in resistance to potyviruses, which is indicative of an essential link between potyviruses and components of the translation initiation complex (Duprat et al., 2002; Lellis et al., 2002; Nicaise et al., 2007). Poly(A)-binding protein (PABP) also appears to be another translation initiation factor required for efficient potyvirus replication. PABP was found to bind to the RNA-dependent-RNA polymerase (RdRp) of *Zucchini yellow mosaic virus* and to the VPg-Pro of TuMV (Léonard et al., 2004; Wang et al., 2000). PABP, as well as eIF4E, are also known to relocalize upon infection to membranous viral replication complexes (VRCs) (Beauchemin and Laliberté, 2007). While these data demonstrate direct interactions between potyviral proteins and eIFs, the roles of these interactions and their requirement in potyviral life cycle are still unclear.

Present results likely have revealed only a small fraction of the underlying virus-host interaction on which potyviral replication depends. Therefore, it is expected that other plant-virus protein interactions are required for the successful completion of the TuMV life cycle. The availability of powerful genetic and biochemical tools is now providing opportunities to isolate and characterize plant factors involve in TuMV infection cycle. A better understanding of the complex network of interactions between

viruses and their hosts is not only improving our comprehension of plant virus replication and disease establishment, but also that of many plant cellular processes.

1.2. Research hypotheses

Our general research hypothesis is that TuMV genome replication and the associated infection depend on a wide range of plant host factors. Thus, plant-virus interactions are necessary for the assembly and function of potyviral replication complexes and their membrane targeting. Specifically, this thesis is based on the following hypotheses:

1. Translation of TuMV genome and replication of its RNA occurs in VRCs, which are associated with intracellular membranes and contain viral and host proteins.
2. The polymerase (RdRp), the P3 protein and VPg-Pro of TuMV are part of the VRC and are required for TuMV replication and/or translation. These proteins can be used as baits to detect interactors of host origin.
3. The cytoplasmic vesicles induced by TuMV 6K-VPg-Pro house the VRC. Identification of the proteins present within these vesicles is a productive approach to characterize the composition of TuMV replicase complex.

1.3. Research objectives

The main objective of this doctoral project was to identify host factors involved in TuMV life cycle. To achieve this global objective, specific targeted objectives were formulated:

1. To identify plant proteins interacting with the viral polymerase (RdRp) of TuMV using a two-step affinity strategy (chapters III and IV).
2. To confirm the presence of RdRp-interacting proteins (PABP, eEF1A, and Hsc70) in the vesicles induced by 6K-VPg-Pro using confocal microscopy (chapters III and IV).
3. To study the involvement of the VPg protein of TuMV in translation using *in vitro* translation systems (chapter V).
4. To identify plant proteins interacting with the viral protein P3 of TuMV using the yeast-two-hybrid system and to assess their requirement *in vivo* (chapter VI).

CHAPTER II

LITERATURE REVIEW

2.1. *Turnip mosaic virus*

2.1.1. General description of *Turnip mosaic virus*

2.1.1.1. Taxonomy and physical description

Turnip mosaic virus (TuMV) is a member of the genus *Potyvirus* in the family *Potyviridae*. The potyvirus is the largest group of plant viruses containing at least 180 members (Riechmann et al., 1992). Potyviruses account for over one-third of viruses known to infect plant species (Fauquet et al., 2005). Viruses of the family *Potyviridae* share general genome organization and many replication strategies with well studied members of the *Picornaviridae* virus family. These similarities have allowed potyviruses, together with plant bipartite como- and nepoviruses, as well as animal picornaviruses, to be organized into the picorna-like super-group (Goldbach, 1987).

Potyvirus virions are non-enveloped (Langenberg and Zhang, 1997), filamentous particles, between 680 nm and 900 nm long, 11 to 15 nm wide (Riechmann et al., 1992). The capsid is made of approximately 2000 units of a single virally encoded protein, the capsid protein (CP) (Martin and Gelie, 1997), which encapsidates a positive-sense single-stranded RNA [(+) ssRNA] genome (Brunt, 1992). A feature shared by most potyviruses is the formation of cylindrical inclusions in the cytoplasm of infected cells (Edwardson and Purcifull, 1970). These cytoplasmic cylindrical inclusions, resulting from the

aggregation of the virus-encoded cylindrical inclusion (CI) protein, are used to identify and classify potyviruses.

2.1.1.2. Host range, transmission and economical importance

The host range of TuMV is large but the *Brassicaceae* family is the most affected. It causes serious losses in many economically important vegetable crops including rutabaga, turnip, Chinese cabbage, broccoli, and cauliflower. TuMV also infects many ornamentals and non-brassica crops such as radish, lettuce, endive, escarole, horseradish, pea, and rhubarb (Walsh, 1997). Characteristic symptoms caused by TuMV are mosaic, mottling, chlorotic rings or color break on foliage, flowers, fruits, and stems. Severe stunting of young plants and drastically reduced yields, as well as leaf, fruit and stem malformations, fruit drop, and necrosis of various tissues are also observed (Shukla et al., 1994). TuMV is transmitted in a non-persistent manner during aphid feeding. It is introduced into plant cells via the stylet of the insect (Walsh and Jenner, 2002).

2.1.1.3. Genome organization and processing

The TuMV genome consists of a (+) ssRNA molecule of 9830 nucleotides (Nicolas and Laliberté, 1992). The 5'-terminus of the genomic RNA is covalently linked to a viral protein known as the viral protein genome-linked (VPg) (Siaw et al., 1985). The genomic RNA has a poly(A) tail of variable length at its 3' end (Hari et al., 1979). The genome codes for a single long open reading frame (ORF) flanked by two untranslated regions (UTRs). The ORF is translated into a single 358-kDa polyprotein, which is co-

and post-translationally processed by three virus-encoded proteinases (Fig. 2.1). The proteins released are: the first protein (P1; 40 kDa), helper component protease (HC-Pro; 52 kDa), the third protein (P3; 40 kDa), 6 kDa protein 1 ($6K_1$; 6 kDa), CI protein (72 kDa), 6 kDa protein 2 ($6K_2$; 6 kDa), VPg protein (22 kDa), the protease from VPg-Pro polypeptide precursor (Pro; 27 kDa), the RNA-dependent RNA polymerase (RdRp; 60 kDa) and the CP (33 kDa) (Fig. 2.1).

2.1.2. The RdRp of TuMV

The central step in virus infection cycle is replication, which depends on viral and host proteins. RdRps function as the catalytic subunit of the viral replicase required for the replication of all positive strand RNA viruses. The recruitment of the RdRp to membranes and its interaction with viral and host proteins are essential for the efficiency, specificity and regulation of viral replication (Buck, 1996). Thus, it is of considerable interest to emphasize on the functions of the RdRp and on the host proteins that can directly interact with it.

2.1.2.1. Function and cellular localization of the RdRp

The RdRp of potyviruses contains the consensus sequence motif GDD found in all viral RdRps (Koonin, 1991) and is the core polypeptide of the viral replicase complex (Hong and Hunt, 1996). Its polymerase activity and RNA-binding properties confirm its direct role in genome amplification (Merits et al., 1998). The RdRp of potyviruses utilize the 3' UTR to produce complementary (negative sense) RNA (Teycheney et al., 2000).

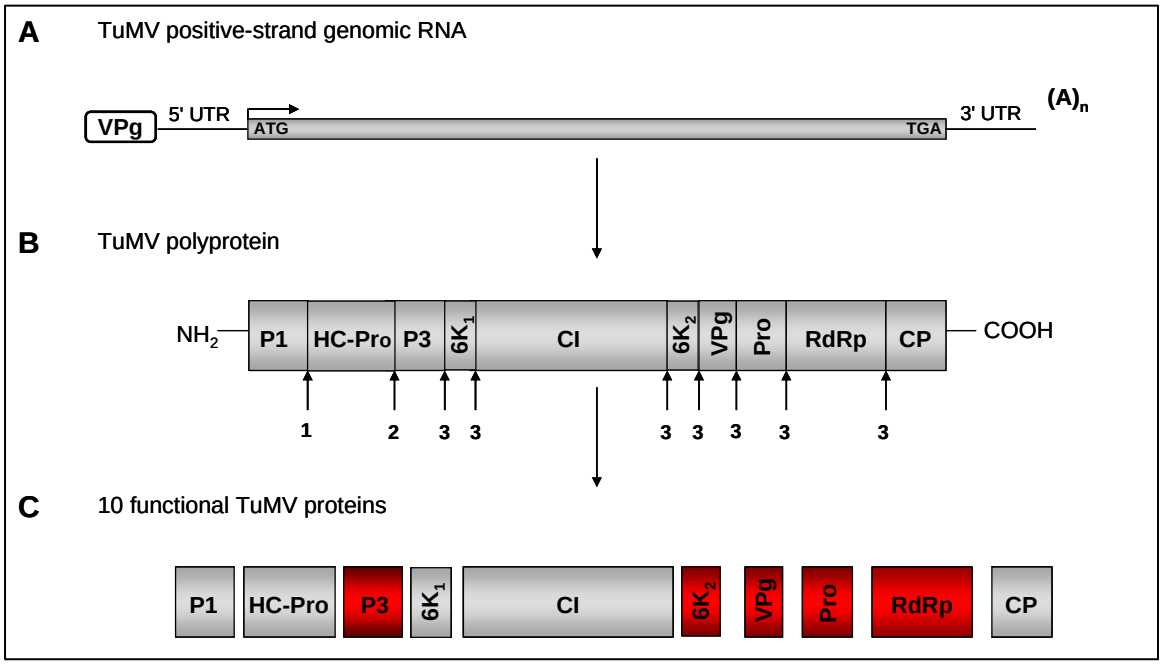

Figure 2.1: Schematic representation of the TuMV genome and polyprotein. (A) Representation of the (+) ssRNA genome of TuMV. The single ORF is flanked by two UTRs. The 5'-terminus of genomic RNA is covalently linked to the VPg. The genome has a poly(A) tail at its 3' end. (B) The TuMV polyprotein and the position of each cleavage sites. The abbreviations of the names of the viral proteins are indicated within the polyprotein. Arrows indicate the positions at which cleavage occurs. VPg-Pro protease (cleavage site 3) cleaves at all sites except those cleaved by P1 (cleavage site 1) and HC-Pro (cleavage site 2) proteases. (C) TuMV individual cleavage products that result from autoproteolytic digestion. Red boxes represent the viral proteins that will be further described in chapter 2.

Elucidation and comparison of the crystal structures of RdRps indicate that their overall shape resembles that of a "right hand" with finger, palm and thumb subdomains; the catalytic domain residing in the palm domain. All viral RdRps described thus far adopt a conformation where the active site is fully enclosed as a result of extensive interactions between the fingers and thumb domains (Thompson and Peersen, 2004).

The RdRp of some potyviruses forms inclusion bodies in the nucleus of infected plants (Baunoch et al., 1991; Li and Carrington, 1993). The RdRp of these potyviruses is known as nuclear inclusion b (NIb) protein. These nuclear inclusions also contain VPg-Pro [known as nuclear inclusion a (NIa) protein] and are crystalline structures that result from excess protein depositions (Baunoch et al., 1991). However, in the case of most potyviruses such as TuMV, *Peanut stripe mosaic virus*, and *Tobacco vein mottling virus* (TVMV), the RdRp and VPg-Pro accumulate in the nucleus but do not form inclusions (Edwardson and Christie, 1991; Hajimorad et al., 1996). The transport of the RdRp to the nucleus is control by two independent nuclear localization signals (NLSs) (Li et al., 1997). The RdRp and VPg-Pro are also found in cytoplasmic membrane-bound replication complexes (Léonard et al., 2004; Schaad et al., 1997a). How the RdRp is recruited to the site of RNA replication is however unclear. There are accumulating evidences suggesting that the polymerase is directed to the site of RNA synthesis through protein-protein interactions with VPg-Pro. In fact, it has been demonstrated that VPg-Pro is directed to membranes in the form of a 6K-VPg-Pro precursor (Beauchemin et al., 2007; Beauchemin and Laliberté, 2007; Schaad et al., 1997a). As the RdRp protein interacts with VPg-Pro, RdRp is thought to be recruited to membranes through

interaction with the 6K-VPg-Pro protein (Léonard et al., 2004; Li et al., 1997; Schaad et al., 1997a).

2.1.2.2. Interaction of the potyviral RdRp with viral and plant proteins

The most documented interaction between the RdRp and other potyviral proteins is the one with VPg-Pro. The interaction was first discovered with the yeast two-hybrid system (YTHS) using TVMV proteins (Hong et al., 1995). Mutation analyses revealed that the RdRp-VPg-Pro interaction arises through interaction with the VPg domain of VPg-Pro. The interaction of VPg with RdRp was again confirmed *in vitro* with purified recombinant proteins of *Tobacco etch virus* (TEV). It is now well established that the Pro domain of VPg-Pro also interacts with the RdRp (Guo et al., 2001; Li et al., 1997; Merits et al., 1999). Using the two-hybrid system with the TEV VPg or Pro domains as bait, Li et al. (1997) identified the Pro domain as necessary for the RdRp-VPg-Pro interaction. Work with *Potato virus A* (PVA) and *Pea seed-borne mosaic virus* (PSbMV) also identified an interaction between the Pro domain and the RdRp. Both VPg-Pro and VPg alone were shown to possess a stimulatory effect on the RdRp activity, a finding that indicates the participation of VPg-Pro in virus replication (Fellers et al., 1998). This interaction was also proposed to be involved in the initiation of viral RNA synthesis as VPg is uridylated by the viral RdRp (Puustinen and Makinen, 2004) and may then act as a primer for negative-strand synthesis as seen with picornaviruses (Semler and Wimmer, 2002).

The RdRp is also able to bind three other potyviral proteins. Whole genome protein-protein interaction studies performed on PVA and PSbMV proteins using various

biochemical methods have identified P1 and P3 as potential interactors of RdRp (Guo et al., 2001; Merits et al., 1999). Finally, the YTHS also showed an interaction between the RdRp and the CP of TVMV (Hong et al., 1995). However, these interactions have not been characterized in detail and their role in virus infection is still unclear.

Only one host protein was found to interact with the potyviral RdRp. The RdRp of *Zucchini yellow mosaic potyvirus* (ZYMV) was shown to interact with host poly(A)-binding protein (PABP) in the YTHS and in *in vitro* binding assays (Wang et al., 2000). The authors proposed that this interaction might facilitate virus replication, either by helping to recruit the RdRp to the virus poly(A) tail or by facilitating removal of PABP from the poly(A) tail and allowing access of the RdRp for initiation of replication. The RdRp of potyviruses has a crucial role in replication, thus, the polymerase surely interacts with more than one host protein. Further characterization of the virus-host interactions involving the RdRp is required.

2.1.3. The VPg and its precursor forms

VPg and its precursor forms are multifunctional and have essential functions in all critical steps of potyvirus replication cycle, i.e. viral RNA replication, RNA translation, local and systemic movement and avirulence. The capacity of VPg and its precursors to interact with RNA and several others viral proteins emphasize their important roles in virus infection. Consequently, the functions of VPg and its precursor forms will be underlined in the following section.

2.1.3.1. Function and cellular localization of VPg and its precursor forms

The VPg is the protein that is covalently linked to the 5' end of the viral RNA. It has a molecular weight of 22 kDa (Laliberté et al., 1992). VPg also exists under two precursor forms: VPg-Pro (49 kDa) and 6K-VPg-Pro (55 kDa) (Léonard et al., 2004). VPg and its precursors have essential functions in the viral replication cycle. The 6K peptide possesses a central hydrophobic domain that is responsible for its binding to membranes (Schaad et al., 1997a). When linked to VPg-Pro, the 6K peptide of TEV and TuMV prevents transport of VPg-Pro to the nucleus and thus seems to override nuclear translocation of the VPg-Pro protein (Beauchemin et al., 2007). The 6K protein induces the formation of large vesicular compartments derived from the ER (Schaad et al., 1997a). It has been suggested that these vesicles harbor the viral replication complex (VRC). Consequently, it has been proposed that the 6K protein is required for genome amplification and that it anchors the replication apparatus to ER-like structures. Targeting to these membranous sites may require 6K-VPg or 6K-VPg-Pro (Beauchemin et al., 2007; Schaad et al., 1997a).

The C-terminal portion of VPg-Pro (i.e. Pro domain) is a serine-type proteinase, which shares homology with the 3C picornaviral protease ($3C^{Pro}$) (Schaad et al., 1996). It is the major proteinase of potyviruses; it processes the polyprotein *in cis* and *in trans* to produce functional products (Riechmann et al., 1992). Figure 2.1 shows the specific cleavage sites of the protease.

The cellular localization of VPg-Pro and 6K-VPg-Pro has been described in section 2.1.2.1. The nuclear localization of VPg-Pro has been attributed to its association with the RdRp as well as to its functional NLS located in its VPg domain (Schaad et al.,

1996). Recently, the VPg-Pro of TuMV was observed in the nucleolus of *Nicotiana benthamiana* cells (Beauchemin et al., 2007). The accumulation of VPg-Pro within the nucleus is essential for viral replication as a mutations resulting in debilitation of VPg nuclear translocation also reduced genome amplification (Schaad et al., 1996). However, the reason for the VPg-Pro localization in the nucleus and nucleolus remains unknown.

Accumulating evidence support a role for VPg and its precursors in viral amplification: its stimulatory effect on the RdRp activity (Fellers et al., 1998), its localization in the virus-induced vesicles (Beauchemin et al., 2007; Beauchemin and Laliberté, 2007), and its capacity to bind RNA in a non-specific manner (Daros and Carrington, 1997; Merits et al., 1998). Its involvement in replication is also supported by the study of Klein et al. (1994) in which mutant TVMV clones with a non-functional VPg-Pro failed to produce detectable amounts of progeny viral RNA.

Beside its role in viral replication, VPg-Pro has been attributed different functions in cell-to-cell movement (Schaad et al., 1997b) and in overcoming resistance in plants (Keller et al., 1998).

2.1.3.2. Interaction of VPg and its precursor forms with viral and plant proteins

Interactions of VPg-Pro with itself, the HC-Pro protein, and the RdRp (see section 2.1.2.2 for more details on the VPg-Pro-RdRp interaction) were studied using the YTHS (Hong et al., 1995; Yambao et al., 2003). VPg-Pro of TVMV was shown to interact with itself (Hong et al., 1995). More recently, a strong interaction between HC-Pro and the central domain of the VPg of *Clover yellow vein virus* (ClYVV) was detected by both YTHS and by *in vitro* far-Western blot analysis (Yambao et al., 2003). Given that the

central domain of VPg determines host specificity for systemic movement (Schaad et al., 1997b), this interaction is believed to be involved in vascular movement of the virus.

Protein-protein interactions were also found between VPg-Pro and host cellular factors. The most documented is the one between VPg-Pro and the mRNA cap-binding eukaryotic initiation factor 4E (eIF4E) or its isoform eIF(iso)4E. This interaction was first identified between the VPg of TuMV or TEV with eIF4E/eIF(iso)4E using the YTHS (Schaad et al., 2000; Wittman et al., 1997). The formation of this complex is important for virus infectivity: *Arabidopsis thaliana* mutants that lack eIF(iso)4E show total resistance to TuMV, *Lettuce mosaic virus* and TEV (Duprat et al., 2002; Lellis et al., 2002), while the disruption of eIF4E isoform results in resistance to ClYVV (Sato et al., 2005). The molecular characterization of naturally occurring recessive resistance loci has also led to the identification of eIF4E/eIF(iso)4E as viral susceptibility factors in different plant species. Recessive resistance genes against potyviruses have been shown to encode defective allelic forms of the eIF4E or eIF(iso)4E gene in pepper (Kang et al., 2005; Ruffel et al., 2002), tomato (Ruffel et al., 2005), lettuce (Nicaise et al., 2003) and pea (Gao et al., 2004).

The VPg-Pro of TuMV also interacts *in planta* and *in vitro* with host PABP (Léonard et al., 2004). The PABP was recently shown to be internalized in TuMV-induced vesicles upon infection (Beauchemin and Laliberté, 2007). As these vesicles are thought to contain the VRC, it suggests a role for PABP in the viral replication/translation.

2.1.4. The P3 protein

2.1.4.1. Function and cellular localization of P3

The P3 remains the least characterized proteins of potyviruses due to its high sequence variability among species, the lack of structural motif, the toxicity for expression in *Escherichia coli* and difficulty in refolding. To gain information on the function of P3 in viral infection, localization of the protein was performed by immunocytology with antibodies raised against P3 of TVMV (Rodriguez-Cerezo et al., 1993) and TEV (Langenberg and Zhang, 1997). The TVMV P3 was localized in the cytoplasm of infected cells in association with the CI protein, whereas TEV P3 protein was observed inside the nucleus in association with the viral RdRp and VPg-Pro proteins. More recently, the subcellular localization of P3 and $6K_1$-P3 proteins of *Papaya ringspot virus* was investigated by expressing their green fluorescent protein (GFP)-fusion proteins in onion epidermal cells. Both fusion proteins were localized at the ER of transfected cells (Eiamtanasate et al., 2007). These contradictory results might arise from different localization between functional and excessive non-functional proteins. Despite these conflicting results, the conclusion with all three viruses is that P3 may be involved in virus amplification. Insertion mutations in TVMV P3 protein gene have been found to prevent replication, again indicating a role for P3 in virus amplification (Klein et al., 1994). Since P3 does not have RNA binding activity (Merits et al., 1998), its participation in replication is postulated to occur through its interaction with CI (Rodriguez-Cerezo et al., 1993), which is part of the replication complex (Klein et al., 1994).

A role for P3 in plant pathogenicity is supported by several studies demonstrating that the P3 protein is the avirulant factor for some resistance genes (Jenner et al., 2003;

Johansen et al., 2001), a pathogenicity determinant relevant for symptom severity (Saenz et al., 2000), and a host range determinant (Suehiro et al., 2004; Tan et al., 2005). However, little is known on how the P3 protein may interact with plant/virus elements in order to elicit different symptomatologies.

2.1.4.2. Interaction of P3 with viral proteins

There is little information on protein-protein interactions involving the P3 protein. As described above, attempts to localize the viral protein in infected cells suggest that P3 interacts with CI, VPg-Pro and RdRp (Langenberg and Zhang, 1997; Rodriguez-Cerezo et al., 1993). *In vitro* binding assays also revealed that PVA P3 protein interacts directly with CI, VPg-Pro and RdRp, although in YTHS the same researchers reported that PVA P3 protein interacts only with the RdRp (Merits et al., 1999). Similarly *in vitro* and *in vivo* assays also showed that P3 of *Wheat streak mosaic virus* is capable of binding to itself, P1, HC-Pro and CI (Choi et al., 2000). None of these interactions have been extensively characterized and their role in virus infection remains to be determined. To date, the P3 protein has not been reported to interact with plant protein.

2.2. General life cycle of potyviruses

The replication cycle of potyviruses involves cell entry, uncoating, viral protein synthesis, genome replication, progeny virus particle assembly, cell-to-cell movement within the infected plant and vector transmission from plant to plant (Ahlquist et al., 2003) (Fig. 2.2).

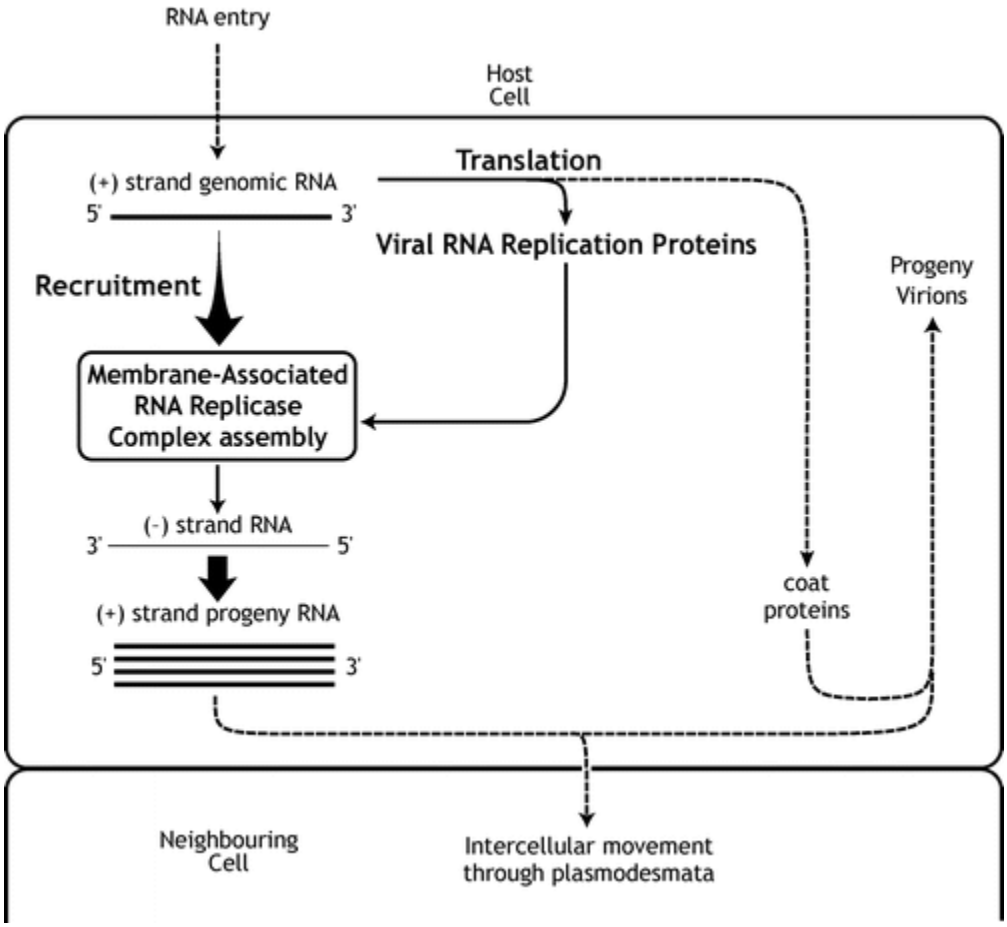

Figure 2.2: General scheme of positive-strand RNA virus replication. The major steps in RNA virus replication are cell entry, uncoating, virus protein synthesis, genome replication, progeny virus particle assembly, cell-to-cell movement within the infected plant and vector transmission from plant to plant. All steps specific to RNA replication are depicted with solid arrows, whereas steps that are not involved in RNA replication are depicted with dashed arrows. In RNA replication, all steps where host factors have been implicated are in bold. Adapted by permission from Annual Reviews Publishers Ltd: Annu. Rev. Phytopathol. (Noueiry and Ahlquist, 2003), copyright 2003.

Viral RNA translation and RNA replication are two fundamental processes required for potyvirus genome amplification. Positive-strand RNA virus genomes are templates for both protein synthesis and RNA replication, leading to interactions between host translation factors and RNA replication components at multiple levels. All known positive-strand RNA viruses carry genes encoding an RdRp used in virus genome replication. Thus, upon infection of a new cell, viral RNA replication begins once the genomic RNA has been translated to produce the polymerase, and additional factors involved in membrane targeting, template recruitment, RNA capping and other functions (Nagy, 2008). The replication/translation of RNA viruses involves several viral and host factors. The following section of this review will be focusing on the translation and replication steps of the viral replication cycle.

2.2.1. Translation of the viral RNA genome

Positive-strand RNA viruses have small genomes that encode a limited number of proteins and depend on their hosts to achieve the synthesis of their proteins. Viruses have therefore evolved many strategies to promote their translation and redirect the host translation apparatus to their advantage (Schneider and Mohr, 2003).

In contrast to most cellular messenger RNAs (mRNAs), potyviral RNAs lack a 5' cap structure. However, the host mRNAs and potyviral RNAs both have a poly(A) tail at their 3' end. Since translation of most eukaryotic mRNAs requires both the 5' cap and 3' poly(A) tail for efficient translation initiation (see section 2.3 for more details) (Gallie, 1998), alternative mechanisms must operate for potyviruses. In the virion, the 5' structure is replaced by VPg, which suggests a role for this protein in the binding of translational

factors prior the recruitment of ribosomes. The finding of an interaction between TuMV VPg and the cap binding protein eIF(iso)4E from *A. thaliana* supports this hypothesis (Wittman et al., 1997). Further characterization of the interaction showed that VPg can effectively compete with the methyl-7-guanidine cap (m^7GTP) for eIF4E/eIF(iso)4E binding, which suggests that VPg and the 5' cap structure of cellular mRNAs might compete for eIF(iso)4E binding *in vivo* (Khan et al., 2007; Léonard et al., 2000; Michon et al., 2006). However, the hypothesis that the VPg of potyviruses can replace the 5' cap structure is still debatable since the 5' structure of the polysome-associated potyviral RNA is unknown.

Another mechanism that could be used by potyviruses to overcome the need for the 5' cap structure is illustrated by some members of the *Picornaviridae* family of viruses. Like potyviruses, picornaviruses all have a VPg, but ribosome entry has been linked to the presence of a long 5' leader sequence that contains an internal ribosome entry site (IRES): a genetic element that facilitates internal ribosome entry and mRNA translation independent of the m^7GTP cap structure (Gale et al., 2000). Picornaviruses use a cap-independent translation mechanism that involves internal ribosome entry (Pelletier and Sonenberg, 1988). IRES-mediated translation provides an advantage for viruses; it avoids the requirement of a pool of specific initiation factors. The 48S translation initiation complex formation on cardiovirus IRES requires eIF4G, which directly binds to the IRES, and eIF4A, but does not require eIF4E (Lomakin et al., 2000; Pestova et al., 1996). An IRES element is also present within the 5'-untranslated leader of TEV, a member of the potyvirus group, which can substitute for the 5' cap structure. Like animal picornavirus IRES, TEV IRES promotes cap-independent translation (Gallie,

2001). To date, evidence suggests that the TuMV 5' UTR may act similarly to the TEV 5' UTR, although no IRES-like structure has been identified (Basso et al., 1994). Thus, the 5' UTR of some potyviruses might have the necessary features to recruit efficiently the host translation machinery.

Finally, following the initiation of translation, the elongation and termination processes of viral RNA translation can proceed. These two possesses are thought to occur in a similar manner as cellular mRNA. The viral RNA translation leads to a large polyprotein, which is then cleaved by the three virus-encoded proteases. The proteins released are all thought to be multifunctional.

2.2.2. Viral replication

After the synthesis of replication factors, positive-strand RNA viruses must switch the role of the incoming genomic RNA from translation to replication. The genome replication of positive-strand RNA viruses consists of a two-step process: first, the minus-strand replication intermediates are produced, which are then used to direct synthesis of excess amounts of (+)RNA progeny. Both processes are catalyzed by the virus RdRp with the help of other viral and host proteins. Positive-strand RNA viruses assemble their RNA replication complexes on intracellular membranes (see section 2.2.2.1 for more details) (Salonen et al., 2005). Based on recent detailed analyses of a single replication cycle of (+)RNA viruses, genome replication can be further divided in the following steps: (i) the recruitment of the viral (+)RNA template for replication, including a requirement for switching of the genomic RNA from translation to replication; (ii) targeting of viral replication proteins to the site of replication; (iii)

preassembly of the viral replicase components; (iv) activation/final assembly of the VRC containing the (+)RNA template on intracellular membranous surfaces; (v) synthesis of the viral RNA progeny by the replicase complexes, including minus- and plus-strand synthesis; (vi) release of the viral (+)RNA progeny from the VRC to the cytosol; and (vii) disassembly of the VRC (Nagy , 2008).

In the case of potyviruses, mutational analyses have shown that the viral VPg-Pro, RdRp, P1, HC-Pro, and P3 are involved in genome amplification (Atreya et al., 1992; Kasschau and Carrington 1995; Kasschau et al., 1997; Klein et al., 1994; Verchot and Carrington, 1995). Several studies have also implicated the CI protein, an RNA helicase, and the CP in potyviral replication (Eagles et al., 1994; Klein et al., 1994; Lain et al., 1990; Urcuqui-Inchima et al., 2001). Evidence indicates that, in addition to the viral replication factors, specific host factors play an essential role in positive-strand RNA virus replication. The potyviral ER-derived vesicles have been shown to contain two host proteins: PABP and eIF(iso)4E (Beauchemin et al., 2007; Beauchemin and Laliberté, 2007). The specific role of these host proteins in viral amplification remains unclear but their presence in viral-induced vesicles suggests the formation of a multiprotein complex during potyviral translation and replication.

2.2.2.1. Assembly of membrane-associated RNA replication complexes

All characterized positive-strand RNA viruses assemble their RNA replication complexes on intracellular membranes, usually in association with membrane vesicle formation or other membrane rearrangements. The host membrane constitutes a crucial component for VRCs serving multiple purposes. First, the membrane provides a surface

on which replication factors are localized and concentrated for assembly. The membrane also protects the VRC in which the RNA replication factors and genomic RNAs are sequestered from competing RNA templates (Salonen et al., 2005). This assembly also helps to protect any dsRNA replication intermediates from dsRNA-host defense responses (Ahlquist, 2002).

For potyviruses, replication complexes associate with membranes of the ER. The 6K protein is known to associate with membranes as an integral protein and to be sufficient for the production of large endoplasmic reticulum (ER)-derived vesicles (Beauchemin et al., 2007; Beauchemin and Laliberté, 2007; Schaad et al., 1997a). The VPg-Pro is anchored to membranes through its association with the 6K protein. The RNA polymerase is thought to be recruited to membranes through its interaction with 6K-VPg-Pro (Beauchemin et al., 2007; Schaad et al., 1997a). Finally, the interactions of VPg-Pro with host eIF4E isoforms and PABP and its capacity to form ER-derived vesicles under its 6K-VPg-Pro precursor form suggest that the viral protein may serve as a focal point for the VRC assembly (Beauchemin et al., 2007; Beauchemin and Laliberté, 2007).

2.3. Translation in eukaryotes

2.3.1. Overview

Translation can be divided into four stages: initiation, elongation, termination, and recycling (Kapp and Lorsch, 2004). During initiation, the ribosome is assembled at the initiation codon of the mRNA with a methionyl initiator transfer RNA (tRNA) bound in its peptidyl (P) site. During elongation, aminoacyl-tRNAs (aa-tRNAs) enter the acceptor (A) site where decoding takes place. If it is the correct (cognate) tRNA, the ribosome

catalyzes the formation of a peptide bond. After the tRNAs and mRNA are translocated such that the next codon is moved into the A site, the process is repeated. Termination occurs when a stop codon is encountered and the finished peptide is released from the ribosome. In the recycling stage, the ribosomal subunits are dissociated, releasing the mRNA and deacylated tRNA and preparing the stage for another round of initiation. A comprehensive review of all four stages of translation is not the scope of this treatise. Therefore, we will limit the discussion to the initiation and elongation stages of translation.

2.3.1.1. Translation initiation

Translation initiation can be subdivided into three steps: first, the recruitment of the ribosome to mRNA, the unwinding of the mRNA 5' secondary structure to facilitate 40S ribosome binding, and the recognition of an initiation codon (for review, see Hersey and Merrick, 2000). The majority of mRNA translation in eukaryotic cells is dependent on the 5'-m^7G cap, a structure at the 5' terminus of the mRNA (Gale et al., 2000). The recruitment of the ribosome to the 5' cap structure is mediated by the multi-subunit eIF4F (Haghighat et al., 1997). The eIF4F factor is a complex of three proteins: eIF4E, eIF4A and eIF4G. In plants, a second heteromeric cap-binding complex, eIF(iso)4F [eIF(iso)4E/eIF(iso)4G], has been identified (Browning, 1996). Despite a low level of amino acid sequence conservation, both cap-binding complexes are functional and facilitate cap-dependent translation (Gallie and Browning, 2001). eIF4E recognizes and binds directly to the m^7G-cap, while eIF4A is a helicase and eIF4G is a scaffolding protein. eIF4G binds eIF4E, eIF4A, eIF3, and PABP (Gingras et al., 1999). By its

association with the 40S ribosomal subunit, which is complexed with eIF2-GTP-$tRNA^{met}$ near the 5' end of the mRNA, eIF3 serves as a link between the mRNA/eIF4F complex and the ribosome. In conjunction with eIF4B and eIF4H, eIF4A is thought to unwind the mRNA 5' secondary structure to facilitate the binding of the 40S ribosome subunit (Hersey and Merrick, 2000). Finally, upon recognition of the AUG codon, most of the initiation factors are released, followed by the recruitment of the 60S ribosomal subunit and the beginning of elongation.

Efficient translation of eukaryotic mRNAs occurs in a closed loop format (Fig. 2.3), in which the 5'- and 3'- ends are brought together into close proximity through the mediation of interactions involving translation initiation factors (Sachs et al., 1997). The key interactions involve PABP bound to the 3'-poly(A) tail and eIF4E bound to the 5' cap, and the interaction of both proteins with eIF4G. The circularization of the mRNA increases the affinity of translation initiation factors, the ribosome and the mRNA for each other, causing a synergistic enhancement of translation (Pestova et al., 2001).

2.3.1.2. Elongation

The sequential addition of amino acids to the growing polypeptide chain involves the use of three sites on the fully assembled 80S ribosome, designated the P, A and E sites (Fig. 2.4). Peptide chain elongation starts with a peptidyl tRNA in the ribosomal P site next to a vacant A site. An aa-tRNA is transported to the A site as part of a tertiary complex with GTP and the eukaryotic elongation factor 1 alpha [eEF1A; elongation factor thermo unstable (EF-Tu) in bacteria].

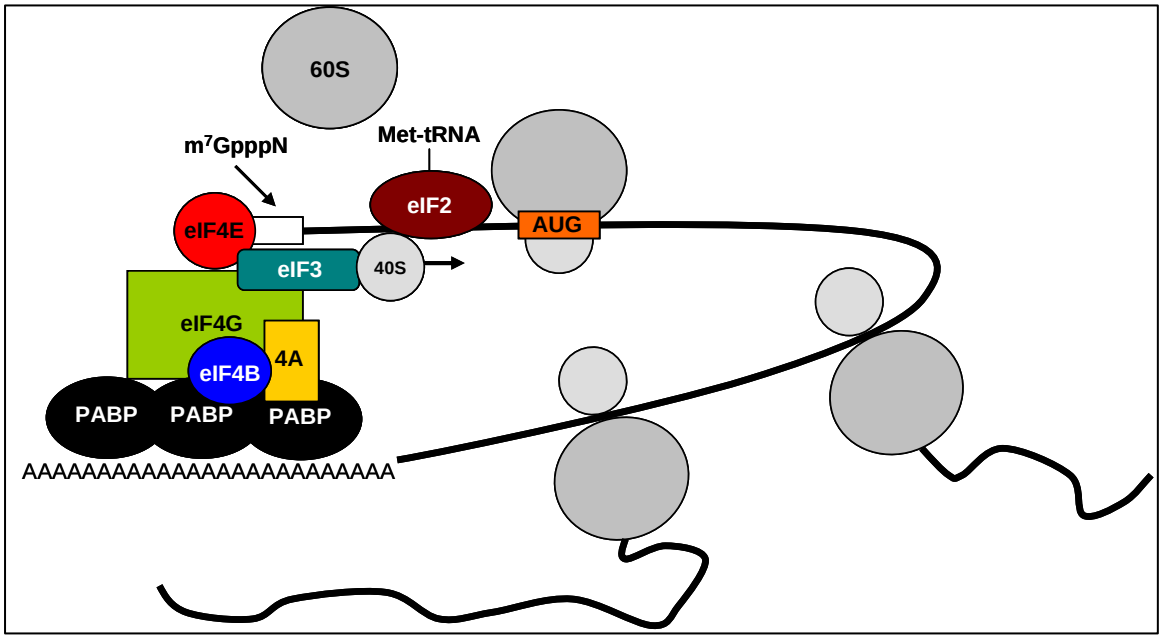

Figure 2.3: Circularization of the eukaryotic translation initiation complex. Capped mRNAs are recruited by the eIF4F complex (composed of eIF4E, eIF4G and eIF4A). The eIF4E binds to the 5'-m^{7}GppN-cap of the mRNA. The eIF4G is a scaffold protein that binds eIF4E, eIF4A, eIF4B and PABP. The assembly of these proteins circularizes the mRNA, which causes a synergetic enhancement of translation. The eIF4G also interacts with the eIF3 complex to position the 40S ribosomal subunit and the eIF2-GTP-tRNA^{met} near the 5' end of the mRNA. With the assistance of the other factors, both ribosomal subunits (40S and 60S) are coupled and elongation can then begin. Adapted by permission from Elsevier Limited: Curr. Opin. Plant Biol. journal, (Kawaguchi and Bailey-Serres, 2002), copyright 2002.

Figure 2.4: The elongation phase of protein synthesis. First, a growing polypeptide chain is covalently attached to the tRNA in the P site. The A site is empty, exposing the next codon in the mRNA. The uncharged tRNA from the previous cycle is in the E site. Secondly, a charged tRNA binds to the ribosomal A site. If its anticodon matches the exposed codon on the mRNA, the tRNA in the E-site is ejected from the ribosome. eEF1A forms a ternary complex with GTP and the charged tRNA and promotes the binding of the charged tRNA to the A site of the ribosome. Thirdly, the peptidyl transferase center is used by the ribosome to catalyze the formation of a peptide bound between the growing polypeptide chain and the new amino acid. The result of this process is that the nascent polypeptide has been transferred from the tRNA in the P site to the new amino acid attached to its tRNA in the A site. The polypeptide is one residue longer, the peptidyl-tRNA is now in the A site, and the tRNA in the P site is free of its amino acid. Finally, the complex is reorganized to expose the next triplet. This process, called the translocation, involves three rearrangements: the deacylated tRNA in the P site moves into the E site; the peptidyl-tRNA in the A-site moves to the P site; and the ribosome moves relative to the mRNA by exactly three nucleotides (one codon), exposing a new triplet in the A site. Adapted by permission from John Wiley and Sons Inc: Biochemistry and Molecular Biology of Plants (Buchanan et al., 2000), copyright 2000.

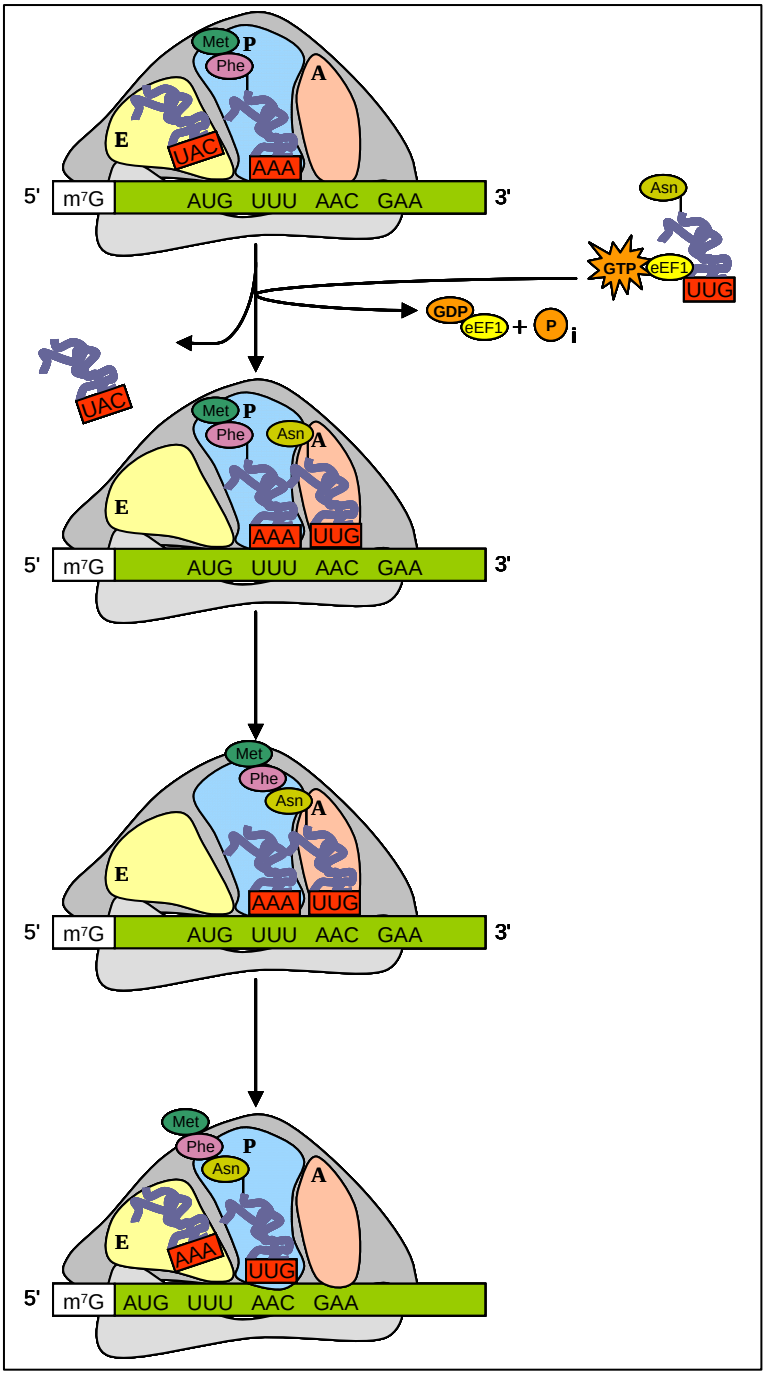
Met
P
Phe
A
E
UAC
AAA
5'
m7G
AUG UUU AAC GAA
3'
Asn
GTP
eEF1
UUG
GDP
eEF1
+
P
i
UAC
Met
P
Phe
Asn
A
E
AAA
UUG
5'
m7G
AUG UUU AAC GAA
3'
Met
Phe
Asn
A
E
AAA
UUG
5'
m7G
AUG UUU AAC GAA
3'
Met
Phe
P
Asn
A
E
AAA
UUG
5'
m7G
AUG UUU AAC GAA

eEF1A•GTPaa•tRNA ternary complexes with either the cognate or non-cognate aa-tRNAs can bind to the ribosome A site. The selection of the correct aa-tRNA, based on codon-anticodon interaction, is a crucial step in translation and involves many steps (reviewed in Rodnina and Wintermeyer, 2001). Codon-anticodon base pairing induces three nucleotides in the small ribosomal subunit's rRNA to swing out and interact with the resulting mRNA-tRNA duplex (Ogle et al., 2001). This activates the GTPase activity of eEF1A. eEF1A•GDP releases the aminoacyl tRNA into the A site in a form that can continue with peptide bond formation. Then, the ribosomal transferase center catalyses the formation of a peptide bond between the incoming amino acid and the peptidyl tRNA (Moore and Steitz, 2003). The result is a deacylated tRNA in a hybrid state with its acceptor end in the E site of the large subunit and its anticodon end in the P site of the small subunit (Green and Noller, 1997). The peptidyl-tRNA is also in a similar hybrid situation with its acceptor end in the P site of the large subunit and its anticodon end in the A site of the small subunit. This complex in then translocated so that the deacylated tRNA is completely in the E site, the peptidyl tRNA completely in the P site, and the mRNA moved by three nucleotides to place the next codon of the mRNA into the A site. This task is accomplished by the elongation factor 2, which hydrolyzes GTP and facilitates translocation (Wintermeyer et al. 2001). This cycle is repeated until a stop codon is encountered and the process of termination initiated.

2.4. Potyviral recruitment and/or modification of translation factors

2.4.1. PABP

PABPs play critical roles in mRNA translation and stability. PABPs also bind a large number of proteins and as described in section 2.3.1.1, the interaction between eIF4E/eIF4G and PABP is sufficient to circularize the mRNA. This closed-loop translation initiation complex stabilizes assembled initiation factors and increases translation efficiency. The functions of PABP and how viruses use or disrupt these functions will be the subject of the following section.

2.4.1.1. Structure and function of the PABP

PABP is a multidomain mRNA-binding protein of ~ 70 kDa (Adam et al., 1986). The N-terminal two-thirds of the protein consists of four conserved RNA recognition motifs (RRMs) (Sachs et al., 1987). It is primarily via the RRM 1 and 2 domains that PABP binds to the poly(A) tail of mRNA (Gray et al., 2000) and to eIF4G (Imataka et al., 1998). The carboxy-terminal one-third of PABP serves as a docking site for a number of proteins, including PABP-interacting protein 1 (paip1), PABP-interacting protein 2 (paip2) and eukaryotic release factor 3 (Craig et al., 1998; Hoshino et al. 1999; Khaleghpour et al., 2001).

PABP is an essential protein; deletion of the yeast *PAB1* gene is lethal (Sachs et al., 1987) and reduction in PABP levels, either by cleavage or by sequestration by virus proteins, can result in shutdown of host translation (Chen et al., 1999; Joachims et al., 1999; Piron et al., 1998). PABP has been shown to bind eIF4G in mammals (Piron et al.,

1998), plants (Le et al., 1997) and yeasts (Tarun and Sachs, 1996). In plants, this interaction stabilizes the binding of PABP to the poly(A) tail and results in a 40-fold increase in the affinity of eIF4F for the 5' cap structure (Wei et al., 1998). The PABP/eIF4G interaction also promotes binding of 40S ribosomal subunits to the mRNA and formation of the 48S initiation complex (Tarun and Sachs, 1995). These studies provide evidence supporting a role for PABP during translation initiation and suggest that efficiently translated mRNAs are circularized via a cap-eIF4E-eIF4G-PABP-poly(A) tail interaction (the closed-loop model). mRNA circularization has been directly demonstrated *in vitro* by using recombinant yeast eIF4E, eIF4G and PABP (Wells et al., 1998) and is thought to increase the efficiency of translation by promoting the novo initiation of new ribosomes and by recycling of terminating ribosomes on the same mRNA (Welch et al., 2000).

PABP is also involved in maintaining the integrity of mRNAs. Once an mRNA is transported to the cytoplasm, the poly(A) tail is shortened until a tail length of 10-25 adenosine residues is reached (Caponigro and Parker, 1995). The 5' cap structure is removed by the decapping enzyme and the coding region is quickly degraded by a 5'→3' RNA exoribonuclease (Beelman et al., 1996). As the presence of PABP on the poly(A) tail prevents this decapping event (Caponigro and Parker, 1995), the means by which PABP exerts its protective effect may be through stabilizing the binding of eIF4E to the cap as mediated through eIF4G (Gallie, 1998).

Accumulating evidence also proposes a role for PABP in the nucleus. The nuclear PABP (PABPN) interacts with component of the polyadenylation machinery and affects polyadenylation processing *in vitro* and *in vivo* (Amrani et al., 1997; Brown and Sachs,

1998). PABPN stimulates the extension and controls the length of the poly(A) (Kuhn and Wahle, 2004; Mangus et al., 2003). PABPN also possess a NLS in its C-terminal domain, which suggests that PABPN shuttles between nucleus and cytoplasm to export the mRNA to the cytoplasm (Hector et al., 2002; Kuhn and Wahle, 2004).

2.4.1.2. PABP and virus infection

2.4.1.2.1. Enhancement of viral replication/translation

The poly(A) tail plays an important role in the replication of polyadenylated positive-strand RNA viruses. Removal of the poly(A) from genomic RNAs of viruses dramatically reduces infectivity (Sanchez et al., 1998; Sarnow, 1989). Numerous reports have also shown that the poly(A)-tail significantly stimulates the IRES-dependent translation of picornaviruses (Bergamini et al., 2000; Khaleghpour et al., 2001; Michel et al., 2000; Michel et al., 2001; Svitkin et al., 2001). PABP is an important mediator of the poly(A)-IRES functional interaction; its displacement from the poly(A) tail by Paip2, a repressor of translation, abolishes the stimulatory effect of the poly(A) tail on translation (Khaleghpour et al., 2001). eEF4G mediates this translational enhancement because its cleavage by 2A viral protease ($2A^{pro}$) or disruption of PABP-eIF4G interaction renders the IRES refractive to the stimulatory activity of poly(A) tail (Michel et al., 2001; Svitkin et al., 2001).

2.4.1.2.2. Proteolysis of PABP: picornaviruses, calciviruses and retroviruses

It has been known for a long time that infection of cultured cells with poliovirus, a member of the *Picornaviridae*, results in the translational inhibition of host but not viral mRNAs (Holland and Peterson, 1964). Initially explained by eIF4GI (Lamphear et al., 1995) and eIF4GII (Gradi et al., 1998) specific cleavage, poliovirus-induced shutoff of host translation is now attributed to an additional event; the proteolysis of PABP (Joachims et al., 1999). Experiments performed *in vitro* and on poliovirus infected cells have shown that both viral $2A^{pro}$ and $3C^{Pro}$ proteases cleave PABP and lead to inhibition of host translation (Joachims et al., 1999). A direct role for the proteolysis of PABP in host translation shutdown was further observed in various members of the *Picornaviridae*, *Caliciviridae* and *Retroviridae* (Alvarez et al., 2006; Kerekatte et al., 1999; Kuyumcu-Martinez et al., 2002; Kuyumcu-Martinez et al., 2004a; Kuyumcu-Martinez et al., 2004b; Rodriguez Pulido et al., 2007; Zhang et al., 2007). This suggests that proteolysis of PABP may be a common mechanism used by different virus families to inhibit host translation.

The cleavage of PABP is particularly intriguing since picorna-, retro- and calicivirus RNAs are polyadenylated at the 3' end of their positive strand which is the site of initiation of minus strand synthesis. If PABP is involved in viral translation/replication, a bypass mechanism is needed to selectively inhibit host translation without affecting viral translation. Kuyumcu-Martinez et al. (2002) reported that ribosome-associated PABP is preferentially cleaved by poliovirus proteases as compared to PABP in other fractions, which may suggest selective inhibition of cellular translation.

2.4.1.2.3. Substitution of PABP: rotaviruses

Rotaviruses (*Reoviridae* family) use another mechanism involving PABP to inhibit host translation machinery. Rotavirus mRNA is capped and non-polyadenylated, but it utilizes a mechanism of circularization to promote its translation (Piron et al., 1998). The rotavirus RNA is circularized via virus protein NSP3 (non-structural protein 3) that bridges the 3' end of viral RNA with eIF4G (Vende et al., 2000). Binding of NSP3 to eIF4G disrupts the cellular interaction between PABP and eEF4G which interferes with circularization of cellular mRNAs. The two consequences of NSP3 expression are inhibition of host protein synthesis and circularization-mediated translational enhancement of rotavirus mRNAs (Padilla-Noriega et al., 2002).

2.4.1.2.4. PABP protein and plant viruses

Compared to animal viruses, the role of PABP in plant viral infection has not been extensively investigated. As described in more details in section 2.1.2.2 and 2.1.3.2, two potyviruses were found to recruit PABP. TuMV VPg-Pro was shown to interact with PABP while the RdRp of ZYMV was demonstrated to bind PABP (Léonard et al., 2004; Wang et al., 2000). More recently (see section 2.1.3.2 for more details), the presence of PABP into TuMV-derived vesicles was demonstrated, which suggests a role for the host protein in virus replication/translation (Beauchemin and Laliberté, 2007).

2.4.2. eEF1A

eEF1A is probably the most extensively studied factor involved in protein synthesis. eEF1A is a multifunctional protein that has more to do in the cell than bringing GTP and aa-tRNA to the elongating ribosome. Therefore, it is not surprising that viruses have evolved mechanisms to take advantage of eEF1A multifunctional character. The following section provides a general overview of eEF1A functions and its involvement in some virus replication cycle.

2.4.2.1. Structure and function of eEF1A

Crystal structures of eEF1A-GDPNP (which is believed to be a good representation of the EF1A-GTP conformation) and of eEF1A-GDP have been determined in different organisms (Abel et al., 1996; Berchtold et al., 1993; Polekhina et al., 1996; Song et al., 1999). These structures show that eEF1A consists of three domains. The G domain (or domain I) of ~200 residues is responsible for binding either GDP (inactive form) or GTP (active form). The two other domains (domain II and III) contain approximately 100 residues and are both β barrels. All three domains are involved in the binding of tRNAs and eEF1B (Kawashima et al., 1996; LaRiviere et al., 2001; Nissen et al., 1995). eEF1B is needed as a catalyst for the reactivation of eEF1A from the GDP form into the GTP form. The available information reveals that eEF1A undergoes dramatic conformational changes between its active and inactive forms depending on the nucleotide bound (LaRiviere et al., 2001; Nissen et al., 1995; Vitagliano et al., 2001).

eEF1A is one of the most abundant proteins in eukaryotic cells, representing up to 5% of soluble proteins (Browning et al., 1990; Lenstra and Bloemendal, 1983). The

traditional role of eEF1 is to bring the cognate aa-tRNA to the A site of the ribosome in preparation for the next peptide bond to be formed during elongation. It is a multimeric protein consisting of four non-identical subunits (α, β, γ, and δ). eEF1A (the α subunit) catalyzes the binding of aa-tRNA to the A site of the ribosome by a GTP dependent mechanism during protein synthesis. Following the hydrolysis of GTP, aa-tRNA is incorporated into the growing polypeptide and GDP-eEF1A is released from the ribosome. The exchange of bound GDP to free GTP regenerates the capacity of eEF1A to catalyze binding of another aa-tRNA and to participate in further cycles of elongation.

Apart from being involved in protein biosynthesis, eEF1A also participates in other cellular processes. Numerous studies have shown the binding of eEF1A to actin filaments and microtubules *in vitro* and *in vivo* (Bassell and Singer, 1997; Durso and Cyr, 1994; Shiina et al., 1994; Yang et al., 1990). The association of eEF1A to microtubules and actin filaments may play a role in the regulation of protein synthesis: a close spatial association of the translation apparatus with the cytoskeleton enhances protein translation (Bassell et al., 1994; Jansen, 1999; Stapulionis and Deutscher, 1995). eEF1A was also found to be involved in protein degradation mediated through ubiquitin-dependent pathways which role implicates eEF1A in the stability of expressed proteins (Gonen et al., 1996).

2.4.2.2. eEF1A and virus infection

The versatility of the highly abundant and conserved eEF1A protein renders it attractive for recruitment by the virus replication machinery. As early as 1972, host-encoded EF-Tu, elongation factor Ts, and ribosomal protein S1 were shown to be

components of Qβ phage RNA replicase (Blumenthal and Carmichael, 1979). This discovery led us to expect the participation of eEF1A in RNA virus replication in eukaryotic cells. More than three decades after the discovery in Qβ, Das et al. (1998) reported an association between eEF1-αβγ and the RNA polymerase of Vesicular stomatitis virus, a negative-stranded RNA virus. This interaction was shown to be necessary for positive-strand RNA synthesis (Das et al., 1998). eEF1A was also reported to bind with the poliovirus and the bovine viral diarrhea polymerase, and the human immunodeficiency virus type 1 Gag polyprotein (Cimarelli and Luban, 1999; Harris et al., 1994; Johnson et al., 2001). Although the exact function of these interactions remains unknown, a role in viral replication has been speculated for the three of them.

An interaction between eEF1A and the 3' stem-loop (SL) region of West Nile virus (WNV) genomic RNA was recently reported to facilitate viral minus-strand RNA synthesis (Blackwell and Brinton, 1997; Davis et al., 2007). Various mutations were introduced into the WNV 3' SL RNA and the effect of these mutations on virus production, viral RNA translation, and viral RNA synthesis was assessed. All the mutations that altered eEF1A binding had a negative effect on viral minus-stranded synthesis. None of these mutations had an effect on the translation of viral proteins (Davis et al., 2007). These results strongly suggest that eEF1A plays a role in the replication of WNV.

eEF1A has also been reported to bind to the viral genomic RNA of plant viruses including *Brome mosaic virus* (BMV) (Bastin and Hall, 1976), *Turnip yellow mosaic virus* (TYMV) (Joshi et al., 1986) and *Tobacco mosaic virus* (TMV) (Zeenko et al., 2002). In the case of TYMV, the binding of eEF1A to the 3'-terminal TLS of the

positive-stranded RNA acts as both a translational enhancer and a repressor of minus-stranded synthesis. It is proposed that minus strand repression by the binding of eEF1A occurs to help coordinate the competing translation and replication functions of the viral genomic RNA. (Matsuda and Dreher, 2004; Matsuda et al., 2004). eEF1A also binds to both the 3' TLS and the viral polymerase of TMV. These interactions have not been extensively characterized yet but were both suggested to be involved in the replication and translation of TMV (Yamaji et al., 2006; Zeenko et al., 2002).

More recently, a proteome-wide approach using the yeast protein array was used to test ~70% of all yeast proteins for their capacities to bind to the viral RNAs of *Tomato bushy stunt virus* (TBSV) or BMV. eEF1A was among the host proteins identified with both TBSV and BMV RNA probes. The translation factor was further shown to be an integral part of TBSV replicase complex and to interact directly with the viral p33 replication co-factor and the $p92^{pol}$ RdRp proteins (Li et al., 2008; 2009). Moreover, eEF1A has been shown to interact with the yeast Tdh2p, which is also a component of the tomusvirus replicase (Gavin et al., 2006). The multiple interactions of eEF1A with various components of the tombusvirus replicase could be important for eEF1A to regulate the functions of the viral replicase complex.

2.5 Heat shock 70 kDa protein

The heat shock proteins (HSPs) constitute an important set of proteins that were first characterized based on their induction in cells exposed to a sublethal heat shock (Ritossa, 1962). Their up-regulation following various stressors such as environmental stresses, infection, and normal physiological processes has also been well documented

(Mayer, 2005). HSPs are highly conserved and present in both eukaryotic and prokaryotic cells. In eukaryotic cells, HSPs are present in the cytosol, mitochondria, ER, and nucleus (Mayer and Bukau, 2005). In this review, we mainly discuss about the heat shock 70 kDa proteins (Hsp70s) family and its involvement in viral infection.

2.5.1. Structure and function of Hsp70

Members of the Hsp70 family of chaperones are involved in a large variety of processes. Among these processes are the folding of newly synthesized polypeptides, the refolding of stress denatured proteins, the disaggregation of protein aggregates, the degradation of misfolded proteins, the translocation of proteins across membranes, the remodelling of large native protein complexes, and the control of the biological activity and stability of regulatory proteins (Craig et al., 1994; Hartl and Hayer-Hartl, 2002; Mayer and Bukau, 2005). Hsp70s are also involved in signal transduction and regulation of cell cycle and death (Beere and Green, 2001; Helmbrecht and Rensing, 1999). In most species, they are encoded by a highly conserved multigene family whose members encode for multiple Hsp70 isoforms. Some of the isoforms are strictly inducible (only expressed under stress conditions), while some are present in cell under normal growth conditions. The latter are said to be “cognate” or “constitutive” and are referred as heat shock cognate 70 kDa protein (Hsc70) (Palter et al., 1986).

All Hsp70 proteins share the same overall structure, consisting of an N-terminal ATPase domain of 45 kDa and a C-terminal substrate-binding domain of at least 25 kDa. The C-terminal binding domain is further subdivided into a β-sandwich subdomain of 15 kDa and a C-terminal α-helical subdomain. ATP binding and hydrolysis to the ATPase

domain provide the essential energy to drive the conformational changes in the other domain (Flaherty et al., 1990; Flaherty et al., 1994). The ATP cycle of Hsc70 consists of an alteration between the ATP and the ADP stage. When ATP is bound, the lid is open and the peptide binds and is released rapidly, while when ADP is bound, the lid is closed and the peptide are tightly bound to the substrate binding domain (Mayer et al., 2000). Protein folding then proceeds through cycles of substrate binding and release regulated by Hsp70 ATPase activity and through interaction with co-chaperones such as Hsp40, Hop, CHIP or Bag-1 (Hartl and Hayer-Hartl, 2002).

2.5.2. Hsp70 and virus infection

Hsp70 proteins are involved in all phases of the viral life cycle including cell entry, virion disassembly, the transfer of viral genome into the nucleus, virus replication and translation, the maturation of the viral proteins, virus cell-to-cell movement, and inhibition of virus-induced apoptosis (Jindal and Malkovsky, 1994; Mayer, 2005; Sullivan and Pipas, 2001). This review will focus mainly on the involvement of Hsp70 chaperones during plant virus infection: their induction following virus infection, their role in virus movements, and their role in virus replication.

2.5.2.1. Induction of Hsp70 following viral infection

Increase in Hsp70 chaperone levels following viral infection of eukaryotic and prokaryotic cells has been widely observed (Jindal and Malkovsky, 1994). In plants, Hsp70 expression is induced by a wide range of viruses in diverse hosts, including *Pisum sativum*, *N. tabacum*, and *A. thaliana* (Aranda et al., 1996; Escaler et al., 2000; Havelda

and Maule, 2000; Jockusch et al., 2001; Whitham et al., 2003). Hsp70 induction in response to plant viral infection is tightly controlled, spatially and temporally, such that recently infected cells accumulate Hsp70 mRNA and proteins. This phenomenon applies to many plant virus genera including the *Potyvirus*, *Tobravirus*, *Potexvirus*, *Geminivirus*, and *Cucumovirus* (Aranda et al., 1996; Escaler et al., 2000; Havelda and Maule, 2000).

While the detailed mechanisms of Hsp70 induction by plant viruses has not been extensively investigated, recent work by Aparicio and colleagues (2005) revealed that plant viruses do not encode a specific inducer of Hsp70. Instead, the induction occurs indirectly through the production of a large number of virus-specific proteins in the cytosol that are in an unfolded, aggregation-prone state (Aparicio et al., 2005). More evidence for this mode of viral heat shock response induction is also provided by Jockusch and coworkers (2001). Analyzing Hsp70 and Hsp18 mRNA and protein levels in tobacco leaves after infection with TMV or a mutant virus, which encodes a temperature sensitive CP, they found that degree and time of induction paralleled the amount of insoluble viral CP suggesting that the amount of unfolded protein is the inducing agent.

2.5.2.2. Involvement of Hsp70 in virus movement

There are several evidences suggesting that Hsp70 plays a role in plant virus cell-to-cell movement. Members of the *Closteroviridae* (positive-strand RNA viruses) encode an Hsp70-like chaperone. This viral Hsp70 homolog has a function in virion assembly (Napuli et al., 2000; Napuli et al., 2003; Satyanarayana et al., 2000; Satyanarayana et al., 2004) and has been implicated in cell-to-cell movement (Alzhanova et al., 2001;

Peremyslov et al., 1999). The viral Hsp70 binds microtubules and assists in the movement of the viral particle through plasmodesmata (Prokhnevsky et al., 2002; Prokhnevsky et al., 2005). In the unrelated *Tomato spotted wilt virus* (TSWV: a negative-stranded RNA virus of the *Bunyaviridae* family), it is the host chaperone Hsp40, from the DnaJ family (Hsp70 bacterial homologs) that has been proposed to be involved in the TSWV movement (Soellick et al., 2000). The Hsp40 protein interacts with the non-structural movement protein (NSm), a viral protein that shows some typical characteristics of movement proteins such as expression only at early stages of infection, intracellular localization of NSm close to plasmodesmata and nucleocapsid associations in the cytoplasm, and a tubule-forming capacity (Kormelink et al., 1994; Storms et al., 1995).

Potato virus Y (PVY) (a member of the family) also relies on chaperone for movement (Hofius et al., 2007). The CP from PVY was recently found to interact with a subset of DnaJ-like proteins from tobacco designated capsid protein interacting proteins (CPIPs) (Hofius et al., 2007). The CP of potyviruses is required for both cell-to-cell and long distance movement (Dolja et al., 1995). Mutational analyses identified the CP core region, previously shown to be essential for plasmodesmal trafficking, as the domain responsible for the CP- CPIPs interaction (Hofius et al., 2007). Hence, transgenic plants with impaired CPIP showed a reduced accumulation of viral RNA and delayed in virus cell-to-cell movement. Taken together, these results suggest that CPIPs act as important susceptibility factors during PVY infection, possibly by recruiting Hsp70 chaperones for viral cellular movement (Hofius et al., 2007).

2.5.2.3. Role of Hsp70 in viral replication

The involvement of Hsp70 in viral polymerase function was first demonstrated by genetic and biochemical means for bacteriophages (for review see Zylicz et al., 1989). The bacterial Hsp70 system of *E. coli* (DnaK, DnaJ and GrpE) was found to be essential for viral replication (Georgopoulos, 1977; Sunshine, 1977; Yochem et al., 1978). Further studies showed that both Hsp70 bacterial homologs (DnaK, DnaJ) were necessary for conformational changes of the polymerase holoenzyme (Zylicz et al., 1989). Since, Hsp70 has also been demonstrated to be involved in transcriptional regulation and activation of the polymerase functions of many other DNA viruses (for review see Mayer, 2005).

The requirement of HSPs for viral polymerase activity has also been demonstrated for numerous eukaryotic RNA viruses (Brown et al., 2005; Frolova et al., 2006; Hu et al., 2002; Hu et al., 2004; Kampmueller and Miller, 2005; Momose et al., 2002; Oglesbee et al., 1996; Stahl et al., 2007; Watashi et al., 2005). The best examples of the involvement of chaperones in RNA viral polymerases function come from yeast model system. For instance, BMV RNA replication in *Saccharomyces cerevisiae* is markedly inhibited by a mutation in host YDJ1 gene, which encodes the chaperone Ydj1p, an ortholog of Hsp40 (Tomita et al., 2003). For BMV, Ydj1p is essential for negative-strand synthesis. It facilitates assembly of RNA replication complexes by maintenance of viral polymerase cytosolic solubility prior to membrane association (Tomita et al., 2003). The tombusviruses are another model group of plant viruses that can replicate in *S. cerevisiae*. Among the host proteins that have been identified within the tombusviral replication complex, the Hsp70 chaperone appears to play multiple and

essential roles in the virus replication. As it is for Ydj1p, the cytosolic Hsp70 proteins (called Ssa1p and Ssa2p in yeast) have been proposed to be involved in the assembly/activation of tombusvirus replicase complex. The double mutant strain (*ssa1 ssa2*) shows 75% reduction in viral RNA replication, whereas overexpression of double either Ssa1 or Ssa2 stimulates viral RNA replication by threefold (Serva and Nagy, 2006). It is possible that the binding of p33 and $p92^{pol}$ replication proteins to Hsp70 results in shielding the hydrophobic membrane transmembrane domains in the replication proteins, which could prevent their aggregation and promote binding to the Pex19p transport protein. The latter interaction is needed for peroxisomal targeting of the replication proteins (Pathak et al., 2008). It was recently demonstrated that Hsp70 is also involved in controlling the subcellular localization of the viral replication proteins. Using confocal microscopy and cellular fractionation experiments, it was demonstrated that the localization of the viral replication proteins (p33 and $p92^{pol}$) change to the cytosol in the mutant cells from the peroximal membranes in the wildtype cells. Furthermore, *in vitro* membrane insertion assay showed that the Hsp70 promotes the integration of the viral replication proteins into subcellular membranes. This step seems critical for the assembly of the replication complex. Taken together, these data suggest a role for Hsp70 proteins in the early steps of tombusvirus replication including subcellular localization of the viral replication proteins, membrane insertion of the replication proteins, and the assembly of the viral replicase complex (Wang et al., 2009a; 2009b). Finally, recent data indicate that Hsp70 remains associated with the viral replicase even after the insertion of the replication proteins into the membranes, suggesting an additional function for Hsp70 during tombusvirus replication (Wang et al., 2009b).

In plant, the Hsp70 association with viral replication complex has only been showed for *Tomato mosaic virus* (ToMV), a positive-strand RNA virus part of the *Tobamovirus* family (Nishikiori et al., 2006). Hsp70 and eEF1A, as well as RdRp activity, were showed to co-purify with the viral replicase from membrane extracts of ToMV-infected protoplasts (Nishikiori et al., 2006).

2.6 Plant esterases/lipases

Lipases and esterases are ubiquitous hydrolytic enzymes that catalyze the hydrolysis of a broad range of compounds containing an ester linkage. Although they hydrolyze vastly different substrates, substantial sequence similarity can be recognized between these enzymes. Many lipase and esterase sequences possess the pentapeptide Gly-Xaa-Ser-Xaa-Gly (GxSxG) motif with the active site serine situated near the center of the conserved sequence. However, not all lipolytic enzymes have this common motif; a subfamily of hydrolytic/lipolytic enzymes show a different motif, Gly-Asp-Ser-(Leu) [GDS(L)] with the active site serine located near the N-terminus (Upton and Buckley, 1995). These so-called GDSL-lipases and esterases will be the focus of this review.

2.6.1. Structure and function of GDSL-lipases and esterases

As lipolytic enzymes, GDSL-lipases are important superfamily of lipases, and active in hydrolysis and synthesis of abundant ester compounds. They have a GDSL-motif with the flexible active site serine located near the N-terminus (Upton and Buckley, 1995), five blocks (block I-V) containing Ser-Asp-His triad and oxyanion hole residues

(Ser, Gly and Asn) (Molgaard et al., 2000). Most GDSL-lipases possess a signal peptide at their N terminus, which targets them for secretion to the cell wall (Ling, 2008). GDSL-lipases are distributed broadly throughout microorganisms, where much progress on their structures, functions and physiological roles has been made. Many bacterial GDSL-lipase genes have been cloned and characterized, and presently the crystal structures of GDSL-lipases from *E. coli* and *Pseudomonas fluorescens* are available (Kim et al., 1993; Li et al., 2000; Lo et al., 2000). GDSL-lipase is made up of several β-strands and α-helices arranged in alternate order, and the substrate-binding pocket between the central β-strand and long α-helix appears to be highly flexible. The flexible pocket brings the conformational changes, so that the active sites are exposed to the solvent and easily bind to substrates, conferring multi-functional character of GDSL-lipases (Derewanda, 1994).

GDSL-lipases are also found in plant species; several candidates from *A. thaliana*, *Rauvolfia serpentine, Medicago sativa, Hevea brasiliensis, Brassica napus,* and *Alopecurus myosuroides* have been isolated, cloned and characterized (Arif et al., 2004; Brick et al., 1995; Cummins and Edwards, 2004; Ling et al., 2006; Oh et al., 2005; Pringle and Dickstein, 2004; Ruppert et al., 2005). GDSL-lipases are involved in many physiological processes. Firstly, these lipases play an important role in the regulation of plant development and morphogenesis. Mayfield et al. (2001) reported six extracellular lipases (EXL1-6) isolated from *A. thaliana* pollen coat. Anther-specific proline-rich protein genes (APGs) have been cloned and sequenced from *A. thaliana* and *B. napus* (Brick et al., 1995). Another GDSL-lipase enzyme from post-germinated sunflower seeds was isolated, purified, and shown to have fatty acyl-ester hydrolase activity (Teissere et al., 1995). More recently, the lipase gene BnLIP2, coding for a GDSL-lipase, from *B.*

napus was isolated from germinated and mature seedling. BnLIPP2 may play multiple roles in plant physiological activities such as germination, flowering and morphogenesis (Ling et al., 2006). Secondly, GDSL-lipases have been found to be involved in the synthesis of secondary metabolites. The acetylajmalan esterase (AAE) of *R. serpentine* plays an essential role in the late stage of ajmaline biosynthesis. Based on its primary structure, AAE is a member of the GDSL-lipase superfamily. Using a plant-virus expression system, AAE has been functionally overexpressed in leaves of *N. benthamiana*, and its enzymatic activity in *Nicotiana* tissues was identified (Ruppert et al., 2005).

Additionally, GDSL-lipases appear to be involved in plant abiotic/biotic stress responses. The *A. thaliana* GDSL-lipase, GLIP1, possesses lipase and anti-microbial activities that disrupted fungal spore integrity. In association with ethylene signalling it might play a key role in plant resistance to *Alternaria brassicicola* (Oh et al., 2005). Another GDSL-lipase, the early nodule specific protein homolog (Hev b 13), was isolated and characterized from *H. brasiliensis* latex (Arif et al., 2004). It was proposed by the authors that the lipase and esterase activities of the purified enzyme might be involved in plant defence. Recently, the expression of the *Capsicum annuum GDSL-lipase 1* (CaGL1) gene was showed to be induced by methyl acid (MeJA) in hot pepper plants. CaGL1 transcripts were also increased in response to mechanical wounding. These results indicate that CaGL1 may be involved in signalling pathway of MeJA and/or the wound response (Kim et al., 2008). Finally, overexpression of AtLTL1 induced by salicylic acid (SA) treatment, encoding a GDSL-motif lipase, increased salt tolerance in yeast and in *Arabidopsis* (Naranjo et al., 2006).

2.6.2. Lipases and virus infection

The potential role of lipases in plant viral infection was first discovered in tobacco leaves reacting hypersensitively to TMV (Dhondt et al., 2000). The authors demonstrated that a strong increase in soluble phospholipase A2 (PLA2) activity occurs in these tobacco leaves at the onset of necrotic lesion appearance. This rapid PLA2 activation occurred before the accumulation of 12-oxophytodienoic and jasmonic acids, two fatty acid-derived defense signals. The induction of PLA2 was suggested to provide precursors for oxylipin synthesis during the hypersensitive response to pathogens (Dhondt et al., 2000). Since then, further involvement of lipases in plant defence against virus was highlighted by the study of Kumar and Klessig (2003). The SA-binding protein SABP2 is required for basal resistance to TMV in a TMV-resistant tobacco variety. Silencing of SABP2 expression suppresses local resistance to TMV (Kumar and Klessig, 2003). SABP2 exhibits homology to acyl-hydrolases, and recombinant SABP2 was shown to hydrolyze synthetic lipid substrates *in vitro*. SA binding stimulates the SABP2 acyl-hydrolase activity, suggesting that SABP2 is required subsequent to SA accumulation in plant defences. (Kumar and Klessig, 2003).

Accumulating evidences that lipases play a role in virus infection are also coming from studies analyzing plant gene expression following viral infection. Diverse RNA viruses induce expression of different type of lipases in susceptible *A. thaliana* plants. Microarray analyses between five positive-strand RNA viruses (including TuMV) and *Arabidopsis* showed that the induction of lipases genes upon infection is widespread in plants (Whitham et al., 2003; Yang et al., 2007). Spatial analyses of *A. thaliana* gene expression have also demonstrated that the degree to which TuMV-responsive genes

(including lipases) were up- or downregulated correlated with the amount of virus accumulation (Yang et al., 2007).

The role of GDSL-lipases in plant viral infection is highlighted by two different studies. Firstly, study of *A. thaliana* resistome in response to *Cucumber mosaic virus* using whole genome microarray has revealed induction of lipase genes, including two GDSL-lipases, following infection. Secondly, in the pathosystem of TuMV and *A. thaliana*, two types of symptoms can be observed (mosaic symptom and veinal necrosis) depending of the *Arabidopsis* ecotype. The Col-0 ecotype develops mosaic symptoms after infection while the Ler ecotype develops veinal necrosis. The Ler phenotype is controlled by a single dominant gene *TuNI* (TuMV necrosis inducer). Fine genetic mapping of *TuNI* locus has revealed the presence three genes predicted to encode GDSL-lipases (Kaneko et al., 2004). These lipases may be the necrosis inducer since lipases are required for the induction of defence responses mediated by SA (Falk et al., 1999; Jirage et al., 1999; Kumar and Klessig, 2003).

CONNECTING STATEMENT BETWEEN CHAPTER II AND III

As described in chapter II, viruses depend on a wide range of host-virus protein-protein interactions to complete the various steps of their replication cycle. For potyviruses, we still have limited knowledge on the plant-virus protein interactions required for their multiplication. In this chapter, we used the preexisting NTAPi-RdRp *A. thaliana* transgenic line to investigate the potential interaction between the plant eEF1A and TuMV RNA polymerase. eEF1A was identified as a host interactor of TuMV RdRp. As the potyviral protein VPg-Pro is known to interact with RdRp, the possibility of a tripartite complex formation between RdRp, VPg-Pro and eEF1A was also investigated. This chapter also describes the construction an infectious TuMV cDNA that additionally codes for green fluorescent protein (GFP) attached to the viral 6K protein. Confocal microscopy experiments using this infectious clone were carried to characterize the 6K-induced vesicles. The inclusion of one viral and four plant proteins into these vesicles was demonstrated. These finding strongly suggest that the vesicles induced by TuMV 6K protein house the virus replication complex.

The results of this section are the subject of a manuscript that has been published in the journal Virology (vol. 377, p. 216-225). I have designed the experimental set-up, conducted almost all of the experiments, wrote the manuscript and prepared all the figures. Sophie Cotton's contribution for this chapter represents 10% and includes the experiments that are related to the immunofluorescence labeling and the construction of pGEXVPgPro24-GST pGEXPro-GST, and pGEXVPg-GST vectors. She also performed the ELISA-based binding assays relatively to the interaction between the VPg-Pro domains and eEF1A. Isabelle Mathieu (Institut national de la recherche scientifique

(INRS), Quebec, Cananda) constructed the binary fluorescent pCambia/6K-VPg-Pro-mCherry vector. Dr. P. J. Dufresne provided the NTAPi-GFP and RdRp-NTAPi transgenic *A. thaliana* plants and the pET28(a)-RdRp vector. Chantal Beauchemin (INRS, Quebec, Canada) provided many of the binary fluorescent constructs for confocal microscopy. Christine Ide assisted in cloning of pGreen/GFP-eEF1A and pGreen/DsRed-eEF1A constructs. Professor Marc G. Fortin provided funding. Jean-François Laliberté provided supervision of the work and contributed to the overall design of the manuscript.

CHAPTER III

Eukaryotic elongation factor 1A interacts with *Turnip mosaic virus* RNA-dependent RNA polymerase and VPg-Pro in virus-induced vesicles

K. Thivierge [1], S. Cotton [1], P. J. Dufresne [1], I. Mathieu [2], C. Beauchemin [2] C. Ide [1], M. G. Fortin [3], J.-F. Laliberté [2]

[1] Department of Plant Science, McGill University, 21,111 Lakeshore, Ste-Anne-de-Bellevue, Quebec, Canada H9X 3V9. [2] Institut national de la recherche scientifique, Institut Armand-Frappier, 531 Boulevard des Prairies, Laval, Quebec, Canada H7V 1B7. [3]Agriculture and Agri-Food Canada, 930 Carling Avenue, Ottawa, Ontario, Canada K1A 0C7.

3.1. Abstract

Eukaryotic elongation factor 1-alpha (eEF1A) was identified as an interactor of *Turnip mosaic virus* (TuMV) RNA-dependent RNA polymerase (RdRp) and VPg-protease (VPg-Pro) using tandem affinity purification (TAP) and/or *in vitro* assays. Subcellular fractionation experiments revealed that the level of eEF1A substantially increased in membrane fractions upon TuMV infection. Replication of TuMV occurs in cytoplasmic membrane vesicles, which are induced by 6K-VPg-Pro. Confocal microscopy indicated that eEF1A was included in these vesicles. To confirm that eEF1A was found in replication vesicles, we constructed an infectious recombinant TuMV that contains an additional copy of the 6K protein fused to the green fluorescent protein (GFP). In cells infected with this recombinant TuMV, fluorescence emitted by 6KGFP was associated with cytoplasmic membrane vesicles that contained VPg-Pro, the eukaryotic initiation factor (iso) 4E, the poly(A)-binding protein, the heat shock cognate 70-3 protein, and eEF1A. These results suggest that TuMV-induced membrane vesicles host at least three plant translation factors in addition to the viral replication proteins.

3.2. Introduction

A body of data demonstrates the potential role for components of the host translation machinery in virus replication. It has been shown that host translation elongation factors (EFs) are involved in the multiplication of a number of RNA viruses infecting animals, plants and bacteria (Lai, 1998). The participation of cellular EFs in viral amplification seems to follow two mechanisms. In some cases, eukaryotic

elongation translation factors interact directly with the viral RNA. Eukaryotic elongation factor 1A (eEF1A) has been shown to interact with the genomic RNA of different plant and animal viruses and was suggested to play a role in viral replication and/or translation (Bastin and Hall, 1976; Blackwell and Brinton, 1997; De Nova-Ocampo et al., 2002; Joshi et al., 1986; Zeenko et al., 2002). In other cases, the EFs bind directly to the viral RdRp. The RdRp is the core polypeptide that catalyzes the synthesis of RNA chains from both negative- and positive-strand templates of viral RNA. A classical example of this type of interactions is the presence of cellular elongation factors thermo unstable (EF-Tu) and Ts (EF-Ts) in the bacteriophage Qβ replicase complex. Removal of these host factors results in the loss of Qβ replicase activity (Blumenthal and Carmichael, 1979). The interactions between eEF1A and RdRp have also been demonstrated for Vesicular stomatitis virus (VSV) (Das et al., 1998), Bovine viral diarrhea virus (BVDV) (Johnson, 2001) and poliovirus (PV) (Harris et al., 1994). These two modes of interactions are not mutually exclusive. In fact, a direct *in vivo* interaction between the RdRp of *Tobacco mosaic virus* (TMV) and host eEF1A was recently reported (Yamaji et al., 2006) after the demonstration that the same EF was interacting with the viral genome (Zeenko et al., 2002).

TuMV belongs to the genus *Potyvirus*. Potyviruses have a positive-strand RNA genome, which is ~10 kb in length. It is polyadenylated at its 3' end and covalently linked at its 5' terminus to a viral genome-linked protein (VPg) (Nicolas and Laliberté, 1992). The genome encodes a single polyprotein that is processed by three viral proteinases into ten mature peptides. The C-terminal portion of this polyprotein yields two non-structural proteins that are required for genome replication: 6K-VPg-Pro precursor polyprotein and

RdRp (Hong and Hunt, 1996). All characterized positive-stranded RNA viruses assemble their RNA replication complexes on intracellular membranes, usually in association with membrane vesicle formation. The recruitment of the RdRp to membranes and its interaction with viral and host factors are critical for the efficiency, specificity and regulation of viral replication (Nagy, 2008). Recent results have revealed that TuMV 6K-VPg-Pro polyprotein induces the formation of large cytoplasmic vesicular compartments derived from the endoplasmic reticulum (ER) (Beauchemin et al., 2007). These vesicles are very similar in size and origin to those induced by the 6K domain of the 6K-VPg-Pro during *Tobacco etch virus* infection (Schaad et al., 1997a).

Positive-strand RNA virus genomes are templates for both translation and replication, leading to interactions between host translation factors and RNA replication components at multiple levels. In the case of TuMV, components of both processes have been found within 6K-VPg-Pro-induced vesicles. First, the RdRp is directed into the vesicles through its interaction with 6K-VPg-Pro (Dufresne et al., 2008a). This interaction suggests that the vesicles induced by 6K-VPg-Pro house the viral replication complex (VRC). Second, the interaction of 6K-VPg-Pro with translation factors poly(A)-binding protein (PABP) and eukaryotic initiation factor (iso) 4E [eIF(iso)4E] within virus-induced vesicles points to the hypothesis that the protein synthesis machinery is trapped during the formation of these vesicles (Beauchemin et al., 2007; Beauchemin and Laliberté, 2007). However, it is not known if viral translation occurs in these vesicles. The identification of host factors enclosed in these virus-induced vesicles is of considerable interest as it sheds light on virus-cell interactions that facilitate infection and reveals the mechanistic components required for RNA replication and translation.

In this study, we investigated eEF1A as a potential host interactor of TuMV RdRp. We found that the translation factor not only interacted with the viral RdRp but also with VPg-Pro. We further observed the presence of eEF1A in vesicles induced by 6K-VPg-Pro during TuMV infection. The inclusion of eIF(iso)4E, PABP, and the heat shock cognate 70-3 (Hsc70-3) into these vesicles was also demonstrated. These data point to the hypothesis that the vesicles induced by 6K-VPg-Pro house the virus replication complex and that at least three translation factors are included in these vesicles.

3.3. Materials and Methods

3.3.1. Plant material and TAP purification procedure

The generation and growth of NTAPi-GFP and RdRp-NTAPi transgenic *A. thaliana* and TAP tag purifications were conducted as previously described (Dufresne et al., 2008a).

3.3.2. Recombinant protein expression in *E. coli* and purification

Recombinant His-tailed RdRp was purified as previously described (Dufresne et al., 2008a). pET-EF1A-his encodes a His/T7-tailed eEF1A of *A. thaliana* and was produced as follows. eEF1A sequence was amplified using *Pfu* Turbo polymerase (Stratagene, Kirkland, WA, USA) from validated SSP gold standard full length open reading frame (ORF) clone U12802 (Yamada et al., 2003) using forward EF1AF-*Bam*HI and reverse EF1AR-*Not*I primers (Table 3.1). The amplified fragment was digested with *Bam*HI and *Not*I and cloned into similarly digested pET28a (Novagen Gibbstown, NJ,

USA). The recombinant plasmid was introduced into *E. coli* BL21 (DE3). Cells (500 ml) containing pET-EF1A-his were grown at 37°C to an OD_{600} of 0.6 and protein expression was induced with 1 mM isopropyl-β-D-galactopyranoside (IPTG) for three hrs. Bacterial cells were collected by centrifugation and resuspended in buffer A (500 mM NaCl, 160 mM Tris-HCl, pH 8). The cells were disrupted by sonication and centrifuged at 39,000 × *g* for 20 min. The insoluble proteins were resuspended in 20 ml of buffer A containing 6 M guanidine, 5 mM β-mercaptoethanol and 0.1 % Tween-20. The solubilized proteins were recovered by ultracentrifugation at 100,000 × *g* and incubated with 2.5 ml of Talon Metal Affinity Resin (Clontech, Mountain View, CA, USA). The resin was washed with buffer A containing 6 M guanidine and bound proteins were eluted using the same buffer but containing 250 mM imidazole. The purified proteins were dialyzed against 20 mM NaCl, 10 mM Tris-HCl pH 8.0. Protein concentration was measured using a Bradford assay (Bio-Rad, Mississauga, On, Canada) with bovine serum albumin (BSA) as standard.

The pGEXVPgPro24-glutathione-S-transferase (GST) encodes an N-terminus GST-fused mutant form of TuMV VPg-Pro and was created by replacing the glutamate (Glu) 192 of VPg-Pro by histidine (His). This mutation abolishes the cleavage site between the VPg and the Pro domains (Laliberté et al., 1992). The mutation was introduced by chimeric polymerase chain reaction (PCR) using full length TuMV cDNA clone p35Tunos as a template (Sanchez et al., 1998). Two individual PCRs were conducted before the chimeric reaction using primers: 1) VPgPro-*Eco*RI F and VPgPro mutation R (Table 3.1) and 2) VPgPro-*Not*I R and VPgPro mutation F (Table 3.1). Then, the two PCR products were diluted 1:1000 and mixed for a second run of PCR using the

VPgPro-*Eco*RI F and VPgPro-*Not*I R primers. The final PCR product was digested with *Eco*RI and *Not*I and ligated into similarly restricted pGEX6P1vector (Amersham Biosciences, Baie d'Urfé, Qc, Canada). The final construct was sequenced to confirm the presence of the mutation. For construction of pGEXPro-GST, the Pro domain of VPg-Pro was amplified from p35Tunos by PCR using primers Pro pGEX6P1-*Eco*RI F and VPgPro-*Not*I R (Table 3.1). The PCR product was introduced into pGEX6P1 as described above. The pGEXPro-GST codes for the N-terminus GST fusion of the Pro domain of TuMV VPg-Pro. The construction of the vector pGEXVPg-GST coding for the N-terminus GST–VPg fusion protein was previously described (Cotton et al., 2006). The recombinant plasmids (pGEXVPgPro24-GST, pGEXPro-GST, and pGEXVPg-GST) were introduced in *E. coli* BL21. BL21 *E. coli* cells containing recombinant plasmids were cultured at 37 °C to an OD_{600} of 0.6 and protein expression was induced with 1 mM IPTG for 3 hrs at 30 °C. Bacterial cells were centrifuged and resuspended in buffer B (4.3 mM Na_2HPO_4, 1.47 mM KH_2PO_4, 137 mM NaCl, 2.7 mM KCl, pH 7.3). The cells were disrupted by sonication and the lysate was centrifuged at 39,000 × *g* for 20 min. The supernatant was used for affinity purification of GST–VPgPro24, GST–VPg or GST–Pro. The protein extract was added to GST-Bind resin (Novagen) according to the manufacturer's protocol and incubated at 4°C for 1 h. Beads were washed three times with buffer B and collected by centrifugation for five min at 500 × *g*. The fusion proteins were eluted from the resin in a buffer containing 10 mM reduced glutathione and 50 mM Tris–HCl pH 8.0. Protein concentration was measured using a Bradford assay using BSA as standard. GST controls (the pGEX-6P1 vector without insert) was expressed and purified using the same conditions.

3.3.3. ELISA-based binding assay

A. thaliana eEF1A protein (100 µl of protein at 15 ng μl^{-1} in PBS buffer) or metal chelation-purified *E. coli* lysate containing pET28(a) was adsorbed to wells of a polystyrene plate (Costar, San Diego, CA, USA) by overnight incubation at 4°C and wells were blocked with 5% milk PBS solution for two hours at room temperature. Appropriate proteins were diluted in PBS with 1% milk and 0.1% Tween 20 and incubated for 1.5 h at 4°C in the previously coated wells. Detection of retained protein was achieved with a rabbit anti-GST (Invitrogen, Carlsbad, CA, USA) or anti-RdRp (Dufresne et al., 2008a) sera, followed by a horseradish peroxidase-coupled goat anti-rabbit immunoglobulin serum (Pierce Rockford, IL, USA). Wells were washed four times with PBS supplemented with 0.05% Tween 20 between incubations. Enzymatic reactions were performed in 100 µl of o-phenylenediamine dihydrochloride (OPD) citrate buffer (50 mM citric acid, 100 mM sodium phosphate dibasic, pH 5.0, 0.5 mg/ml OPD and 0.1% hydrogen peroxide) and stopped with a solution of 3 M H_2SO_4. Absorbance was measured at 492 nm. Standard error of the mean (SEM) was calculated for three biological replicates from a minimum of three technical replicates.

3.3.4. Cellular fractionation

Three-week-old *N. benthamiana* plants were agroinfiltrated with pCambiaTunos/6KGFP or P19 vector. After infiltration, the plants were kept for 4 days in a growth chamber before collection of leaves. Leaf tissue (1 g) was ground in 4 ml of homogenization buffer [50 mM Tris-HCl, pH 7.6, 15 mM $MgCl_2$, 10 mM KCl, 20 % glycerol, 0.1 % β-mercaptoethanol, plant proteinase inhibitor (Sigma-Aldrich, St-Louis,

MO, USA)]. Cell wall, nuclei, chloroplasts and debris were removed by two centrifugations at 3000 × *g* at 4°C for 10 min. The supernatant (S3) was centrifuged at 30 000 × *g* at 4°C for 30 min, resulting in soluble (S30) and crude membrane (P30) fractions. The P30 pellet was resuspended in the same volume as the supernatant in homogenization buffer. Twenty microliters of total, soluble, and membrane fractions were collected, diluted in 1:5 in protein dissociation buffer, and subjected to immunoblot analysis following sodium dodecyl sulfate-polyacrylamide electrophoresis (SDS-PAGE). The antigen-antibody complexes were visualized using a horseradish peroxidase coupled goat anti-rabbit IgG under standard conditions. Complexes were visualized with Super Signal West Pico substrate (Pierce).

3.3.5. Plasmid construction for expression in plants

Plasmids for co-localization were constructed as follows. The sequence of eEF1A was amplified with *Pfu* Turbo polymerase (Stratagene) from full length ORF clone U12802 (Yamada et al., 2003) using primers eEF1F EGFP-*Xba*I and eEF1R EGFP-*Bam*HI (Table 3.1) and inserted into the *Xba*I/*Bam*HI sites of pGreen/GFP or pGreen/DsRed2. The resulting plasmids were identified as pGreen/eEF1A-GFP and pGreen/eEF1A-DsRed2. The sequence of lipase protein (GenBank accession no. **AY065046**) was amplified with *Pfu* Turbo polymerase (Stratagene) from full length ORF clone pda02401 (RIKEN) using primers LipaseF mCherry-*Xba*I and LipaseR mCherry-*Bam*HI (Table 3.1) and inserted into the *Xba*I/*Bam*HI sites of pCambia/mCherry. TuMV P3 sequence was amplified from p35Tunos (Sanchez et al., 1998) with primers P3F mCherry-*Hind*III and P3R mCherry-*Hind*III (Table 3.1). The amplified fragment was

digested with *Hind*III and cloned into similarly digested pCambia/mCherry. The resulting plasmids were identified as pCambia/lipase-mCherry and pCambia/P3-mCherry, respectively. The plasmids pGreen/GFP, pGreen/ER-GFP, pGreen/DsRed2, pGreen/6K-Vpg-Pro-GFP, pGreen/6K-VPg-Pro-ct, pCambia/PABP-mCherry, pCambia/6K-VPg-Pro-mCherry, pGreen/Hsc70-3-DsRed2, pCambia/eIF(iso)4E-DsRed, and pCambia/GFP-RdRp have previously been described (Beauchemin et al., 2007; Beauchemin and Laliberté, 2007, Dufresne et al., 2008a). All plasmid constructs were verified by sequencing.

The plasmid pCambiaTunos/6KGFP contains an infectious TuMV cDNA that contained an additional copy of the 6K protein fused to the GFP and was constructed as follow. A fragment containing 6K and a part of CI sequence was amplified with primers JFCI and FT6K-*Bam*HI (Table 3.1) from pSK/TuMV ClaI (Léonard et al., 2000) and introduced into pGreen/GFP (Beauchemin et al., 2007) using *Xba*I-*Bam*HI restriction sites. 6KGFP was then amplified using primers JF6K-*Sac*II and FTGFP-*Sac*II (Table 3.1) and introduced into *Sac*II site of p35Tunos/*Sac*II plasmid (Beauchemin et al., 2005). 35S-TuMV-tunos was then inserted into the *Sma*1-*Apa*1 restriction sites of pCambia 0390 binary vector.

3.3.6. Agroinfiltration and confocal microscopy

Binary vectors containing genes for fluorescent fusion proteins were transformed into *Agrobacterium tumefaciens* AGL1 by electroporation. Transformed cells confirmed to contain the binary vector were used for agroinfiltration assays. Bacterial cultures grown overnight were centrifuged, and the pellet was resuspended in water supplemented

with 10 mM $MgCl_2$ and 150 mM acetosyringone. The resulting preparation was used to agroinfiltrate leaves from 3-week-old *N. benthamiana* plants. To allow optimal expression of the fusion proteins, the P19 protein of *Tomato bushy stunt virus* was coexpressed in the agroinfiltrated plant cells to prevent induction of posttranscriptional gene silencing (Qu and Morris, 2002). After infiltration, the plants were kept for 2 to 4 days in a growth chamber before observation. Fluorescence was visualized 2 to 4 days post-infiltration by confocal microscopy, which was carried as previously described (Beauchemin and Laliberté, 2007). The data for green and red channels were collected simultaneously. Images were collected with a charge-coupled-device camera and treated with Adobe Photoshop or Image J (http://rsb.info.nih.gov/ij/) software.

3.3.7. Protoplast isolation and immunofluorescence

N. benthamiana leaves agroinfiltrated with pCambiaTunos/6KGFP were collected at 4 days post-inoculation and sliced in 1 mm wide stripes and incubated in an enzyme solution (1.5 % cellulose R10, 0,2 % macerozyme R10, 0,5 M mannitol, 20 mM KCl, 20 mM MES pH 5,7, 10 mM $CaCl_2$, 0,1 % BSA) for 3 hrs in the dark under vacuum. The protoplast solution was filtered through a 45 µm nylon filter and centrifuged for 4 min at 100 × *g*. The supernatant was removed. Protoplasts were incubated for 15 min at room temperature with one volume of fixing solution (4 % formaldehyde, 0,25 M mannitol, 50 mM sodium phosphate in PBS). They were centrifuged and resuspended for 30 min with 2 volumes of fixing solution at room temperature. Protoplasts were washed three times with PBS for 10 min. Then, they were put on cover slide pretreated with 0,1 % poly-L-lysine. They were treated with Triton X-100 0,5 % in PBS for 10 min and incubated for

20 min in a blocking solution of 5 % BSA in PBS. They were incubated for 1 h with the first antibody, washed three times with PBS for 10 min, incubated for another hour with the secondary antibody conjugated to Alexa Fluor 568 (Invitrogen) and finally washed three times with PBS for 10 min. Pro-long Gold Antifade was used to prepare the slides. Confocal microscope visualization was carried as previously described (Beauchemin and Laliberté, 2007). The data for green and red channels were collected simultaneously. Images were collected with a charge-coupled-device camera and treated with Adobe Photoshop or Image J (http://rsb.info.nih.gov/ij/) software.

3.4. Results

3.4.1. Identification of *Arabidopsis thaliana* eEF1A as TuMV RdRp interactor

We took advantage of our existing *A. thaliana* NTAPi-RdRp and NTAPi-GFP T_4 lines to investigate eEF1A as a potential cellular interactor of the RdRp. The NTAPi-RdRp line expresses TuMV RdRp with a TAP-tag fused at its N-terminal end while the NTAPi-GFP line expresses a TAP-tagged GFP protein (Dufresne et al., 2008a). Protein extracts from 3-week-old RdRp-NTAPi *A. thaliana* plants were incubated with IgG-coated beads and absorbed proteins were then released by protease cleavage of the Protein A moiety. A second affinity purification step was performed by incubating the protease-released proteins with calmodulin-coated resin in presence of calcium and elution was performed using an EGTA-containing buffer. As a control for the TAP procedure, extracts from NTAPi-GFP were subjected to the same purification strategy as RdRp-NTAPi transgenic plants. The eluted material was separated by SDS-PAGE and

analyzed by immunoblotting using anti-calmodulin-binding protein (CBP) and anti-eEF1A antibodies. RdRp and GFP TAP fusions were detected at the expected molecular masses of ~65 and 32 kDa respectively following IgG-agarose and CAM–agarose chromatography (Fig. 3.1). We then investigated the presence of eEF1A in the NTAPi-RdRp extract. Immunoblotting using a rabbit serum directed against eEF1A confirmed the co-purification of eEF1A with the viral protein in the NTAPi-RdRp but not in the NTAPi-GFP extract (Fig.3.1). This data suggests an interaction between the TuMV RdRp and eEF1A.

3.4.2. *In vitro* interaction between TuMV RdRP and *A. thaliana* eEF1A

The co-purification of eEF1A with TuMV RdRp may be the result of a direct interaction between the two proteins or may occur indirectly through a complex formation involving another protein. An enzyme linked immunosorbent assay (ELISA)-based binding assay was used to show the direct interaction of eEF1A with RdRp. Recombinant His-tagged RdRp and His-tagged eEF1A from *A. thaliana* were purified from *Escherichia coli* by metal chelating chromatography. ELISA plate wells were coated with His-tagged eEF1A and were incubated with increasing concentrations of His-tagged RdRp. Complex retention was detected using an anti-RdRp rabbit serum. Figure 3.2 shows a saturation binding curve of eEF1A with RdRp. Control experiments showed that no interaction was detected when His-tagged eEF1A was replaced with metal chelating chromatography purified *E. coli* lysate containing pET-28a, which is the vector that was used for eIF1A expression. This experiment indicates that the co-purification of eEF1A in NTAPi-RdRp transgenic plants results from a direct protein-protein interaction.

3.4.3. Membrane association of eEF1A

We have previously shown the redistribution of PABP2 and Hsc70-3 to membrane-associated fractions during TuMV infection (Beauchemin and Laliberté, 2007; Dufresne et al., 2008a). To determine whether eEF1A could be modulated in a similar way, we examined the distribution of the translation factor among soluble and membrane-enriched fractions in *Nicotiana benthamiana*, a natural host of TuMV. Three-week-old *N. benthamiana* plants were agroinfiltrated with pCambiaTunos/6KGFP. This plasmid contains an infectious TuMV cDNA that contains an additional gene that codes for the 6K protein linked to GFP (see complete description of the vector below). Infiltrated leaves were collected four days later and used for subcellular fractionation assays. Total, soluble, and membrane-associated proteins were separated by SDS-PAGE and analyzed by immunoblot experiments using an anti-eEF1A rabbit serum. eEF1A was found mainly in the soluble fraction of control P19-agroinfiltrated plants, although a small quantity was observed in the membrane-enriched fraction (Fig. 3.3). However, in TuMV-agroinfiltrated plants, a substantially higher level of eEF1A was found in the membrane-enriched fractions when compared to the control plants.

To investigate further the membrane association of the elongation factor, eEF1A was fused to the fluorescent protein GFP or DsRed2 (Figs. 3.4B and 3.4C, respectively) and expressed transiently in *N. benthamiana* using agroinfiltration. Expression of the fluorescent fusions was assessed by immunoblot analysis using a rabbit serum raised against eEF1A. In both cases (i.e. eEF1A-DsRed2 and eEF1A-GFP), a signal corresponding to the expected molecular mass of the analyzed protein was observed, indicating that full length proteins had been expressed (data not shown).

Fluorescence was visualized 2 to 5 days post-infiltration by confocal microscopy. No notable differences in cellular localization were observed during this time period. Fluorescence was generally observed in 40 to 60% of the cells in the infiltrated area. GFP and DsRed2 markers with or without ER-targeting signals were co-expressed with the fluorescent eEF1A proteins to facilitate the cellular localization of the translation factor. The coexpresion of GFP and eEF1A-DsRed2 clearly showed that the translation factor was mainly a soluble cytoplasmic protein, and was excluded from the nucleus (Fig. 3.5A). A similar pattern was observed when eEF1A was fused to GFP and coexpressed with DsRed (data not shown). When ER-targeted GFP (ER-GFP) was coexpressed with the eEF1A-DsRed2 fusion, only partial co-localization was noted (Fig. 3.5B). These results are in agreement with the cellular fractionation data, in which eEF1A was detected mostly in the soluble fraction and that a small proportion of the eEF1A was membrane-associated.

The presence of TuMV RdRp into cytoplasmic vesicles results from its association with 6K-VPg-Pro (Dufresne et al., 2008a). We consequently investigated whether expression of a non-cleavable form of 6K-VPg-Pro (Beauchemin et al., 2007; Dufresne et al., 2008a) can alter the subcellular localization of eEF1A. We previously showed that expression of 6K-VPg-Pro-ct induced the formation of cytoplasmic vesicles (Beauchemin et al., 2007), within which RdRp was found (Dufresne et al., 2008a). Figure 3.5C shows that RdRp and eEF1A localized within the vesicles induced by 6K-VPg-Pro-ct. We also found that eEF1A could be retargeted to the vesicles induced by 6K-VPg-Pro-GFP in the absence of RdRp (Fig. 3.5D). A similar pattern was observed when eEF1A was fused to GFP and coexpressed with 6K-VPg-Pro fused to the fluorescent

protein mCherry (6K-VPg-Pro-mCherry) (data not shown). These data suggest that the elongation factor can be internalized within 6K-VPg-Pro -induced vesicles and that a tripartite complex between eEF1A, 6K-VPg-Pro and RdRp is likely.

3.4.4. *In vitro* interaction between VPg-Pro, RdRP and eEF1A

The presence of the translation elongation factor into the vesicles induced by 6K-VPg-Pro raised the possibility of a direct interaction between the two proteins. To investigate this possibility, ELISA plate wells were coated with His-tagged eEF1A and were incubated with increasing concentrations of GST-tagged VPg-Pro. Complex retention was detected using a polyclonal anti-GST antibody. Figure 3.6A shows a saturation binding curve of eEF1A with VPg-Pro. Control experiments showed the specificity of the *in vitro* interaction as no signal was detected when GST-tagged VPg-Pro was replaced with GST. VPg-Pro auto-catalytically cleaves itself into two functional domains: VPg and Pro (Laliberté et al., 1992). ELISA-based binding assays were conducted to test if the interaction with eEF1A was mediated by either one of the two domains. Figure 3.6A shows that each domain was also able to bind eEF1A. Interestingly, the optical density (OD) value for saturation with VPg or Pro was half of that obtained with VPg-Pro, suggesting that VPg-Pro can bind two molecules of the elongation factor.

The ELISA-based binding assays indicated that eEF1A interacts with RdRp and VPg-Pro. The possibility of a trimolecular complex was thus investigated. ELISA plate wells were coated with His-tagged eEF1A and were incubated with increasing amounts of GST-tagged VPg-Pro in the absence or in the presence of a saturating binding

concentration of His-tagged RdRp. Complex retention was detected using either a polyclonal anti-GST antibody or polyclonal anti-RdRp antibody. Figure 3.6B shows a saturation binding curve of VPg-Pro with the eEF1A. A similar saturation curve was observed with a saturating binding concentration of RdRp to all concentration of VPg-Pro. The RdRp was retained in the wells in the presence of VPg-Pro since a constant signal was detected with the anti-RdRp. This experiment indicates that both viral proteins bind to eEF1A in a non-competitive manner. This also suggests that a tripartite complex of VPg-Pro, RdRp and eEF1A exists in TuMV-infected plants.

3.4.5. Vesicle localization of eEF1A during TuMV infection

The retargeting of eEF1A within the membrane vesicles induced by 6K-VPg-Pro was analyzed by ectopic expression of individual viral proteins. To confirm that the eEF1A protein is found in viral-derived vesicles during TuMV infection, we constructed the plasmid pCambiaTunos/6KGFP (Fig. 3.4A). This plasmid contains an infectious TuMV cDNA that contains an additional copy of the 6K protein fused to GFP. The 6KGFP coding sequence was inserted between the P1 and HC-Pro coding genes as an in-frame translational fusion containing flanking P1 and VPg-Pro cleavage sites (Beauchemin et al., 2005).

The ability of this modified TuMV to replicate and form fluorescent vesicles was investigated by expressing pCambiaTunos/6KGFP in *N. benthamiana* by agroinfiltration. Fluorescence was observed four days later in infiltrated leaves and systemic infection became apparent after six days. Expression of 6KGFP was assessed by immunoblot analysis using a rabbit serum raised against GFP. A signal corresponding to the expected

molecular mass of 6KGFP was observed in the membrane associated fraction (data not shown). This result suggests that 6KGFP was expressed and correctly released from the polyprotein by the viral proteinases. When observed by confocal microscopy, fluorescence emitted by 6KGFP was associated with cytoplasmic vesicles. On average, there were one to three ~10µm vesicles per cell, although several smaller fluorescing structures were also observed (Fig. 3.7A).

To further characterize these GFP-tagged vesicles, the presence of 6K-VPg-Pro within these vesicles was first investigated by co-expressing pCambia/6K-VPg-Pro-mCherry with pCambiaTunos/6KGFP. Red fluorescence emitted by 6K-VPg-Pro-mCherry was found in all GFP-tagged vesicles (Fig. 3.7B). We have previously shown that the 6K-VPg-Pro-derived vesicles house the host factors PABP, eIF(iso)4E and Hsc70-3 (Beauchemin et al., 2007; Beauchemin and Laliberté, 2007; Dufresne et al., 2008a). The presence of these factors in the vesicles induced by 6KGFP during TuMV infection was investigated. Each protein was co-expressed with pCambiaTunos/6KGFP in *N. benthamiana*. When PABP2-mCherry was coexpressed with pCambiaTunos/6KGFP, red fluorescence was seen throughout the cytoplasm, but was also observed in viral-induced vesicles exactly where green fluorescence was emitted by 6KGFP (Fig. 3.7C). Similarly, the red fluorescence produced by eIF(iso)4E-DsRed (Fig. 3.7D) or Hsc70-3-DsRed2 (Fig. 3.7E) was observed throughout the cytoplasm but was also found within the green fluorescing vesicles induced by 6KGFP. These results indicate that the GFP-tagged vesicles observed upon TuMV infection were not empty structures but contained proteins previously found to be included in 6K-VPg-Pro-induced vesicles. To test whether eEF1A is also present in the vesicles formed by 6KGFP,

eEF1A-DsRed2 was coexpressed with pCambiaTunos/6KGFP in *N. benthamiana*. Fluorescence was visualized four days postagroinfiltration by confocal microscopy. Red fluorescence was seen throughout the cytoplasm but also accumulated in punctuate locations that co-localized with the 6K-GFP fluorescence (Fig. 3.7F). This experiment indicated that eEF1A was internalized in the vesicles formed by 6KGFP during TuMV infection.

To verify that the presence of PABP, eIF(iso)4E, Hsc70-3 and eEF1A within the 6KGFP-induced vesicles was not the result of a non-specific entrapment, lipase-mCherry (Fig. 3.4D) was coexpressed with Tunos/6KGFP. The lipase-mCherry was previously found to localize in the cytoplasm 2 days post-infiltration and to localize in the intercellular space 4 days post-infiltration (Thivierge and Laliberté, unpublished results). To date, there is no data involving the lipase in TuMV replication so this protein should not localize in the vesicles. As expected, the lipase-mCherry was not redistributed in the virus-induced vesicles when coexpressed with Tunos/6KGFP (Fig. 3.7G). The specificity of the vesicular localization of PABP2, eEF(iso)4E, eEF1A and Hsc70-3 was further confirmed by the co-expression of TuMV P3-mCherry (Fig. 3.4E) with Tunos/6KGFP. TuMV P3-mCherry did not co-localize with the green fluorescence produced by the 6KGFP. Instead, the viral protein was found in the nucleus of the infected plant cell (Fig.3.7H)

Immunofluorescence was also used to confirm the presence of the elongation factor within the vesicles. *N. benthamiana* plants were agroinfiltrated with pCambiaTunos/6KGFP and infiltrated leaves were collected four days later for protoplast isolation. Protoplasts were then fixed and labeled with rabbit sera raised against VPg-Pro

or eEF1A. The distribution of the tested proteins was visualized with Alexa Fluor 568-conjugated secondary antibody. The presence of VPg-Pro within the vesicles formed by 6KGFP during the course of TuMV infection was first investigated. Fluorescence associated with VPg-Pro was coincident with that of the vesicles formed by 6KGFP (Fig. 3.8A). Every vesicles formed by 6KGFP were positive for the presence of VPg-Pro. Additionally, presence of PABP and eIF(iso)4E in the 6KGFP derived vesicles was tested using anti-PABP and anti-eIF(iso)4A sera. As expected, PABP and eIF(iso)4E were found in the GFP-tagged vesicles (data not shown). Likewise, red fluorescence associated with endogenous eEF1A was found within the 6KGFP-induced vesicles (Fig. 3.8B). A proportion of eEF1A was also observed in the cytoplasm. These data point to the hypothesis that the vesicles tagged with 6KGFP house the virus replication complex and that at least three translation factors are included in these vesicles.

Table 3.1: Primers used for vector construction

Primer	Sequence (5'→ 3')
EF1AF-*Bam*HI	ATCTTCGGATCCATGGGTAAAGAGAAGTTTC
EF1AR-*Not*I	ATCGTAGCGGCCGCTCACTTGGCACCCTTCTTGAC
VPgPro-*Eco*RI F	ATCCGAATTCGCGAAAGGTAAGAGGCAAAG
VPgPro mutation R	CATGGAGTTACTGTGGTGGTCCACTGG
VPgPro-*Not*I R	CTTCGCGGCCGCTTATTGTGCGTAGACTGCCGTG-
VPgPro mutation F	CCAGTGGACCACCACAGTAACTCCATGTTC
Pro pGEX6P1-*Eco*RI F	ATCCGAATTCAGTAACTCCATGTTCAGAG
eEF1F EGFP-*Xba*I	ACTTCTCTAGAATGGGTAAAGAGAAGTTTCA
eEF1R EGFP-*Bam*HI	ATCTTCGGATCCCTTGGCACCCTTCTTGACTG
LipaseF mCherry-*Xba*I	ATCTTCTAGAATGGAGAGTTACTTAACGAAATG
LipaseR mCherry-*Bam*HI	ATCTGGATCCAAGCTGTGCCAGCCTTGAA
P3F mCherry-*Hind*III	ATCTTCAAGCTTATGGGAACAGAATGGGAGG
P3R mCherry-*Hind*III	TTCAAGCTTGCTTGATGAACCACCGCCTTTTC
JFCI	ACATCCCAGAAAAACTTCATCT
FT6K-*Bam*HI	ACCTTTGGATCCATGGGTTACGGGTTG
JF6K-*Sac*II	GCAGTTCCCGCGGAAAACACCAGCCACATGAGC
FTGFP-*Sac*II	AAACCTCCGCGGCTGCCTGGTGATAGACACAAGCTTTGTATAGTTCATCCAT

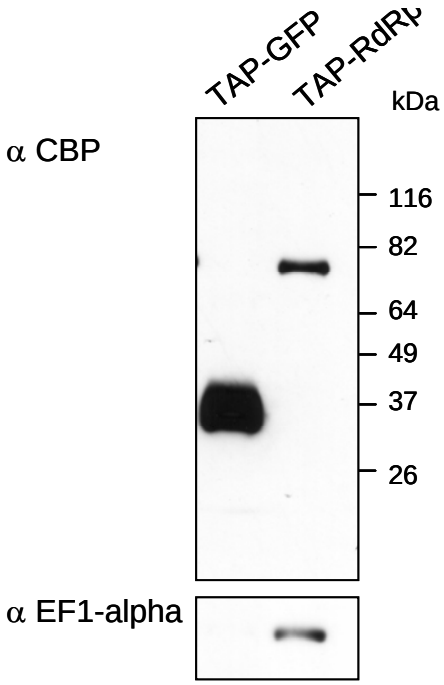

Figure 3.1: Expression and purification of NTAPi-tagged RdRp fusion and identification of eEF1A as an interactor. Western blot analysis of eEF1A purified in *A. thaliana* NTAPi-RdRp lines. Protein extracts from *A. thaliana* NTAPi-RdRp and NTAPi-GFP (control) lines were separated by SDS-PAGE and analyzed by immunoblotting using antibodies directed against eEF1A or calmodulin binding protein (CBP). The CBP antibody detects TuMV RdRp and GFP tag fusion product (the CBP is present in the TAP fusion).

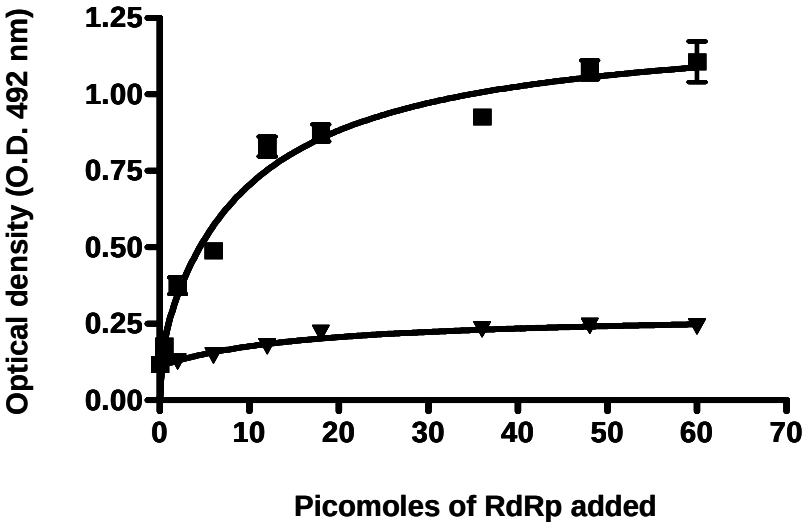

Figure 3.2: Interaction of TuMV RdRp protein with *A. thaliana* eEF1A in an ELISA-based binding assay. Wells were coated with 2.5 μg of His-tailed purified eEF1A (■) or metal chelation-purified *E. coli* lysate containing pET28(a) (▲) and incubated with increasing amounts of His-tailed RdRp. Protein retention was detected using a rabbit anti-RdRp serum and horseradish peroxidase-coupled goat anti-rabbit immunoglobulin serum. Data represent the mean ± SEM of three replicates. Error bars are specified for each data, but the small SEM values for some data are masked by the data point symbols.

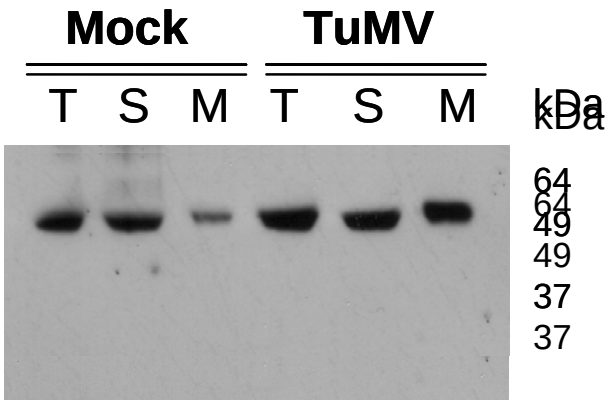

Figure 3.3: Immunoblot analysis of soluble and membrane-associated proteins from P19 or pCambiaTunos/6KGFP-agroinfiltrated plants. *N. benthamiana* plants were agroinfiltrated with P19 or pCambiaTunos/6KGFP. Four days later, total proteins (T) were extracted and soluble proteins (S) were separated from membrane-associated proteins (M) by centrifugation at 30,000 x *g*. Proteins were separated by SDS-PAGE and analyzed by immunoblotting using a rabbit serum against eEF1A.

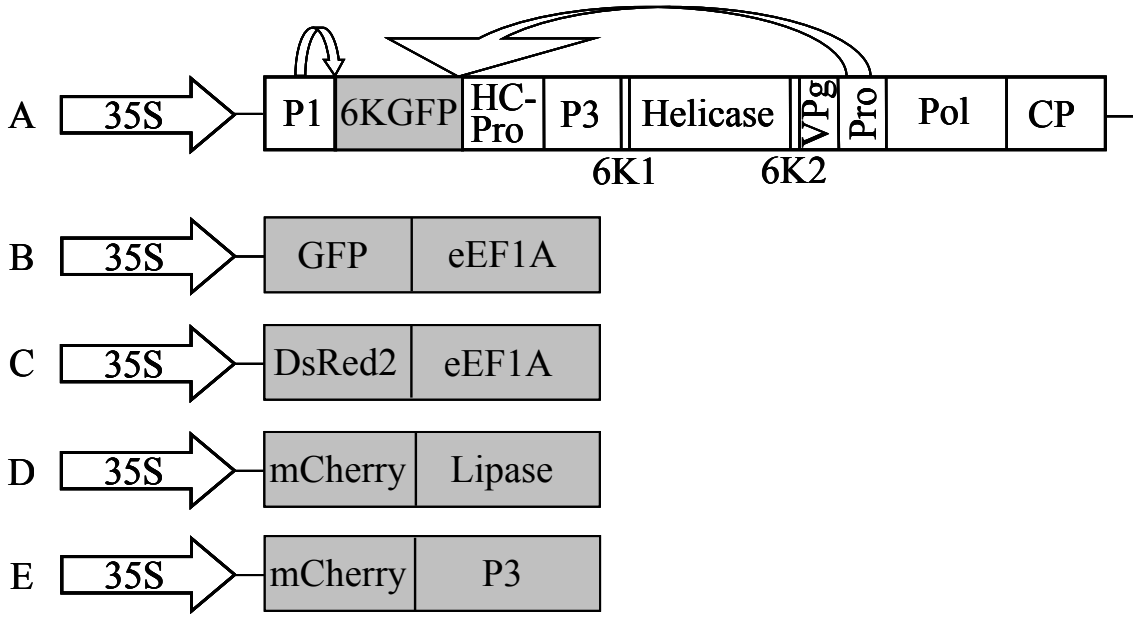

Figure 3.4: Construction of the plasmids used for co-localization experiments. Schematic representation of pCambiaTunos/6KGFP (A), pGreen/eEF1A-GFP (B), pGreen/eEF1A-DsRed2 (C), pCambia/lipase-mCherry (D), and pCambia/P3-mCherry (E). Straight arrow represents the 35S promoter of *Cauliflower mosaic virus* and boxes the coding region of listed protein. Curved arrows indicate cleavage of 6KGFP by P1 and Pro.

Figure 3.5: Subcellular localization of eEF1A, RdRp, and 6K-VPg-Pro. *N. benthamiana* leaves were infiltrated with *A. tumefaciens*, and expression of fluorescent proteins was visualized by confocal microscopy 4 to 5 days later. *A. tumefaciens* suspensions contained binary Ti plasmids encoding eEF1A-DsRed2 and GFP (A), eEF1A-DsRed2 and ER-GFP (B), eEF1A-DsRed2, GFP-RdRp, and non-fluorescent 6K-VPg-Pro-ct (C), and eEF1A-DsRed2 and non-fluorescent 6K-VPg-Pro-ct (D). Left panels show fluorescence emitted by the red channel only, while middle panels show fluorescence emitted by the green channel only, and right panels show the merging of the red and green channels with the yellow color representing areas where the red and green fluorescence coincide. Scale bar = 15 μm. All agroinfiltrations were performed in the presence of the P19 inhibitor of silencing as previously described.

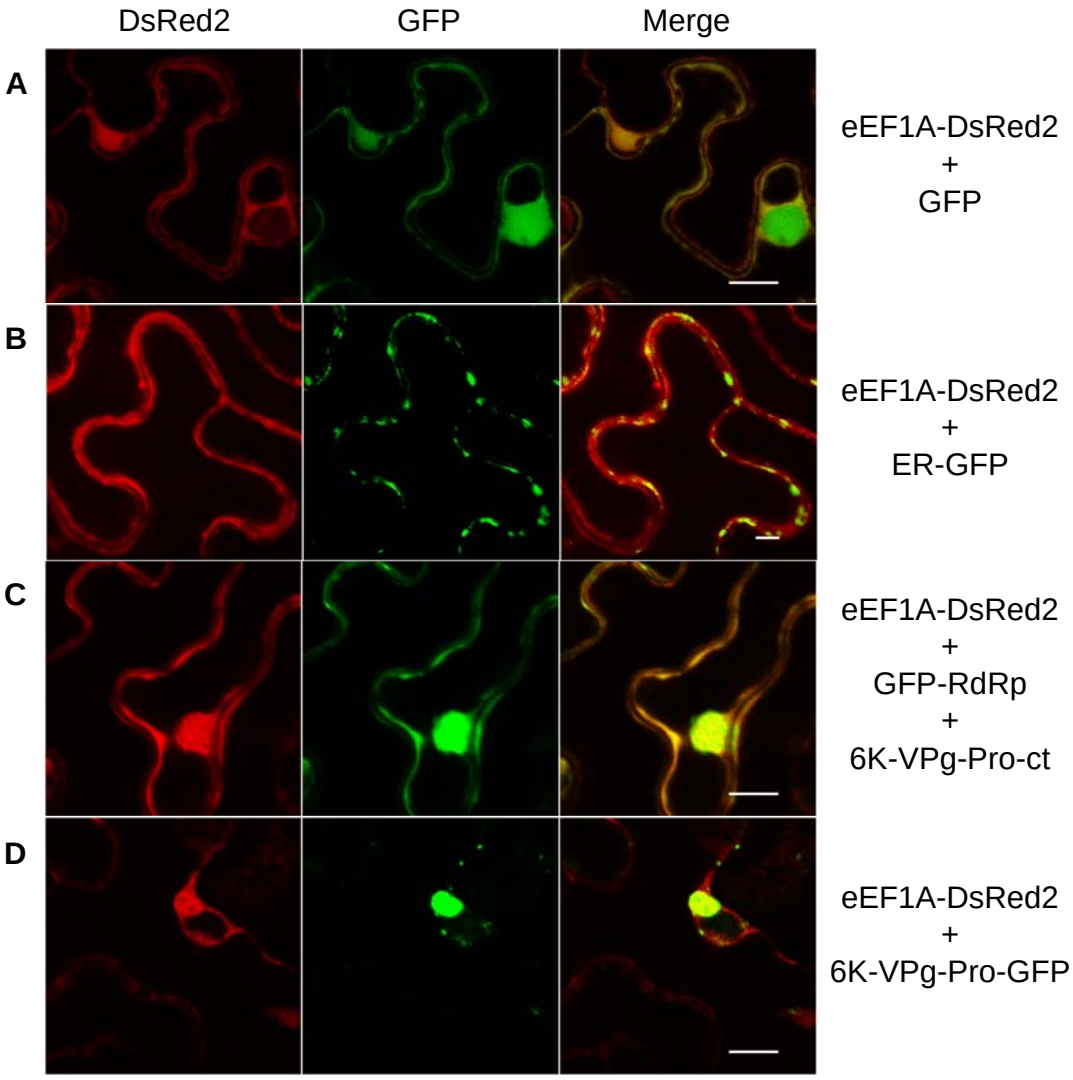
DsRed2
GFP
Merge
A
eEF1A-DsRed2
+
GFP
B
eEF1A-DsRed2
+
ER-GFP
C
eEF1A-DsRed2
+
GFP-RdRp
+
6K-VPg-Pro-ct
D
eEF1A-DsRed2
+
6K-VPg-Pro-GFP

Figure 3.6: *In vitro* interaction between VPg-Pro, RdRP and eEF1A. (A) VPg-Pro interaction with eEF1A of *A. thaliana* as demonstrated by ELISA-based binding assay. Wells were coated with 48 picomoles of purified His-tailed eEF1A and incubated with increasing amounts of GST–tagged VPg-Pro (■), GST-tagged VPg (▲), GST-tagged Pro (▼) or GST (□). Protein retention was detected using a polyclonal anti-GST antibody. (B) Trimolecular complex made up of eEF1A, RdRp and VPg-Pro demonstrated by ELISA-based binding assay. Wells were coated with 48 picomoles of purified His-tailed eEF1A and incubated with increasing concentration of purified GST–tagged VPg-Pro with (□) or without (Δ) His-tailed RdRp (48 picomoles). Retention of the complex was detected using polyclonal anti-GST (open symbols) or polyclonal anti-RdRp (filled symbols). Data represent the mean ± SEM of three replicates. Error bars are specified for each data, but the small SEM values for some data are masked by the data point symbols.

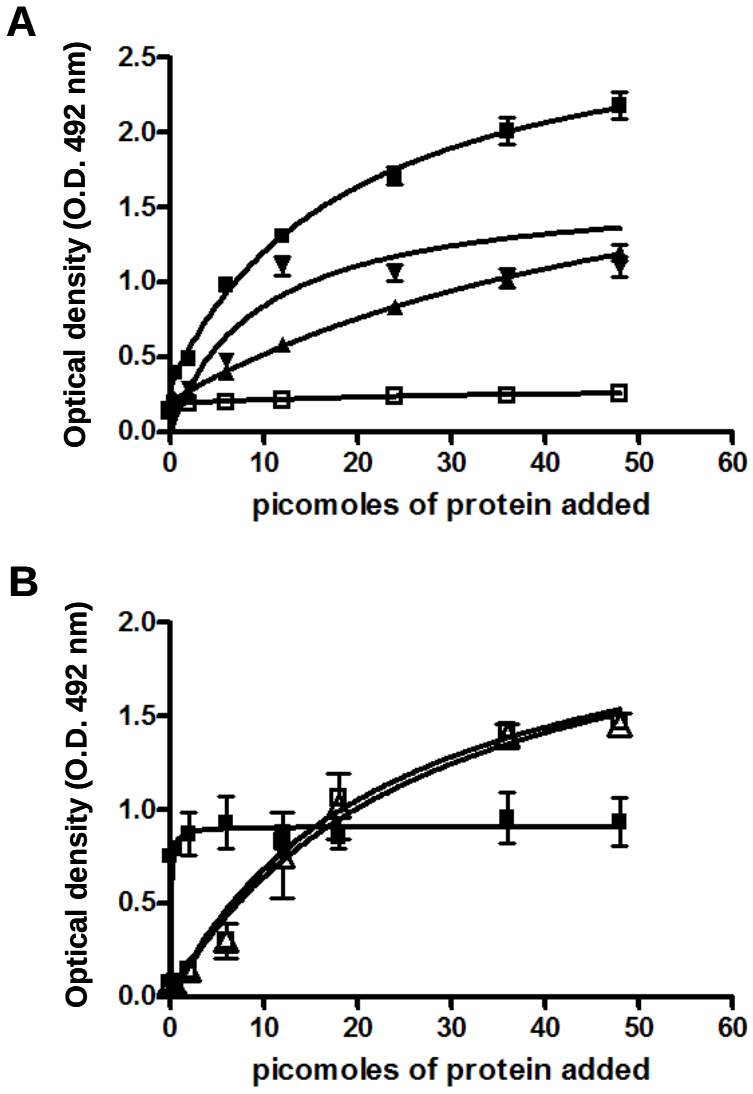
A
Optical density (O.D. 492 nm)
2.5
2.0
1.5
1.0
0.5
0.0
0
10
20
30
40
50
60
picomoles of protein added
B
Optical density (O.D. 492 nm)
2.0
1.5
1.0
0.5
0.0
0
10
20
30
40
50
60
picomoles of protein added

Figure 3.7: Intracellular distribution of recombinant 6K-VPg-Pro, PABP2, eIF(iso)4E, Hsc70-3, eEF1A, P3, and lipase proteins in *N. benthamiana* infected with Tunos/6KGFP. *N. benthamiana* leaves were infiltrated with *A. tumefaciens*, and expression of fluorescent proteins was visualized by confocal microscopy four days later. *A. tumefaciens* suspensions contained binary Ti plasmids encoding Tunos/6KGFP and ER-DsRed2 (A), Tunos/6KGFP and 6K-VPg-Pro-mCherry (B), Tunos/6KGFP and PABP2-mCherry (C), Tunos/6KGFP and eIF(iso)4E-DsRed (D), Tunos/6KGFP and Hsc70-3-DsRed2 (E), Tunos/6KGFP and eEF1A-DsRed2 (F), Tunos/6KGFP and Lipase-mCherry (G), and Tunos/6KGFP and P3-mCherry (H). Left panels show fluorescence emitted by the red channel only, while middle panels show fluorescence emitted by the green channel only, and right panels show the merging of the red and green channels with the yellow color representing areas where the red and green fluorescence coincide. Scale bar = 15 μm. All agroinfiltrations were performed in the presence of the P19 inhibitor of silencing as previously described.

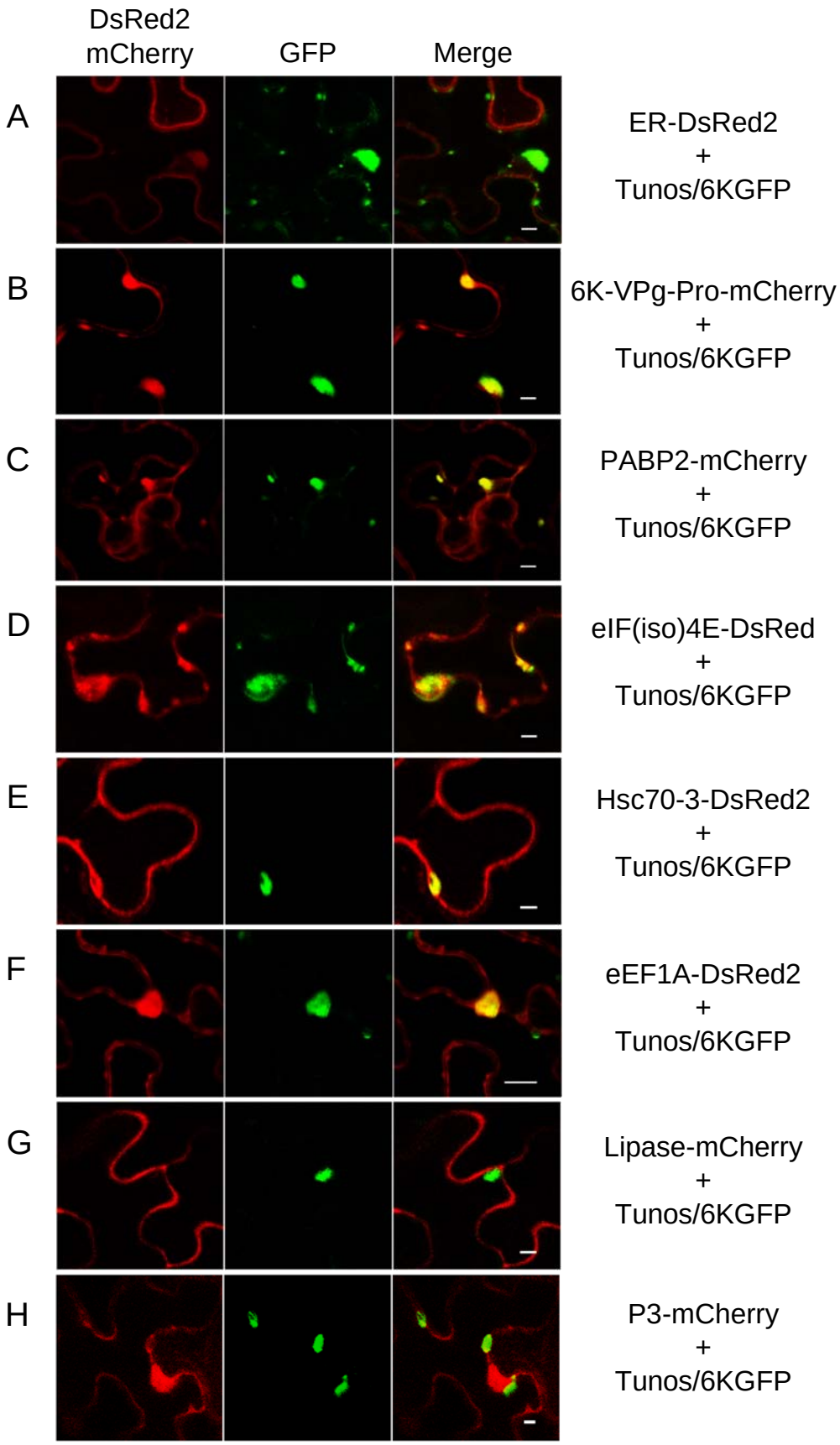
DsRed2
mCherry
GFP
Merge
A
ER-DsRed2
+
Tunos/6KGFP
B
6K-VPg-Pro-mCherry
+
Tunos/6KGFP
C
PABP2-mCherry
+
Tunos/6KGFP
D
eIF(iso)4E-DsRed
+
Tunos/6KGFP
E
Hsc70-3-DsRed2
+
Tunos/6KGFP
F
eEF1A-DsRed2
+
Tunos/6KGFP
G
Lipase-mCherry
+
Tunos/6KGFP
H
P3-mCherry
+
Tunos/6KGFP

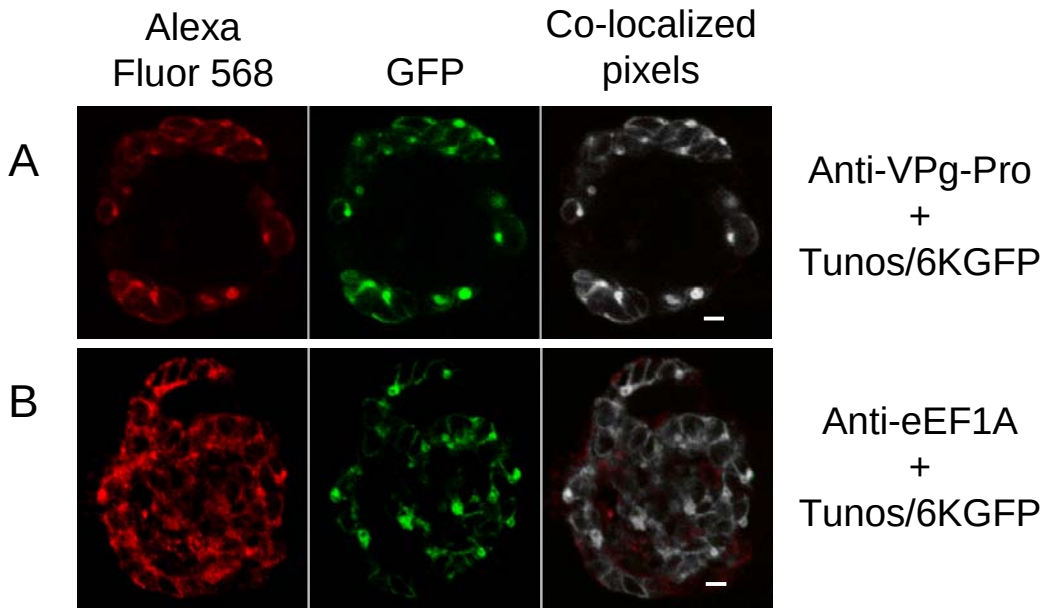

Figure 3.8: Intracellular distribution of viral VPg-Pro and endogenous eEF1A in protoplast infected with Tunos/6KGFP. Four days post-infiltration *N. benthamiana* leaves agroinfiltrated with pCambiaTunos/6KGFP were collected and used for protoplast isolation. Protoplasts were fixed and labeled with antisera raised against VPg-Pro (A) or eEF1A (B) and Alexa Fluor 568-conjugated secondary antibody. The fluorescent signals from 6KGFP and Alexa Fluor-labeled VPg-Pro or eEF1A proteins were scanned in separated channels through confocal laser scanning microscopy. Left panels show fluorescence emitted by the red channel only, while middle panels show fluorescence emitted by the green channel only, and right panels show co-localized pixels highlighted in white. Scale bar = 15 μm.

3.5. Discussion

eEF1A is essential for cell viability by virtue of its role in the formation of peptide bonds during protein synthesis. eEF1A also participates in protein degradation mediated through ubiquitin-dependent pathways (Gonen et al., 1996) and in cytoskeletal attachment of polysome (Yang et al., 1990). The identification of eEF1A as a cellular factor interacting with TuMV RdRp and 6K-VPg-Pro indicates that the elongation factor is also involved in potyvirus infection. Interaction of the host factor with the TuMV proteins has been demonstrated by TAP tag chromatography and/or ELISA-based binding experiments. Interestingly, VPg-Pro could simultaneously bind RdRp along with eEF1A, thus forming a multi-protein complex. The interaction was shown to take place within virus-induced vesicles, which are likely to contain the virus replication complex. However, it is as yet unclear what exact role eEF1A plays in TuMV infection through its association with RdRp and 6K-VPg-Pro.

There have been a number of studies implicating eEF1A with viruses. This was first shown for the positive-strand bacteriophage Qβ. Bacteriophage Qβ replicase complex contains the bacterial homolog of eEF1A, EF-Tu, which interacts with the viral RdRp and is indispensable for both positive- and negative-strand RNA syntheses (Blumenthal and Carmichael., 1979). RNA polymerase of PV, VSV and BVDV also associates with eEF1A (Das et al., 1998; Harris et al., 1994; Jonhnson et al., 2001). In the case of TMV, eEF1A interacts not only with the RdRp but as well with the upstream pseudoknot domain in the 3'-untranslated region (3'-UTR) of the genomic RNA (Yamaji et al., 2006; Zeenko et al., 2002). Likewise, interaction of the elongation factor with the 3'-terminal stem-loop of the genomic RNA of the West Nile virus (WNV) was reported

and was shown to facilitate minus-strand RNA synthesis (Davis et al., 2007). Furthermore, eEF1A was found to co-localize with replication complexes in both Dengue-2 and WNV infected cells (Davis et al., 2007; De Nova-Ocampo et al., 2002). The above studies suggest that eEF1A plays, somehow, a role in virus RNA replication. eEF1A can also be involved in viral translation. The interaction between eEF1A and the 3'-UTR of *Turnip yellow mosaic virus* (TYMV) (Matsuda and Dreher, 2004) genomic RNA was suggested to enhance the translation of TYMV RNA and to suppress the minus-strand RNA synthesis (Matsuda et al., 2004). Finally, reports have demonstrated the binding of eEF1A to microfilaments and microtubules both *in vivo* and *in vitro* (Bassell et al., 1994; Bassell et al., 1999; Condeelis, 1995; Jansen, 1999; Moore and Cyr, 2000). Since intracellular trafficking of viral VRC on microfilaments has been demonstrated for TMV (Liu et al., 2005) and TuMV (Cotton et al., 2009), it is possible that eEF1A participates in TuMV vesicle movement by its interaction with viral proteins (RdRp and VPg-Pro) and microfilaments. It must be added that the above possible functions of eEF1A in TuMV infection are not mutually exclusive.

Interaction of eEF1A with the viral proteins was shown to take place within 6K-VPg-Pro-induced vesicles, which contains the VRC (Schaad et al., 1997a). These same vesicles were previously shown to contain eIF(iso)4E, PABP2 and Hsc70-3 (Beauchemin et al., 2007; Beauchemin and Laliberté, 2007; Dufresne et al., 2008a). The presence of translation factors along with virus replication proteins may provide a mechanistic explanation for the coupling of viral RNA translation with viral RNA replication. In positive-strand RNA viruses, RNA replication and translation pathways conflict with each other, because genomic RNA can serve as a template for synthesis of negative-

strand RNA by viral RNA replicase and as a template for translation of viral proteins by ribosomes. However, there are increasing reports indicating that viral RNA translation and replication are coupled *in cis*. For instance, mutation in the RNA1 of *Brome mosaic virus* translation initiation codon significantly decreased its accumulation even when wild-type 1a and 2a proteins were provided *in trans*, indicating that RNA1 replication requires 1a translation from RNA1 *in cis* (Yi and Kao, 2008). Translation and replication are also coupled for *Red clover necrotic mosaic virus* (Mizumoto et al., 2006) and Sindbis virus (Sanz et al., 2007). Interestingly, formation of the poliovirus replication complex requires that viral RNA translation be coupled to viral RNA synthesis in a *cis* pathway, which integrates vesicle production (Egger and Bienz, 2000; Egger et al., 2005). Further evidence for physical linkage of viral RNA translation with transcription comes from the DNA poxvirus. Poxviruses replicate in cytoplasmic foci known as DNA factories, which contain virus-encoded transcription factor, viral mRNA, translation initiation factors eIF4E and eIF4G, and ribosomal proteins. Each factory is formed from a single genome and is the site of transcription and translation as well as DNA replication (Katsafanas and Moss, 2007). It is possible that release of 6K-VPg-Pro from the polyprotein upon translation of the invading genomic RNA induces the formation of vesicles that trap the host protein machinery. Translation continues within the vesicles until sufficient replication proteins accumulate so that virus translation stops and a switch to minus-stand RNA synthesis takes place.

This work also underlies the importance of 6K-VPg-Pro and RdRp as scaffold proteins for the formation of a multi-protein complex within virus-induced vesicles. At the present time, we have been able, in addition to the above mentioned viral proteins, to

demonstrate the presence of eIF(iso)4E, PABP2, Hsc70-3 and eEF1A in the vesicles. Interaction of eIF(iso)4G with VPg-Pro through the intermediary of eIF(iso)4E has also been reported (Plante et al., 2004), although interaction within the vesicles remain to be demonstrated. Interestingly, many of the proteins have several, sometimes common, interacting partners. For example 6K-VPg-Pro and RdRp each bind to PABP2 and eEF1A. In the case of VPg, its propensity to have several binding partners has been explained by its intrinsically disordered protein state (Grzela et al., 2008).

CONNECTING STATEMENT BETWEEN CHAPTERS III AND IV

The ability of TuMV VPg-Pro to bind directly to eEF1A protein and the enclosure of three translation factors in 6K-VPg-Pro-induced vesicles was demonstrated in chapters III. These results suggest that TuMV VPg and its precursor forms play a role in viral translation. The involvement of VPg-Pro in translation is also supported by the well studied interaction between VPg-Pro and the eukaryotic initiation translation factor 4E [eIF(iso)4E]. Chapter IV describes the use of *in vitro* translation systems to further characterize the role of VPg-Pro in translation.

The results of this section are the subject of a manuscript that has been published in Virology (vol. 351, p. 92-100). My 30% contribution to this chapter is described in details below.

1. I have contributed equally with Sophie Cotton and Philippe Dufresne to the overall experimental set-up.
2. I have conducted all experiments dealing with the production of all the recombinant proteins including TuMV GST-VPgPro, GST-D77N, NV GST-VPg and wheat eIF(iso)4E (Section 4.3.1. of Materials and Methods). The resulting purified recombinant proteins are shown in Figure 4.1, and were eventually used by the other authors, Sophie Cotton and Philippe Dufresne in order to generate all subsequent figures (Figs. 4.2, 4.3, 4.4, 4.5, 4.6, and 4.7).
3. I have contributed equally with Sophie Cotton and Philippe Dufresne to the writing of the following sections: Abstract, Introduction, Results and Discussion. My contribution to the methodology is limited to section 4.3.1.

Philippe Dufresne performed all the cloning of the vectors described in section 4.3.1 of Materials and Methods. He carried the ELISA binding-assays (Fig. 4.3B) and the analysis of the reporter RNA in absence of translation (Fig.4.5). He also studied the effect of EDTA and heat denaturation on the RNase activity of TuMV VPgPro (Fig. 4.7). Finally, he analyzed the capacity of the VPg domain to degrade plant total RNA (Fig. 4.6B). Sophie Cotton performed all the experiments related to the inhibition of translation (Figs. 4.2 and 4.3A), and the RNA degradation assays shown in Figures 4.4 and 4.6A. Christine Ide assisted in cloning of constructs expressing TuMV GST-VPgPro, GST-VPg, and GST-D77N proteins. She prepared the m^7G-luciferase reporter RNA and the *B. perviridis* total RNA. She also assisted in Northern blot and RNA degradation analysis. Professor M. G. Fortin provided supervision and funding throughout the study. He provided valuable suggestions and corrected the manuscript.

CHAPTER IV

The VPgPro protein of *Turnip mosaic virus*: *in vitro* inhibition of translation from a ribonuclease activity

S. Cotton[1], P. J. Dufresne[1], K. Thivierge[1], C. Ide[1], and M. G. Fortin[2]

[1]Department of Plant Science, McGill University, 21,111 Lakeshore, Ste-Anne-de-Bellevue, Québec, Canada H9X 3V9. [2]Agriculture and Agri-Food Canada, 930 Carling Avenue, Ottawa, Ontario, Canada K1A 0C7.

4.1. Abstract

A role for viral encoded genome-linked (VPg) proteins in translation has often been suggested because of their covalent attachment to the 5′ end of the viral RNA, reminiscent of the cap structure normally present on most eukaryotic mRNAs. We tested the effect of the VPgPro of *Turnip mosaic virus* (TuMV) on translation of reporter RNAs in *in vitro* translation systems. The presence of VPgPro in either wheat germ extract or rabbit reticulocyte lysate systems lead to inhibition of translation. The inhibition did not appear to be mediated by the interaction of VPg with the eIF(iso)4E translation initiation factor since a VPg mutant that does not interact with eIF(iso)4E still inhibited translation. Monitoring the fate of RNAs revealed that they were degraded as a result of addition of TuMV VPgPro or of Norwalk virus (NV) VPg protein. The RNA degradation was not the result of translation being arrested and was heat labile and partially EDTA sensitive. The capacity of TuMV VPgPro and of NV VPg to degrade RNA suggests that these proteins have a ribonucleolytic activity which may contribute to the host RNA translation shutoff associated with many virus infections.

4.2. Introduction

TuMV (family of *Potyviridae*) is a member of the picorna-like supergroup of positive-sense RNA viruses. For many plant and animal RNA viruses, the virus-encoded VPg protein (Viral Protein genome-linked) is covalently attached to the 5′ terminus of their genomic RNA (van Regenmortel et al., 2000). This protein is positioned on the viral RNA where the m^7G cap structure is normally found on cellular mRNAs; it is not clear whether the VPg plays the same functional role as the cap structure in translation initiation for viral RNA.

The VPg protein, and its VPgPro precursor form, are multi-functional proteins that play important roles in the replication cycle of potyviruses (Urcuqui-Inchima et al., 2001). The VPg was shown to interact with translation initiation factors eIF(iso)4E (eukaryotic initiation factor (iso)4E) and PABP (poly(A)-binding protein) (Léonard et al., 2004; Wittmann et al., 1997). These interactions suggest a role for the VPg in the recruitment of translation initiation factors for viral RNA translation. Mutations in either VPg or eIF(iso)4E result in reduced ability of the virus to infect its host. Mutations in the eIF(iso)4E-interacting domain of VPg lead to loss of virus infectivity (Léonard et al., 2000), and disruption of plant eIF(iso)4E gene prevented TuMV infection (Duprat et al., 2002; Lellis et al., 2002). The involvement of VPg in facilitating viral RNA translation was shown for Feline calicivirus (FCV) (Goodfellow et al., 2005) where FCV translation is dependent on the presence of VPg at the 5′ end of the viral genome. The VPg-eIF4E interaction is required for virus RNA translation since sequestration of eIF4E by 4E-binding protein 1 inhibited translation. It was suggested that FCV VPg acts as a ‘cap substitute’ during translation initiation of virus mRNA.

Viruses that infect eukaryotic cells use a variety of mechanisms for subverting the functions of the host cell. Several viruses alter the translation machinery such that they effectively block translation of host mRNAs. Viruses often target translation initiation factors as a mean to increase their own translation at the expense of that of their host. The main strategies are either to compromise eIF4G or PABP functions by proteolytic cleavage, to sequester eIF4E or to alter the phosphorylation state of host translation factors (reviewed by Gale et al., 2000). Another key aspect of virus infection in plants and animals is the associated host transcription shut-down (Aranda and Maule, 1998; Jen et al., 1980). For instance, infection of plant cells with a potyvirus (carrying a 5′-bound VPg) leads to transient disappearance of most cellular mRNAs in cells supporting active viral replication (Aranda et al., 1996). It is not clear whether the disappearance of RNAs is the consequence of mRNA destabilization resulting from a stress response, of host transcription inhibition, or of targeted degradation resulting from a viral ribonuclease activity.

A more direct line of evidence implicating VPg in cellular translation inhibition was found for NV. NV VPg was shown to inhibit translation of a reporter RNA in rabbit reticulocyte lysate (RRL; Daughenbaugh et al., 2003). VPg added to cell-free translation reactions that contained either capped RNA or RNA with an internal ribosomal entry site inhibited translation of these reporter RNAs in a dose-dependent manner. Although potyviral VPgPro protein was found to have non-specific RNA-binding properties (Daròs and Carrington, 1997) as well as a deoxyribonuclease activity (Anindya and Savithri, 2004), no link has been made between those activities and an inhibition of translation or

the disappearance of mRNAs in plant cells. The mechanism by which this occurs remains unclear.

In this report, we investigated the effect of addition of TuMV VPgPro on the translation of reporter RNA in *in vitro* translation systems. Purified TuMV VPgPro inhibited translation of capped reporter RNA, as was observed when VPg of NV was added to an *in vitro* translation system. The VPgPro-eIF(iso)4E interaction was likely not involved in the inhibition of translation since a VPg mutant that does not interact with eIF(iso)4E did inhibit translation. We observed that this inhibition of translation was concurrent with degradation of reporter RNA in a rabbit reticulocyte lysate. Purified total plant RNA was also degraded when VPgPro was added; the same effect was observed with the VPg domain alone. A similar ribonucleolytic activity was also observed with NV VPg. The ribonucleolytic activity of VPg proteins may contribute to the disappearance of most mRNAs previously observed during potyvirus infection and to the transient inhibition of translation documented for host cell mRNAs during picornavirus infection.

4.3. Materials and Methods

4.3.1. Expression and purification of recombinant proteins

Sequences encoding TuMV VPgPro and TuMV D77N were amplified by polymerase chain reaction (PCR) from the full-length TuMV cDNA clone (p35Tunos) and its mutant form p35Tunos-D77N, respectively (Sanchez et al., 1998; Léonard et al., 2000), in order to construct vectors for the expression of glutathione-S-transferase (GST)-fused VPgPro and D77N proteins. Primers used for amplification were VPgPro-*NcoI* (5'-

ATCGTACCATGGCGAAAGGTAAGAGGCAAAG-3') and VPgPro-*EcoRI* (5'-ATCTTCGAATTCTTATTGTGCTAGACTGCCGTG-3'). The amplified fragments were digested with *NcoI*/*Eco*RI and cloned into similarly digested pET41(b) (Novagen, Gibbstown, NJ, USA). Both constructions resulted in the expression of a fusion protein containing a S-Tag, six histidine residues and a GST tag at the N terminus.

For construction of the vector coding for the N-terminus GST-VPg fusion protein, TuMV VPg sequences were PCR-amplified from p35Tunos using primers VPg-*EcoRI* (5'-ATCCGAATTCCGGAAAGGTAAGAGGCAAAG-3') and VPg-*NotI* (5'-CTTCGCGGCCGCTTACTCGTGGTCCACTGGGAC-3'). The amplified fragments were digested with *EcoRI/NotI* and cloned into similarly digested pGEX-6P1 (Amersham Biosciences, Baie d'Urfé, Qc, Canada).

BL21(DE3) (for pET41(b)-based constructs) and BL21 (for the pGEX-6P1-derived construct) *E. coli* cells containing recombinant plasmids were cultured at 37°C to an OD_{600} of 0.6 and protein expression was induced with 1 mM isopropyl-β-D-galactopyranoside for three hrs at 30°C. Bacterial cells were collected by centrifugation and resuspended in buffer A (4.3 mM Na_2HPO_4, 1.47 mM KH_2PO_4, 137 mM NaCl, 2.7 mM KCl, pH 7.3). The cells were disrupted by sonication and the lysate was centrifuged at 39,000 *g* for 20 min. The supernatant was used for affinity purification of either GST-VPgPro, GST-VPg or GST-D77N.

The protein extract was added to GST-Bind resin (Novagen) according to the manufacturer's protocol and incubated at room temperature with agitation for 30 min. Beads were washed three times with buffer A and collected by centrifugation for five min at 500 *g*. The fusion proteins were eluted from the resin in a buffer containing 10 mM

reduced glutathione and 50 mM Tris-Cl pH 8.0. Protein concentration was measured using a Bradford assay (Bio-Rad, Mississauga, On, Canada) using bovine serum albumin as standard. GST controls (the pET41(b) or pGEX-6P1 vectors without inserts) were expressed and purified using the same conditions.

The bacterial clones for expression of NV GST-VPg (pGEX-4T1 NV GST-VPg) and wheat eIF(iso)4E (pETtag(iso)4E*Ta*) were kindly provided by M.E. Hardy (Montana State University, MT, USA) and J.-F. Laliberté (INRS-Armand Frappier, QC, Canada) respectively. NV GST-VPg and wheat eIF(iso)4E were expressed and purified as described previously (Daughenbaugh et al., 2003; Léonard et al., 2000).

4.3.2 *In vitro* translation

The pGEM-luc vector (Promega, Madison, WI, USA) containing a luciferase cDNA was linearized with *Xho*I and used as template for synthesis of capped RNA. m^7G-luciferase RNA was transcribed using the mMessage mMachine SP6 system (Ambion, Austin, TX, USA). RNA was denatured for three min at 65°C before use. One µg of reporter RNA was translated in a 50 µl reaction containing 25 µl of wheat germ extract (WGE), 40 U of RNAGuard RNase inhibitor (Amersham Biosciences) and 10 µM of amino acid mixture (Promega). Different concentrations of GST, TuMV GST-VPgPro, TuMV GST-D77N and NV GST-VPg protein were added to the translation mix. The reactions were incubated at 25°C for two hours and light emission was measured after the addition of 100 µl of luciferase substrate (Promega). The experiment was conducted at least three times. The *in vitro* translation assays using RRL were performed similarly but incubated at 30°C for 90 min. Experiments on the effect of the VPgPro-eIF(iso)4E

interaction on translation of reporter RNA in WGE were conducted using to the same protocol but the GST and GST-VPgPro proteins were pre-incubated with eIF(iso)4E at 25°C for 15 min before addition to the translation system. In these assays, concentrations of 24, 48 or 96 pmol of eIF(iso)4E were used with 12, 24 or 48 pmol of GST or of GST-VPgPro.

4.3.3. VPgPro-eIF(iso)4E ELISA binding assays

GST-VPgPro protein (100 µl of protein at 15 ng μl^{-1} in PBS buffer) was adsorbed to wells of a polystyrene plate (Costar, San Diego, CA, USA) by overnight incubation at 4°C and wells were blocked with 5% milk PBS solution for two hours at room temperature. T7-labelled wheat eIF(iso)4E or β-galactosidase proteins were diluted in PBS with 1% milk and 0.1% Tween 20 and incubated for 1.5 h at 4°C in the previously coated wells. Detection of retained protein was achieved with a mouse monoclonal anti-T7-tag antibody (Novagen) and horseradish peroxidase-coupled goat anti-mouse immunoglobulin (Pierce, Rockford, IL, USA). Between each incubation, wells were washed five times with PBS supplemented with 0.04% Tween 20. Enzymatic reactions were performed in 100 µl of o-phenylenediamine dihydrochloride (OPD) citrate buffer (50 mM citric acid, 100 mM sodium phosphate dibasic, pH 5.0, 0.5 mg/ml OPD and 0.1% hydrogen peroxide) and stopped with a solution of 3 M H_2SO_4. Absorbance was measured at 492 nm. Statistical analyses were performed using the GLM procedure of SAS in a randomized complete block design (RCBD). ANOVA was used to detect statistical differences and LSD method used to determine significant differences among

means. SEM and statistics were calculated for three biological replicates from a minimum of three technical replicates (replicate of the assay on the same microplate).

4.3.4. RNA stability assays

To assess RNA stability in translation reactions that were arrested (in presence or not of VPgPro protein), *in vitro* translation of luciferase RNA in WGE was performed in presence of 600 µM of cycloheximide, an inhibitor of ribosome translocation. Five µl of each translation reaction were removed at 0, 5, 15 and 60 min after the addition of luciferase RNA and RNA degradation was monitored using Northern blot hybridizations with a ^{32}P-labelled luciferase RNA probe.

4.3.5. Total plant RNA degradation assays

RNA was extracted from *Brassica perviridis* using the RNeasy Plant Mini Kit (Qiagen, Mississauga, On, Canada). Five µg of RNA (eluted in RNase-DNase free water) were incubated with 48 pmol of GST, TuMV GST-VPgPro, GST-VPg or NV GST-VPg (eluted in 10 mM reduced glutathione and 50 mM Tris-Cl pH 8.0) for 30 min at 25°C. The volume of the reaction was completed with RNase-DNase free water. RNA degradation experiments following addition of EDTA and heat denaturation (15 min at 95°C) were carried out similarly. Samples were run on an agarose gel and stained with ethidium bromide.

4.3.6. Agarose gel electrophoresis and Northern blot analysis

RNA samples were purified using the RNeasy MinElute cleanup kit (Qiagen). A wash step with 200 µl of the RW1 buffer (Qiagen) was added after the application of the sample on the column to remove residual protein. RNA samples were eluted in 14 µl of RNase-free water and combined with four µl of RNA sample buffer (20 mM HEPES, 1 mM EDTA, pH 7.8, with 50% formamide and 6% formaldehyde). Following a 10 min incubation at 65°C, 2 µl of RNA loading buffer (95% formamide, 0.025% xylene cyanol, 0.025% bromophenol blue, 18 mM EDTA pH 8, 0.025% sodium dodecyl sulfate (SDS)) were added and the RNA samples were separated through a 1.5% agarose gel containing 6% formaldehyde in running buffer (20 mM HEPES, 1 mM EDTA, pH 7.8, 6% formaldehyde). The gel was washed for one hour in diethyl pyrocarbonate-treated water. RNA was transferred to a nylon membrane (Zeta-Probe, Bio-Rad) in 10X SSC pH 7 (1.5 M sodium chloride, 0.15 M sodium citrate). Following UV cross-linking, the membrane was stained for five min in a solution of 0.02% methylene blue and 0.3 M sodium acetate and washed in water. The membrane was scanned and the coloration was removed in 1 mM EDTA pH 8, 1% SDS. The membrane was incubated for four hours at 65°C in 10 ml of hybridization buffer (1 mg/ml bovine serum albumin (BSA), 50% formamide, 5% SDS, 1 mM EDTA, 400 mM $NaPO_4$ pH 7.2) and incubated for 16 hours with the ^{32}P-labelled riboprobe. The membrane was washed twice with washing buffer (0.1X SSC pH 7, 0.1% SDS, 1 mM EDTA) and exposed to Kodak Biomax MS film.

4.3.7. Synthesis of ^{32}P-labelled riboprobes

The plasmid pGEM-luc (Promega) was linearized with *Eco*RV. The riboprobe was synthesized for two hours at 37ºC in T7 polymerase buffer (10 mM of DTT, 20 U of RNAGuard RNase Inhibitor (Amersham Biosciences), 500 µM of CTP, GTP and ATP (Invitrogen, Carlsbad, CA, USA), 50 µCi of [α-^{32}P]-UTP (Amersham Biosciences), 500 ng of pGEM-luc/*Eco*R*V*) and 50 units of T7 polymerase (Invitrogen). RNase-free DNase I (10 U; Qiagen) was added and incubated for 15 min at 37ºC. The probe was purified with the QIAquick nucleotide removal kit (Qiagen).

4.4. Results

4.4.1. Expression and purification of VPg, VPgPro and eIF(iso)4E proteins

TuMV VPgPro was expressed as a fusion protein with the S-tag, GST and histidines fused at the N-terminus (a fusion tag of 33 kDa). SDS-polyacrylamide electrophoresis (PAGE) analysis of the protein extracts obtained from soluble fractions following GST affinity chromatography showed that protein bands corresponding to both the VPg and VPgPro proteins were present. This is consistent with the data of Ménard et al. (1995) that showed that recombinant TuMV VPgPro self-cleaves into two functional domains, the VPg and Pro domains. A prominent 55 kDa band [VPg domain (22 kDa) + N-terminal tag (33 kDa)] and a fainter 82 kDa band [VPgPro domain (49 kDa) + N-terminal tag (33 kDa)] (Fig. 4.1) corresponding to GST-VPg and GST-VPgPro, respectively, were found in the preparation. Both the GST-VPg and GST-VPgPro fusions were obtained since the GST domain was fused at the N-terminus of the protein. The

D77N mutant of VPgPro was similarly expressed and purified (Fig. 4.1). The identity of the proteins was confirmed by Western blot analysis using an anti-GST monoclonal antibody and a polyclonal anti-VPgPro serum (data not shown). The lower molecular weight products resulted from degradation of the fused GST moiety. NV and TuMV VPg proteins were also expressed in *E. coli* cells as N-terminal GST fusions (a fusion tag of 26 kDa); fusion proteins of 53 kDa (Fig. 4.1) [NV VPg domain (27 kDa) + N-terminal tag (26 kDa)] and a 48 kDa [VPg domain (22 kDa) + N-terminal tag (26 kDa)] were obtained for NV and TuMV, respectively. *Triticum aestivum* eIF(iso)4E protein was expressed as an N-terminal T7 fusion protein of 28 kDa (Fig. 4.1).

4.4.2. VPgPro inhibits *in vitro* translation of capped reporter RNA

A capped luciferase reporter RNA was translated either in WGE (Fig. 4.2A) or in RRL (Fig. 4.2B) translation systems in the presence of increasing concentrations of TuMV GST-VPgPro or of GST protein. Luciferase luminescence was used to measure translation efficiency of the m^7G-luciferase RNA. Translation of the reporter mRNA decreased sharply when increasing amounts of GST-VPgPro were added to the translation systems. As a control for the presence of contaminants in our protein purifications, the same amounts of GST protein alone, produced and purified using the same procedure as GST-VPgPro, were added to the *in vitro* translation systems; no inhibition of translation was observed.

4.4.3. Role of the eIF(iso)4E-VPgPro interaction in translation inhibition

We tested the D77N mutant of VPgPro on its capacity to interfere with translation *in vitro*. The D77N mutant contains an asparagine at position 77 of the protein instead of an aspartic acid residue; the resulting protein is unable to interact with eIF(iso)4E and virus infectivity is abolished (Léonard et al., 2000). We reasoned that if the eIF(iso)4E-VPgPro interaction is essential for the inhibition of translation, the addition of D77N into WGE or RRL translation systems would not interfere with translation of the m^7G-luciferase RNA. Increasing amounts of GST-VPgPro, GST or GST-D77N were added to translation reactions (WGE and RRL). GST-VPgPro or GST-D77N both decreased translation of the reporter gene in the same fashion, in both the RRL and WGE systems. Addition of GST had no effect on translation of the reporter RNA (Fig. 4.2).

Furthermore, to test whether the VPgPro-mediated translation inhibition was linked to the sequestration of eIF(iso)4E by VPgPro, different concentrations of VPgPro were pre-incubated with *T. aestivum* eIF(iso)4E before addition to the translation reaction. Addition of 24 or 48 pmol of VPgPro inhibited capped luciferase RNA translation even in the presence of excess eIF(iso)4E (Fig. 4.3A). Miyoshi et al. (2005) have previously reported that the GST portion of GST-VPg interferes with the binding of TuMV VPg to eIF(iso)4E from *A. thaliana* in pull-down assays. However, in our study, GST-tagged TuMV VPgPro did interact with wheat eIF(iso)4E in enzyme-linked immunosorbent assay (ELISA)-based binding assays (Fig.4.3B). Binding was specific as no signal was detected in absence of primary antibody or when eIF(iso)4E was replaced with T7-tagged β-galactosidase.

4.4.4. TuMV VPgPro and NV VPg degrade reporter RNA

We monitored the fate of reporter RNA during *in vitro* translation to investigate how VPgs affect protein translation. After addition of luciferase RNA in the RRL in presence of GST or GST-VPgPro from TuMV, or in presence of NV VPg, RNA was collected at different times and purified. Figure 4.4 shows that reporter RNA is degraded when TuMV GST-VPgPro or NV GST-VPg, but not GST, is added to the translation assay. An incubation period as short as 5 min was sufficient to allow TuMV GST-VPgPro to degrade the reporter RNA. Ribosomal RNA was not affected by the addition of either protein to the *in vitro* RRL.

We tested whether or not RNA degradation was triggered by the absence of translation. Reporter RNA was incubated without added protein or with 48 pmol of GST or GST-VPgPro from TuMV in WGE in presence of cycloheximide. The addition of 600 μM of cycloheximide to the *in vitro* translation system completely inhibited translation of the reporter luciferase RNA since no light emission was detected (data not shown). Samples were collected at different times and RNA was electrophoresed, blotted and hybridized with a ^{32}P-labelled RNA probe complementary to the luciferase RNA. Figure 4.5 shows that the reporter luciferase RNA was degraded more rapidly in the presence of TuMV GST-VPgPro compared to controls where no protein was added or where GST was added.

4.4.5. TuMV VPgPro and NV VPg degrade total plant RNA

To test the involvement of cellular factors for the VPgPro ribonucleolytic activity, 48 pmol of TuMV GST-VPgPro, NV GST-VPg and GST were incubated with total plant

RNA. Figure 4.6A shows that TuMV GST-VPgPro and NV GST-VPg degraded total plant RNA within 30 min. In contrast with the RNA degradation observed in the *in vitro* translation system (see Fig. 4.4), ribosomal RNA was degraded by GST-VPgPro and GST-VPg. Total plant RNA incubated with GST was not degraded nor was the RNA sample incubated with no added protein.

4.4.6. The VPg domain of TuMV is sufficient for the degradation of total plant RNA

VPgPro auto-catalytically cleaves itself into two functional domains: VPg and Pro (Laliberté et al., 1992). Since NV VPg degraded RNA, we verified if the VPg domain of VPgPro was responsible for the observed ribonucleolytic activity. We constructed and purified the VPg domain of TuMV VPgPro and added the protein to total plant RNA. TuMV GST-VPg was able to degrade total plant RNA as efficiently as GST-VPgPro (Fig. 4.6B). No RNA degradation was observed when total RNA was incubated without protein or with GST.

4.4.7. Effect of EDTA and heat treatment on TuMV VPgPro ribonucleolytic activity

The requirement for divalent cations for VPgPro catalytic activity was tested by incubating total plant RNA with TuMV GST-VPgPro in increasing concentrations of EDTA. The results showed that GST-VPgPro nuclease activity was not completely inactivated by the addition of EDTA concentrations ranging from 1 to 10 mM (Fig. 4.7A). However, degradation products increased in size with increasing amounts of EDTA. To investigate whether RNA degradation is due to enzymatic cleavage, heat-

denatured GST-VPgPro was incubated with total plant RNA; no RNA degradation was observed (Fig. 4.7B).

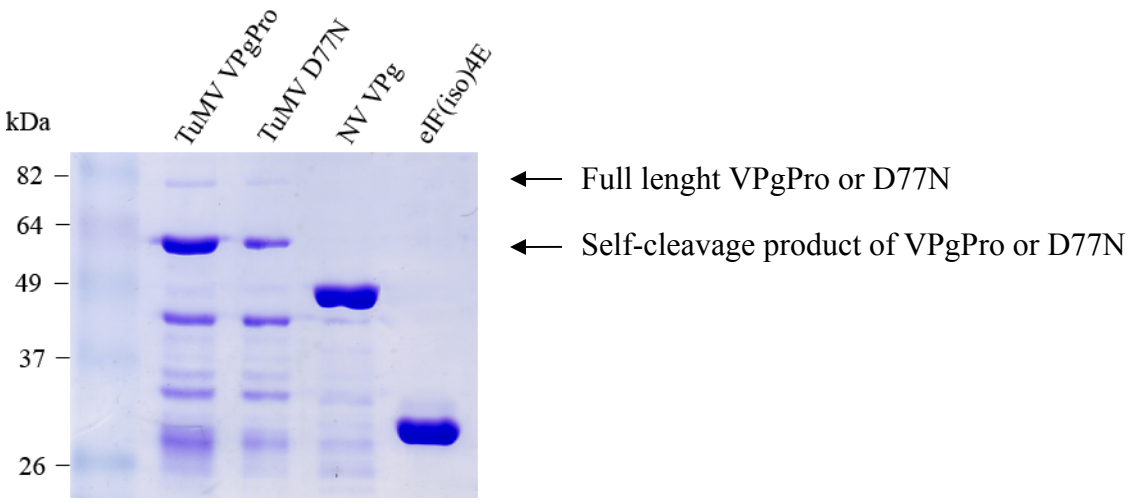

Figure 4.1: Expression and purification of GST-VPgPro and D77N of TuMV, GST-VPg of NV and wheat eIF(iso)4E as described under Materials and Methods. In both TuMV VPgPro and D77N protein preparations the prominent 55 kDa band corresponds to the self-cleavage product of VPgPro (or D77N) while the 82 kDa fainter band corresponds to the full length VPgPro species. Samples were loaded on a SDS-polyacrylamide gel and were stained with Coomassie blue.

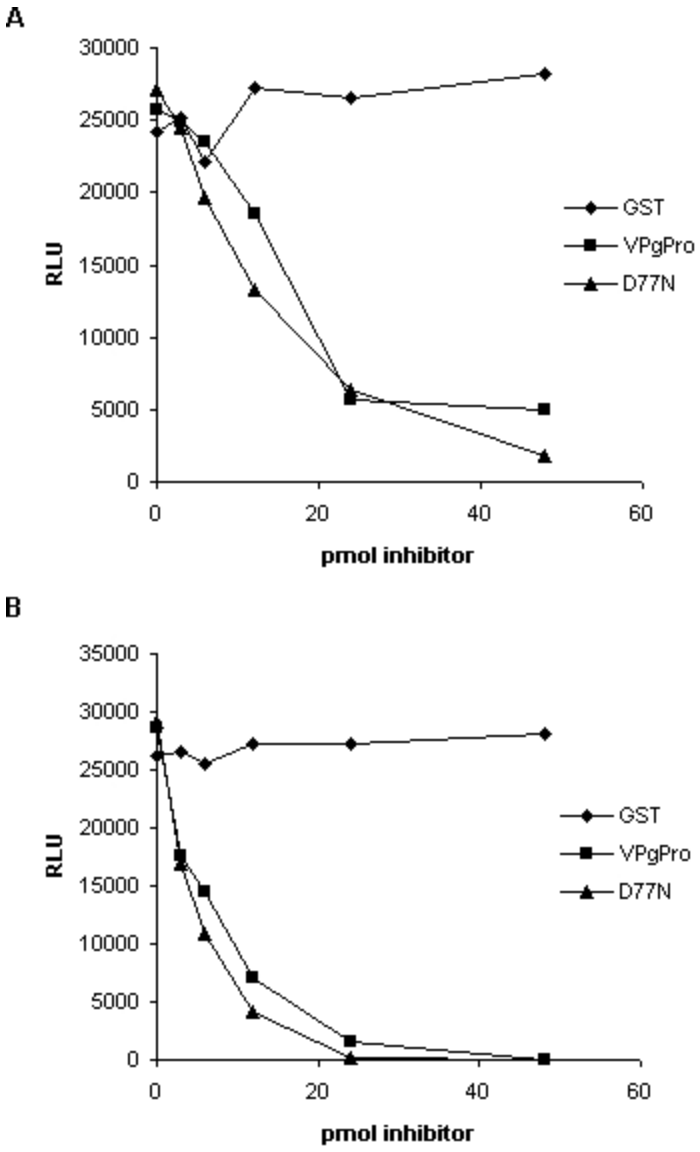

Figure 4.2: Translation inhibition of reporter RNA by GST-VPgPro. (A) Relative light units (RLU) of luciferase obtained when adding capped luciferase RNA in WGE translation system in the presence of GST, GST-VPgPro or GST-D77N. (B) Capped luciferase RNA was added to RRL translation system in the presence of GST, GST-VPgPro or GST-D77N and luciferase RLU was measured. These experiments were repeated at least three times.

Figure 4.3: Inhibition of translation of luciferase reporter RNA by GST-VPgPro in the presence of eIF(iso)4E. (A) Ratio of the luciferase light units (synthesized from capped luciferase RNA) from translation reactions containing GST-VPgPro over that of reactions containing GST in WGE incubated or not with eIF(iso)4E. (B) GST-VPgPro interaction with wheat T7-eIF(iso)4E as demonstrated by ELISA-based binding assay. Wells were coated with 1.5 µg of purified GST-VPgPro and incubated with 1.5 µg of *E. coli* recombinant T7-tagged eIF(iso)4E (bar 1) or T7-tagged β-galactosidase (bar 3). Protein retention was detected using a monoclonal anti-T7-tag antibody. Non-specific binding of the secondary antibody was verified by incubating VPgPro and eIF(iso)4E in absence of anti-T7 tag antibody (bar 2). Error bars represent the standard error of the mean. Groups a and b are statistically different ($p < 0.001$).

A

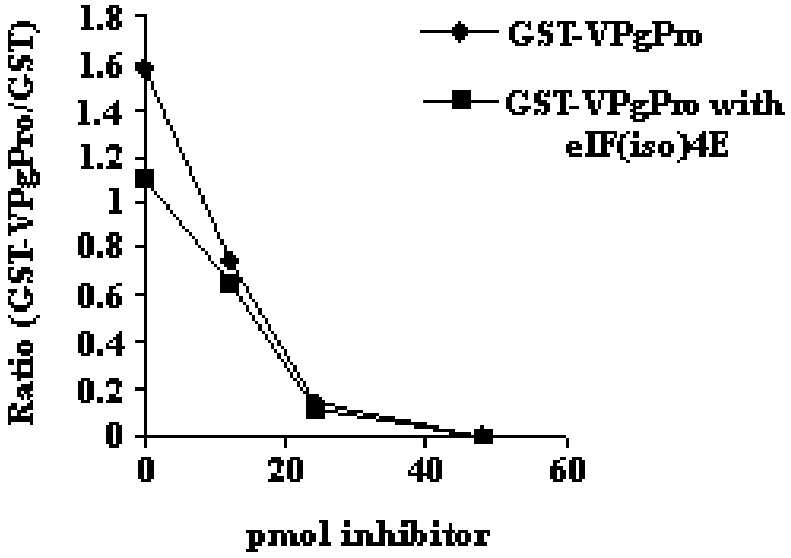
Ratio (GST-VPgPro/GST)
1.8
1.6
1.4
1.2
1
0.8
0.6
0.4
0.2
0
0
20
40
60
pmol inhibitor
GST-VPgPro
GST-VPgPro with eIF(iso)4E

B

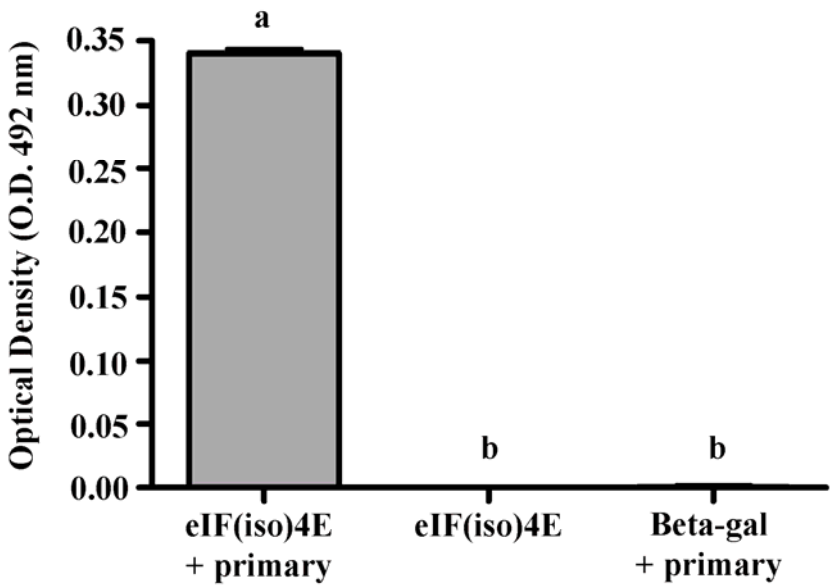
Optical Density (O.D. 492 nm)
0.35
0.30
0.25
0.20
0.15
0.10
0.05
0.00
a
b
b
eIF(iso)4E + primary
eIF(iso)4E
Beta-gal + primary

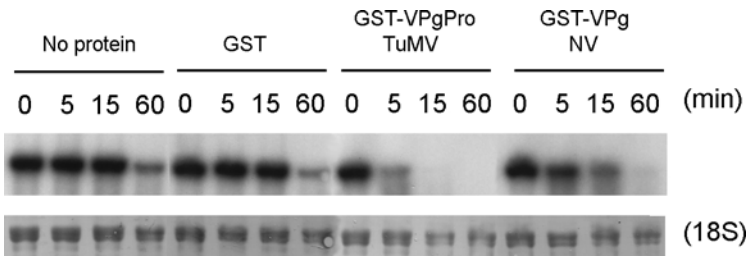

Figure 4.4: Reporter RNA degradation in the presence of GST, TuMV GST-VPgPro or NV GST-VPg in a RNA stability assay. The proteins were incubated in a RRL in the presence of capped luciferase RNA and RNA samples were collected at different time points. Total RNA was run on an agarose-formaldehyde gel and transferred to a nylon membrane which was incubated with a ^{32}P-labelled RNA probe complementary to luciferase RNA. The 18S rRNA was used as a loading reference.

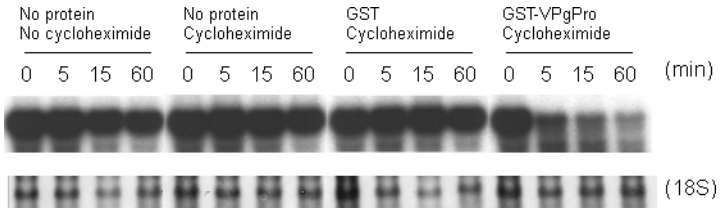

Figure 4.5: Reporter RNA degradation in the presence of GST or TuMV GST-VPgPro in absence of translation.48 pmol of GST or TuMV GST-VPgPro proteins were incubated in WGE in the presence of capped luciferase RNA with 600 μM of cycloheximide to arrest translation of the reporter RNA. Samples were collected at different times and RNA was purified. Total RNA was run on an agarose-formaldehyde gel and transferred to nylon. The membrane was incubated with a ^{32}P-labelled RNA probe complementary to luciferase RNA. 18S rRNA was used as a loading reference.

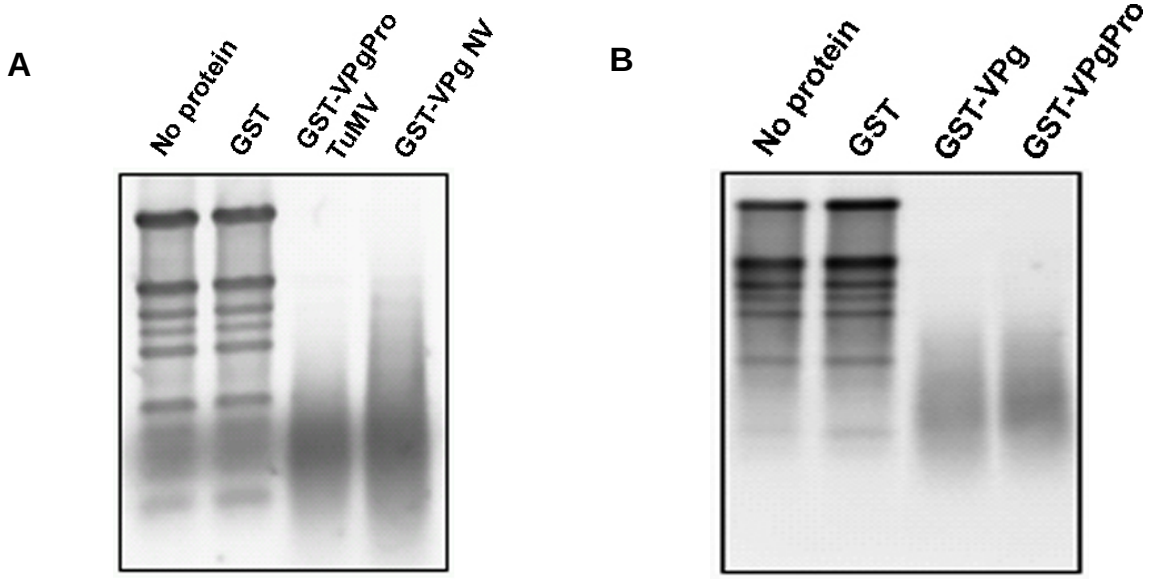

Figure 4.6: Plant total RNA degradation. (A) Plant total RNA degradation by GST-VPgPro of TuMV and GST-VPg of NV. Total RNA was incubated without protein or with 48 pmol of GST, TuMV GST-VPgPro or NV GST-VPg for 30 min. The RNA was purified, run on an agarose gel and stained with ethidium bromide. (B) Plant total RNA degradation by GST-VPg domain of TuMV. Total RNA was incubated without protein or with 48 pmol of GST, TuMV GST-VPg or TuMV GST-VPgPro for 30 min. The RNA was purified, run on an agarose gel and stained with ethidium bromide.

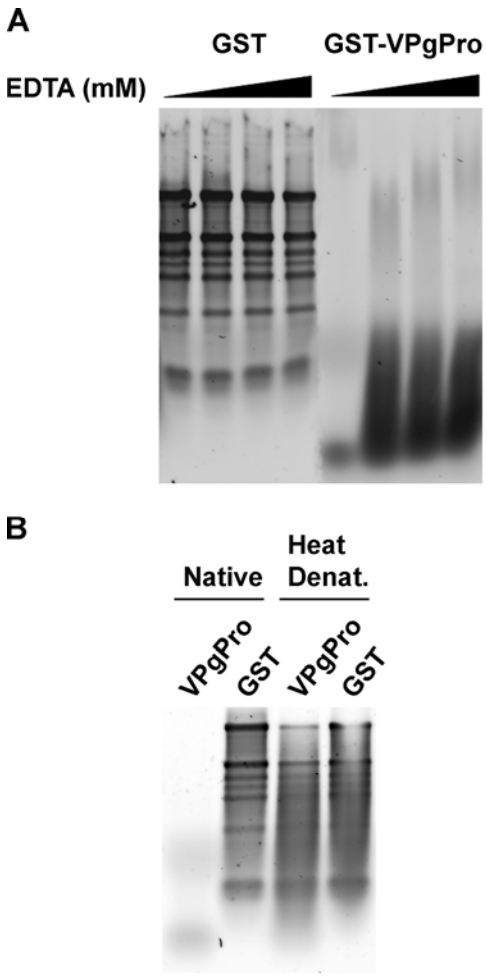

Figure 4.7: Effect of EDTA and heat denaturation on the RNase activity of TuMV VPgPro. (A) Total RNA was incubated with 48 pmol of GST or TuMV GST-VPgPro for 30 min at 25°C with increasing concentrations of EDTA (0, 1, 5, and 10 mM, as depicted by the sliding scale). (B) Total RNA was incubated with 48 pmol either native or heat denatured (95°C for 15 min) of GST or TuMV GST-VPgPro for 30 min at 25°C.

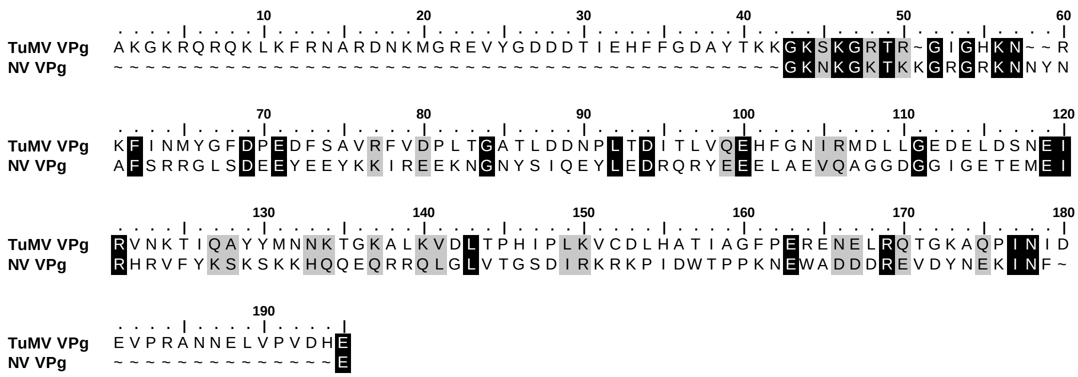

Figure 4.8: Alignment of TuMV VPg (NP_062866) and NV VPg (NP_786948). Gaps were introduced to obtain best alignment and are represented by the (~) symbol. Identical amino acids are found shaded in black and similar ones shaded in grey. The most conserved domain is found for amino acids residues at position 43-56 for TuMV VPg and 1-15 for NV VPg (60% identity and 80% similarity). This conserved region overlaps with previously experimentally validated potyviral VPg NTP binding domain (Puustinen and Makinen, 2004) found at position 38-51 in TuMV VPg. Alignment was performed using the BioEdit alignment program.

4.5. Discussion

One of the roles of the cap structure found at the 5′ end of most eukaryotic mRNAs and some viral RNAs is to interact with the cellular host translation initiation machinery, namely the eIF4F complex (Pestova and Hellen, 2000). eIF4E is part of this complex and recognizes the 5′ cap structure which will eventually lead to the recruitment of the small ribosomal subunit (reviewed by Sachs et al., 1997). The presence of a VPg at the 5′ end of many viral RNAs suggests that a different mechanism is at play for translation initiation of these viral genomes.

Potyvirus VPgs have been shown to interact with eIF4E isoforms (Kang et al., 2005; Myoshi et al., 2005; Wittmann et al., 1997), as is also the case for calicivirus VPg (Goodfellow et al., 2005). The VPg-eIF4E interaction is important for virus infection since mutations in either VPg or eIF4E of potyviruses lead to the reduction of symptoms or the absence of infection (Duprat et al., 2002; Lellis et al., 2002; Léonard et al., 2000). TuMV VPgPro can also interact with PABP *in planta* (Léonard et al., 2004). Interaction of VPg proteins with translation factors has lead to the suggestion that they may play a critical role in assembly of the viral translation initiation complex (Daughenbaugh et al., 2003; Léonard et al., 2004). The VPg of caliciviruses was shown to act as a 'cap substitute' for viral RNA translation and the effect is dependent on the interaction with eIF4E. However, it is paradoxical that the addition of NV VPg to an *in vitro* translation system was found to inhibit translation of reporter RNAs (Daughenbaugh et al., 2003).

We report here on the effect of TuMV VPgPro on mRNA translation *in vitro*. We show that recombinant VPgPro inhibits translation of capped reporter RNA, both in plant and animal *in vitro* translation systems. One hypothesis that would explain the effect of

VPg on translation is that sequestration of eIF(iso)4E by VPgPro in the extract could interfere with translation. eIF4E has been reported to be the least abundant translation factor, and perhaps the rate limiting one, in animal cells (Duncan et al., 1987). However, the inhibition of translation was not relieved by addition of supplementary eIF(iso)4E in the translation system. A VPgPro mutant that could no longer interact with eIF(iso)4E (Léonard et al., 2000) was also tested. The mutant could still inhibit translation. Our results do not support the hypothesis that the interaction between VPgPro-eIF(iso)4E is responsible for the inhibition of translation.

Given these results, we investigated whether the presence of VPg or VPgPro in the translation system could have a destabilizing effect on the reporter RNA. The addition of TuMV GST-VPgPro led to the degradation of reporter RNA over time. RNA remained intact when GST protein purified in the same way as VPgPro was added to the translation system. The effect was linked to the presence of VPgPro as the rest of the fusion protein expressed without viral sequences did not lead to RNA degradation, therefore eliminating the possibility that a contaminating RNase from *E. coli* was co-purified along with the fusion tags. RNA degradation was not the result of translation inhibition as it was observed in translation reactions arrested by the addition of cycloheximide; RNA degradation was observed only in samples that contained VPgPro protein.

Daughenbaugh et al. (2003) also observed an inhibition of translation when NV VPg was added to an *in vitro* translation system. We speculated that both the NV VPg and TuMV VPgPro proteins inhibit translation through RNA destabilisation and/or degradation. In our experiments, the addition of NV to the *in vitro* translation system lead to the degradation of reporter RNAs as was observed for TuMV. Given that the TuMV

VPgPro and NV VPg proteins were purified according to different protocols and share little homology, it is unlikely that both proteins interact with the same contaminating RNAse from *E. coli*. Since the VPg protein was always prominent versus the full length VPgPro protein in the protein preparation, we examined the capacity of the VPg domain alone to degrade RNA. As seen with NV, we also observed that the VPg domain of TuMV was sufficient for RNA degradation. The proteinase portion of VPgPro was not required for ribonuclease activity.

We studied the effect of purified recombinant proteins incubated with total plant RNA, without the components of a translation reaction. Purified RNA was degraded in the presence of either TuMV GST-VPgPro or NV GST-VPg. This suggests that both proteins have a ribonucleolytic activity *in vitro* without the need for cellular factors. The ribonuclease activity is therefore associated with the VPg, and is not the result of the activation of a latent RNAse activity from a cellular protein present in the translation system.

Since both NV and TuMV VPg displayed RNAse activity, we examined the two sequences for homology; alignment of the two sequences revealed less than 13% overall identity (Fig. 4.8). A stretch of 15 amino acids is well conserved between the two proteins (60% identity and 80% similarity). This region overlaps with the nucleotide tri-phosphate binding domain identified and experimentally confirmed for *Potato virus A*, another potyvirus (Puustinen and Makinen, 2004). A phosphate-binding site may be correlated with a ribonuclease activity as was observed in other plant ribonucleases with no clear homology to known ribonucleases (Bantignies et al., 2000; Hoffmann-Sommergruber et al., 1997).

The RNAse activity displays the characteristic feature of an enzyme, i.e. sensitivity to heat denaturation. The ribonuclease activity of VPgPro was not completely inactivated by the addition of EDTA. This is not uncommon as EDTA insensitive RNases are widespread and have been previously reported in different organisms (Mishra, 2002; Yen and Green, 1991).

It was previously shown that potyvirus replication is associated with disappearance of cellular mRNAs. It was suggested that host mRNA shutoff could be achieved, in part, through the degradation of host transcripts (Aranda et al., 1996). Interestingly, viral proteins inducing host shutoff through their ability to degrade host mRNAs have been reported for many animal viruses (Hulst and Moormann, 2001; Laidlaw et al., 1998; Smiley et al., 2001). For example, proteins of RNA viruses such as the Influenza virus, Leishmania RNA virus 1-4, of flaviviruses and of coronaviruses were shown to have ribonuclease activity (Bhardwaj et al., 2004; Hulst and Moormann, 2001; Klumpp et al., 2001; Ro and Patterson, 2000). We hypothesize that TuMV VPg contributes to host mRNA degradation through its ribonucleolytic activity. TuMV could enhance its access to the translation and replication components of the cell by degrading host mRNAs. For example, influenza virus proteins, using a similar strategy, binds to capped mRNA and hnRNA molecules in the nucleus of infected cells and cleave the capped host RNA molecules (Klumpp et al., 2001).

The VPgPro of PVBV was shown to have DNase activity (Anindya and Savithri, 2004) and could explain in part the transcriptional shutdown associated with potyviral infection (Aranda and Maule, 1998). The D77N mutation, which impairs eIF(iso)4E binding, did not result in reduction of translation inhibition or ribonuclease activity. This

is interesting in light of the results obtained by Anyanda et al., 2004) with the D81N mutant of PVBV (equivalent to D77N mutant of TuMV) which showed reduced DNase activity. The eIF4E-interacting domain does not seem to be important for VPg ribonuclease activity; this suggests that distinct regions of VPg might be important for its nuclease activities.

It is interesting that rRNA was degraded when VPgPro was added to purified plant RNA (i.e. where proteins had been removed). However, rRNA remained intact but reporter RNA was degraded when VPg was added to RRL translation system. The unspecific RNase activity displayed by VPg raises the question of how TuMV protects its own RNA against degradation. It is possible that cellular factors present in infected plant cells (and absent from the *in vitro* translation systems) regulate VPg's ribonucleolytic activity. Consistent with this hypothesis is the observation that the RNase activity associated with the herpes simplex virus vhs protein exhibits a higher specificity *in vivo* (Krikorian and Read, 1991; Kwong and Frenkel, 1987; Oroskar and Read, 1989; Zelus et al., 1996) than in an *in vitro* RRL (Lu et al., 2001). Vhs-mediated host shutoff is characterized by disruption of pre-existing polyribosomes, and accelerated turnover of host mRNA. Vhs displays little sequence specificity *in vitro* and targets most, if not all, cellular and viral mRNAs, *in vivo* other cytoplasmic transcripts such as rRNA, tRNA and 7SL RNA are spared during infection. We speculate that rRNA was not degraded in our *in vitro* translation system because of the protection offered by the ribosome ribo-nucleoprotein complex. The number of host proteins involved in replication/translation of virus RNA is growing and the involvement of a large ribonucleoprotein complex is an emerging theme across positive-strand RNA viruses (reviewed by Thivierge et al., 2005).

It is also possible that the ribonucleoprotein complex formed during replication and translation of the viral RNA may protect that RNA from degradation, as we observed with rRNA embedded in ribosomes. The association of viral RNA with different cellular factors, perhaps as a result of different subcellular localizations, may regulate the specificity of the nucleolytic activity. It is also possible that the conditions used *in vitro* altered the specificity of the activity. The localization of ribonuclease activity to the nucleus, and not the cytoplasm, would allow an extensive reprogramming of host gene expression while protecting viral RNA. The VPgPro protein of potyviruses is normally found in the nucleus of infected cells (Schaad et al., 1996).

In this report, we have shown *in vitro* that TuMV VPg exhibits an RNase activity. The involvement of VPg as stimulator of viral translation by acting as a cap substitute and its participation in host mRNA translation shutoff by acting as a nuclease are not mutually exclusive activities. VPg may interact with eIF4E isoforms to facilitate the recruitment of the host translation apparatus to its RNA, while removing host mRNAs to reduce competition. Further work is needed however to assess the role of VPg RNase activity during potyvirus infection *in planta* and how TuMV's RNA, if it's the case, avoids degradation.

CONNECTING STATEMENT BETWEEN CHAPTERS IV AND V

In chapters III, we identified plant interactors of the TuMV viral replicase using the TAP procedure. This chapter describes the use of the yeast two-hybrid system to identify cellular factors that interact with the TuMV P3 protein. One host factor, a GDSL-lipase, was found to interact with the viral protein. This chapter also reports the cellular localization of P3 and its lipase interactor using confocal microscopy. The biological relevance of this interaction was further analyzed in TuMV infected *A. thaliana* lipase knockout plants. The role of this interaction in the viral replication cycle is discussed in the following chapter.

The results of this section are the subject of a manuscript that is in preparation. I have designed the experimental set-up, conducted all of the laboratory experiments, and wrote the manuscript. Christine Ide assisted me in the yeast two-hybrid assay and in the plant RNA extraction. Professor M. G. Fortin provided funding throughout the study. Drs S. Jabaji and J.-F. Laliberté contributed to the overall design of the manuscript and its correction.

CHAPTER V

Identification and characterization of a turnip mosaic virus P3-interacting protein: GDSL-lipase Protein.

K. Thivierge[1], C. Ide[1], S. H. Jabaji[1], J.-F. Laliberté[2], and M. G. Fortin[3]

[1]Department of Plant Science, McGill University, 21,111 Lakeshore, Ste-Anne-de-Bellevue, Québec, Canada H9X 3V9. [2] Institut national de la recherche scientifique, Institut Armand-Frappier, 531 Boulevard des Prairies, Laval, Québec, Canada H7V 1B7. [3]Agriculture and Agri-Food Canada, 930 Carling Avenue, Ottawa, Ontario, Canada K1A 0C7.

5.1. Abstract

Turnip mosaic virus (TuMV; *Potyviridae*) has a single-stranded, positive-sense RNA genome, encoding a large polyprotein that is cleaved into 10 proteins, including the non-structural P3 protein. P3 has been identified as a key component of host-viral interactions specifying both pathogenicity and virulence. Its roles in these two processes suggest that different host factors interact with P3 during virus infection. By using a yeast two-hybrid system (YTHS), P3 was found to interact with a GDSL-lipase protein, the product of the At1g29670 gene. An enzyme-linked immunosorbent assay (ELISA)-based binding assay confirmed the specificity of the interaction. Lipase and P3 were expressed as full-length fluorescent protein fusions in *Nicotiana benthamiana*, and their subcellular localizations were visualized by confocal microscopy. P3 was observed in the cytoplasm and in association with the endoplasmic reticulum (ER), and the lipase protein was localized in the cytoplasm to be eventually excreted out of the cell. Co-expression of P3 and lipase fusions revealed that the two proteins partially co-localized in the cytoplasm of the cell. To assess the role of the lipase-P3 interaction during TuMV infection, the infection of TuMV in *lipase* T-DNA insertional *Arabidopsis thaliana* mutant (gene At1g29670) was analyzed. Our results show that viral replication was not affected in the *lipase* knockout plants. Possibly, the remaining lipase-coding genes can compensate for the loss of the disrupted one to allow viral replication or plant defense. Given the involvement of lipases in the induction of defense responses, the interaction between P3 and a GDSL-lipase reinforces the importance of the P3 protein as a symptom determinant.

5.2. Introduction

Infection by plant viruses relies on a number of processes such as viral genome amplification, cell-to-cell movement, long distance movement and aphid transmission, in which host factors play an essential role (Nagy, 2008). Defense mechanisms such as the hypersensitive response (HR) or the systemic acquired resistance (SAR) also involve interactions between the plant and the pathogen (Loake and Grant, 2007). These interactions may cause symptom development and serious diseases in the infected plants. Thus, identification of host proteins that interact with viral proteins is informative on the molecular events that must occur for successful infection and is also helpful for the development of antiviral strategies and viral resistant plants.

TuMV is a member of the large and economically important genus *Potyvirus* of the family *Potyviridae*. Its genome consists of a positive polarity single-stranded RNA molecule encoding one large open reading frame (ORF). This genomic RNA is translated into a polyprotein that is proteolitically cleaved by three self-encoded proteinases to produce 10 mature proteins, including the non-structural P3 protein (Riechmann et al., 1992). Little is known about the function of P3 in the infection cycle, but it has been suggested that P3 plays a role in virus movement (Dougherty and Semler, 1993) and as a protease co-factor (Riechmann et al., 1995). Its participation in viral replication was postulated through an interaction with the viral helicase (Guo et al., 2001; Merits et al., 1999) although P3 lacks RNA binding activity (Merits et al., 1998). The primary structure of P3 protein contains one or two putative hydrophobic domains, which suggests its possible membrane-bound character (Kyte and Doolittle, 1982; Rodriguez-Cerezo and Shaw, 1991). Attempts to localize P3 in infected plant cells using

immunogold labeling have led to inconsistent results. The protein was found either in association with viral cylindrical inclusion (CI) protein in the cytoplasm (Rodriguez-Cerezo et al., 1993) or in association with viral nuclear inclusion b (NIb) and nuclear inclusion a (NIa) proteins inside the nucleus of infected cells (Langenberg and Zhang, 1997). More recently, P3 of *Papaya ringspot virus* was shown to localize at the ER when expressed as a green fluorescent-tagged protein (Eiamtanasate et al., 2007).

P3 protein is the most variable component of the polyprotein among the genus members (Shulka et al., 1994), suggesting its role in virus-host interactions. Published evidence supporting a correspondence between the potyviral P3-$6K_1$ region and hypothetical host factors comes from recent studies linking P3-$6K_1$ to host range. In TuMV, the C-terminal part of P3-$6K_1$ was shown to be an important factor in determining the viral host range and the type symptoms (Suehiro et al., 2004). Additionally, a substitution in the C-terminal P3 region was shown to be associated with adaptation of TuMV from *Brassica rapa* to *Raphanus sativus* (Tan et al., 2005). Thus, the role of P3 in pathogenicity determination and host resistance suggests that different host proteins may interact directly with P3 during virus infection. However, to date, direct protein-protein interaction between P3 and a host protein has not been characterized. The YTHS has been successfully used to identify host proteins that interact with potyviral proteins such as HC-Pro (Anandalakshmi et al., 2000; Guo et al., 2003), viral genome-linked protein (VPg) (Dunoyer et al., 2004; Léonard et al., 2000; Schaad et al., 2000; Wittmann et al., 1997), NIb (Wang et al., 2000) or CI (Jimenez et al., 2006). In this study, the TuMV P3 protein was used as a bait to screen an *A. thaliana* cDNA library in the YTHS. The host GDSL-lipase protein was identified as a P3-interacting protein, and the cellular

localization of the interaction was studied by confocal microscopy. A partial co-localization between the viral and the host proteins was observed in the cytoplasm of the cell. The relevance of this interaction was studied by analyzing the effect of the complete abolition of the lipase gene in TuMV infection.

5.3. Materials and Methods

5.3.1. Yeast Two-Hybrid Screening and Analysis

The ProQuest™ YTHS (Invitrogen, Carlsbad, CA, USA) was used to screen for interacting partners of TuMV P3. Construction of P3 in frame with the GAL4 DNA binding domain (DBD) was performed using GATEWAY technology (Invitrogen). The P3 coding sequence was amplified by polymerase chain reaction (PCR) from full-length TuMV UK1 p35Tunos (Sanchez et al., 1998) using primer set P3F-pENTR and P3R-pENTR (Table 5.1). The purified PCR product was cloned in pENTR™/D-TOPO® vector (Invitrogen) and the attL sites within this clone were used to clone the P3 in the pDEST™32 vector with LR clonase according to the manufacturer's recommendation (Invitrogen). Sequencing (Genome Quebec Center at McGill University) confirmed that the P3 gene was in frame with the GAL4 DBD sequence in pDEST™32.

The *A. thaliana* cDNA library was constructed in the pDEST™22 vector (Invitrogen) that produces proteins fused to the yeast GAL4 activation domain (AD). The dsDNA from the SuperScript Pre-made cDNA *A. thaliana* library (Invitrogen #11474-012) was prepared with the S.N.A.P. MidiPrep Kit according to the manufacturer's instruction (Invitrogen). The Entry library was created using pDONR-221 vector (Invitrogen) as the

donor plasmid. Plasmid pDEST^{TM}22 was used as destination vector to generate the *A. thaliana* AD library. The BP clonase reaction to introduce *A. thaliana* dsDNA into pDONR-221 vector, and the LR clonase reaction to transfer the Entry library from the pDONR-221 to the pDEST^{TM}22 vectors to create the AD library were carried out according to the manufacturer's instructions (Invitrogen).

Screening was performed by sequential transformation of bait and library vectors in the *Saccharomyces cerevisiae* reporter strain MaV203 (*MATα leu*2-3, 112, *trp* 1-901, *his*3Δ200, *ade*2-101, *gal*4Δ, *gal*80Δ, *SPAL*10::*URA*3, *GAL*1::*lacZ*, *HIS*3$_{UAS\ GAL1}$::*HIS*3@*LYS*2, *can*1^{R}, *cyh*2^{R}) according to the manufacturer's instructions. Approximately 1.6 million clones were screened for interaction with P3. Transformants were plated on SC-Leu-Trp-Ura-His + 3-aminotriazole (3-AT) (50 mM) and incubated at 30°C for 72 hrs. Positive clones were confirmed using the ProQuest Two-Hybrid system protocol (including replicating, replica cleaning, β-D-galactosidase analysis, and retransformation assay). The interacting partners were sequenced and homology searches were performed using the BLAST algorithm from the *Arabidopsis Information Resource* (www.arabidopsis.org). All culture media used in these studies were prepared according to ProQuest Two-Hybrid system protocols.

5.3.2. Bacterial and plant expression constructs

The sequence encoding P3 was PCR-amplified from the full-length TuMV cDNA clone p35Tunos (Sanchez et al., 1998) using primer set P3F-*Eco*RI and P3R-*Not*I (Table 5.1). The resulting fragment was digested with *Eco*RI/*Not*I and ligated into similarly digested pGEX-6P1 (Amersham Biosciences, Baie d'Urfé, Qc, Canada). The resulting

plasmid was identified as pGEX-P3-glutathione-S-transferase (GST). pETLipase-his encodes a His/T7-tailed lipase of *A. thaliana* (At1g29670; GenBank accession no. **AY065046**) and was produced as follows. *A. thaliana* lipase sequence was PCR-amplified from cDNA clone pda02401 (RIKEN) using primers LipaseF-*Bam*HI and LipaseR-*Not*I (Table 5.1). The amplified fragment was digested with *Bam*HI/*Not*I and cloned into similarly digested pET28(a) (Novagen, Gibbstown, NJ, USA).

Plasmids for co-localization were constructed as follows. The sequence of lipase protein was PCR-amplified from full length ORF clone pda02401 using primers LipaseF mCherry-*Xba*I and LipaseR mCherry-*Bam*HI (Table 5.1) and inserted into the *Xba*I/*Bam*HI sites of pCambia/mCherry. P3 sequence was PCR-amplified from p35Tunos (Sanchez et al., 1998) with primers P3F EGFP-*Sac*I and P3R EGFP-*Sac*I (Table 5.1). The amplified fragment was digested with *Sac*I and cloned into similarly digested pCambia/EGFP. The resulting plasmids were identified as pCambia/lipase-mCherry and pCambia/P3-EGFP, respectively. All PCR amplifications were performed with *Pfu* Turbo polymerase (Stratagene, Kirkland, WA, USA) and all plasmid constructs were verified by sequencing at Genome Quebec Center at McGill University. The plasmids pCambia/mCherry and pCambia/EGFP have previously been described (Beauchemin et al., 2007; Dufresne et al., 2008a). The construction of the plasma membrane (PM) marker was previously described (Ivanchenko et al., 2000; Prokhnevsky et al., 2005).

5.3.3. Expression and purification of recombinant proteins in *E. coli*

The recombinant plasmid pGEX-P3-GST was introduced into *Escherichia coli* BL21. BL21 *E. coli* cells containing recombinant plasmids were cultured at 37 °C to an

OD_{600} of 0.6 and protein expression was induced with 1 mM isopropyl-β-D-galactopyranoside (IPTG) for 3 hrs at 30°C. Bacterial cells were centrifuged, resuspended in buffer A (4.3 mM Na_2HPO_4, 1.47 mM KH_2PO_4, 137 mM NaCl, 2.7 mM KCl, pH 7.3), disrupted by sonication and the lysate was centrifuged at 39,000 × *g* for 20 min. The supernatant was used for affinity purification of GST–P3. The protein extract was added to GST-Bind resin (Novagen) according to the manufacturer's protocol and incubated at 4°C for 1 hr. Beads were washed three times with buffer A and collected by centrifugation for five min at 500 × *g*. The fusion proteins were eluted from the resin in a buffer containing 10 mM reduced glutathione and 50 mM Tris–HCl pH 8.0. GST controls (the pGEX-6P1 vector without insert) was expressed and purified using the same conditions.

The recombinant plasmid pETLipase-his was introduced into *E. coli* BL21 (DE3). *E. coli* cells containing recombinant plasmids were cultured at 37°C to an OD_{600} of 0.6 and protein expression was induced with 1 mM IPTG for four hrs at 37°C. Bacterial cells were collected by centrifugation and resuspended in lysis buffer (100 mM NaH_2PO_4, 10 mM Tris-HCl, 8 M urea, pH 8). The cells were stirred at room temperature for 1 hr and the resulting lysate centrifuged at 10, 000 × *g* for 20 min to pellet the cellular debris. The supernatant was incubated with Ni-NTA resin (Novagen) for 1 hr at room temperature. The resin was washed with lysis buffer pH 6.3 and bound proteins were eluted using the same buffer but at pH 4.5. The purified proteins were extensively dialyzed against 20 mM NaCl, 10 mM Tris-HCl pH 8.0. Concentration of all recombinant proteins was measured using a Bradford assay (Bio-Rad, Mississauga, On, Canada) using bovine serum albumin (BSA) as standard. Protein purity and molecular weight was assessed by

Coomassie staining and immunoblot analysis using monoclonal anti-GST (Novagen) for GST-P3, and monoclonal anti-histidine (Novagen) for his-tagged lipase (data not shown).

5.3.4. ELISA-based binding assay

A. thaliana lipase protein (100 µl of protein at 15 ng μl^{-1} in PBS buffer) was adsorbed to wells of a polystyrene plate (Costar, San Diego, CA, USA) by overnight incubation at 4°C and wells were blocked with 5% milk PBS solution for two hrs at room temperature. GST-P3 or GST proteins were diluted in PBS with 1% milk and 0.1% Tween 20 and incubated for 1.5 hr at 4°C in the previously coated wells. Detection of retained protein was achieved with a rabbit polyclonal anti-GST-tag (Invitrogen) followed by a horseradish peroxidase (HRP)-coupled goat anti-mouse immunoglobulin (Pierce, Rockford, IL, USA). Wells were washed several times with PBS supplemented with 0.05% Tween 20 between incubations. Enzymatic reactions were performed in 100 µl of o-phenylenediamine dihydrochloride (OPD) citrate buffer (50 mM citric acid, 100 mM sodium phosphate dibasic, pH 5.0, 0.5 mg/ml OPD and 0.1% hydrogen peroxide) and stopped with a solution of 3 M H_2SO_4. Absorbance was measured at 492 nm. Standard error of the mean (SEM) was calculated for three biological replicates from a minimum of three technical replicates.

5.3.5. Agroinfiltration and confocal microscopy

Binary vectors containing genes for fluorescent fusion proteins were transformed into *Agrobacterium tumefaciens* AGL1 by electroporation and the transformed cells

containing the binary vector were used for agroinfiltration assays. Overnight bacterial cultures were centrifuged, and the pellet was resuspended in water supplemented with 10 mM $MgCl_2$ and 150 mM acetosyringone. The resulting preparation was used to agroinfiltrate two leaves of 3-week-old *N. benthamiana* plants. For optimal expression of the fusion proteins, the P19 protein of *Tomato bushy stunt virus* (TBSV) was coexpressed in the agroinfiltrated plant cells to prevent induction of posttranscriptional gene silencing (Qu and Morris, 2002). After infiltration, the plants were kept for 2 to 5 days in a growth chamber at 22°C/18°C (day/night) temperature regime with a photoperiod of 16 hrs of light/8 hrs of dark. Irradiance was set at 150 µmol m^{-2} sec^{-1} with fluorescent and incandescent lights.

Confocal microscope visualization was carried out as previously described (Beauchemin and Laliberté, 2007). Briefly, sections (1 cm^2) from agroinfiltrated leaves were cut out and placed in immersion oil on a microscope coverslide. Individual cells were observed with a 40 X oil immersion objective on a Radiance 2000 confocal microscope (Bio-Rad). Fluorescent proteins were excited with Argon-Krypton laser. The data for green and red channels were collected simultaneously. Images were collected with a charge-coupled-device camera and treated with Adobe Photoshop or Image J (http://rsb.info.nih.gov/ij/) software.

5.3.6. Plant material, growth conditions and confirmation of *lipase* knockout

Potential *lipase* (SALK_005724C) T-DNA insertion mutant T4 line from the SALK T-DNA collection (Alonso et al., 2003) was obtained from the Ohio State University Arabidopsis Biological Resource Center seed collection. Seeds of wild-type

and *lipase* knockout plants were grown on peat-based growing medium and fertilized with 13-13-13 (N-P-K) slow-release fertilizer. Plants were grown at 22°C/18°C (day/night) temperature regime with a photoperiod of 16 hrs of light/8 hrs of dark in a growth chamber. Irradiance was set at 150 µmol m^{-2} sec^{-1} with fluorescent and incandescent lights.

The *lipase* homozygous mutant plants were first confirmed by PCR using a T-DNA left border primer (LBb1; Table 5.1) and gene specific primers (SALK_005724cLP and SALK_005724cRP; Table 5.1) designed using the SiGnAL iSect T-DNA primer design tool (http://signal.salk.edu/tdnaprimers.2.html). Genomic DNA was extracted using the DNeasy plant mini-kit (Qiagen, Mississauga, On, Canada). PCR parameters were 94°C for 4 min for initial denaturation, 32 cycles of 94 °C for 30 sec, 50°C for 30 sec, 72°C for 1 min, and 72°C for 7 min for the final extension. The 25 µl reactions were composed of 2mM dNTPs, 1 U of *Pfu* Turbo polymerase (Stratagene), 500 nM of each forward and reverse primers, 20 mM Tris-Cl (pH 8.8), 2 mM $MgSO_4$, 10 mM KCl, 10 mM $(NH_4)_2SO_4$, 0.1% Triton X-100, and 0.1 mg/ml nuclease-free BSA. PCR products were separated on 1 % TBE agarose gels. *Lipase* homozygous mutant plants were further characterized by Reverse transcription reverse-transcriptase PCR (RT-PCR). Total RNA was isolated as described in section 5.3.8. Two µl of cDNA were amplified using gene specific primers FcDNA and RcDNA (Table 5.1) in a 25 µl PCR reaction. The gene encoding actin, *ACTIN2* (*ACT2*) (At3g18780) mRNA was used as a positive control for amplification. PCR parameters and electrophoresis conditions were as described in section 5.3.6.

5.3.7. TuMV inoculation of *A. thaliana*

Three weeks-old wild-type and *lipase* knockout plants were infected with TuMV by rubbing fresh extract of previously infected plants (1 g in 2 ml of 5 mM sodium phosphate buffer pH 7.4) onto leaves dusted with Carborundum. Leaves were collected at 4, 7 and 21 days post-infection and freeze dried in liquid nitrogen until further used. Plants were kept in a growth chamber at 16 hrs of light/8 hrs of dark at 22°C/18°C (day/night) temperature regime.

5.3.8. RNA isolation and quantitative real-time RT-PCR analysis

Total RNA was isolated from 4, 7, and 17 days post infection (dpi) of wild-type and *lipase* mutant *A. thaliana* plants using the RNeasy plant mini-kit (Qiagen). The concentration of total RNA was determined by measuring absorbance at 260 nm using a Nanodrop spectrophotometer (Nanodrop Technologies, Wilmington, DE, USA). RNAs (1 µg aliquots) were reverse-transcribed to cDNA using the Omniscript RT Kit (Qiagen) according to the manufacturer's protocol and treated with RNase-free DNAse I (Qiagen).

Quantitative real-time RT-PCR was performed in a 25 µl reaction using SYBR Green MasterMix (Stratagene) on a MX3000p thermal cycler (Stratagene). The thermal cycling conditions were 10 min at 95 °C, 40 to 55 cycles of 30 sec at 95°C, 45 sec at 56 or 55°C and 45 sec at 72°C, followed by melting curve analysis. Relative amounts of all mRNAs were calculated from threshold cycle values and standard curves. In calculating relative expression ratios, the reference gene *ACT2* was used for normalization and differences in PCR efficiency was taken into account according to the following formula: Ratio = $(E_{target})^{\Delta CP\ target\ (control\text{-}sample)}$/ $(E_{ref})^{\Delta CP\ ref\ (control\text{-}sample)}$ (Pfaffl, 2001). RNA samples for each

time point were independently extracted three times from a pool of four different plants and quantitative real-time PCR was repeated twice. Primer set CP-F and CP-R was used for TuMV detection while primers ACT2F and ACT2R were used to amplify the reference gene (Table 5.1).

5.3.9. Immunoblot analysis of wild-type and *lipase* mutants

Protein extracts were prepared from 4, 7, and 17 dpi of wild-type and *lipase* mutant *A. thaliana* plants as follow. Total protein extracts were prepared by grinding leaf tissue (0.5 g) in four volumes (2 ml) of protein extraction buffer (50 mM Tris-HCl pH 7.5, 50 mM KCl, 0.5 mM EDTA, 20 mM NaCl, 5% (v/v) glycerol, 0.1% (v/v) Triton-100, 0.01% (w/v) sodium dodecyl sulfate (SDS), and 1mM phenylmethanesulphonyl fluoride). The supernatant was collected by centrifugation at 5 000 x *g* for 1 min and the protein concentration of each sample was measured using the Bradford assay (Bio-Rad). For each sample, 25 µg of proteins were resolved on SDS-polyacrylamide electrophoresis (SDS-PAGE) gel (10% acrylamide), electroblotted to nitrocellulose membrane (Bio-Rad) and subjected to Western blot analysis. Coat protein (CP) and actin protein were immuno-detected with a polyclonal rabbit anti-CP or monoclonal mouse anti-AtActin8 (Sigma-Aldrich, St-Louis, MO, USA) using a goat anti-rabbit or goat anti-mouse HRP-coupled antibody (Pierce) using the SuperSignal West Pico chemiluminescent substrate (Pierce).

5.3.10. Mouse monoclonal and rabbit polyclonal antibodies

The primary antibodies were used as follows: rabbit polyclonal anti-green fluorescent protein (GFP) 1:1000 (Invitrogen) and mouse monoclonal Anti-Actin (plant) 1:1000 (Sigma-Aldrich).

The recombinant clone pET-CP in *E. coli* BL21 (DE3) cells was used for antibody production as follows. Full-length coding sequence of CP (Nicolas and Laliberté, 1992) was cloned in frame in the pET11d vector (Novagen). The resulting recombinant protein was overproduced in *E. coli* and purified as insoluble inclusion bodies. Inclusion bodies were resuspended in TBS buffer pH 7.5 and used for rabbit injection and serum production at McGill University Animal Resources Center.

5.3.11. Statistical analyses

The data of the ELISA-based binding assay were analyzed using one-way ANOVA and analysis of variance was conducted using Tukey's test using SAS 9.0 software (at p = 0.05). Statistical analyses of quantitative RT-PCR were performed by REST MCS relative expression software tool 1.9.12 that uses a pair-wise fixed reallocation randomization test (Pfaffl, 2001; Pfaffl et al., 2002).

5.4. Results

5.4.1. TuMV P3 interacts with a lipase protein in a YTHS.

To identify plant P3-interacting proteins, we performed a yeast two-hybrid screen using the viral protein as bait. The P3-coding gene was fused to the GAL-4 DBD in the

vector pDEST^{TM}32 and an *A. thaliana* cDNA library was fused to the GAL-4 AD in the vector pDEST^{TM}22 as described in Materials and Methods. P3-pDEST^{TM}32 was first introduced into the host strain, MaV203, and the transformed strain was plated on various concentrations of 3-AT to detect background activation of the *HIS*3 reporter gene. In plates lacking 3-AT, nonspecific activation of the bait was observed. However, as low as 5 mM of 3-AT inhibited background activation of the *HIS*3 reporter gene of P3 protein. Accordingly, to make the selection more stringent, 50 mM 3-AT was used throughout the screening. Twenty-five colonies out of 10^6 transformants tested were histidine positive and of these, 3 colonies were histidine and uracil positive. Retransformation of the 3 plasmids from positive colonies yielded two clones that tested positive for interaction with TuMV P3 protein and negative for interaction with the GAL4 DBD alone. The sequences at the 5' and 3' ends of the insert of the two plasmids were found to match the sequence *A. thaliana* At1g29670 gene. According to the *Arabidopsis Information Resource* (www.arabidopsis.org), the corresponding protein is a member of the GDSL-motif lipase/hydrolase family protein.

5.4.2. TuMV P3 binds to GDSL-lipase protein *in vitro*

To test for the specific and direct interaction of P3 with the GDSL-lipase protein, an ELISA-based binding assay was performed. ELISA plate wells were coated with purified 6×histidine-tagged GDSL-lipase protein. The coated wells were then incubated with increasing concentrations of purified GST-tagged P3 and complex retention was detected using an anti-GST antiserum. Figure 5.1 shows a saturation binding curve of GDSL-lipase with P3. Control experiments showed the specificity of the *in vitro*

interaction as no signal was detected when GST-tagged P3 was replaced with the GST (Fig. 5.1). This experiment suggests that the GDSL-lipase/P3 interaction is specific and is the result of a direct protein-protein interaction.

5.4.3. Cellular localizations of P3 and GDSL-lipase fusions

TuMV P3 was fused to the GFP and expressed transiently in *N. benthamiana* (a natural host for TuMV) using agroinfiltration to determine its subcellular distribution. P19 from TBSV was used as a suppressor of gene silencing. Expression of the fusion protein was assessed by immunoblot analysis using a rabbit serum raised against GFP. A signal corresponding to the expected molecular mass of the analyzed protein (66 kDa) was observed (Fig. 5.2; lane 2). This indicated that the full-length protein had been expressed in agroinfiltrated leaves with both P19 and GFP-P3 plasmids. No band was observed in the control plants agroinfiltrated with P19 only (Fig. 5.2; lane 1). Fluorescence was visualized 2 to 5 days post-infiltration by confocal microscopy. No notable differences were observed during this time period in cellular localization for P3. DsRed2 markers with or without ER targeting signal were co-expressed with GFP-P3 to facilitate its cellular localization. The co-expression of GFP-P3 and DsRed2 clearly showed that P3 was mainly a soluble cytoplasmic protein, and was excluded from the nucleus (Fig. 5.3A). A similar pattern was observed when P3 was fused to mCherry and coexpressed with GFP soluble marker (data not shown). The ER-targeted fluorescent marker (ER-DsRed2) was co-expressed along with the GFP-P3 fusion. Merging of the fluorescence observed for ER-DsRed2 and P3-GFP showed that a subpopulation of P3 was also ER associated (Fig. 5.3B).

To investigate the cellular localization of the *A. thaliana* lipase protein *in planta*, the plant protein was fused to the fluorescent protein mCherry and expressed transiently in *N. benthamiana* using agroinfiltration. GFP markers with or without ER or plasma PM targeting signal were co-expressed with the fluorescent lipase protein to facilitate its cellular localization. Fluorescence was visualized 2 to 5 days post-infiltration by confocal microscopy. A notable difference in cellular localization of the fluorescent lipase was observed during this time period. At 2 days post-infiltration, red fluorescence associated with lipase-mCherry was observed in the cytoplasm and in the intercellular space (data not shown). At 5 days post-infiltration, the red fluorescence was observed only in the intercellular space (Fig. 5.3C-E; red panel). Upon co-expression of lipase-mCherry and the GFP, GFP-PM or GFP-ER marker, no merged fluorescence signal was found between the lipase and the markers (Fig. 5.3C, 5.3D, and 5.3E; merge panel, respectively). The localization data indicate that the lipase protein, following its synthesis in the cytoplasm of the cell, is secreted outside of the cell.

A final set of experiment was performed to visualize the co-expression of the GFP-P3 and the lipase-mCherry *in planta*. When the lipase-mCherry was coexpressed with GFP-P3 two days post-infiltration, merge data indicated that the lipase partially co-localized with TuMV P3 in the cytoplasm of the cell (Fig. 5.4A; merge panel). However, no co-localization between the two proteins was observed 5 days post-infiltration (Fig. 5.4B; merge panel). Thus, the expression of GFP-P3 is not sufficient to retain the lipase in the cytoplasm or to redistribute the plant protein in the ER membranes, nor is the lipase sufficient for the redistribution of P3 into the intercellular space.

5.4.4. The isolated viable *lipase* mutant expresses an aberrant *LIPASE* mRNA

To analyze the role of the lipase protein in TuMV infection, we used the potential *lipase* (SALK_005724C) T-DNA insertion mutant T4 line. The T-DNA insertion is located in the third exon of the *LIPASE* gene At1g29670 (Fig. 5.5A), and the corresponding single null mutant was designated as *lipase*. The homozygous knockout genotype and presence of T-DNA insertion was confirmed by PCR on plant genomic DNA (data not shown) and by RT-PCR on expressed mRNA. The *LIPASE* mRNA was not detected in the corresponding mutant (Fig.5.5B). The *lipase* (SALK_005724C) T-DNA insertion mutant did not display apparent phenotypic defects (data not shown).

5.4.5. TuMV replication in the *lipase A. thaliana* knockout

To assess the possible role of the P3-lipase interaction during TuMV infection, the viral infection was monitored in *lipase* T-DNA insertional mutant. No difference in growth and symptoms between the control and the mutant plants could be observed at 4, 7 and 21 days dpi. All plants showed typical inflorescence stunting that result from TuMV infection, indicating that the *lipase* knockout plants were not resistant to TuMV (data not shown). In order to obtain a quantitative assessment of viral replication in the *lipase* knockout versus the control Col-0 plants, quantitative real-time PCR analysis of TuMV-infected and mock Col-0 at 4, 7, 17 dpi was performed using viral coat CP specific primers. No significant difference ($p>0.05$; n = 3) in relative TuMV RNA levels was estimated in the *lipase* mutant as compared to the Col-0 control (Fig. 5.6A). The accumulation level of the CP was also measured in leaves of TuMV-infected control and

knock-out plants by immunoblot analysis. At 7 and 14 dpi, the CP protein was detected in Col-0 and *lipase* mutant plants (Fig. 5.6B). However, no difference in the expression level was observed between the mutant and the control at both time points. Overall, these experiments indicate that the complete depletion of the At1g29670 gene product did not impair the capacity of TuMV to replicate *in planta*. The *LIPASE* gene At1g29670 codes for a protein that is part of the GDSL-motif lipase/hydrolase family. Thus, the remaining members of the GDSL-motif lipase/hydrolase family might compensate for the loss of the At1g29670 gene product either to allow viral replication or to increase the capacity of the plant to defend itself.

Table 5.1: Primers used for vectors construction and for the analysis of the *lipase* mutants

Primer	Sequence (5'→ 3')
P3F-pENTR	CACCGGAACAGAATGGGAGGACAC
P3R-pENTR	TTATTGATGAACCACCGCGTTTTC
P3F-*Eco*RI	ATCTTCGAATTCGGAACAGAATGGGAGGACAC
P3R-*Not*I	ATCTTCTCAGCGGCCGCTTGATGAACCACCGCCTTTTC
LipaseF-*Bam*HI	ATCTTCGGATCCATGGAGAGTACTTAACGAAATG
LipaseR-*Not*I	ATCGTAGCGGCCGCTCAAAGCTGTGCCAGCCTTG
LipaseF mCherry-*Xba*I	ATCTTCTAGAATGGAGAGTTACTTAACGAAATG
LipaseR mCherry-*Bam*HI	ATCTGGATCCAAGCTGTGCCAGCCTTGAA
P3F EGFP-*Sac*I	TTAAATGAGCTCGGAACAGAATGGGAGGACAC
P3R EGFP-*Sac*I	TTCGAGCTCTCATTGATGAACCACCGCCTTTTC
CP-F	CTGCCTAAATGTGGGTTTGG
CP-R	TGGCTGATTACGAACTGACG
ACT2F	ACCAGCTCTTCCATCGAGAA
ACT2R	GAACCACCGATCCAGACACT
LBb1	GCGTGGACCGCTTGCTGCAACT
SALK_005724cLP	TGGAGAGTTACTTAACGAAATGG
SALK_005724cRP	CCAAACCCACGTCTAAAAACC
FcDNA	TAACGAAATGGTGTGTAGTGC
RcDNA	TCTCCTAGAAGCTGCACAAC

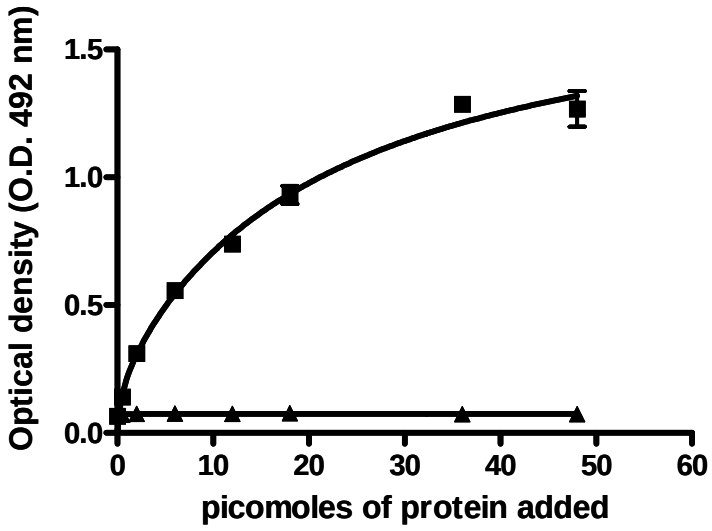

Figure 5.1: Interaction of TuMV P3 protein with *A. thaliana* lipase protein in an ELISA-based binding assay. Wells were coated with 36 pmol of purified His-tailed lipase protein and incubated with increasing concentrations of purified GST-P3 (■) or GST (▲). Protein retention was detected using a polyclonal anti-GST antibody. Data represent the mean ± SEM of three replicates. Error bars are specified for each data, but the small SEM values for some data are masked by the data point symbols.

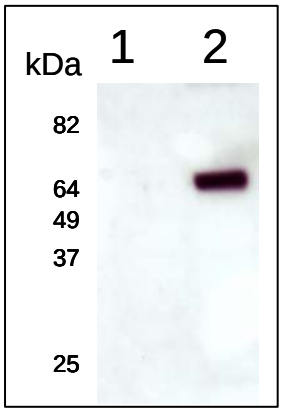

Figure 5.2: Expression of GFP-P3 fusion in *N. benthamiana*. Leaves were infiltrated with *A. tumefaciens*. Total proteins were extracted 4 days post-infiltration, separated by SDS-PAGE, and analyzed by Western blotting using a rabbit serum against the GFP tag. *A. tumefaciens* suspensions containing Ti plasmid encoding P19 (lane 1) and Ti plasmids encoding GFP-P3 + P19 (lane 2).

Figure 5.3: Subcellular localizations of TuMV GFP-P3 and lipase-mCherry proteins. *N. benthamiana* leaves were infiltrated with *A. tumefaciens*, and expression of fluorescent proteins was visualized by confocal microscopy 2 to 5 days later. *A. tumefaciens* suspensions contained binary Ti plasmids encoding GFP-P3 and mCherry (A), GFP-P3 and ER-DsRed2 (B), lipase-mCherry and GFP (C), lipase-mCherry and GFP-PM marker (D), lipase-mCherry and GFP-ER (E). Left panels show fluorescence emitted by the red channel only, while middle panels show fluorescence emitted by the green channel only, and right panels show the merging of the red and green channels with the yellow color representing areas where the red and green fluorescence coincide. Bar = 15 μm. All agroinfiltrations were performed in the presence of the P19 inhibitor of silencing as previously described.

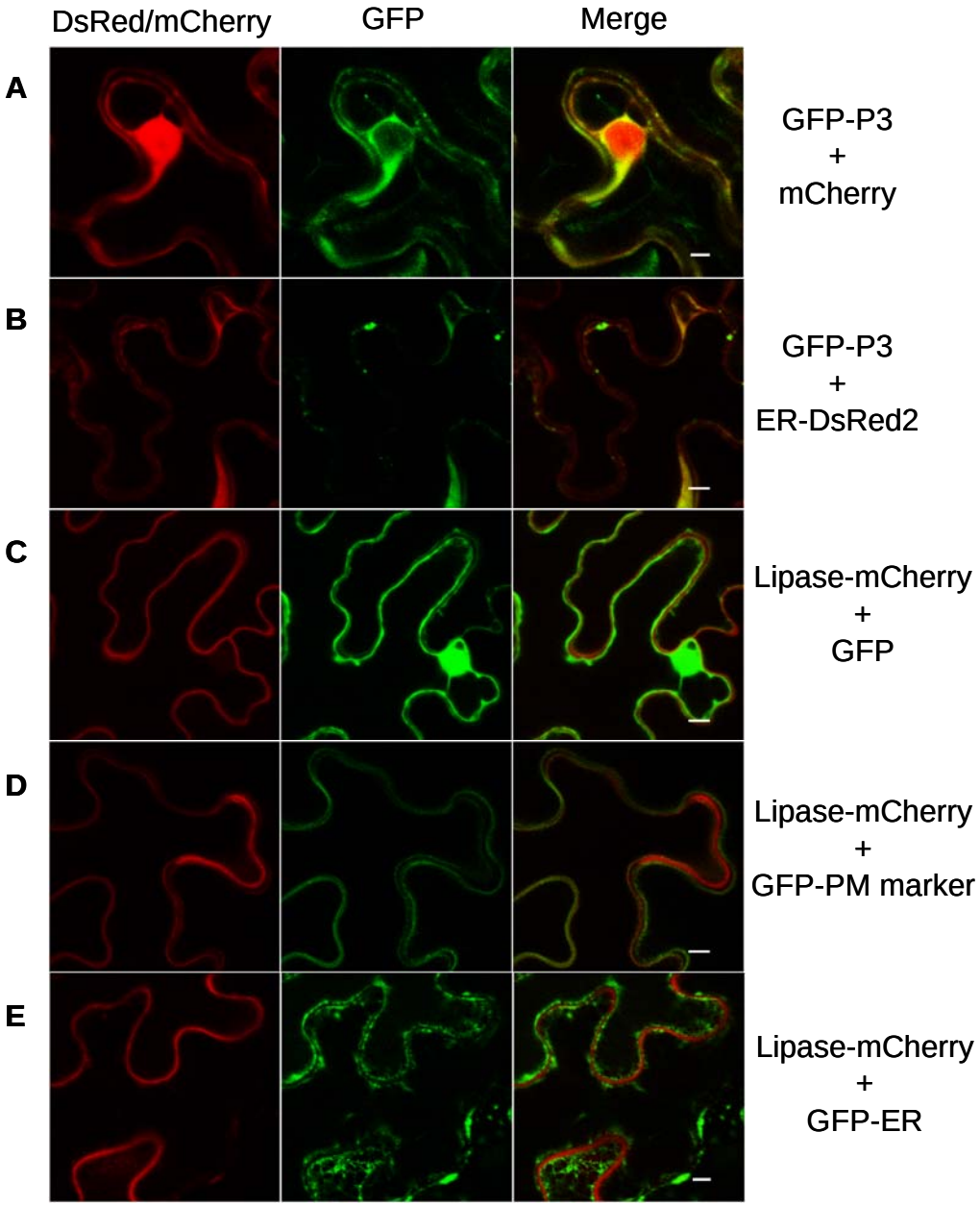
DsRed/mCherry
GFP
Merge
A
GFP-P3
+
mCherry
B
GFP-P3
+
ER-DsRed2
C
Lipase-mCherry
+
GFP
D
Lipase-mCherry
+
GFP-PM marker
E
Lipase-mCherry
+
GFP-ER

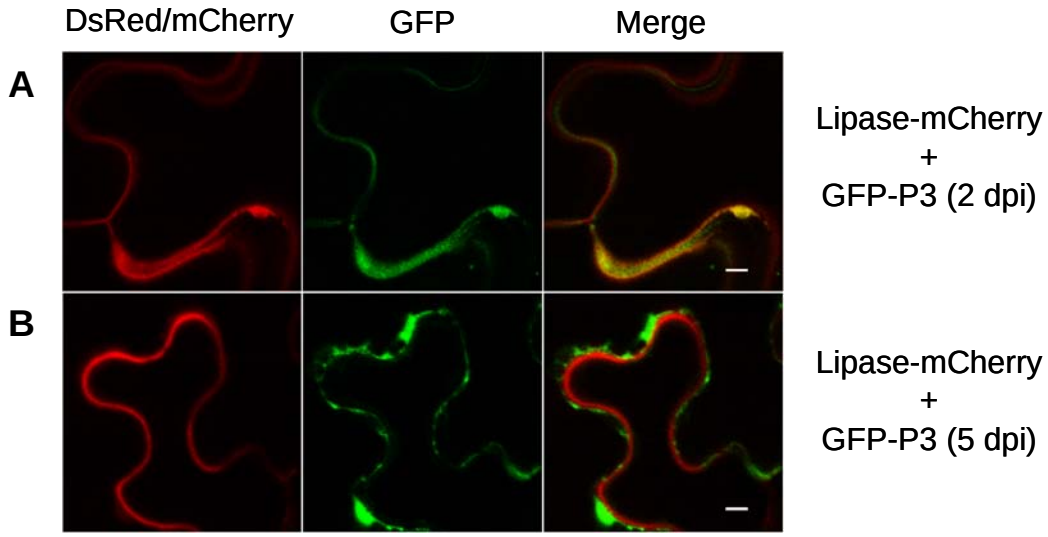

Figure 5.4: TuMV P3 and the *A. thaliana* lipase co-localization *in planta. N. benthamiana* leaves were infiltrated with *A. tumefaciens*, and expression of fluorescent proteins was visualized by confocal microscopy 2 to 5 days later. *A. tumefaciens* suspensions contained binary Ti plasmids encoding lipase-mCherry and GFP-P3 2 days post-infiltration, (A), lipase-mCherry and GFP-P3 4 days post-infiltration (B). Left panels show fluorescence emitted by the red channel only, while middle panels show fluorescence emitted by the green channel only, and right panels show the merging of the red and green channels with the yellow color representing areas where the red and green fluorescence coincide. Bar = 15 µm. All agroinfiltrations were performed in the presence of the P19 inhibitor of silencing as previously described (Qu and Morris, 2002).

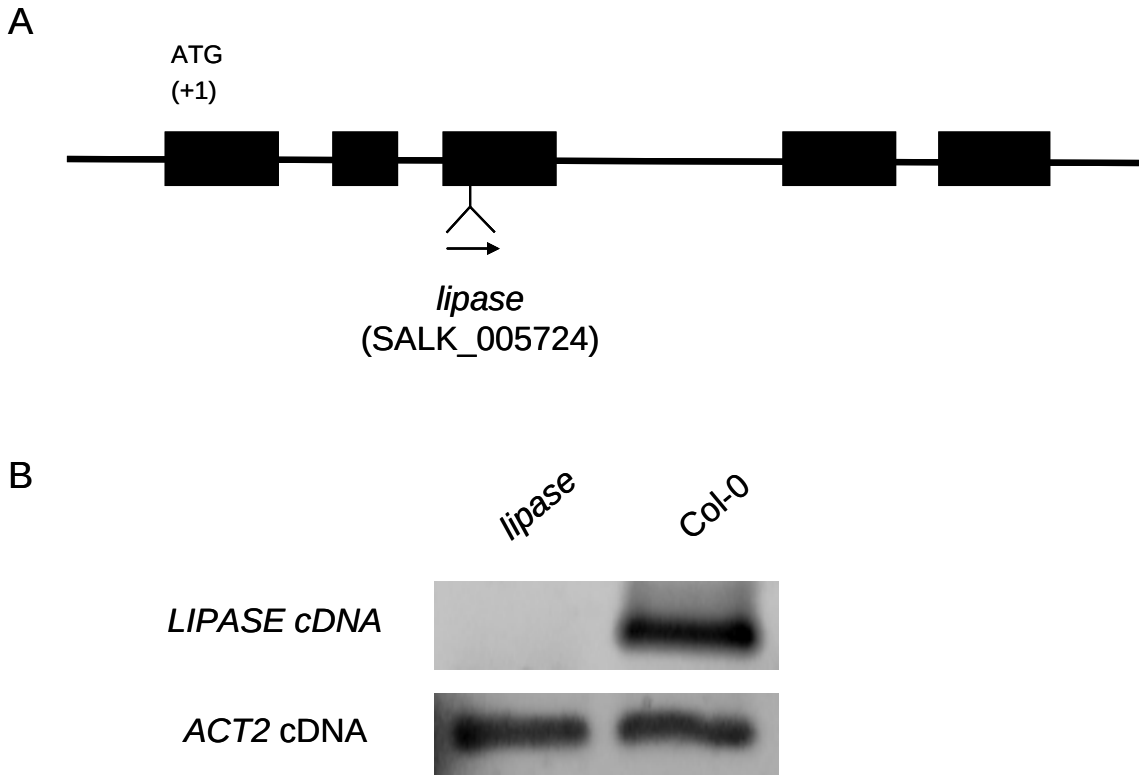

Figure 5.5: Confirmation of *A. thaliana lipase* knockout. (A) *LIPASE* gene structure and T-DNA insertion. Map of *A. thaliana LIPASE* locus [At1g29670.1]. Translated exons are shown as rectangles, introns as black lines. The site of the SALK T-DNA insertion and its orientation is depicted with an arrow. (B) RT-PCR analysis of *LIPASE* expression in four-weeks-old *A. thaliana* Col-1 and *lipase* mutant. PCR was performed with primers flanking the insertion. The *ACTIN2* gene (*ACT2*) was amplified as an internal control.

Figure 5.6: Infection of *lipase A. thaliana* mutant and wild-type Col-0 lines with TuMV. (A) Relative quantification of TuMV genomic RNA in TuMV infected *A. thaliana lipase* mutants at 4, 7 and 17 days post-infection by quantitative RT-PCR amplification using primers flanking the coat protein region. Relative viral RNA accumulation was calculated with threshold cycle values obtained for the *lipase* mutant versus that of wild-type Col-0 plants. Bootstrap analysis performed using REST 2 multicomponent analysis software (10000 iterations). Actin gene (*ACT2*) was used as internal reference to normalize the data. (B) CP expression in *lipase A. thaliana* knockout versus wild-type Col-0. Immunoblot analysis of CP protein in TuMV infected *lipase A. thaliana* mutants or wild-type Col-0 at 4, 7 and 17 dpi using polyclonal anti-CP antibody. The western blot showing the actin protein was used as a loading control.

A

	4 DPI	7 DPI	17 DPI
Lipase mutant (SALK_005724)	-2.108	-1.394	-2.177

B

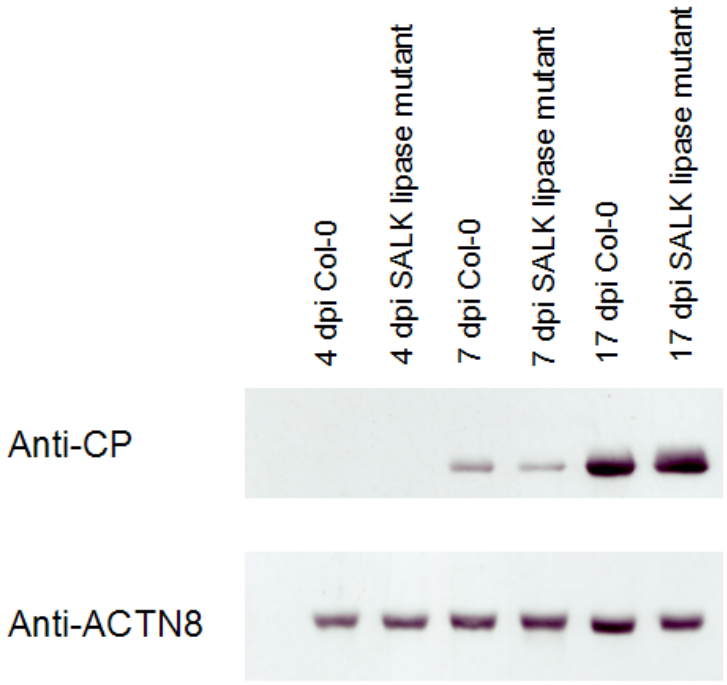

5.5. Discussion

Identification of cellular factors that interact with viral proteins is of key importance to characterize the molecular basis of the infection process. In this work, a cDNA library from *A. thaliana*, a natural host of TuMV, was screened in a yeast two-hybrid interaction assay, leading to the identification of one interactor of the TuMV P3 protein, a GDSL-lipase protein. The P3-lipase interaction was confirmed *in vitro* by an ELISA-based binding assay. Confocal imaging partially co-localized P3 and the lipase in the cytoplasm of the cell 2 days post-infiltration. Even if co-localization of two proteins does not mean that they actually interact, their localization in the same compartment is consistent with a potential interaction between the two proteins.

P3 protein is one of the least characterized proteins of potyviruses. The high sequence variability of P3 among species suggests a role for the viral protein in some virus-specific processes, e.g. in virus interactions with specific host plants. This is in agreement with experimental data demonstrating that the potyviral P3 protein is the avirulant factor for some resistance genes (Jenner et al., 2003; Johansen et al., 2001), a pathogenicity determinant relevant for symptom severity (Saenz et al., 2000), and a host range determinant (Suehiro et al., 2004; Tan et al., 2005). In the pathosystem TuMV-*A. thaliana*, two distinct symptoms (mosaic symptom or veinal necrosis) are observed that are dependent upon the combination of the TuMV isolate and the *Arabidopsis* ecotype. Interestingly, two genes encoding lipase proteins reside in the genetic locus controlling the type of symptoms induced by TuMV (Kaneko et al., 2004). The viral pathogenicity determinant responsible for the *A. thaliana* symptoms occurs within the region containing

P3 and CI genes (Kaneko et al., 2004). Accumulating evidences suggested a role for P3 in pathogenesis and symptom determination (Jenner et al., 2003; Johansen et al., 2001; Saenz et al., 2000; Suehiro et al., 2004; Tan et al., 2005), however, knowledge on the biochemical basis underlying the recognition process is lacking.

Disease resistance in plants is mediated by corresponding gene pairs in the plant (resistance or *R* gene) and pathogen (avirulence or *avr* gene) that condition specific recognition and activate plant defenses (Baker et al., 1997). After pathogen recognition, necrotic lesions, characteristic of the HR, appears at the site of attack. The HR is accompanied by the release of active oxygen species, the induction of defense genes such as those coding for pathogenesis-related proteins (PR), and a rise in salicylic acid (SA) levels. Subsequent to the local response, plants develop a broad-based long-lasting resistance to secondary pathogen infection known as SAR.

As lipolytic enzymes, GDSL-lipases are an important superfamily of lipases, and active in hydrolysis and synthesis of abundant ester compounds. Their flexible pocket brings conformational changes, so that the active sites are exposed to the solvent and easily bind to substantive substrates, conferring multi-functional character of GDSL-lipases (Derewenda, 1994). In plants, GDSL-lipases that have been characterized so far are mainly involved in the regulation of plant development, morphogenesis, synthesis of secondary metabolites and (Ling et al., 2006; Shah, 2005). Mutational analyses of *Arabidopsis* to screen for genes required for R gene-mediated resistance or SAR, identified two lipase-encoding genes, the enhanced disease susceptibility1 (*EDS1*) and phytoalexin deficient4 (*PAD4*) (Falk et al., 1999; Jirage et al., 1999). Inactivation of both of these genes by mutation suppressed disease resistance conferred by R proteins. In

tobacco, SA binding protein2 (SABP2) binds strongly SA and belongs to the α/β-Ser hydrolase superfamily. SABP2 displays SA-stimulated lipase activity and is required for full local and systemic resistance to *Tobacco mosaic virus* (Kumar and Klessig, 2003). In a differential screening study, a different lipase gene family of *Arabidopsis* was also identified (Jakab et al., 2003). It contains nine genes encoding pathogenesis-related lipase proteins (PRLIP1 to PRLIP9), which are induced by treatment with SA, jasmonate acid, or ethylene. More recently, a secreted lipase with a GDSL-motif designated GDSL-LIPASE1 (GLIP1) was shown to be implicated in both short and long-distance defense responses to pathogen infection (Oh et al., 2005). The mechanism through which GLIP1 transduces the defense signal is not known but its extracellular localization lead to the notion that it may produce a lipid-derived defense signaling molecule. The defense signaling may be activated by a lipid-derived molecule generated by the lipid-hydrolyzing activity of GLIP1.

All these lipases, including the GDSL-lipase protein that we have isolated share little sequence homology but contain the catalytic triad (Ser, Asp, His) and either one of the two lipases signature sequences (GxSxG or GxSxxxxG). Similar to GLIP1, the lipase protein interacting with P3 was shown to localize in the extracellular space 4 days post-infiltration. The possibility exists that the lipase meets P3 in the cytoplasm before being targeted at the periphery of the cell where it then influences the defense signaling in the plant.

The P3 interactor was further characterized for its function in disease resistance by monitoring the viral infection in plants carrying the disrupted *LIPASE* At1g29670 gene. This approach has been successfully used to study the function of different host

factors in TuMV and other potyviruses life cycle (Duprat et al., 2002; Lellis et al., 2002; Nicaise et al; 2007). In this study, the disruption of the *A. thaliana* gene coding for the P3 interactor, the lipase protein, did not lead to any morphological or developmental modifications in the *lipase* mutant plants. Also, the complete depletion of the At1g29670 gene product did not have any effect on the capacity of TuMV to replicate *in planta*. The At1g29670 gene is part of the *Arabidopsis* GDSL-lipase gene family which contains 108 members (Ling, 2008). Protein sequence analyses indicate that at least four GDSL-lipases (At1g29660, At5g45670, At4g18970, and At1g33810) exhibit more than 50% sequence identity to the At1g29670 corresponding protein. These observations are indicative of a possible functional redundancy among these proteins. The functional redundancy between the genes could explain why the growth of the knockout *lipase* plants was not affected in absence of the At1g29670 gene product. Also, it is highly probable that the remaining lipases can compensate for the loss of the disrupted lipase products to allow viral replication and/or plant defense. One way to circumvent the redundancy associated problem would be to generate double or triple *lipase* mutants and to challenge them with TuMV. This approach was recently successfully used in the TuMV-*A.thaliana* pathosystem where depletion of the poly(A)-binding protein in double knockout plants was shown to result in reduced TuMV RNA accumulation (Dufresne et al., 2008b).

One other approach that would provide evidence for the role of GDSL-lipases during potyvirus infection would be to isolate *Arabidopsis* mutants with increased or decreased susceptibility to TuMV, to determine the genome position of the affected loci in the mutants, and to examine the candidate genes in the defective locus. The identification of non-susceptible mutants of TuMV with GDSL-lipase defects would

provide evidence for a role of GDSL-lipase during potyvirus infection. While, if the GDSL-lipase was part of a defensive mechanism, then loss of GDSL-lipase function would lead to an increased susceptibility to TuMV.

In summary, the results presented here strongly suggest that *A. thaliana* lipase protein interacts with TuMV P3 protein. This specific interaction reinforces the role of P3 in pathogenicity determination and host resistance. Unfortunately, the corresponding *lipase* mutant did not exhibit an altered response to TuMV infection following inoculation; the remaining similar lipase genes can probably compensate for the lost of the disrupted one. Further experiments are needed to unravel the precise role of the P3-lipase interaction.

CHAPTER VI

GENERAL DISCUSSION

6.1. General discussion

The principal aim of this project was to identify host factors involved in TuMV life cycle. Two viral proteins were used as baits to identify interacting host proteins using two different protein-protein interaction methodologies. First, three host proteins that bind to TuMV RdRp *in vitro* (ELISA-based binding assays) and *in planta* (TAP tag strategy) were identified: the PABP2, Hsc70-3 protein (chapter III; Dufresne et al., 2008a), and the eEF1A (chapter IV; Thivierge et al., 2008). These interactions appear to be relevant since each of these proteins were found to relocalize in ER-derived vesicles during TuMV infection. In other viral systems, the recruitment of RdRp to membranes and its interaction with viral and host proteins are essential for its polymerase activity. Thus, the three host proteins described here may be important components of the replication complex and may play a role in the regulation of the polymerase activity. For TuMV, the ER-derived vesicles are known to be induced by the viral 6K protein and are though to house the virus replication complex (VRC). The presence of replication (VPg-Pro, RdRp, Hsc70) and translation [VPg-Pro, PABP, eEF1A, and eIF(iso)4E] proteins in 6K-derived vesicles add to accumulating evidence that TuMV 6K-derived vesicles not only house the VRC, but may be the site for viral translation as well. The later hypothesis and the possibility of an involvement of host and viral proteins in the coordination of the

translation and replication functions into the 6K-induced viral vesicles will be discussed in the following section.

The second protein that was used as a bait to recover plant-virus interactions is the P3 protein. Using the yeast two-hybrid system, we found an interaction between P3 and an *Arabidopsis* GDSL-lipase. This interaction may be significant as some of the lipases are known to be involved in plant defence against different type of pathogens.

6.1.1. Model for translation and replication of TuMV genome in cytoplasmic vesicles induced by 6K

The assembly of RNA replication complexes on intracellular membranes is an essential step in the life cycle of positives-sense RNA viruses. Various viruses assemble their replication complexes on different membranes such as endosomal and lysosomal membranes, ER membranes, mitochondrial and peroxisomal membranes (Salonen et al., 2005). While many positives-sense RNA viruses form spherical invaginations, others form distinct membranes structures, including vesicles. The mechanisms whereby replication complexes are fixed to membranes remain incompletely understood, although the involvement of viral proteins as membrane anchors has been proposed (see review by Wimmer et al., 1993). The proliferation or reorganization of cellular membranes and vesicles induced by viruses may be a common mechanism to increase the available surface area for RNA synthesis. The membrane rearrangements may also serve in protecting the virus-induced replication complexes from host defense responses, as well as in providing a mechanism to limit diffusion of viral constituents.

For potyviruses, it is the 6K protein that mediates association of the RNA replication apparatus with ER-derived membranes as an integral protein (Beauchemin et al., 2007; Schaad et al., 1997a). When present in the same polyprotein, the membrane-binding activity of the 6K protein dominates over the nuclear localization activity of VPg-Pro (Beauchemin et al., 2007; Restrepo-Hartwig and Carrington, 1994). For TuMV, previous studies have revealed that the 6K-VPg-Pro polyprotein induces the formation of large cytoplasmic vesicular compartments derived from the ER (Beauchemin et al., 2007). The localization data obtained in our study using a fluorescently labelled 6K-GFP TuMV infectious clone have reconfirmed the anchoring of TuMV replication complexes to ER membranes through a mechanism involving the 6K protein. The vesicles induced by the recombinant virus were indistinguishable from the one induced by the ectopic expression of 6K-VPg-Pro; they accumulated around the nucleus and were 2-10 μm in diameter. Thus, the 6K protein, in the presence or absence of TuMV infection, mediates an association with membranes.

After the assembly of viral replication complexes on cellular membranes, at least some viruses require additional contributions from host factors to initiate viral translation and RNA synthesis. Our data indicates that Hsc70 plays a role in TuMV replication. Its association with RdRp and its relocalization in virus-induced vesicles suggest that Hsc70 is a constituent of the potyvirus replicase complex as seen for plant tobamo- and tombusvirus (Nishikiori et al., 2006; Serva and Nagy, 2006). Hsp70 proteins and additional members of the heat shock protein (HSP) family play a role in the replication of other viruses as well. For example, the RNA replication of *Brome mosaic virus* (BMV) and *Flock house virus* (FHV) is blocked in *YDJ1* mutants. *YDJ1* encodes the yeast

ortholog of Hsp40/DnaJ, whose deletion is not lethal but still disrupts Hsp70 chaperone complex activity (Tomita et al., 2003; Weeks and Miller, 2008). The function of *YDJ1* in BMV and FHV RNA replication appears to be different. For BMV, the *YDJ1* mutant cells support many early steps in RNA replication, including the assembly of RNA replication complexes to membrane and the recruitment and accumulation of the polymerase on ER membranes (Tomita et al., 2003). However, *YDJ1* mutant cells do not support the negative-strand RNA synthesis, which suggest that the chaperone may be responsible for proper polymerase folding required for RNA synthesis. For FHV, yeast cells with an *YDJ1* deletion show a dramatic reduction in replication due in part to reduced viral polymerase accumulation (Weeks and Miller, 2008). The authors proposed three hypotheses to explain the role of cellular chaperones in positive-strand RNA virus replication. First, the chaperones might have an indirect role in viral replication in promoting the maturation of particular cellular proteins that subsequently facilitate viral RNA replication complex assembly or function. Secondly, the chaperones may interact directly yet transiently with viral RNA replication complex constituents to facilitate protein folding and stabilization during translation, intracellular targeting or membrane association. Thirdly, the cellular chaperones may constitute an essential component of the membrane-associated RNA replication complex and may stabilize viral proteins or RNA. This later hypothesis is consistent with our results that show the presence of Hsc70 in the viral-induced vesicles as well as its co-purification in membrane-associated replicase complexes (chapters III and IV). The three hypotheses outlined above are not mutually exclusive, and there is a possibility that specific cellular chaperones might have virus- and cellular-particular mechanisms of action. The best examples to support the major

roles for chaperones in many steps of the viral infection cycle come from the model virus tombusviruses. The cytosolic Hsp70 play several roles in TBSV replication, such as affecting the subcellular localization and membrane insertion of the viral replication proteins as well as the assembly of the viral replicase (Wang et al., 2009a; 2009b).

There is evidence that indicates that PABP is also an important host factor involved in potyvirus life cycle. Like Hsc70, PABP is internalized in virus-induced vesicles (Beauchemin and Laliberté, 2007) and interacts with TuMV RdRp (chapters III and IV). This host factor also interacts with VPg-Pro and is up regulated following TuMV infection (Dufresne et al., 2008b; Léonard et al., 2004). The precise function of PABP in potyvirus infection remained to be clearly defined. One possibility is that PABP is necessary for efficient cap-independent translation of the viral RNA. End-to-end RNA interactions are found in several picornaviruses. For example, circularization of poliovirus (PV) RNA is mediated by PABP; interaction between 3CD (the viral polymerase precursor), poly(C) binding protein (a host protein regulating the stability and expression of several cellular mRNAs; Ostareck-Lederer et al., 1998), and PABP hold both ends of PV RNA together (Herold and Andino, 2001). These interactions are necessary for PV replication and stimulate viral RNA translation. PABP might be involved in the circularization of the potyvirus RNA by linking VPg and eIF(iso)4G to the virus poly(A) tail in a VPg-eIF(iso)4E-eIF(iso)4G-PABP protein bridge (Fig. 6.1A). Alternatively, a more direct interaction between VPg-Pro and PABP might achieve the same result. This end-to-end communication might increase viral translation by stabilizing the translation complex and promoting the recycling of terminating ribosomes on the same mRNA.

Figure 6.1: Model of TuMV translation/replication through circularization of the genomic viral RNA.

(A) Circularization of TuMV mRNA during viral translation. Circularization of the RNA of TuMV is mediated by simultaneous interactions between VPg or precursor forms (6K-VPg-Pro or VPg-Pro) at the 5' extremity of the RNA with the eIF4E-eIF4G-PABP complex bound to 3' poly(A) tail. Components of the eIF4F complex recruit ribosomes at 5' end of the RNA and result in a cap-independent translation of the RNA, which proceeds from 5' to 3' end. eEF1A fulfills its functional role in protein synthesis which is, in this case, to elongate the viral polypeptide. Translation might possibly occur on membranes if membrane-binding 6K-VPg-Pro polypeptide is involved as depicted.

(B) A model for initiation of negative strand synthesis during TuMV replication. As the viral genome is translated, the viral polymerase (RdRp) accumulates and its combined interaction with VPg-Pro and PABP evicts the eIF4F complex and engaged ribosomes (composed of 40S and 60S subunits) on the viral RNA. Translation is down regulated and replication can proceed. Interaction of VPg-Pro with both PABP and RdRp maintains the circular conformation of the genomic RNA. Interaction of the RdRp with PABP bound to poly(A) tail positions the RdRp in close proximity of 3' poly(A) tail and allows, following recruitment of an uridylated VPg primer (VPg-UUUUU), initiation of negative strand synthesis in 3' to 5' direction. By interacting with the RdRp on membranes, Hsc70 and eEF1A could possibly assist in the assembly and stabilization of the replication complex. Adapted by permission from the Ph.D. thesis of Dr. P. J. Dufresne: Involvement of poly(A)-binding and heat shock 70 kDa proteins in *Turnip mosaic virus* infection, copyright 2008.

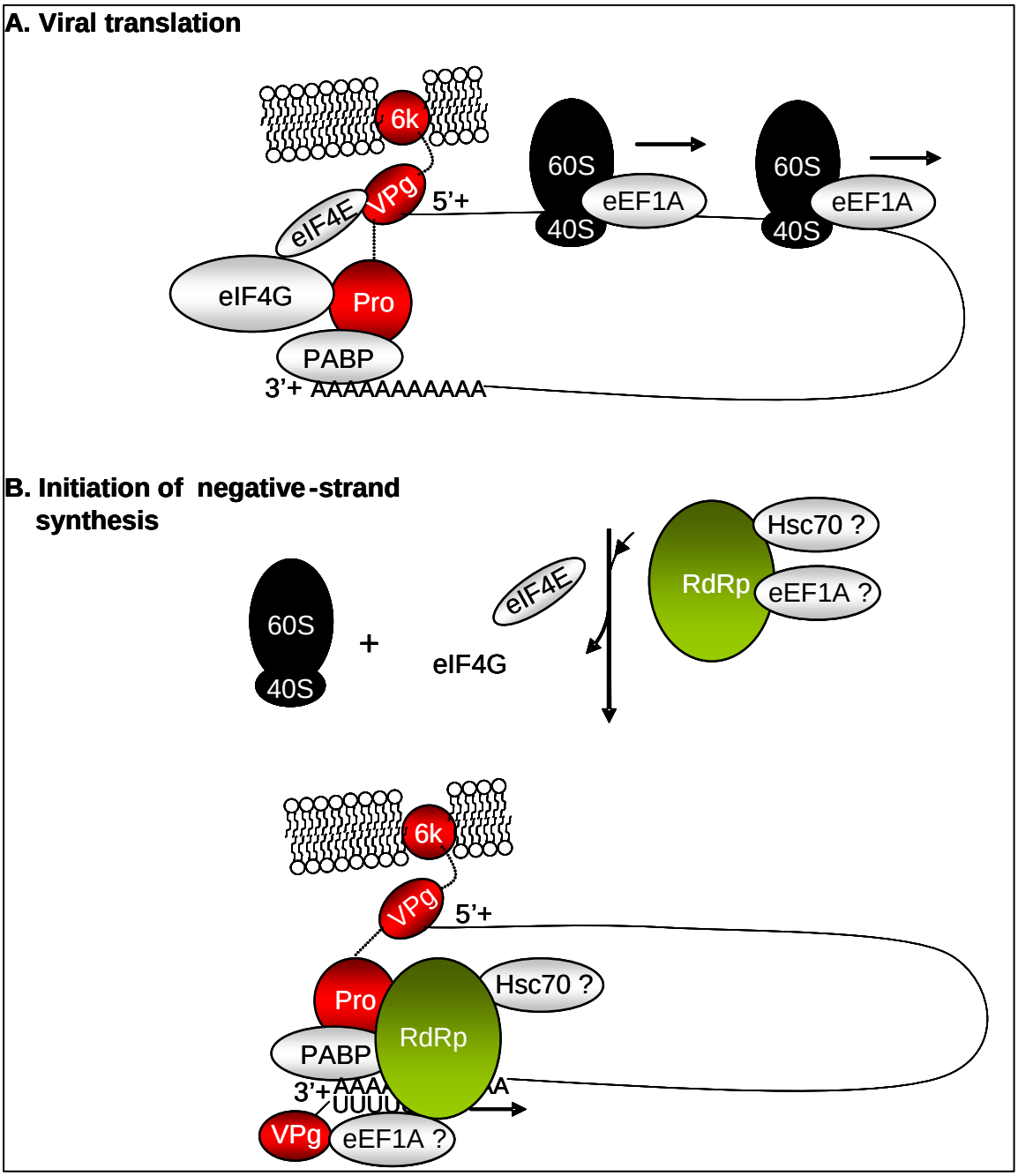
A. Viral translation
6k
VPg
eIF4E
5'+
60S
40S
eEF1A
60S
40S
eEF1A
eIF4G
Pro
PABP
3'+ AAAAAAAAAAA
B. Initiation of negative-strand synthesis
60S
40S
+
eIF4E
eIF4G
RdRp
Hsc70 ?
eEF1A ?
6k
VPg
5'+
Pro
RdRp
Hsc70 ?
PABP
3'+AAA
UUUU
A
VPg
eEF1A ?

Another hypothesis is that the interaction of the RdRp with both PABP and VPg-Pro may regulate the coupling of viral translation with viral RNA synthesis. As genome translation progresses, RdRp accumulates and its interaction with PABP and VPg-Pro would destabilize the VPg-Pro-eIF(iso)4G-PABP-poly(A) translation complex. The interaction of RdRp with VPg-Pro may also interfere with the translation complex by interfering with the VPg-Pro-eIF(iso)4E interaction. As a consequence, ribosomes on the viral RNA would disengage and the interaction of RdRp with PABP linked to poly(A) tail would bring the polymerase to the 3' end of the RNA template for replication to proceed (Fig. 6.1B). This later model is consistent with the observation that PABP2 can form a tripartite complex with VPg-Pro and eIF(iso)4E *in vitro* (Beauchemin and Laliberté, 2007).

The eEF1A interaction with both RdRp and VPg-Pro as well as its vesicular localization during TuMV infection reinforce the potential role for eEF1A in the replication cycle of positive-stranded RNA viruses. The first evidence that a translation elongation factor (EF) is involved in positive-stranded RNA virus replication cycle was obtained more than 30 years ago with bacteriophage Qβ (Blumenthal et al., 1976). Subsequently, EF1A was found to bind to many viral RNAs, to be part of several virus replicase complexes, and to interact directly with various viral replication proteins (for a review, see chapter II). Functional studies in several virus-host models have revealed that eEF1A is involved in many steps of the viral replication cycle including viral translation, replication and movement. For TuMV, the association of eEF1A with the viral replicase and its presence in the 6K-induced vesicles suggest that the elongation factor participates in the replication of the viral genomic RNA. This hypothesis is consistent with previous

studies in which eEF1A was shown to be essential for the replication of Qβ and Vesicular stomatitis virus (Blumenthal and Carmichael, 1979; Das et al., 1998). More recently, mutational analyses have demonstrated that eEF1A is important for the replication of *Tomato bushy stunt virus* (TBSV) and directly interacts with the viral RNA, the p33 replication co-fator and the $p92^{pol}$ RdRp. The downregulation of eEF1A in yeast mutants leads to decreased TBSV RNA accumulation and reduced p33 levels (Li et al., 2008; 2009). Overall, the multiple interactions of eEF1A with components of the of TBSV replicase suggest a role for eEF1A in the regulation of the functions of the viral replicase complex. The mechanism by which eEF1A contribute to the regulation of viral replication is still unclear and seems to be different among various RNA viruses.

Another possibility is that the eEF1A-RdRp interaction contributes to TuMV translational regulation. Because eEF1A is a translation factor, possible functions of eEF1A in translation have been proposed. Binding of eEF1A to the 3'-untranslated region (3'-UTR) of *Tobacco mosaic virus* has been suggested to enhance translation of the viral RNA by increasing the local concentration of eEF1A on virus mRNAs (Zeenko et al., 2002). eEF1A may then fulfill its functional role in protein synthesis on virus mRNAs which is to participate in translation elongation. Like PABP, eEF1A may also help coordinate the competing translation and replication functions of genomic RNA via its interaction with the viral RNA and/or RdRp and VPg-Pro proteins.

There is also the possibility that the eEF1A/VPg-Pro/RdRp complex may be involved in the attachment of TuMV genomic RNA to the cytoskeleton and ER, thereby regulating the efficiency of protein synthesis. Protein synthesis can be enhanced by a close spatial association of the ribosome and other translation factors with the

cytoskeleton (Bassell et al., 1999; Jansen, 1999; Stapulionis and Deutscher, 1995). eEF1A interacts with microfilaments, microtubules, and the ER and mediates the attachment of cellular mRNA to the cytoskeleton (Bassell et al., 1994, 1999; Condeelis, 1995; Moore and Cyr, 2000). Moreover, TuMV VRCs are transported intracellularly, probably via microfilaments along the ER throughout the infection cycle (Cotton et al., 2009). eEF1A may be implicated as a cofactor of the viral transport process. Again, all these hypotheses are not mutually exclusive; the high abundance of eEF1A in cell might facilitate its recruitment in many steps of the TuMV infection cycle.

Overall, this work highlights the importance of 6K-VPg-Pro and RdRp as scaffold proteins for the formation of a multi-protein complex within virus-induced vesicles. Both proteins have several and common interacting partners. For example, 6K-VPg-Pro and RdRp each bind to PABP2 and eEF1A. 6K-VPg-Pro polypeptide is sufficient to redirect the RdRp and Hsc70 (chapter III) as well as PABP2, eIF(iso)4E (Beauchemin et al., 2007; Beauchemin and Laliberté, 2007), and eEF1A (chapter IV) to ER-induced vesicles. Localization data described in chapter IV reconfirmed the retargeting of these host and viral proteins in 6K-induced vesicles during the course of TuMV infection.

The presence of three translation factors along with proteins of the replicase complex in 6K-induced vesicles strongly suggests that translation and replication of TuMV are coupled in these viral structures. For at least some viruses, both processes occur on membrane-associated vesicles. Notably, the DNA poxyviruses replicate in cytoplasmic foci called DNA factories, which are known to be the site of viral RNA and protein synthesis as well as genome replication and virion assembly (Katsafanas and Moss, 2007). Like 6K-induced vesicles, the poxyvirus factories are associated to the ER

and contain translation host factors such as eIF4E, eEF4G, and ribosomal proteins (Katsafanas and Moss, 2007; Tolonen et al., 2001). Our data add to accumulating evidence that translation and replication are also coupled in TuMV-induced vesicles. The coordination of both processes probably depends on specific interactions between the viral RNA genome and viral and host proteins. As described above, the interactions RdRp-PABP and RdRp-eEF1A translation factors may be involved in this coordination.

6.1.2. P3-GDSL-lipase interaction

During evolution, plants have developed multiple mechanisms to cope with numerous biotic stresses. Plants can recognize a pathogen early in the interaction and activate defence responses. Rapid recognition of a pathogen is based on the presence of resistance (*R*) genes in the host, the product of which are presumed to bind with the products of avirulence (*Avr*) genes of the pathogen. P3 is likely to function as a specific *Avr* determinant to elicit resistance mediated by a given *R* gene. Several studies have identified virulence determinants in the P3-$6K_1$ region of potyviruses for overcoming plant resistance. In TuMV, amino acids in central and C-terminal P3 have been shown to be virulence determinants for two dominant *R* genes in *Brassica napus* (Jenner et al., 2002; Jenner et al., 2003). At the cellular level, *R*-gene mediated resistance is often associated with localized plant cell necrosis, called the hypersensitive response (HR). Accompanying the HR are a number of early cellular changes, such as an oxidative burst producing reactive oxygen intermediates (ROI), accumulation of the signalling molecules, nitric oxide (NO) and salicylic acid (SA), and the transcriptional activation of defense-related genes such as those coding for pathogenesis-related (PR) proteins (Jirage

et al., 2001; Kunkel and Brooks, 2002). Such a localized induced defence response often leads to the activation of systemic resistance mechanisms (systemic acquired resistance, SAR) (Sticher et al., 1997).

Mutational analyses in *Arabidopsis* have led to the identification of genes required for *R* gene-mediated resistance or for SAR (Feys and Parker, 2000). Interestingly, genes with homology to lipases such as the enhance disease susceptibility (*EDS1*) and the phytoalexin deficient (*PAD4*) genes have been characterized. *EDS1* has been shown to function upstream of SA-dependent plant defense mechanism (Falk et al., 1999). Mutation of *EDS1* leads to enhanced susceptibility, loss of SA accumulation, and PR proteins genes expression (Falk et al., 1999). *PAD4* has also been identified as playing a role in SA-dependent defense mechanism and as *EDS1*, it is required for accumulation of SA.

In this study, we show that P3 and LIPASE proteins interact specifically, both in yeast two-hybrid system and in ELISA based-binding assay. The physical association between these two proteins may contribute to their activities in disease resistance and/or pathogenesis. One possibility could be that P3 stimulates the hydrolytic activity of LIPASE. Once activated, LIPASE could function upstream of SA-dependent localized plant defense mechanism, like the previously characterized EDS1 and PAD4 proteins. The lipid-hydrolyzing activity of LIPASE may also be required for the activation of the systemic defence signalling. The existence of a lipid-derived mobile signal that promotes long-distance signalling has been proposed previously (Maldonado et al., 2002). It was shown that *defective in induced resistance1* (*dir1*) was defective in developing SAR to virulent *Pseudomonas* or *Peronospora parasitica*. DIR1 is an apoplastic lipid transfer

protein (LTP) and thus may function in the generation of an essential mobile signal or its transmission from the induced leaf. It is conceivable that a LIPASE-derived mobile signal moves around as an LTP-bound form, which would implicate LIPASE in long-distance defense responses. The extracellular location of GDSL-lipase protein following its synthesis in the cytoplasm is consistent with a role in signalling. However, a fuller examination of the P3-GDSL-lipase interaction remains to be achieved to define its exact role in potyvirus infection.

CHAPTER VII

GENERAL CONCLUSION AND FUTURE DIRECTION

7.1. Conclusion

The identification of eEF1A as a cellular factor interacting with TuMV RdRp and 6K-VPg-Pro and its localization in virus-induced vesicles indicate that the elongation factor is involved in potyvirus infection. Further experiments should aim at clarifying the role of these interactions in their associated infection events. Accordingly, development of translation and replication systems should be pursued.

The characterization of the 6K-induced vesicles has revealed the presence of translation factors as well as proteins involved in the viral replication. These data may provide a mechanistic explanation for the coupling of viral RNA translation with viral RNA replication. However, it is still unclear whether the 6K-induced vesicles are the site of viral RNA and protein synthesis, thus, they should be analyzed for presence of active replicating RNA and translation activity.

Taken together, our findings underline the importance of VPg and its precursor forms and RdRp as scaffold proteins for the formation of a multi-protein complex within TuMV-induced vesicles. Present results likely have revealed only a fraction of the proteins present in TuMV-induced vesicles. Consequently, the same approach could be used to further identify host and viral proteins in these vesicles.

Finally, discovery of GDSL-lipase as interactor of the P3 protein of potyviruses is in agreement with many studies involving P3 in pathogenicity determination and host

resistance (Chu et al., 1997; Hjulsager et al., 2002; Johansen et al., 2001; Jenner et al., 2002). Further studies should attempt to investigate the biological relevance of this interaction *in planta*.

7.2. Future direction

The following experimental work should be conducted to further characterize the role of eEF1A in TuMV infection cycle as well as the content and function of the 6K-induced vesicles:

1. *Development of RdRp activity assays to study the effect of eEF1A on the viral polymerase functions. In vitro* experiments could be conducted to characterize the effect of the addition of recombinant eEF1A on the polymerase activity. A similar approach was successfully used to demonstrate the stimulating effect of VPg on the RdRp of *Tobacco vein mottling virus* (Fellers et al., 1998). RdRp assays could also be performed *in vivo* by comparing the accumulation of both positive and negative RNAs in TuMV-infected eEF1A overexpressing or depleted plants.

2. *Precise delineation of the interaction domain of TuMV RdRp with* A. thaliana *eEF1A*. Recombinant clones for the expression of truncated subdomains of RdRp are already available in our laboratory (Dr. Dufresne, unpublished results) while recombinant clones for the expression of truncated subdomains for eEF1A could be developed for that purpose. The finding of critical molecular contact points would be useful to further characterize the functional role of this specific interaction.

3. *Purification and characterization of the content 6K vesicles.* Present results on the content of the 6K-induced vesicles likely have revealed only a small fraction of its composition in host and viral factors. Progress in this area should continue to accelerate due to the development of the fluorescently labeled 6K-GFP TuMV infectious clone. Proteomic analyses of host and viral protein present within these vesicles are informative on the constitution of the replication complex.

4. *Visualization of viral RNA translation in 6K-induced vesicles*. Despite the presence of three translation factors in TuMV 6K-induced vesicles, it is still unclear whether viral translation occurs in these vesicles. Thus, there is a requirement for a way to follow newly synthesized proteins from their site of translation. A recently developed method called translation site imaging should be considered in the quest of visualizing viral RNA translation in 6K-induced vesicles. The approach can identify polypeptides as they are synthesized in living cell based on genetically encodable tetracysteine tags that associate with the biarsenical dyes FiAsH and ReAsH (Estevez and Somerville, 2006; Rodriguez et al., 2006, Zhang et al., 2002).

5. *Visualization of viral RNA replication in 6K-induced vesicles.* The presence of RdRp, cellular factors and VPg-Pro in the 6K-induced vesicles strongly suggests that the viral replication occurs in these structures. However, to date, the presence of actively replicating RNA in TuMV-induced vesicles has not been shown. Thus, experimental work should be conducted to visualized RNA replication sites inside of these vesicles by immunofluorescence staining using antibodies either directed against double-stranded

RNA or neosynthesized 5-bromouridine-labelled RNA. The presence of translation and replication activity in these vesicles would reinforce our model in which both processes are coupled in 6K-induced vesicles.

To further clarify the role the P3-lipase interaction in viral infection, the following experimental work should be achieved:

1. *Assessment of the role of the P3-GDSL-lipase interaction during TuMV infection.* Our attempt to analyze TuMV infection in *lipase* knockout plants has lead to inconclusive results. The functional redundancy among *A. thaliana* GDSL-lipase gene members may explain these results. One way to circumvent the redundancy associated problematic would be to generate double or triple mutants and to challenge them with TuMV. This approach was recently used in the TuMV-*A. thaliana* pathosystem where depletion of PABP in double knockout plants was shown to result in reduced TuMV accumulation (Dufresne et al., 2008b). Another alternative would be to analyze the infection of TuMV in plants in which *lipase* gene expression has been silenced by RNA interference (RNAi). RNAi technology has previously been used successfully with other potyvirus to demonstrate the importance of particular host-virus interactions (Jimenez et al., 2006).

2. *Analysis of the effect of TuMV infection on the expression level of GDSL-lipases.* Level of at least some lipases is known to be altered following infection by certain plant viruses (Marathe et al., 2004, Whitham et al., 2003; Yang et al., 2007). The availability of a TuMV infectious clone expressing GFP and our expertise in quantitative real-time

PCR open the way for spatial and temporal analysis of GDSL-lipases mRNA expression level during TuMV infection. This type of dissection strategy was recently employed to analyze *A. thaliana* gene expression in response to viral infection (Yang et al., 2007). Defining how the expression of GDSL-lipases is altered during the course of TuMV infection could lead to a better understanding of their roles in plant defense and/or in pathogenesis.

3. *Precise delineation of the interaction domain of TuMV P3 with A. thaliana GDSL-lipase.* Identification of the critical molecular contact points may be achieved either by the generation of recombinant clones for the expression of truncated subdomains of both proteins or by targeted point mutations. The finding of critical mutations would be useful to further characterize the functional role of this specific interaction.

CHAPTER VIII

CONTRIBUTION TO KNOWLEDGE

Chapter 3:

1) Two TuMV proteins, VPg-Pro and RdRp, were found to interact with *A. thaliana* host factor eEF1A. According to our knowledge, it is the first report demonstrating an interaction between VPg-Pro and eEF1A, while it is the first time that the eEF1A/RdRp interaction is shown for potyviruses. The identification of eEF1A as a host interacting partner of VPg-Pro and RdRp strongly suggest its involvement in potyvirus infection and open new avenues of research on potyvirus replication cycle.

2) The fact that eEF1A level is substantially higher in membrane-associated fractions of infected plants when compared to healthy plants is relevant knowledge as TuMV replication complexes are known to be associated to membranes. The redistribution of eEF1A and RdRP to membranes was shown to be driven by the polypeptide 6K-VPg-Pro. These data suggest that eEF1A can be internalized within 6K-VPg-Pro-induced vesicles and that a tripartite complex between eEF1A, 6K-VPg-Pro and RdRp is likely to happen. This theory is supported by the *in vitro* studies which indicate that both viral proteins bind to eEF1A in a non-competitive manner. Taken together, these results strengthen the notion of the potential involvement eEF1A in potyviral replication.

3) To date, the retargeting of host and viral proteins to 6K-VPg-Pro-induced vesicles was analyzed by ectopic expression of individual proteins in a non-infectious context. To circumvent this limitation, a fluorescent-labeled 6K-GFP TuMV infectious clone was developed and characterized. This pCambiaTunos/6KGFP vector represents a powerful tool to analyze the composition of the replication complex, and can be used by other researchers working on the characterization of TuMV.

4) The presence of three translation factors, the heat shock cognate 70-3, and viral replication proteins in TuMV-induced vesicles adds significant knowledge to accumulating evidence that viral translation and replication are coupled. Additionally, the results of this chapter highlight the importance of 6K-VPg-Pro and RdRp as scaffold proteins for the formation of a multi-protein complex within virus-vesicles.

Chapter 4:

The finding that TuMV and Norwalk virus (NV) VPg(s) possess a ribonucleolytic activity represents new evidence that such an enzymatic activity is associated to the VPg protein. The capacity of TuMV and NV VPg(s) to degrade RNA suggests that these proteins may contribute to the host RNA translation shutoff associated with many virus infections.

Chapter 5:

1) The finding that P3 interacts with an *A. thaliana* GDSL-lipase protein is, to our knowledge, the first report on the interaction between the potyviral P3 protein and a host

protein. It has been reported previously that lipases are implicated in plant defense. Thus, the P3-GDSL-lipase interaction is likely part of a defensive mechanism and progress in this area should continue to allow a better understanding of the molecular basis of the infection process. This in return provides new targets for the development of antiviral strategies and virus resistant plants.

2) The cellular localization of TuMV P3 and its host interactor (At1g29670 gene product: *A. thaliana* GDSL-lipase) was established *in planta*. This is the first time, to our knowledge, that both proteins are visualized *in planta*. A partial co-localization between the two proteins was also demonstrated. Such localization studies provide key insights into protein function, while the co-localization study reinforce the proposed P3-GDSL-lipase interaction role in disease resistance and/or pathogenesis.

Appendix 1:

1) Two *A. thaliana* host factors, PABP2 and Hsc70, were found to interact with the RdRp of TuMV. This is the first report on RdRp/Hsc70 interaction for potyviruses, whereas it is the first time that the RdRp/PABP2 interaction is described for TuMV. These interactions are likely important for RdRp functions and provide insights on the molecular contacts points and events that must occur for successful infection.

2) The data obtained from the localization studies revealed that TuMV 6K-VPg-Pro polypeptide alone was sufficient to redirect RdRp and Hsc70-3 to ER-derived vesicles. These results raise the possibility that Hsc-70-3 is an integral component of the replicase

complex and may contribute to the regulation of the RdRp activity. Taken together, the results presented in chapter 3 increase our knowledge on viral replication/translation.

REFERENCES

Abel, K., Yoder, M. D., Hilgenfeld, R., and Jurnak, F. 1996. An alpha to beta conformational switch in EF-Tu. Structure 4, 1153-1159.

Adam, S. A., Nakagawa, T., Swanson, M. S., Woodruff, T. K., and Dreyfuss, G. 1986. mRNA polyadenylate-binding protein: Gene isolation and sequencing and identification of a ribonucleoprotein consensus sequence. Mol. Cell. Biol. 6, 2932-2943.

Ahlquist, P. 2002. RNA-dependent RNA polymerases, viruses, and RNA silencing. Science 296, 1270-1273.

Ahlquist, P., Noueiry, A. O., Lee, W.-M., Kushner, D. B., and Dye, B. T. 2003. Host factors in positive-strand RNA virus genome replication. J. Virol. 77, 8181-8186.

Alonso, J. M., Stepanova, A. N., Leisse, T. J., Kim, C. J., Chen, H., Shinn, P., Stevenson, D. K., Zimmerman, J., Barajas, P., Cheuk, R., Gadrinab, C., Heller, C., Jeske, A., Koesema, E., Meyers, C. C., Parker, H., Prednis, L., Ansari, Y., Choy, N., Deen, H., Geralt, M., Hazari, N., Hom, E., Karnes, M., Mulholland, C., Ndubaku, R., Schmidt, I., Guzman, P., Aguilar-Henonin, L., Schmid, M., Weigel, D., Carter, D. E., Marchand, T., Risseeuw, E., Brogden, D., Zeko, A., Crosby, W. L., Berry, C. C., and Ecker, J. R. 2003. Genome-wide insertional mutagenesis of *Arabidopsis thaliana*. Science 301, 653-657.

Alvarez, E., Castella, A., Menandez-arias, L., and Carrasco, L. 2006. HIV protease cleaves poly(A)-binding protein. Biochem. J. 396, 219-226.

Alzhanova, D., Napuli, A., Creamer, R., and Dolja, V. 2001. Cell-to-cell movement and assembly of a plant closterovirus: roles for the capsid proteins and Hsp70 homolog. EMBO J. 20, 6997-7007.

Amrani, N., Minet, M., Le Gouar, M., Lacroute, F., and Wyers, F. 1997. Yeast Pab1 interacts with Rna15 and participates in the control of the poly(A) tail length *in vitro*. Mol. Cell. Biol. 17, 3694-3701.

Anandalakshmi, R., Marathe, R., Ge, X., Herr, J. M. Jr., Mau, C., Mallory, A., Pruss, G., Bowman, L., and Vance, V. B. 2000. A calmodulin-related protein that suppresses posttranscriptional gene silencing in plants. Science 290, 142-144.

Anindya, R. and Savithri, H. S. 2004. Potyviral NIa proteinase, a proteinase with novel deoxyribonuclease activity. J. Biol. Chem. 279, 32159-32169.

Aparicio, F., Thomas, C. L., Lederer, C., Niu, Y., Wang, D., and Maule, A. J. 2005. Virus induction of heat shock protein 70 reflects a general response to protein accumulation in the plant cytosol. Plant Physiol. 138, 529-536.

Aranda, M. A. and Maule, A. J. 1998. Virus-induced host gene shutoff in animals and plants. Virology 243, 261-267.

Aranda, M. A., Escaler, M., Wang, D., and Maule, A. J. 1996. Induction of Hsp70 and polyubiquitin expression associated with plant virus replication. Proc. Natl. Acad. Sci. U.S.A. 93, 15289-15293.

Arif, S. A., Hamilton, R. G., Yusof, F., Chew, N. P., Loke, Y. H., Nimkar, S., Beintema, J. J., and Yeang, H. Y. 2004. Isolation and characterization of the early nodule-specific protein homologue (Hev b 13), an allergenic lipolytic esterase from *Hevea brasiliensis* latex. J. Biol. Chem. 279, 23933-23941.

Atreya, C. D., Atreya, P. L., Thornburu, D. W., and Pirone, T. P. 1992. Site-directed mutations in potyvirus HC-Pro gene affect helper component activity, virus accumulation, and symptom expression in infected tobacco plants. Virology 191, 106-111.

Baker, B., Zambryski, P., Staskawicz, B., and Dinesh-Kumar, S. P. 1997. Signaling in plant-microbe interactions. Science 276, 726-733.

Bantignies, B., Séguin, J., Muzac, I., Dédaldéchamp, F., Gulick, P., and Ibrahim, R. 2000. Direct evidence for ribonucleolytic activity of a PR-10-like protein from white lupin roots. Plant Mol. Biol. 42, 871-881.

Bassell, G. J. and Singer, R. H. 1997. mRNA and cytoskeletal filaments. Curr. Opin. Cell Biol. 9, 109-115.

Bassel, G. J., Oleynikov, Y., and Singer, R. H. 1999. The travels of mRNAs through all cells large and small. FASEB J. 13, 3450-3454.

Bassel, G. J., Powers, C., Taneja, K. L., and Singer, R. H. 1994. Single mRNAs visualized by ultrastructural in situ hybridization are principally localized at actin filament intersections in fibroplasts. J. Cell Biol. 126, 863-876.

Basso, J., Dallaire, P., Charest, P. J., Devantier, Y., and Laliberté, J.-F. 1994. Evidence for an internal ribosome entry site within the 5' non-translated region of *Turnip mosaic potyvirus* RNA. J. Gen. Virol. 75, 3157-3165.

Bastin, M. and Hall, T. C. 1976. Interaction of elongation factor 1 with aminoacylated *Brome mosaic virus* and tRNA's. J. Virol. 20**,** 117-122.

Baunoch, D. A., Das, P., Browning, M. E., and Hari, V. 1991. A temporal study of the expression of the capsid, cytoplasmic inclusion and nuclear inclusion proteins of *Tobacco etch potyvirus* in infected plants. J. Gen. Virol. 72, 487-492.

Beauchemin, C. and Laliberté, J.-F. 2007. The poly(A) binding protein is internalized in virus-induced vesicles or redistributed to the nucleolus during *Turnip mosaic virus* infection. J. Virol. 81, 10905-10913.

Beauchemin, C., Bougie, V., and Laliberté, J.-F. 2005. Simultaneous production of two foreign proteins from a potyvirus-based vector. Virus Res. 112, 1-8.

Beauchemin, C., Boutet, N., and Laliberté, J.-F. 2007. Visualization of the interaction between the precursors of VPg, the viral protein linked to the genome of *Turnip mosaic virus*, and the translation eukaryotic initiation factor iso 4E *in planta*. J. Virol. 81, 775-782.

Beelman, C. A., Stevens, A., Caponigro, G., LaGrandeur, T. E., Hatfield, L., Fortner, D., and Parker, R. 1996. An essential component of the decapping enzyme required for normal rates of mRNA turnover. Nature 382, 642-646.

Beere, H. M. and Green, D. R. 2001. Stress management - heat shock protein-70 and the regulation of apoptosis. Trends Cell Biol. 11, 6-10.

Berchtold, H., Reshetnikova, L., Reiser, C. O., Schirmer, N. K., Sprinzl, M., and Hilgenfeld, R. 1993. Crystal structure of active elongation factor Tu reveals major domain rearrangements. Nature 365, 126-132.

Bergamini, G., Preiss, T., and Hentze, M. W. 2000. Picornavirus IRESes and the poly(A) tail jointly promote cap-independent translation in a mammalian cell-free system. RNA 6, 1781-1790.

Bhardwaj, K., Guarino, L., and Kao, C. C. 2004. The severe acute respiratory syndrome coronavirus Nsp15 protein is an endoribonuclease that prefers manganese as a cofactor. J. Virol. 78, 12218-12224.

Blackwell, J. L. and Brinton, M. A. 1997. Translation elongation factor-1 alpha interacts with the 3' stem-loop region of West Nile virus genomic RNA. J. Virol. 71**,** 6433-6444.

Blumenthal, T. and Carmichael, G. G. 1979. RNA replication: function and structure of Qbeta-replicase. Annu. Rev. Biochem. 48, 525-548.

Blumenthal, T., Young, R. A., and Brown, S. 1976. Function and structure in phage Qbeta RNA replicase. Association of EF-Tu-Ts with the other enzyme subunits. J. Biol. Chem. 251, 2740-2743.

Brick, D. J., Brumlik, M. J., Buckley, J. T., Cao, J. X., Davies, P. C., Misra, S., Tranbarger, T. J., and Upton, C. 1995. A new family of lipolytic plant enzymes with members in rice, *Arabidopsis* and maize. FEBS Lett. 377, 475-480.

Brown, G., Rixon, H. W. M., Steel, J., McDonald, T. P., Pitt, A. R., Graham, S., and Sugrue, R. J. 2005. Evidence for an association between heat shock protein 70 and the respiratory syncytial virus polymerase complex within lipid-raft membranes during virus infection. Virology 338, 69-80.

Brown, C. E. and Sachs, A. B. 1998. Poly(A) tail length control in *Saccharomyces cerevisiae* occurs by message-specific deadenylation. Mol. Cell. Biol. 18, 6548-6559.

Browning, K. S. 1996. The plant translational apparatus. Plant Mol. Biol. 32, 107-144.

Browning, K. S., Humphreys, J., Hobbs, W., Smith, G. B., and Ravel, J. M. 1990. Determination of the amounts of the protein synthesis initiation and elongation factors in wheat germ. J. Biol. Chem. 265, 17967-17973.

Brunt, A. A. 1992. The general properties of potyviruses. Arch. Virol. Suppl. 5, 3-16.

Buchanan, B. B., Gruissem, W., and Jones, R. L. 2000. Biochemistry and molecular biology of plants. John Wiley and Sons Inc.

Buck, K. W. 1996. Comparison of the replication of positive-stranded RNA viruses of plants and animals. Adv. Virus Res. 47, 159-251.

Caponigro, G. and Parker, R. 1995. Multiple functions for the poly(A)-binding protein in mRNA decapping and deadenylation in yeast. Genes Dev. 9, 2421-2432.

Chen, Z., Li, Y., and Krug, R. M. 1999. Influenza A virus NS1 protein targets poly-(A)-binding protein II of the cellular 3'-end processing machinery. EMBO J. 18, 2273-2283.

Choi, I. R., Stenger, D. C., and French, R. 2000. Multiple interactions among proteins encoded by the mite-transmitted *Wheat streak mosaic tritimovirus*. Virology 267, 185-198.

Chu, M., Lopez-Moya, J. J., Llave-Correas, C., and Pirone T. P. 1997. Two separate regions in the genome of the *Tobacco etch virus* contain determinants of the wilting response of Tabasco pepper. Mol. Plant Microbe Interact. 10, 472-480.

Cimarelli, A. and Luban, J. 1999. Translation elongation factor-α interacts specifically with the human immunodeficiency virus type 1 gag polyprotein. J. Virol. 73, 5388-5401.

Condeelis, J. 1995. Elongation factor 1-alpha, translation and the cytoskeleton. Trends Biochem. Sci. 20, 169-170.

Cotton, S., Dufresne, P. J., Thivierge, K., Ide, C., and Fortin, M. G. 2006. The VPgPro protein of *Turnip mosaic virus*: *in vitro* inhibition of translation from a ribonuclease activity. Virology 351, 92-100.

Cotton, S., Grangeon, R., Thivierge, K., Mathieu, I., Ide, C., and Laliberté, J.-F. *Turnip mosaic virus* RNA replication complex vesicles are mobile, align with microfilaments and are each derived from a single viral genome. J. Virol. 83, 10460-10471.

Craig, E. A., Baxter, B. K., Becker, J., Halladay, J., and Ziegelhoffer, T. 1994. Cytosolic hsp70s of *Saccharomyces cerevisae*: roles in protein synthesis, protein translocation, proteolysis and regulation. In The biology of heat shock proteins and molecular chaperones, pp. 31-52. Edited by R. I. Morimoto, A. Tissieres & C. Georgopoulos. New York: Cold Spring Harbor Laboratory Press.

Craig, A. W. B., Haghighat, A., Yu, A. T. K., and Sonenberg, N. 1998. Interaction of polyadenylate-binding protein with the eIF4G homologue PAIP enhances translation. Nature 392, 520-523.

Cummins, I. and Edwards, R. 2004. Purification and cloning of an esterase from the weed black-grass (*Alopecurus myosuroides*), which bioactivates aryloxyphenoxypropionate herbicides. Plant J. 39, 894-904.

Daros, J.-A. and Carrington, J. C. 1997. RNA binding activity of NIa proteinase of *Tobacco etch potyvirus*.Virology 237, 327–336.

Das, T., Mathur, M., Gupta, A. K., Janssen, G. M., and Banerjee, A. K. 1998. RNA polymerase of vesicular stomatitis virus specifically associates with translation elongation factor-1 alphabetagamma for its activity. Proc. Natl. Acad. Sci. U.S.A 95, 1449-1454.

Daughenbaugh, K. F., Fraser, C. S., Hershey, J. W., and Hardy, M. E. 2003. The genome-linked protein VPg of the Norwalk virus binds eIF3, suggesting its role in translation initiation complex recruitment. EMBO J. 22, 2852–2859.

Davis, W. G., Blackwell, J. L., Shi, P.-Y., and Brinton, M. A. 2007. Interaction between the cellular protein eEF1A and the 3'-terminal stem-loop of West Nile virus genomic RNA facilitates viral minus-strand RNA synthesis. J. Virol. 81, 10172-10187.

De Nova-Ocampo, M., Villegas-Sepulveda, N., and del Angel, R. M. 2002. Translation elongation factor-1alpha, La, and PTB interact with the 3' untranslated region of dengue 4 virus RNA. Virology 295, 337-347.

Derewenda, Z. S. 1994. Structure and function of lipases. Adv. Protein Chem. 45, 1-52.

Dhondt, S., Geoffroy, P., Stelmach, B. A., Legrand, M., and Heitz, T. 2000. Soluble phospholipase A2 activity is induced before oxylipin accumulation in *Tobacco mosaic virus*-infected tobacco leaves and is contributed by patatin-like enzymes. Plant J. 23, 431-440.

Dolja, V. V., Haldeman, R., Montgomery, A. E., Vandenbosch, K. A., and Carrington, J. C. 1995. Capsid protein determinants involved in cell-to-cell and long distance movement of *Tobacco etch potyvirus*. Virology 206, 1007-1016.

Dougherty, W. G. and Semler, B. L. 1993. Expression of virus-encoded proteinases: functional and structural similarities with cellular enzymes. Microbiol. Rev. 57, 781-822.

Dufresne, P. J., Thivierge, K., Cotton, S., Beauchemin, C., Ide, C., Ubalijoro, E., Laliberté, J.-F., and Fortin, M. G. 2008a. Heat shock 70 protein interaction with *Turnip mosaic virus* RNA-dependent RNA polymerase within virus-induced membrane vesicles. Virology 374, 217-227.

Dufresne, P. J., Ubalijoro, E., Fortin, M. G., and Laliberté, J.-F. 2008b. *Arabidopsis thaliana* class II poly(A)-binding proteins are required for efficient multiplication of *Turnip mosaic virus*. J. Gen. Virol. 89, 2339-2348.

Duncan, R., Milburn, S. C., and Hershey, J. W. 1987. Regulated phosphorylation and low abundance of HeLa cell initiation factor eIF-4F suggest a role in translational control. Heat shock effects on eIF-4F. J. Biol. Chem. 262, 380-388.

Dunoyer, P., Thomas, C., Harrison, S., Revers, F., and Maule, A. 2004. A cysteine-rich plant protein potentiates Potyvirus movement through an interaction with the virus genome-linked protein VPg. J. Virol. 78, 2301-2309.

Duprat, A., Caranta, C., Revers, F., Menand, B., Browning, K. S., and Robaglia, C. 2002. The *Arabidopsis* eukaryotic initiation factor (iso)4E is dispensable for plant growth but required for susceptibility to potyviruses. Plant J. 32, 927–934.

Durso, N. A. and Cyr, R. J. 1994. A calmodulin-sensitive interaction between microtubules and a higher plant homolog of elongation factor-1 alpha. Plant Cell 6, 893-905.

Eagles, R. M., Balmori-Melian, E., Beck, D. L., Garner, R. C., and Foster, R. L. S. 1994. Characterization of NTPase, RNA-biding and RNA-helicase activities of the cytoplasmic inclusion protein of *Tamarillo mosaic potyvirus*. Eur. J. Biochem. 224, 677-684.

Edwardson, J. and Christie, R. 1991. Potyviruses, pp. 24: Fla. Agric. Exp. Stat. Monogr. Ser.

Edwardson, J. and Purcifull, D. 1970. *Turnip mosaic virus*-induced inclusions. Phytopathology 60, 85-87.

Egger, D. and Bienz, K. 2005. Intracellular location and translocation of silent and active poliovirus replication complexes. J. Gen. Virol. 86, 707-718.

Egger, D., Teterina, N., Ehrenfeld, E., and Bienz, K. 2000. Formation of the poliovirus replication complex requires coupled viral translation, vesicle production, and viral RNA synthesis. J. Virol. 74, 6570-6580.

Eiamtanasate, S., Juricek, M., and Yap, Y. K. 2007. C-terminal hydrophobic region leads PRSV P3 protein to endoplasmic reticulum. Virus Genes 35, 611-617.

Escaler, M., Aranda, M. A., Thomas, C. L., and Maule, A. J. 2000. Pea embryonic tissues show common responses to the replication of a wide range of viruses. Virology 267, 318-325.

Estevez, J. M. and Somerville, C. 2006. FlAsH-based live-cell fluorescent imaging of synthetic peptides expressed in Arabidopsis and tobacco. Biotechniques 41, 569-570.

Falk, A., Feys, B. J., Frost, L. N., Jones, J. D., Daniels, M. J., and Parker, J. E. 1999. EDS1, an essential component of R gene-mediated disease resistance in *Arabidopsis* has homology to eukaryotic lipases. Proc. Natl. Acad. Sci. U.S.A 96, 3292-3297.

Fauquet, C., Mayo, M., Maniloff, J., Desselberger, U., and Ball, L. A. 2005. "Virus taxonomy: VIIIth report of the International Committee on Taxonomy of Viruses." Elsevier Academic Press, San Diego.

Fellers, J., Wan, J., Hong, Y., Collins, G. B., and Hunt, A. G. 1998. *In vitro* interactions between a potyvirus-encoded, genome-linked protein and RNA-dependent RNA polymerase. J. Gen. Virol. 79, 2043-2049.

Feys, B. J. and Parker, J. E. 2000. Interplay of signaling pathways in plant disease resistance. Trends Genet. 16, 449-455.

Flaherty, K. M., DeLuca-Flaherty, C., and McKay, D. B. 1990. Three-dimensional structure of the ATPase fragment of a 70K heat-shock cognate protein. Nature 346, 623-628.

Flaherty, K. M., Wilbanks, S. M., DeLuca-Flaherty, C., and McKay, D. B. 1994. Structural basis of the 70-kilodalton heat shock cognate protein ATP hydrolytic activity. II. Structure of the active site with ADP or ATP bound to wild-type and mutant ATPase fragment. J. Biol. Chem. 269, 12899-12907.

Frolova, E., Gorchakov, R., Garmashova, N., Atasheva, S., Vergara, L. A., and Frolov, I. 2006. Formation of nsP3-specific protein complexes during Sindbis virus replication. J. Virol. 80, 4122-4134.

Gale, M. J. R., Tan, S.-L., and Katze, M. G. 2000. Translational control of viral gene expression in eukaryotes. Microbiol. Mol. Biol. Rev. 64, 239-280.

Gallie, D. R. 1998. A tale of two termini: a functional interaction between the termini of an mRNA is a prerequisite for efficient translation initiation. Gene 216, 1-11.

Gallie, D. R. 2001. Cap-independent translation conferred by the 5' leader of *Tobacco etch virus* is eukaryotic initiation factor 4G dependent. J. Virol. 75, 12141-12152.

Gallie, D. R. and Browning, K. S. 2001. eIF4G functionally differs from eIFiso4G in promoting internal initiation, cap-independent translation, and translation of structured mRNAs. J. Biol. Chem. 276, 36951-36960.

Gao, Z., Johansen, E., Eyers, S., Thomas, C. L., Noel Ellis, T. H., and Maule, A. J. 2004. The potyvirus recessive resistance gene, *sbm1*, identifies a novel role for translation initiation factor eIF4E in cell-to-cell trafficking. Plant J. 40, 376-385.

Gavin, A. C., Aloy, P., Grandi, P., Krause, R., Boesche, M., Marzioch, M., Rau, C., Jensen, L. J., Bastuck, S., Dümpelfeld, B., Edelmann, A., Heurtier, M. A., Hoffman, V., Hoefert, C., Klein, K., Hudak, M., Michon, A. M., Schelder, M., Schirle, M., Remor, M., Rudi, T., Hooper, S., Bauer, A., Bouwmeester, T., Casari, G., Drewes, G., Neubauer, G., Rick, J. M., Kuster, B., Bork, P., Russell, R. B., and Superti-

Furga, G. 2006. Proteome survey reveals modularity of the yeast cell machinery. Nature 440, 631-636.

Georgopoulos, C. P. 1977. A new bacterial gene (groPC) which affects lambda DNA replication. Mol. Gen. Genet. 151, 35-39.

Gingras, A.-C., Raught, B., and Sonenberg, N. 1999. eIF4 initiation factors: Effectors of mRNA recruitment to ribosomes and regulators of translation. Annu. Rev. Biochem. 68, 913-963.

Goldbach, R. 1987. Genome similarities between plant and animal RNA viruses. Microbiol. Sci. 4, 197-202.

Gonen, H., Dickman, D., Schwartz, A. L., and Ciechanover, A. 1996. Protein synthesis elongation factor EF-1 alpha is an isopeptidase essential for ubiquitin-dependent degradation of certain proteolytic substrates. Adv. Exp. Med. Biol. 389, 209-219.

Goodfellow, I., Chaudhry, Y., Gioldasi, I., Gerondopoulos, A., Natoni, A., Labrie, L., Laliberté, J.-F., and Roberts, L. 2005. Calicivirus translation initiation requires an interaction between VPg and eIF4E. EMBO J. 6, 968-972.

Gradi, A., Svitkin, Y. V., Imataka, H., and Sonenberg, N. 1998. Proteolysis of human eukaryotic translation initiation factor eIF4GII, but not eIF4GI, coincides with the shutoff of host protein synthesis after poliovirus infection. Proc. Natl. Acad. Sci. U.S.A. 95, 11089-11094.

Gray, N. K., Coller, J. M., Dikson, K. S., and Wickens, M. 2000. Multiple portions of poly(A)-binding protein stimulate translation *in vivo*. EMBO J. 19, 4723-4733.

Green, R. and Noller, H. F. 1997. Ribosomes and translation. Annu. Rev. Biochem. 66, 679-716.

Grzela, R., Szolajska, E., Ebel, C., Madern, D., Favier, A., Wojtal, I., Zagorski, W., and Chroboczek, J. 2008. Virulence Factor of *Potato Virus Y*, Genome-attached Terminal Protein VPg, Is a Highly Disordered Protein. J. Biol. Chem. 283, 213-221.

Guo, D., Rajamaki, M.-L., Saarma, M., and Valkonen, J. P. T. 2001. Towards a protein interaction map of potyviruses: protein interaction matrixes of two potyviruses based on the yeast two-hybrid system. J. Gen. Virol. 82, 935-939.

Guo, D., Spetz, C., Saarma, M., and Valkonen, J. P. 2003. Two potato proteins, including a novel RING finger protein (HIP1), interact with the potyviral multifunctional protein HCpro. Mol. Plant Microbe Interact. 16, 405-410.

Haghighat, A., Mader, S., Pause, A., and Sonenberg, N. 1997. eIF4G dramatically enhances the binding of eIF4E to the mRNA 5'-cap structure. J. Biol. Chem. 272, 21677-21680.

Hajimorad, M. R., Ding, X. S., Flasinski, S., Mahajan, S., Graff, E., Haldeman-Cahill, R., Carrington, J. C., and Cassidy, B. G. 1996. NIa and NIb of *Peanut stripe potyvirus* are present in the nucleus of infected cells, but do not form inclusions. Virology 224, 368-379.

Hari, V., Siegel, A., Rozek, C., and Timberlake, W. E. 1979. The RNA of *Tobacco etch virus* contains poly(A). Virology 92, 568-571.

Harris, K. S., Xiang, W., Alexander, L., Lane, W. S., Paul, A. V., and Wimmer, E. 1994. Interaction of poliovirus polypeptide 3CDpro with the 5' and 3' termini of the poliovirus genome. Identification of viral and cellular cofactors needed for efficient binding. J. Biol. Chem. 269**,** 27004-27014.

Hartl, F. U. and Hayer-Hartl, M. 2002. Molecular chaperones in the cytosol: from nascent chain to folded protein. Science 295, 1852-1858.

Havelda, Z. and Maule, A. J. 2000. Complex spatial responses to *Cucumber mosaic virus* infection in susceptible *Cucurbita pepo* cotyledons. Plant Cell 12, 1975-1986.

Hector, R. E., Nykamp, K. R., Dheur, S., Anderson, J. T., Non, P. J., Urbinati, C. R., Wilson, S. M., Minvielle-Sebastia, L., and Swanson, M. S. 2002. Dual requirement for yeast hnRNP Nab2p in mRNA poly(A) tail length control and nuclear export. EMBO J. 21, 1800-1810.

Helmbrecht, K. and Rensing, L. 1999. Different constitutive heat shock protein 70 expression during proliferation and differentiation of rat C6 glioma cells. Neurochem. Res. 24, 1293-1299.

Herold, J. and Andino, R. 2001. Poliovirus RNA replication requires genome circularization through a protein-protein bridge. Mol. Cell 7, 581-591.

Hersey, J. W. B. and Merrick, W. C. 2000. Pathway and mechanism of initiation of protein synthesis. In translational control of gene expression (ed. N. Sonenberg et al.), p. 33. Cold Spring Harbor Laboratory Press, Cold Spring Harbor, NY.

Hjulsager, C. K., Lund, O.S., and Johansen, I. E. 2002. A new pathotype of *Pea seedborne mosaic virus* explained by properties of the P3-6K1- and viral genome-linked protein (VPg)-coding regions. Mol. Plant Microbe Interact. 15, 169-171.

Hoffmann-Sommergruber, K., Vanek-Krebitz, M., Radauer, C., Wen, J., Ferreira, F., Scheiner, O., and Breiteneder, H. 1997. Genomic characterization of members of

the Bet v 1 family: genes coding for allergens and pathogenesis-related proteins share intron positions. Gene 197, 91-100.

Hofius, D., Maier, A. T., Dietrich, C., Jungkunz, I., Bornke, F., Maiss, E., and Sonnewald, U. 2007. Capsid protein-mediated recruitment of host dnaJ-like proteins is required for *Potato virus Y* infection in tobacco plants. J. Virol. 81, 11870-11880.

Holland, J. J. and Peterson, J. A. 1964. Nucleic acid and protein synthesis during poliovirus infection of human cells. J. Mol. Biol. 8, 556-573.

Hong, Y. and Hunt, A. G. 1996. RNA polymerase activity catalyzed by a potyvirus-encoded RNA-dependent RNA polymerase. Virology 226, 146-151.

Hong, Y., Levay, K., Murphy, J. F., Klein, P. G., Shaw, J. G., and Hunt, A. G. 1995. A potyvirus polymerase interacts with the viral coat protein and VPg in yeast cells. Virology 214, 159-166.

Hoshino, S.-I., Imai, M., Kobayashi, T., Uchida, N., and Katada, T. 1999. The eukaryotic polypeptide chain releasing factor (eRF3/GSPT) carrying the translation termination signal to the 3'-poly(A) tail of mRNA. direct association of eRF3/GSPT with polyadenylate-binding protein. J. Biol. Chem. 274, 16677-16680.

Hu, J., Flores, D., Toft, D., Wang, X., and Nguyen, D. 2004. Requirement of heat shock protein 90 for human hepatitis B virus reverse transcriptase function. J. Virol. 78, 13122-13131.

Hu, J., Toft, D., Anselmo, D., and Wang, X. 2002. *In vitro* reconstitution of functional hepadnavirus reverse transcriptase with cellular chaperone proteins. J. Virol. 76, 269-279.

Hulst, M. M. and Moormann, R. J. 2001. Erns protein of pestiviruses. Meth. Enzymol. 342, 431-440.

Imataka, H., Gradi, A., and Sonenberg, N. 1998. A newly identified N-terminal amino acid sequence of human eIF4G binds poly(A)-binding protein and functions in poly(A)-dependant translation. EMBO J. 17, 7480-7489.

Ivanchenko, M., Vejlupkova, Z., Quatrano, R. S., and Fowler, J. E. 2000. Maize ROP7 GTPase contains a unique, CaaX box-independent plasma membrane targeting signal. Plant J. 24, 79-90.

Jakab, G., Manrique, A., Zimmerli, L., Metraux, J. P., and Mauch-Mani, B. 2003. Molecular characterization of a novel lipase-like pathogen-inducible gene family of *Arabidopsis*. Plant Physiol. 132, 2230-2239.

Jansen, R. P. 1999. RNA-cytoskeletal associations. FASEB J. 13, 455-466.

Jen, G., Morgan-Detjen, B., and Thach, R. E. 1980. Shutoff of HeLa cell protein synthesis by encephalomyocarditis virus and poliovirus: a comparative study. J. Virol. 35, 150-156.

Jenner, C. E., Tomimura, K., Ohshima, K., Hughes, S. L., and Walsh, J. A. 2002. Mutations in *Turnip mosaic virus* P3 and cylindrical inclusion proteins are separately required to overcome two Brassica napus resistance genes. Virology 300, 50-59.

Jenner, C. E., Wang, X., Tomimura, K., Ohshima, K., Ponz, F., and Walsh, J. A. 2003. The dual role of the potyvirus P3 protein of *Turnip mosaic virus* as a symptom and avirulence determinant in brassicas. Mol. Plant Microbe Interact. 16, 777-784.

Jiang, Y., Serviene, E., Gal, J., Panavas, T., and Nagy, P. D. 2006. Identification of essential host factors affecting Tombusvirus RNA replication based on the yeast Tet promoters Hughes collection. J. Virol. 80, 7394-7404.

Jimenez, I., Lopez, L., Alamillo, J. M., Valli, A., and Garcia, J. A. 2006. Identification of a *Plum pox virus* CI-interacting protein from chloroplast that has a negative effect in virus infection. Mol. Plant Microbe Interact. 19, 350-358.

Jindal, S. and Malkovsky, M. 1994. Stress responses to viral infection. Trends Microbiol. 2, 89-91.

Jirage, D., Tootle, T. L., Reuber, T. L., Frost, L. N., Feys, B. J., Parker, J. E., Ausubel, F. M., and Glazebrook, J. 1999. *Arabidopsis thaliana* PAD4 encodes a lipase-like gene that is important for salicylic acid signaling. Proc. Natl. Acad. Sci. U.S.A. 96, 13583-13588.

Jirage, D., Zhou, N., Cooper, B., Clarke, J. D., Dong, X., and Glazebrook, J. 2001. Constitutive salicylic acid-dependent signaling in cpr1 and cpr6 mutants requires PAD4. Plant J. 26, 395-407.

Joachims, M., Van Breugel, P. C., and Lloyd, R. E. 1999. Cleavage of poly(A)-binding protein by enterovirus proteases concurrent with inhibition of translation *in vitro*. J. Virol. 73, 718-727.

Jockusch, H., Wiegand, C., Mersch, B., and Rajes, D. 2001. Mutants of *Tobacco mosaic virus* with temperature-sensitive coat proteins induce heat shock response in tobacco leaves. Mol. Plant Microbe Interact. 14, 914-917.

Johansen, I. E., Lund, O. S., Hjulsager, C. K., and Laursen, J. 2001. Recessive resistance in *Pisum sativum* and potyvirus pathotype resolved in a gene-for-cistron correspondence between host and virus. J. Virol. 75, 6609-6614.

Johnson, C. M., Perez, D. R., French, R., Merrick, W. C., and Donis, R. O. 2001. The NS5A protein of bovine viral diarrhea virus interacts with the alpha subunit of translation elongation factor-1. J. Gen. Virol. 82, 2935-2943.

Joshi, R. L., Ravel, J. M., and Haenni, A. L. 1986. Interaction of *Turnip yellow mosaic virus* Val-RNA with eukaryotic elongation factor EF-1 [alpha]. Search for a function. EMBO J. 5**,** 1143-1148.

Kampmueller, K. M. and Miller, D. J. 2005. The cellular chaperone heat shock protein 90 facilitates Flock house virus RNA replication in *Drosophila* cells. J. Virol. 79, 6827-6837.

Kaneko, Y.-H., Inukai, T., Suehiro, N., Natsuaki, T., and Masuta, C. 2004. Fine genetic mapping of the *TuNI* locus causing systemic veinal necrosis by *Turnip mosaic virus* infection in *Arabidopsis thaliana*. Theor. Appl. Genet. 110, 33-40.

Kang, B.-C., Yeam, I., Frantz, J. D., Murphy, J. F., and Jahn, M. M. 2005. The *pvr1* locus in *Capsicum* encodes a translation initiation factor eIF4E that interacts with *Tobacco etch virus* VPg. Plant J. 42, 392-405.

Kapp, L. D. and Lorsch, J. R. 2004. The molecular mechanics of eukaryotic translation. Annu. Rev. Biochem. 73, 657-704.

Kasschau, K. D. and Carrington, J. C. 1995. Requirement for HC-Pro processing during genome amplification of *Tobacco etch potyvirus*. Virology 209, 268-273.

Kasschau, K. D., Cronin, S., and Carrington, J. C. 1997. Genome amplification and long distance movement functions associated with the central domain of *Tobacco etch potyvirus* helper-component proteinase. Virology 228, 251-262.

Katsafanas, G. C. and Moss, B. 2007. Colocalization of transcription and translation within cytoplasmic poxvirus factories coordinates viral expression and subjugates host functions. Cell Host Microbe 4, 221-228.

Kawashima, T., Berthet-Colominas, C., Wulff, M., Cusack, S., and Leberman, R. 1996. The structure of the *Escherichia coli* EF-Tu.EF-Ts complex at 2.5 A resolution. Nature 379, 511-518.

Keller, K. E., Johansen, I. E., Martin, R. R., and Hampton, R. O. 1998. Potyvirus genome-linked protein (VPg) determines *Pea seed-borne mosaic virus* pathotype-specific virulence in *Pisum sativum*. Mol. Plant Microbe Interact. 11, 124-130.

Kerekatte, V., Keiper, B. D., Badorff, C., Cai, A., Knowlton, K. U., and Rhoads, R. E. 1999. Cleavage of poly(A)-binding protein by coxsackievirus 2A protease *in vitro* and *in vivo*: another mechanism for host protein synthesis shutoff? J. Virol. 73, 709-717.

Khaleghpour, K., Svitkin, Y. V., Craig, A. W., DeMaria, C. T., Deo, R. C., Burley, S. K., and Sonenberg, N. 2001. Translational repression by a novel partner of human poly(A)-binding protein, Paip2. Mol. Cell 7, 205-216.

Khan, M. A., Miyoshi, H., Gallie, D. R., and Goss, D. J. 2007. Potyvirus genome-linked protein, VPg, directly affects wheat germ *in vitro* translation: interactions with translation initiation factors eIF4F and eIFiso4F. J. Biol. Chem. 283, 1340-1349.

Kim, K. K., Hwang, K. Y., Choi, K. D., Kang, J. H., Yoo, O. J., and Suh, S. W. 1993. Crystallization and preliminary X-ray crystallographic analysis of arylesterase from *Pseudomonas fluorescens*. Proteins 15, 213-215.

Kim, K. J., Lim, J. H., Kim, M. J., Kim, T., Chung, H. M., and Paek, K. H. 2008. GDSL-lipase1 (CaGL1) contributes to wound stress resistance by modulation of CaPR-4 expression in hot pepper. Biochem. Biophys. Res. Commun. 374, 693-698.

Klein, P. G., Klein, R. R., Rodriguezcerezo, E., Hunt, A. G., and Shaw, J. G. 1994. Mutational analysis of the *Tobacco vein mottling virus* genome. Virology 204, 759-769.

Klumpp, K., Hooker, L., and Handa, B. 2001. Influenza virus endoribonuclease. Meth. Enzymol. 342, 451-466.

Koonin, E. 1991. The phylogeny of RNA-dependent RNA polymerases of positive-strand RNA viruses. J. Gen. Virol. 72, 2197-2206.

Kormelink, R., Storms, M., Van Lent, J., Peters, D., and Goldbach, R. 1994. Expression and subcellular location of the NSM protein of *Tomato spotted wilt virus* (TSWV), a putative viral movement protein. Virology 1, 56-65.

Krikorian, C. R. and Read, G. S. 1991. *In vitro* mRNA degradation system to study the virion host shutoff function of Herpes simplex virus. J. Virol. 65, 112–122.

Kuhn, U. and Wahle, E. 2004. Structure and function of poly(A) binding proteins. Biochim. Biophys. Acta 25, 67-84.

Kumar, D. and Klessing, D. F. 2003. High-affinity salicylic acid-binding protein 2 is required for plant innate immunity and has salicylic acid-stimulated lipase activity. Proc. Natl. Acad. Sci. U.S.A. 100, 16101-16106.

Kunkel, B. N. and Brooks, D. M. 2002. Cross talk between signaling pathways in pathogen defense. Curr. Opin. Plant Biol. 5, 325-331.

Kuyumcu-Martinez, N. M., Belliot, G., Sosnovtsev, S. V., Chang, K.-O., Green, K. Y., and Lloyd, R. E. 2004a. Calicivirus 3C-like proteinase inhibits cellular translation by cleavage of poly(A)-binding protein. J. Virol. 78, 8172-8182.

Kuyumcu-Martinez, N. M., Joachims, M., and Lloyd, R. E. 2002. Efficient cleavage of ribosome-associated poly(A)-binding protein by enterovirus 3C protease. J. Virol. 76, 2062-2074.

Kuyumcu-Martinez, N. M., Van Eden, M. E., Younan, P., and Lloyd, R. E. 2004b. Cleavage of poly(A)-binding protein by poliovirus 3C protease inhibits host cell translation: a novel mechanism for host translation shutoff. Mol. Cell. Biol. 24, 1779-1790.

Kwong, A. D. and Frenkel, N. 1987. Herpes simplex virus-infected cells contain a function(s) that destabilizes both host and viral mRNAs. Proc. Natl. Acad. Sci. U.S.A. 84, 1926-1930.

Kyte, J. and Doolittle, R. F. 1982. A simple method for displaying the hydropathic character of a protein. J. Mol. Biol. 157, 105-132.

Lai, M. M. 1998. Cellular factors in the transcription and replication of viral RNA genomes: a parallel to DNA-dependent RNA transcription. Virology 244, 1-12.

Laidlaw, S. M., Arif Anwar, M., Thomas, W., Green, P., Shaw, K., and Skinner, M. A. 1998. Fowlpox virus encodes nonessential homologs of cellular alpha-SNAP, PC-1, and an orphan human homolog of a secreted nematode protein. J. Virol. 72, 6742-6751.

Lain, S., Riechmann, J. L., and Garcia, J. A. 1990. RNA helicase: A novel activity associated with a protein encoded by a positive-strand RNA virus. Nucleic Acids Res. 18, 7003-7006.

Laliberté, J.-F., Nicolas, O., Chatel, H., Lazure, C., and Morosoli, R. 1992. Release of a 22-kDa protein derived from the amino-terminal domain of the 49-kDa NIa of *Turnip mosaic potyvirus* in *Escherichia coli*. Virology 190, 510-514.

Lamphear, B. J., Kirchweger, R., Skern, T., and Rhoads, R. E. 1995. Mapping of functional domains in eukaryotic protein synthesis initiation factor 4G (eIF4G) with picornaviral proteases-implications for cap-dependent and cap-independent translational initiation. J. Biol. Chem. 270, 21975-21983.

Langenberg, W. G. and Zhang, L. 1997. Immunocytology shows the presence of *Tobacco etch virus* P3 protein in nuclear inclusions. J. Struct. Biol. 118, 243-247.

LaRiviere, F. J., Wolfson, A. D., and Uhlenbeck, O. C. 2001. Uniform binding of aminoacyl-tRNAs to elongation factor Tu by thermodynamic compensation. Science 294, 165-168.

Le, H., Tanguay, R. L., Balasta, M. L., Wei, C.-C., Browning, K. S., Metz, A. M., Goss, D. J., and Gallie, D. R. 1997. Translation initiation factors eIF-iso4G and eIF-4B

interact with the poly(A)-binding protein and increase its RNA binding activity. J. Biol. Chem. 272, 16247-16255.

Lellis, A. D., Kasschau, K. D., Whitham, S. A., and Carrington, J. C. 2002. Loss-of-susceptibility mutants of *Arabidopsis thaliana* reveal an essential role for eIF(iso)4E during potyvirus infection. Curr. Biol. 12, 1046-1051.

Lenstra, J. A. and Bloemendal, H. 1983. The major proteins from HeLa cells. Identification and intracellular localization. Eur. J. Biochem. 130, 419-426.

Léonard, S., Plante, D., Wittmann, S., Daigneault, N., Fortin, M. G., and Laliberté, J.-F. 2000. Complex formation between potyvirus VPg and translation eukaryotic initiation factor 4E correlates with virus infectivity. J. Virol. 74, 7730-7737.

Léonard, S., Viel, C., Beauchemin, C., Daigneault, N., Fortin, M. G., and Laliberté, J.-F. 2004. Interaction of VPg-Pro of *Turnip mosaic virus* with the translation initiation factor 4E and the poly(A)-binding protein *in planta*. J. Gen. Virol. 85, 1055-1063.

Li, X. H. and Carrington, J. C. 1993. Nuclear transport of *Tobacco etch potyviral* RNA-dependent RNA polymerase is highly sensitive to sequence alterations. Virology 193, 951-958.

Li, J., Derewenda, U., Dauter, Z., Smith, S., and Derewenda, Z. S. 2000. Crystal structure of the *Escherichia coli* thioesterase II, a homolog of the human Nef binding enzyme. Nat. Struct. Biol. 7, 555-559.

Li, Z., Barajas, D., Pavanas, T., Herbst, D. A., Nagy, P. D. 2008. Cdc34p ubiquitin conjugating enzyme is a component of the tombusvirus replicase complex and ubiquitinates p33 replication protein. J. Virol. 82, 6911-6926.

Li, Z., Pogany, J., Panavas, T., Xu, K., Esposito, A. M., Kinzy, T. G., and Nagy, P.D. 2009. Translation elongation factor 1A is a component of the tombusvirus replicase complex and affects the stability of the p33 replication co-factor. Virology 385, 245-260.

Li, X. H., Valdez, P., Olvera, R. E., and Carrington, J. C. 1997. Functions of the *Tobacco etch virus* RNA polymerase (NIb): subcellular transport and protein-protein interaction with VPg/proteinase (NIa). J. Virol. 71, 1598-1607.

Ling, H. 2008. Sequence analysis of GDSL-Lipase gene family in *Arabidopsis thaliana*. Pak. J. Biol. Sci. 11, 763-767.

Ling, H., Zhao, J., Zuo, K., Qiu, C., Yao, H., Qin, J., Sun, X., and Tang, K. 2006. Isolation and expression analysis of a GDSL-like lipase gene from *Brassica napus* L. J. Biochem. Mol. Biol. 39, 297-303.

Liu, J. Z., Blancaflor, E. B., and Nelson, R. S. 2005. The *Tobacco mosaic virus* 126-kilodalton protein, a constituent of the virus replication complex, alone or within the complex aligns with and traffics along microfilaments. Plant Physiol. 138, 1853-1865.

Lo, Y. C., Lee, Y. L., Shaw, J. F., and Liaw, Y. C. 2000. Crystallization and preliminary X-ray crystallographic analysis of thioesterase I from *Escherichia coli*. Acta Crystallogr. D Biol. Crystallogr. 56, 756-757.

Loake, G. and Grant, M. 2007. Salicylic acid in plant defence – the players and the protagonists. Curr. Opin. Plant Biol. 10, 466-472.

Lomakin, I. B., Hellen, C. U., and Petova, T. V. 2000. Physical association of eukaryotic initiation factor 4G (eIF4G) with eIF4A strongly enhances binding of eIF4G to the internal ribosomal entry site of encephalomyocarditis virus and is required for internal initiation of translation. Mol. Cell. Biol. 20, 6019-6029.

Lu, P., Saffran, H. A., and Smiley, J. R. 2001. The vhs1 mutant form of Herpes simplex virus virion host shutoff protein retains significant internal ribosome entry site-directed RNA cleavage activity. J. Virol. 75, 1072-1076.

Maldonado, A. M., Doerner, P., Dixon, R. A., Lamb, C. J., and Cameron, R. K. 2002. A putative lipid transfer protein involved in systemic resistance signalling in Arabidopsis. Nature 419, 399-403.

Mangus, D., Evans, M., and Jacobson, A. 2003. Poly(A)-binding proteins: multifunctional scaffolds for the post-transcriptional control of gene expression. Genome Biol. 4, 1-14.

Marathe, R., Guan, Z., Anandalakshmi, R., Zhao, H., and Dinesh-Kumar, S. P. 2004. Study of *Arabidopsis thaliana* resistome in response to *Cucumber mosaic virus* infection using whole genome microarray. Plant Mol. Biol. 55, 501-520.

Martin, M. T. and Gelie, B. 1997. Non-structural *Plum pox potyvirus* proteins detected by immunogold labeling. Eur. J. Plant Pathol. 103, 427-431.

Matsuda, D. and Dreher, T. W. 2004. The tRNA-like structure of *Turnip yellow mosaic virus* RNA is a 3'-translational enhancer. Virology 321, 36-46.

Matsuda, D., Yoshinari, S., and Dreher, T. W. 2004. eEF1A binding to aminoacylated viral RNA represses minus strand synthesis by TYMV RNA-dependent RNA polymerase. Virology 321, 47-56.

Mayer, M. P. 2005. Recruitment of Hsp70 chaperones: a crucial part of viral survival strategies. Rev. Physiol. Biochem. Pharmacol. 153, 1-46.

Mayer, M. P. and Bukau, B. 2005. Hsp70 chaperones: cellular functions and molecular mechanism. Cell. Mol. Life Sci. 62, 670-684.

Mayer, M. P., Schroder, H., Rudiger, S., Paal, K., Laufen, T., and Bukau, B. 2000. Multistep mechanism of substrate binding determines chaperone activity of Hsp70. Nat. Struct. Mol. Biol. 7, 586-593.

Mayfield, J. A., Fiebig, A., Johnstone, S. E., and Preuss, D. 2001. Gene families from the *Arabidopsis thaliana* pollen coat proteome. Science 292, 2482-2485.

Ménard, R., Chatel, H., Dupras, R., Plouffe, C., and Laliberté, J.-F. 1995. Purification of *Turnip mosaic potyvirus* viral protein genome-linked proteinase expressed in *Escherichia coli* and development of a quantitative assay for proteolytic activity. Eur. J. Biochem. 229, 107-112.

Merits, A., Guo, D., Jarvekulg, L., and Saarma, M. 1999. Biochemical and genetic evidence for interactions between *Potato A potyvirus*-encoded proteins P1 and P3 and proteins of the putative replication complex. Virology 263, 15-22.

Merits, A., Guo, D., and Saarma, M. 1998. VPg, coat protein and five non-structural proteins of *Potato A potyvirus* bind RNA in a sequence-unspecific manner. J. Gen. Virol. 79, 3123-3127.

Michel, Y. M., Borman, A. M., Paulous, S., and Kean, K. M. 2001. Eukaryotic initiation factor 4G-poly(A) binding protein interaction is required for poly(A) tail-mediated stimulation of picornavirus internal ribosome entry segment-driven translation

but not for X-mediated stimulation of hepatitis C virus translation. Mol. Cell. Biol. 21, 4097-4109.

Michel, Y. M., Poncet, D., Piron, M., Kean, K. M., and Borman, A. M. 2000. Cap-poly(A) synergy in mammalian cell-free extracts. Investigation of the requirements for poly(A)-mediated stimulation of translation initiation. J. Biol. Chem. 275, 32268-32276.

Michon, T., Estevez, Y., Walter, J., German-Retana, S., and Gall, O. 2006. The potyviral virus genome-linked protein VPg forms a ternary complex with the eukaryotic initiation factors eIF4E and eIF4G and reduces eIF4E affinity for a mRNA cap analogue. Eur. J. Biochem. 273, 1312-1322.

Mishra, N. C. 2002. Nucleases: Molecular Biology and Applications. Wiley-Interscience, New Jersey.

Mizumoto, H., Iwakawa, H.-O., Kaido, M., Mise, K., and Okuno, T. 2006. Cap-independent translation mechanism of *Red clover necrotic mosaic virus* RNA2 differs from that of RNA1 and is linked to RNA replication. J. Virol. 80, 3781-3791.

Molgaard, A., Kauppinen, S., and Larsen, S. 2000. Rhamnogalacturonan acetylesterase elucidates the structure and function of a new family of hydrolases. Structure 8, 373-383.

Momose, F., Naito, T., Yano, K., Sugimoto, S., Morikawa, Y., and Nagata, K. 2002. Identification of Hsp90 as a stimulatory host factor involved in influenza virus RNA synthesis. J. Biol. Chem. 277, 45306-45314.

Moore, R. C. and Cyr, R. J. 2000. Association between elongation factor-1α and microtubules in vivo is domain dependent and conditional. Cell Motil. Cytoskeleton 45, 279-292.

Moore, P. B. and Steitz, T. A. 2003. After the ribosome structures: how does peptidyl transferase work? RNA 9, 155-159.

Myoshi, H., Suehiro, N., Tomoo, K., Muto, S., Takahashi, T., Tsukamoto, T., Ohmori, T., and Natsuaki, T. 2005. Binding analyses for the interaction between plant virus genome-linked protein (VPg) and plant translational initiation factors. Biochimie 5, 1-12.

Nagy, D. P. 2008. Yeast as a model host to explore plant virus-host interactions. Annu. Rev. Phytopathol. 46, 217-242.

Napuli, A. J., Alzhanova, D. V., Doneanu, C. E., Barofsky, D. F., Koonin, E. V., and Dolja, V. V. 2003. The 64-kilodalton capsid protein homolog of *Beet yellows virus* is required for assembly of virion tails. J. Virol. 77, 2377-2384.

Napuli, A. J., Falk, B. W., and Dolja, V. V. 2000. Interaction between HSP70 homolog and filamentous virions of the *Beet yellows virus*. Virology 274, 232-239.

Naranjo, M. A., Forment, J., Roldan, M., Serrano, R., and Vicente, O. 2006. Overexpression of *Arabidopsis thaliana* LTL1, a salt-induced gene encoding a GDSL-motif lipase, increases salt tolerance in yeast and transgenic plants. Plant Cell Environ. 29, 1890-1900.

Nicaise, V., Gallois, J. L., Chafiai, F., Allen, L. M., Schurdi-Levraud, V., Browning, K. S., Candresse, T., Caranta, C., Le Gall, O., and German-Retana, S. 2007. Coordinated and selective recruitment of eIF4E and eIF4G factors for potyvirus infection in *Arabidopsis thaliana*. FEBS Lett. 581, 1041-1046.

Nicaise, V., German-Retana, S., Sanjuan, R., Dubrana, M.-P., Mazier, M., Maisonneuve, B., Candresse, T., Caranta, C., and LeGall, O. 2003. The eukaryotic translation initiation factor 4E controls lettuce susceptibility to the potyvirus *Lettuce mosaic virus*. Plant Physiol. 132, 1272-1282.

Nicolas, O. and Laliberté, J.-F. 1992. The complete nucleotide sequence of *Turnip mosaic potyvirus* RNA. J. Gen. Virol. 73, 2785-2793.

Nishikiori, M., Dohi, K., Mori, M., Meshi, T., Naito, S., and Ishikawa, M. 2006. Membrane-bound *Tomato mosaic virus* replication proteins participate in RNA synthesis

and are associated with host proteins in a pattern distinct from those that are not membrane bound. J. Virol. 80, 8459-8468.

Nissen, P., Kjeldgaard, M., Thirup, S., Polekhina, G., Reshetnikova, L., Clark, B. F., and Nyborg, J. 1995. Crystal structure of the ternary complex of Phe-tRNAPhe, EF-Tu, and a GTP analog. Science 270, 1464-1572.

Noueiry, A. O. and Ahlquist, P. 2003. *Brome mosaic virus* RNA replication: revealing the role of the host in RNA virus replication. Ann. Rev. Phytopathol. 41, 77-98.

Ogle, J. M., Brodersen, D. E., Clemons, W. M., Tarry, M. J., Carter, A. P., and Ramakrishnan, V. 2001. Recognition of cognate transfer RNA by the 30S ribosomal subunit. Science 292, 897-902.

Oglesbee, M. J., Liu, Z., Kenney, H., and Brooks, C. L. 1996. The highly inducible member of the 70 kDa family of heat shock proteins increases canine distemper virus polymerase activity. J. Gen. Virol. 77, 2125-2135.

Oh, I. S., Park, A. R., Bae, M. S., Kwon, S. J., Kim, Y. S., Lee, J. E., Kang, N. Y., Lee, S., Cheong, H., and Park, O. K. 2005. Secretome analysis reveals an *Arabidopsis* lipase involved in defense against *Alternaria brassicicola*. Plant Cell 17, 2832-2847.

Oroskar, A. A. and Read, G. S. 1989. Control of mRNA stability by the virion host shutoff function of Herpes simplex virus. J. Virol. 63, 1897-1906.

Ostareck-Lederer, A., Ostareck, D. H., and Hentze, M. W. 1998. Cytoplasmic regulatory functions of the KH-domain proteins hnRNPs K and E1/E2. Trends Biochem. Sci. 23, 409-411.

Padilla-Noriega, L., Paniagua, O., and Guzman-Leon, S. 2002. Rotavirus protein NSP3 shuts off host cell protein synthesis. Virology 298, 1-7.

Palter, K. B., Watanabe, M., Stinson, L., Mahowald, A. P., and Craig, E. A. 1986. Expression and localization of *Drosophila melanogaster* hsp70 cognate proteins. Mol. Cell. Biol. 6, 1187-1203.

Pathak, K. B., Sasvari, Z., and Nagy, P. 2008. The host Pex19p plays a rle in peroxisomal localization of tombusvirus replication proteins. Virology 379, 294-305.

Pelletier, J. and Sonenberg, N. 1988. Internal initiation of translation of eukaryotic mRNA directed by a sequence derived from poliovirus RNA. Nature 334, 320-325.

Peremyslov, V. V., Hagiwara, Y., and Dolja, V. V. 1999. HSP70 homolog functions in cell-to-cell movement of a plant virus. Proc. Natl. Acad. Sci. U.S.A. 96, 14771-14776.

Pestova, T. V. and Hellen, C. U. T. 2000. Ribosome recruitment and scanning: What's new? Trends Biochem. Sci. 24, 85-87.

Pestova, T. V., Hellen, C. U. T., and Shatsky, I. N. 1996. Canonical eukaryotic initiation factors determine initiation of translation by internal ribosomal entry. Mol. Cell. Biol. 16, 6859-6869.

Pestova, T. V., Kolupaeva, V. G., Lomakin, I. B., Pilipenko, E. V., Shatsky, I. N., Agol, V. I., Hellen, C. U. T. 2001. Molecular mechanisms of translation initiation in eukaryotes. Proc. Natl. Acad. Sci. U.S.A. 98, 7029-7036.

Pfaffl, M. W. 2001. A new mathematical model for relative quantification in real-time RT-PCR. Nucleic Acids Res. 29, e45.

Pfaffl, M. W., Horgan, G. W., and Dempfle, L. 2002. Relative expression software tool (REST) for group-wise comparison and statistical analysis of relative expression results in real-time PCR. Nucleic Acids Res. 30, e36.

Piron, M., Vende, P., Cohen, J., and Poncet, D. 1998. Rotavirus RNA-binding protein NSP3 interacts with eIF4GI and evicts the poly(A) binding protein from eIF4F. EMBO J. 17, 5811-5821.

Plante, D., Viel, C., Léonard, S., Hiroyuki, T., Laliberté, J.-F., and Fortin, M. G. 2004. *Turnip mosaic virus* VPg does not disrupt the translation initiation complex but interferes with cap binding. Physiol. Mol. Plant Pathol. 64, 219-226.

Polekhina, G., Thirup, S., Kjeldgaard, M., Nissen, P., Lippmann, C., and Nyborg, J. 1996. Helix unwinding in the effector region of elongation factor EF-Tu-GDP. Structure 4, 1141-1151.

Pringle, D. and Dickstein, R. 2004. Purification of ENOD8 proteins from *Medicago sativa* root nodules and their characterization as esterases. Plant Physiol. Biochem. 42, 73-79.

Prokhnevsky, A. I., Peremyslov, V. V., and Dolja, V. V. 2005. Actin cytoskeleton is involved in targeting of a viral Hsp70 homolog to the cell periphery. J. Virol. 79, 14421-14428.

Prokhnevsky, A. I., Peremyslov, V. V., Napuli, A. J., and Dolja, V. V. 2002. Interaction between long-distance transport factor and Hsp70-related movement protein of *Beet yellows virus*. J. Virol. 76, 11003-11011.

Puustinen, P. and Makinen, K. 2004. Uridylylation of the potyvirus VPg by viral replicase NIb correlates with the nucleotide binding capacity of VPg. J. Biol. Chem. 279, 38103-38110.

Qu, F. and Morris, T. J. 2002. Efficient infection of *Nicotiana benthamiana* by *Tomato bushy stunt virus* is facilitated by the coat protein and maintained by p19 through suppression of gene silencing. Mol. Plant Microbe Interact. 15, 193-202.

Restrepo-Hartwig, M. A. and Carrington, J. C. 1994. The *Tobacco etch potyvirus* 6-kilodalton protein is membrane associated and involved in viral replication. J. Virol. 68, 2388-2397.

Riechmann, J. L., Cervera, M. T., and Garcia, J. A. 1995. Processing of the *Plum pox virus* polyprotein at the P3-6K1 junction is not required for virus viability. J. Gen. Virol. 76, 961-966.

Riechmann, J. L., Lain, S., and Garcia, J. A. 1992. Highlights and prospects of potyvirus molecular biology. J. Gen. Virol. 73, 1-16.

Riedel, D., Lesemann, D. E., and Maiss, E. 1998. Ultrastructural localization of nonstructural and coat proteins of 19 potyviruses using antisera to bacterially expressed proteins of plum pox potyvirus. Arch. Virol. 143, 2133-2158.

Ritossa, F. 1962. A new puffing pattern induced by temperature shock and DNP in Drosophila. Experientia 18, 571-573.

Ro, Y.-T. and Patterson, J. L. 2000. Identification of the minimal essential RNA sequences sesponsible for site-specific targeting of the Leishmania RNA virus 1-4 capsid endoribonuclease. J. Virol. 74, 130-138.

Robaglia, C. and Caranta, C. 2006. Translation initiation factors: a weak link in plant RNA virus infection. Trends Plant Sci. 11, 40-45.

Rodnina, M. V. and Wintermeyer, W. 2001. Fidelity of aminoacyl-tRNA selection on the ribosome: kinetic and structural mechanisms. Annu. Rev. Biochem. 70, 415-435.

Rodriguez, A. J., Shenoy, S. M., Singer, R. H., and Condeelis, J. 2006. Visualization of mRNA translation in living cells. J. Cell. Biol. 175, 67-76.

Rodriguez-Cerezo, E. and Shaw, J. G. 1991. Two newly detected nonstructural viral proteins in potyvirus-infected cells. Virology 185, 572-579.

Rodriguez-Cerezo, E., Ammar, E. D., Pirone, T. P., and Shaw, J. G. 1993. Association of the non-structural P3 viral protein with cylindrical inclusions in potyvirus-infected cells. J. Gen. Virol. 74, 1945-1949.

Rodriguez Pulido, M., Serrano, P., Saiz, M., and Martinez-Salas, E. 2007. Foot-and-mouth disease virus infection induces proteolytic cleavage of PTB, eIF3a,b, and PABP RNA-binding proteins. Virology 364, 466-474.

Ruffel, S., Dussault, M.-H., Palloix, A., Moury, B., Bendahmane, A., Robaglia, C., and Caranta, C. 2002. A natural recessive resistance gene against *Potato virus Y* in pepper corresponds to the eukaryotic initiation factor 4E (eIF4E). Plant J. 32, 1067-1075.

Ruffel, S., Gallois, J., Lesage, M., and Caranta, C. 2005. The recessive potyvirus resistance gene *pot-1* is the tomato orthologue of the pepper *pvr2-eIF4E* gene. Mol. Genet. Gen. 274, 346-353.

Ruppert, M., Woll, J., Giritch, A., Genady, E., Ma, X., and Stöckigt, J. 2005. Functional expression of an ajmaline pathway-specific esterase from Rauvolfia in a novel plant-virus expression system. Planta 222, 888-898.

Sachs, A. B., David, R. W., and Kornberg, R. D. 1987. A single domain of yeast poly(A)-binding protein is necessary and sufficient for RNA binding and cell viability. Mol. Cell. Biol. 7, 3268-3276.

Sachs, A. B., Sarnow, P., and Hentze, M. W. 1997. Starting at the beginning, middle, and end: translation initiation in eukaryotes. Cell 89, 831-838.

Saenz, P., Cervera, M. T., Dallot, S., Quiot, L., Quiot, J.-B., Riechmann, J. L., and Garcia, J. A. 2000. Identification of a pathogenicity determinant of *Plum pox virus* in the sequence encoding the C-terminal region of protein P3 + $6K_1$. J. Gen. Virol. 81, 557-566.

Salonen, A., Ahola, T., and Kaariainen, L. 2005. Viral RNA replication in association with cellular membranes. Curr. Top. Microbiol. Immunol. 285, 139-173.

Sanchez, F., Martinez-Herrera, D., Aguilar, I., and Ponz, F. 1998. Infectivity of *Turnip mosaic potyvirus* cDNA clones and transcripts on the systemic host *Arabidopsis thaliana* and local lesion hosts. Virus Res. 55, 207-219.

Sanz, M. A., Castello, A., and Carrasco, L. 2007. Viral translation is coupled to transcription in Sindbis Virus-infected cells. J. Virol. 81, 7061-7068.

Sarnow, P. 1989. Role of 3'-end sequences in infectivity of poliovirus transcripts made *in vitro*. J. Virol. 63, 467-470.

Sato, M., Nakahara, K., Yoshii, M., Ishikawa, M., and Uyeda, I. 2005. Selective involvement of members of the eukaryotic initiation factor 4E family in the infection of *Arabidopsis thaliana* by potyviruses. FEBS Lett. 579, 1167-1171.

Satyanarayana, T., Gowda, S., Ayllon, M. A., and Dawson, W. O. 2004. Closterovirus bipolar virion: evidence for initiation of assembly by minor coat protein and its restriction to the genomic RNA 5' region. Proc. Natl. Acad. Sci. U.S.A. 101, 799-804.

Satyanarayana, T., Gowda, S., Mawassi, M., Albiach-Marti, M. R., Ayllon, M. A., Robertson, C., Garnsey, S. M., and Dawson, W. O. 2000. Closterovirus encoded

HSP70 homolog and p61 in addition to both coat proteins function in efficient virion assembly. Virology 278, 253-265.

Schaad, M. C., Anderberg, R. J., and Carrington, J. C. 2000. Strain-specific interaction of the *Tobacco etch virus* NIa protein with the translation initiation factor eIF4E in the yeast two-hybrid system. Virology 273, 300-306.

Schaad, M. C., Haldeman-Cahill, R., Cronin, S., and Carrington, J. C. 1996. Analysis of the VPg-proteinase (NIa) encoded by *Tobacco etch potyvirus*: effects of mutations on subcellular transport, proteolytic processing, and genome amplification. J. Virol. 70, 7039-7048.

Schaad, M. C., Jensen, P. E., and Carrington, J. C. 1997a. Formation of plant RNA virus replication complexes on membranes: role of an endoplasmic reticulum-targeted viral protein. EMBO J. 16, 4049-4059.

Schaad, M. C., Lellis, A. D., and Carrington, J. C. 1997b. VPg of *Tobacco etch potyvirus* is a host genotype-specific determinant for long-distance movement. J. Virol. 71, 8624-8631.

Schneider, R. J. and Mohr, I. 2003. Translation initiation and viral tricks. Trends Biochem. Sci. 28, 130-136.

Semler, B. L. and Wimmer, E. 2002. Molecular biology of picornaviruses, pp. 502. Washington: ASM Press.

Serva, S. and Nagy, P. D. 2006. Proteomics analysis of the Tombusvirus replicase: Hsp70 molecular chaperone is associated with the replicase and enhances viral RNA replication. J. Virol. 80, 2162-2169.

Shah, J. 2005. Lipids, lipases, and lipid-modifying enzymes in plant disease resistance. Annu. Rev. Phytopathol. 43, 229-260.

Shiina, N., Gotoh, Y., Kubomura, N., Iwamatsu, A., and Nishida, E. 1994. Microtubule severing by elongation factor 1 alpha. Science 266, 282-285.

Shukla, D. D., Ward, C. W., and Brunt, A. A. 1994. The Potyviridae. Wallingford, UK: CAB International.

Siaw, M. F., Shahabuddin, M., Ballard, S., Shaw, J. G., and Rhoads, R. E. 1985. Identification of a protein linked to the 5' terminus of *Tobacco vein mottling virus* RNA. Virology 142, 134-143.

Smiley, J. R., Elgadi, M. M., and Saffran, H. A. 2001. Herpes simplex virus vhs protein. Meth. Enzymol. 342, 440-451.

Soellick, T. R., Uhrig, J. F., Bucher, G. L., Kellmann, J. W., and Schreier, P. H. 2000. The movement protein NSm of *Tomato spotted wilt tospovirus* (TSWV): RNA binding, interaction with the TSWV N protein, and identification of interacting plant proteins. Proc. Natl. Acad. Sci. U.S.A. 97, 2373-2378.

Song, H., Parsons, M. R., Rowsell, S., Leonard, G., and Phillips, S. E. 1999. Crystal structure of intact elongation factor EF-Tu from Escherichia coli in GDP conformation at 2.05 A resolution. J. Mol. Biol. 285, 1245-1256.

Stahl, M., Retzlaff, M., Nassal, M., and Beck, J. 2007. Chaperone activation of the hepadnaviral reverse transcriptase for template RNA binding is established by the Hsp70 and stimulated by the Hsp90 system. Nucleic Acids Res. 35, 6124-6136.

Stapulionis, R. and Deutscher, M. P. 1995. A channeled tRNA cycle during mammalian protein synthesis. Proc. Natl. Acad. Sci. U.S.A. 92, 7158-7161.

Sticher, L., Mauch-Mani, B., and Métraux, J. P. 1997. Systemic acquired resistance. Annu. Rev. Phytopathol. 35, 235-270.

Storms, M. M., Kormelink, R., Peters, D., Van Lent, J. W., and Goldbach, R. W. 1995. The nonstructural NSm protein of *Tomato spotted wilt virus* induces tubular structures in plant and insect cells. Virology 2, 485-493.

Suehiro, N., Natsuaki, T., Watanabe, T., and Okuda, S. 2004. An important determinant of the ability of *Turnip mosaic virus* to infect *Brassica* spp. and/or *Raphanus sativus* is in its P3 protein. J. Gen. Virol. 85, 2087-2098.

Sullivan, C. S. and Pipas, J. M. 2001. The virus-chaperone connection. Virology 287, 1-8.

Sunshine, M. F. M., Stuart, J., and Yochem, J. 1977. A new host gene (groPC) necessary for lambda DNA replication. Mol. Gen. Genet. 151, 27-34.

Svitkin, Y. V., Imataka, H., Khaleghpour, K., Kahvejian, A., Liebig, H. D., and Sonenberg, N. 2001. Poly(A)-binding protein interaction with elF4G stimulates picornavirus IRES-dependent translation. RNA 7, 1743-1752.

Tan, Z. Y., Gibbs, A. J., Tomitaka, Y., Sanchez, F., Ponz, F., and Ohshima, K. 2005. Mutations in *Turnip mosaic virus* genomes that have adapted to *Raphanus sativus*. J. Gen. Virol. 86, 501-510.

Tarun, S. Z. Jr. and Sachs, A. B. 1995. A common function for mRNA 5' and 3' ends in translation initiation in yeast. Genes Dev. 9, 2997-3007.

Tarun, S. Z. Jr. and Sachs, A. B. 1996. Association of the yeast poly(A) tail binding protein with translation initiation factor eIF-4G. EMBO J. 15, 7168-7177.

Teissere, M., Borel, M., Caillol, B., Nari, J., Gardies, A. M., and Noat, G. 1995. Purification and characterization of a fatty acyl-ester hydrolase from post-germinated sunflower seeds. Biochim. Biophys. Acta 1255, 105-112.

Teycheney, P.-Y., Aaziz, R., Dinant, S., Salanki, K., Tourneur, C., Balazs, E., Jacquemond, M., and Tepfer, M. 2000. Synthesis of (-)-strand RNA from the 3' untranslated region of plant viral genomes expressed in transgenic plants upon infection with related viruses. J. Gen. Virol. 81, 1121-1126.

Thivierge, K., Cotton, S., Dufresne, P. J., Mathieu, I., Beauchemin, C., Ide, C., Fortin, M. G., and Laliberté, J.-F. 2008. Eukaryotic elongation factor 1A interacts with *Turnip mosaic virus* RNA-dependent RNA polymerase and VPg-Pro in virus-induced vesicles. Virology 377, 216-225.

Thivierge, K., Nicaise, V., Dufresne, P. J., Cotton, S., Laliberté, J.-F., Le Gall, O., and Fortin, M. G. 2005. Plant virus RNAs. Coordinated recruitment of conserved host functions by (+) ssRNA viruses during early infection events. Plant Physiol. 138, 1822-1827.

Thompson, A. and Peersen, O. (2004). Structural basis for proteolysis-dependent activation of the poliovirus RNA-dependent RNA polymerase. EMBO J. 23, 3462-3471.

Tolonen, N., Doglio, L., Schleich, S., and Krijnse Locker, J. 2001. Vaccinia virus DNA replication occurs in endoplasmic reticulum-enclosed cytoplasmic mini-nuclei. Mol. Biol. Cell. 12, 2031-2046.

Tomita, Y., Mizuno, T., Diez, J., Naito, S., Ahlquist, P., and Ishikawa, M. 2003. Mutation of host dnaJ homolog inhibits *Brome mosaic virus* negative-strand RNA synthesis. J. Virol. 77, 2990-2997.

Upton, C. and Buckley, J. T. 1995. A new family of lipolytic enzymes? Trends Biochem. Sci. 20, 178-179.

Urcuqui-Inchima, S., Haenni, A. L., and Bernardi, F. 2001. Potyvirus proteins: a wealth of functions. Virus Res. 74, 157-175.

van Regenmortel, M. H. V., Fauquet, C. M., Bishop, D. H. L., Carstens, E. B., Estes, M. K., Lemon, S. M., Maniloff, J., Mayo, M. A., McGeoch, D. J., Pringle, C. R., and Wickner, R. B. 2000. Virus Taxonomy. Seventh report of the international committee on taxonomy of viruses. Academic Press, San Diego.

Vende, P., Piron, M., Castagne, N., and Poncet, D. 2000. Efficient translation of rotavirus mRNA requires simultaneous interaction of NSP3 with the eukaryotic translation initiation factor eIF4G and the mRNA 3' end. J. Virol. 74, 7064-7071.

Verchot, J. and Carrington, J. C. 1995. Debilitation of plant potyvirus infectivity by P1 proteinase-inactivating mutations and restoration by second-site modifications. J. Virol. 69, 1582-1590.

Vitagliano, L., Masullo, M., Sica, F., Zagari, A., and Bocchini, V. 2001. The crystal structure of *Sulfolobus solfataricus* elongation factor 1alpha in complex with GDP reveals novel features in nucleotide binding and exchange. EMBO J. 20, 5305-5311.

Walsh, J. A. 1997. *Turnip mosaic virus*. Data sheet for Commonwealth Agriculture Bureau International Global Crop Protection Compendium. Wallingford, UK: CAB International.

Walsh, J. A. and Jenner, C. E. 2002. *Turnip mosaic virus* and quest for durable resistance. Mol. Plant Pathol. 3, 289-300.

Wang, X., Ullah, Z., and Grumet, R. 2000. Interaction between *Zucchini yellow mosaic potyvirus* RNA-dependent RNA polymerase and host poly(A)-binding protein. Virology 275, 433-443.

Wang, Y.-L., Stork, J., and Nagy, P. 2009a. A key role for heat shock protein 70 in the localization and insertion of tombusvirus replication proteins to intracellular membranes. J. Virol. 83, 3276-3287.

Wang, Y.-L., Stork, J., Pogany, J., and Nagy, P. 2009b. A temperature sensitive mutant of heat shock protein 70 reveals an essential role during the early steps of tombusvirus replication. Virology, *i:10.1016/j.virol.2009.08.003.*

Watashi, K., Ishii, N., Hijikata, M., Inoue, D., Murata, T., Miyanari, Y., and Shimotohno, K. 2005. Cyclophilin B is a functional regulator of hepatitis C virus RNA polymerase. Mol. Cell 19, 111-122.

Weeks, S. A. and Miller, D. J. 2008. The heat shock protein 70 cochaperone YDJ1 is required for efficient membrane-specific Flock House Virus RNA replication complex assembly and function in *Saccharomyces cerevisiae*. J. Virol. 82, 2004-2012.

Wei, C. C., Balasta, M. L., Ren, J., and Goss, D. J. 1998. Wheat germ poly(A) binding protein enhances the binding affinity of eukaryotic initiation factor 4F and (iso)4F for cap analogues. Biochemistry 37, 1910-1916.

Welch, E. M., Wang, W., and Peltz, S. W. 2000. Translation termination: it's not the end of the story. In: N Sonenberg, JWB Hershey, MB Mathews, eds, Translational Control of Gene Expression, Cold Spring Harbor Laboratory Press, Cold Spring Harbor, pp 467-486.

Wells, S. E., Hillner, P. E., Vale, R. D., and Sachs, A. B. 1998. Circularization of mRNA by eukaryotic translation initiation factors. Mol. Cell 2, 135-140.

Whitham, S. A., Quan, S., Chang, H.-S., Cooper, B., Estes, B., Zhu, T., Wang, X., and Hou, Y.-M. 2003. Diverse RNA viruses elicit the expression of common sets of genes in susceptible *Arabidopsis thaliana* plants. Plant J. 33, 271-283.

Wimmer, E., Hellen, C. U., and Cao, X. 1993. Genetics of poliovirus. Annu. Rev. Genet. 27, 353-436.

Wintermeyer, W., Savelsbergh, A., Semenkov, Y. P., Katunin, V. I., and Rodnina, M. V. 2001. Mechanism of elongation factor G function in tRNA translocation on the ribosome. Cold Spring Harbor Symp. Quant. Biol. 66, 449-458.

Wittmann, S., Chatel, H., Fortin, M. G., and Laliberté, J.-F. 1997. Interaction of the viral protein genome linked of *Turnip mosaic potyvirus* with the translational eukaryotic initiation factor (iso)4E of *Arabidopsis thaliana* using the yeast two-hybrid system. Virology 234, 84–92.

Yamada, K., Lim, J., Dale, J. M., Chen, H., Shinn, P., Palm, C. J., Southwick, A. M., Wu, H. C., Kim, C., Nguyen, M., Pham, P., Cheuk, R., Karlin-Newmann, G., Liu, S. X., Lam, B., Sakano, H., Wu, T., Yu, G., Miranda, M., Quach, H. L., Tripp, M., Chang, C. H., Lee, J. M., Toriumi, M., Chan, M. M. H., Tang, C. C., Onodera, C. S., Deng, J. M., Akiyama, K., Ansari, Y., Arakawa, T., Banh, J., Banno, F., Bowser, L., Brooks, S., Carninci, P., Chao, Q., Choy, N., Enju, A., Goldsmith, A. D., Gurjal, M., Hansen, N. F., Hayashizaki, Y., Johnson-Hopson, C., Hsuan, V. W., Iida, K.,

Karnes, M., Khan, S., Koesema, E., Ishida, J., Jiang, P. X., Jones, T., Kawai, J., Kamiya, A., Meyers, C., Nakajima, M., Narusaka, M., Seki, M., Sakurai, T., Satou, M., Tamse, R., Vaysberg, M., Wallender, E. K., Wong, C., Yamamura, Y., Yuan, S., Shinozaki, K., Davis, R. W., Theologis, A., and Ecker, J. R. 2003. Empirical analysis of transcriptional activity in the *Arabidopsis* genome. Science 302, 842-846.

Yamaji, Y., Kobayashi, T., Hamada, K., Sakurai, K., Yoshii, A., Suzuki, M., Namba, S., and Hibi, T. 2006. *In vivo* interaction between *Tobacco mosaic virus* RNA-dependent RNA polymerase and host translation elongation factor 1A. Virology 347, 100-108.

Yambao, M. L., Masuta, C., Nakahara, K., and Uyeda, I. 2003. The central and C-terminal domains of VPg of *Clover yellow vein virus* are important for VPg-HC-Pro and VPg-VPg interactions. J. Gen. Virol. 84, 2861-2869.

Yang, F., Demma, M., Warren, V., Dharmawardhane, S., and Condeelis, J. 1990. Identification of an actin-binding protein from Dictyostelium as elongation factor 1a. Nature 347, 494-496.

Yang, C., Guo, R., Jie, F., Nettleton, D., Peng, J., Carr, T., Yeakley, J. M. , Fan, J. B., and Whitham, S. A. 2007. Spatial analysis of *Arabidopsis thaliana* gene expression in response to *Turnip mosaic virus infection*. Mol. Plant Microbe Interact. 20, 358-370.

Yen, Y. and Green, P. 1991. Identification and properties of the major ribonucleases of *Arabidopsis thaliana*. Plant Physiol. 97, 1487-1493.

Yi, G. and Kao, C. C. 2008. *Cis*- and *trans*-acting function of *Brome mosaic virus* protein 1a in genomic RNA1 replication. J. Virol. 82, 3045-3053.

Yochem, J., Uchida, H., Sunshine, M., Saito, H., Georgopoulos, C., and Feiss, M. 1978. Genetic analysis of two genes, dnaJ and dnaK, necessary for *Escherichia coli* and bacteriophage lambda DNA replication. Mol. Gen. Genet. 164, 9-14.

Zeenko, V. V., Ryabova, L. A., Spirin, A. S., Rothnie, H. M., Hess, D., Browning, K. S., and Hohn, T. 2002. Eukaryotic elongation factor 1A interacts with the upstream pseudoknot domain in the 3' untranslated region of *Tobacco mosaic virus* RNA. J. Virol. 76, 5678-5691.

Zelus, B. D., Stewart, R. S., and Ross, J. 1996. The virion host shutoff protein of Herpes simplex virus type 1: messenger ribonucleolytic activity in vitro. J. Virol. 70, 2411-2419.

Zhang, J., Campbell, R. E., Ting, A. Y., and Tsien R. Y. 2002. Creating new fluorescent probes for cell biology. Nat. Rev. Mol. Cell Biol. 3, 906-918.

Zhang, B., Morace, G., Gauss-Muller, V., and Kusov, Y. 2007. Poly(A) binding protein, C-terminally truncated by the hepatitis A virus proteinase 3C, inhibits viral translation. Nucleic Acids Res. 35, 5975-5984.

Zylicz, M., Ang, D., Liberek, K., and Georgopoulos, C. 1989. Initiation of lambda DNA replication with purified host- and bacteriophage-encoded proteins: the role of the dnaK, dnaJ and grpE heat shock proteins. EMBO J. 8, 1601-1608.

APPENDIX 1

Other significant contributions

Heat shock 70 protein interaction with Turnip mosaic virus RNA-dependent RNA polymerase within virus-induced membrane vesicles

P. J. Dufresne, K. Thivierge, S. Cotton, C. Beauchemin, C. Ide, E. Ubalijoro, J.-F. Laliberté, and M. G. Fortin

Virology (2008): 374: 217-227.

My contribution to this publication represents 20% and is described in detail below.

1. I have designed the experimental set-up for the following experiments:
    i. The membrane flotation assay (Fig. 4).
    ii. The confocal microscopy experiment in relative to the redistribution of RdRp and Hsc70 to membranous vesicles (Fig. 7).
2. I have conducted the experiments that dealt with the:
    i. *The membrane flotation assays*. I grew the plants, performed all of the inoculation trials, conducted the membrane fractionation assays, and the step sucrose gradient experiment. The obtained protein extracts were further used by P. Dufresne in order to generate results for Figure 3.4.

ii. *Construction of plasmid pCambia/EGFP*. The plasmid was used for the construction of pCambia/GFP-RdRp which was further used for the confocal microscopy experiment described in Figures 6 and 7.

iii. *Performance of all the confocal microscopy experiments*. I grew the plants, performed the agroinfiltration and performed the microscopy experiments.

3. I have contributed to the writing of the methodology section that is related to all of the experiments that I have conducted. I also helped in proofreading the final draft of the manuscript.

Available online at www.sciencedirect.com
ScienceDirect
Virology 374 (2008) 217–227
VIROLOGY
www.elsevier.com/locate/yviro

Heat shock 70 protein interaction with *Turnip mosaic virus* RNA-dependent RNA polymerase within virus-induced membrane vesicles

Philippe J. Dufresne [a], Karine Thivierge [a], Sophie Cotton [a], Chantal Beauchemin [b], Christine Ide [a], Eliane Ubalijoro [a], Jean-François Laliberté [b,*], Marc G. Fortin [a]

[a] *Department of Plant Science, McGill University, 21,111 Lakeshore, Ste-Anne-de-Bellevue, Quebec, Canada H9X 3V9*
[b] *Institut national de la recherche scientifique, Institut Armand-Frappier, 531 Boulevard des Prairies, Laval, Quebec, Canada H7V 1B7*

Received 9 November 2007; returned to author for revision 4 December 2007; accepted 9 December 2007
Available online 28 January 2008

Abstract

Tandem affinity purification was used in *Arabidopsis thaliana* to identify cellular interactors of *Turnip mosaic virus* (TuMV) RNA-dependent RNA polymerase (RdRp). The heat shock cognate 70-3 (Hsc70-3) and poly(A)-binding (PABP) host proteins were recovered and shown to interact with the RdRp *in vitro*. As previously shown for PABP, Hsc70-3 was redistributed to nuclear and membranous fractions in infected plants and both RdRp interactors were co-immunoprecipitated from a membrane-enriched extract using RdRp-specific antibodies. Fluorescently tagged RdRp and Hsc70-3 localized to the cytoplasm and the nucleus when expressed alone or in combination in *Nicotiana benthamiana*. However, they were redistributed to large perinuclear ER-derived vesicles when co-expressed with the membrane binding 6K-VPg-Pro protein of TuMV. The association of Hsc70-3 with the RdRp could possibly take place in membrane-derived replication complexes. Thus, Hsc70-3 and PABP2 are potentially integral components of the replicase complex and could have important roles to play in the regulation of potyviral RdRp functions.
© 2007 Elsevier Inc. All rights reserved.

Keywords: *Arabidopsis thaliana*; Heat shock protein; Hsp70; Poly(A)-binding protein; PABP; Potyvirus; RNA-dependent RNA polymerase; 6K-VPg-Pro; *Turnip mosaic virus*

Introduction

The RNA-dependent RNA polymerase (RdRp) is the core polypeptide that catalyzes the synthesis of RNA chains from both negative- and positive-strand templates of RNA viruses. The recruitment of the RdRp to membranes and its interaction with viral and host factors are critical for the efficiency, specificity and regulation of viral replication (Buck, 1996). Recent data from genome-wide screens in yeast (Jiang et al., 2006; Kushner et al., 2003; Panavas et al., 2005) have revealed the importance and multiplicity of viral–cellular interactions required for productive infection by positive-strand RNA viruses. A number of cellular proteins have been proposed as necessary for viral RdRp functions. Such factors were characterized following the co-purification of host proteins from the viral membrane replication complex and/or through the identification of host proteins that can directly interact with viral RdRps. The identification of host factors recruited to the replicase complex is of considerable interest as it sheds light on virus–cell interactions that facilitate infection and reveals the mechanistic components required for RNA replication.

In plants, different subunits of the translation initiation factor eIF3 were shown to interact with the membrane bound replicases of *Brome mosaic virus* (Quadt et al., 1993) and *Tobacco mosaic virus* (Osman and Buck, 1997), and the addition or immunodepletion of the eIF3 components modulated the *in vitro* RdRp activity of both viruses (Osman and Buck, 1997; Quadt et al., 1993). Similarly, the heat shock 70 protein (Hsp70) and the eukaryotic translation elongation factor 1A (eEF1A) were found in solubilized tobamovirus RdRp preparations (Nishikiori et al., 2006; Yamaji et al., 2006). In yeast, the Hsp70 homologues Ssa1/2p were recently reported to interact specifically with the

* Corresponding author. Fax: +1 450 686 5501.
E-mail address: jean-francois.laliberte@iaf.inrs.ca (J.-F. Laliberté).

0042-6822/$ - see front matter © 2007 Elsevier Inc. All rights reserved.
doi:10.1016/j.virol.2007.12.014

Cucumber necrosis virus (CNV) p33 replicase protein (Serva and Nagy, 2006). The activity of the replicase and level of viral replication correlated with the level of expression Ssa1/2p chaperones and it was suggested that Ssa1/2p is important for CNV replicase assembly.

Turnip mosaic virus (TuMV) is a *potyvirus* (Fauquet et al., 2005). Its positive single stranded RNA genome of almost 10 kilobases contains one long open reading frame and bears a viral genome-linked protein (VPg) covalently linked at its 5′ terminus and a poly(A) tail at the 3′ terminus (Nicolas and Laliberté, 1992). All TuMV-encoded proteins arise by synthesis of a large polyprotein followed by processing by viral proteinases. The C-terminal portion of this polyprotein yields two non-structural proteins that play important roles in replication: the 6K-VPg-Pro precursor polyprotein and the RdRp (Hong and Hunt, 1996).

A subset of the RdRp protein localizes to endoplasmic reticulum (ER) membranes where RNA synthesis takes place (Martin et al., 1995; Martin and Garcia, 1991; Schaad et al., 1997). The ER association of RdRp is likely due to its interaction with the 6K-VPg-Pro polypeptide (Léonard et al., 2004; Li et al., 1997; Restrepo-Hartwig and Carrington, 1994; Schaad et al., 1997). The 6K domain of the 6K-VPg-Pro polyprotein has been shown to be necessary for ER membrane targeting of VPg-Pro. For some potyviruses, the RdRp was also shown to accumulate in the nucleus (Baunoch et al., 1991; Restrepo et al., 1990; Riedel et al., 1998), where its function is unclear.

Potyviral RdRp interacts specifically with VPg-Pro (Daros et al., 1999; Fellers et al., 1998; Guo et al., 2001; Hong et al., 1995; Li et al., 1997). This interaction is thought to be essential since mutations that abolish or reduce the interaction have deleterious effects on replication (Daros et al., 1999; Li et al., 1997). One cellular interactor of the RdRp polymerase has been identified thus far for potyviruses. A yeast two-hybrid study has revealed the interaction of *Zucchini yellow mosaic virus* RdRp with the poly (A)-binding protein (PABP) of cucumber (Wang et al., 2000), but its biological significance has not been explored *in planta*.

In this study, we investigated host interactors of TuMV RdRp and found that *Arabidopsis thaliana* Hsc70-3 and PABP2 co-purify and directly interact with the viral RdRp. Upon inoculation, Hsc70-3 was relocalized to membranes and was co-immunoprecipitated with the RdRp polymerase from the microsomal fraction of an infected extract. Expression of 6K-VPg-Pro was sufficient to redirect the RdRp polymerase and host Hsc70-3 to large perinuclear ER-derived vesicles where replication likely takes place. Thus, Hsc70-3 and PABP2 are potentially integral components of the replicase complex and could have important roles to play in the regulation of potyviral RdRp functions.

Results and discussion

Identification of A. thaliana Hsc70-3 and PABP2 as TuMV RdRp interactors

To investigate cellular interactors of TuMV RdRp, we engineered an N-terminal fusion of the RdRp coding sequence with an improved tandem affinity purification (NTAPi) tag (Rohila et al., 2004). The NTAPi tag strategy has been used for the two-step isolation of highly purified native protein complexes in yeast and plants (Rigaut et al., 1999; Rohila et al., 2004; Rubio et al., 2005). The NTAPi tag is composed of the calmodulin binding peptide (CBP) domain, an AcTEV protease cleavage site (✂) and the *Staphylococcus aureus* Protein A (ProtA) domain preceded by the catalase intron (*CAT1*; Fig. 1A). The *Cauliflower mosaic virus* 35S promoter driven pNTAPi-RdRp construct was introduced in *Agrobacterium tumefaciens* and used for transformation of *A. thaliana* plants. Plants were also transformed with an NTAPi-tagged green fluorescent protein construct (pNTAPi-GFP; Rohila et al., 2004) to be used as a control for non-specific protein interactions.

A minimum of twenty putative *A. thaliana* transgenics for NTAPi-RdRp and NTAPi-GFP were evaluated by immunoblot analysis using anti-RdRp, anti-GFP, and/or anti-Protein A antibodies. The RdRp- and GFP-NTAPi fusions were detected in the crude cell lysate at the expected molecular masses of 82 kDa and 49 kDa, respectively (data not shown). Anti-CBP antibodies also allowed detection of RdRp- and GFP-NTAPi fusions at expected molecular masses of ~65 and 32 kDa respectively following human IgG sepharose beads chromatography and protease cleavage (see below, Fig. 1D).

NTAPi-RdRp lines were immune to TuMV infection as opposed to NTAPi-GFP lines, which showed typical TuMV symptoms and for which the viral capsid protein could be detected (data not shown). This is not unexpected as RdRp transgenics have previously been reported to be resistant to potyvirus infection (Audy et al., 1994; Jones et al., 1998; Simon-Mateo et al., 2003). RdRp levels were greatly reduced in TuMV-infected NTAPi-RdRp transgenics, which suggests that resistance could result from targeted RNA silencing of the RdRp sequence (data not shown).

Since NTAPi purification with TuMV-infected plant material was not possible, healthy 3-week-old *A. thaliana* NTAPi-RdRp plants were used. Protein extracts were incubated with IgG-coated beads and absorbed proteins then released by protease cleavage of the Protein A moiety. A second affinity purification step was performed by incubating the digested eluates with calmodulin-coated resin in presence of calcium and elution of native protein complexes was performed using an EGTA containing buffer. Eluates were subjected to SDS–PAGE and silver stained (Fig. 1B).

Mass spectrometric analysis was performed on two bands excised from a SDS–PAGE gel at 65 and 70 kDa, respectively. These bands were present in the RdRp purified extract but absent from GFP extract (Fig. 1B). Analysis of the 65 and 70 kDa bands in the RdRp purified extract allowed the identification of the RdRp and of another protein. Four peptide matches were obtained for the AtHsc70-3 protein in the 70 kDa band (Fig. 1C). Immunoblotting using a mouse monoclonal serum directed against human Hsc70/Hsp70 protein confirmed the co-purification of the host protein with the viral protein in the NTAPi-RdRp but not in the NTAPi-GFP extract (Fig. 1D). As Hsc70-3 is part of a multigene family (see below), it is possible that the sera used could react with other related Hsc70 proteins. To indicate this possibility, the general term “Hsc70” rather than specific “Hsc70-3”

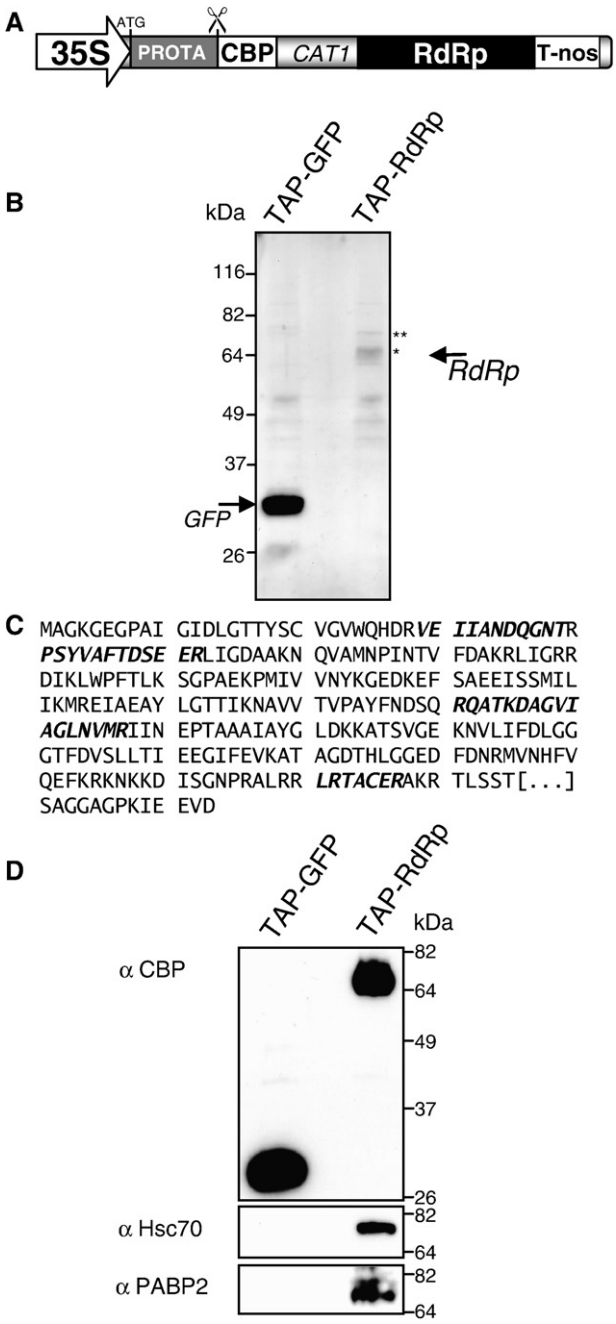

Fig. 1. Expression and purification of NTAPi-tagged RdRp fusion and identification of interactors in *A. thaliana*. (A) Diagram of NTAPi-RdRp construct used. Expression cassette is driven by 35S *Cauliflower mosaic virus* promoter (35S) followed by the coding sequence for *S. aureus* protein A (PROT A), AcTEV protease cleavage site (✂), calmodulin binding peptide (CBP), catalase intron 1 (*CAT1*), the RdRp, and ends with the nopaline synthase terminator (T-nos). (B) Silver stained SDS–PAGE of proteins co-purified in *A. thaliana* NTAPi-GFP (TAP-GFP) and NTAPi-RdRp (TAP-RdRp) lines following NTAPi purification. GFP and RdRp products are indicated with arrows. Positions of the excised bands used for mass spectrometric identification are indicated by asterisks. (C) Identification of *A. thaliana* Hsc70-3 as an RdRp interactor by mass spectrometric analysis (LC/MS). The four significant peptide matches are depicted in bold and italic. (D) Immunoblot analysis of cellular proteins purified in *A. thaliana* NTAPi-GFP (TAP-GFP) and NTAPi-RdRp (TAP-RdRp) lines. Proteins were separated by SDS–PAGE and analyzed by immunoblotting using rabbit antibodies directed against Hsc70, PABP2, or CBP moiety found in the NTAPi fusion.

denomination is used throughout the text when presenting immunoblots from complex plant protein extracts using these antibodies (Figs. 3–5). AtRNase L inhibitor 2 (At4g19210; NM11 8041) was also identified in the 70 kDa band but was not investigated further.

Based on previous work showing that the RdRp of *Zucchini yellow mosaic virus* interacted with PABP of *Cucumis sativus* in the yeast two-hybrid system (Wang et al., 2000), we also investigated and confirmed the presence of AtPABP2 in the NTAPi-RdRp extract but not in the NTAPi-GFP extract (Fig. 1D). The data presented here indicate that PABP/RdRp interaction is detected *in planta* in the *A. thaliana*/TuMV pathosystem and could be a broad conserved feature among other potyviruses.

PABP is an abundant RNA-binding protein which binds specifically to 3′ poly(A) tracts of mRNAs and is important factors in the regulation of protein synthesis initiation, mRNA maturation, and mRNA decay (Mangus et al., 2003). Interaction of PABP with the potyviral RdRp could be mechanistically analogous to that of PABP interacting with poliovirus 3CD polypeptide (polymerase precursor; $3D_{pol}$). The 3CD protein interacts with both PABP and poly(rC)-binding protein (PCBP). As PABP can still bind to poly (A) tail at 3′ end of viral genomic RNA and PCBP to the cloverleaf structure at its 5′ end, these interactions bridge the ends of the viral RNA and form a stable circular ribonucleoprotein complex thought to enhance replication/translation (Barton et al., 2001; Herold and Andino, 2001). Interaction of the RdRp with PABP could also position the RdRp on the polyadenylated 3′ end of the viral genomic RNA of TuMV to allow initiation of negative-strand synthesis.

Hsc70-3 and PABP2 interact with RdRp in vitro

Hsc70-3 and PABP2 co-purification with TuMV RdRp may be the result of direct interaction with the viral protein or occur through the intermediary of another protein that interacts with the RdRp. To test for the direct interaction of Hsc70-3 and PABP2 with the RdRp, an enzyme linked immunosorbent assay (ELISA)-based binding assay was performed. ELISA plate wells were coated with purified TuMV 6× histidine-tagged RdRp. The coated wells were then incubated with increasing concentrations of purified GST-tagged Hsc70-3 or PABP2. Complex retention was detected using an anti-GST antiserum. A saturation binding curve was observed for Hsc70-3 (Fig. 2A) and PABP2 (Fig. 2B). Binding was specific as no signal was detected in the absence of primary antibody (data not shown) or when GST-Hsc70-3 or GST-PABP2 was replaced with the GST protein. Overall this suggests that RdRp/Hsc70-3 and RdRp/PABP2 interactions are specific and result from direct protein–protein interaction.

In plant cells, Hsc70 is involved in protein folding, protein translocation, assembly of macromolecular complexes, and protein degradation functions (Craig et al., 1994; Mayer and Bukau, 2005). Hsc70-3 is a member of the Hsp70 chaperone family. In *A. thaliana*, this family comprises at least 14 members, five of which, including Hsc70-3, are predicted to be cytosolic (Lin et al., 2001; Sung et al., 2001). Hsc70-3 and three other cytosolic members were reported to be transcriptionally induced at high levels following TuMV infection (Aparicio et al.,

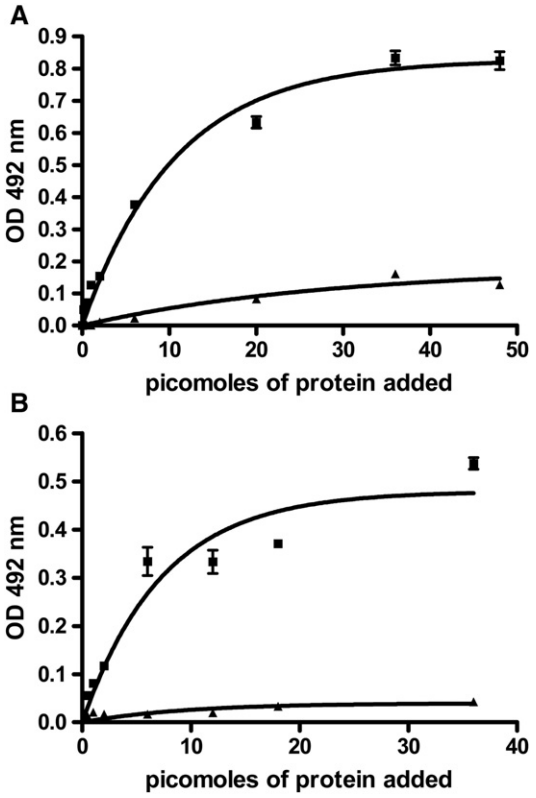

Fig. 2. *A. thaliana* Hsc70-3 and PABP2 interaction with RdRp *in vitro*. (A) Interaction of TuMV RdRp protein with *A. thaliana* Hsc70-3 protein in ELISA-based binding assays. Wells of a microtiter plate were coated with 25 pmol of *E. coli* purified 6×-histidine-tagged RdRp protein and incubated with increasing amounts of *E. coli* purified GST-tagged Hsc70-3 protein (■) or GST recombinant protein alone (▲). Retention of the complex was detected with polyclonal anti-GST antibodies. (B) Interaction of TuMV RdRp protein with *A. thaliana* PABP2 protein in ELISA-based binding assays. Wells of microtiter plate were coated with 25 pmol of *E. coli* purified 6×-histidine-tagged RdRp protein and incubated with increasing amounts of *E. coli* purified GST-tagged PABP2 protein (■) or GST recombinant protein alone (▲). Retention of the complex was detected with monoclonal anti-GST antibodies. In A and B, error bars are specified for GST control data, but the small S.E.M. values are masked by the data point symbols.

2005) and are expected to be abundant proteins in cells where viral replication takes place.

The identification of Hsc70 as a host factor interacting with TuMV RdRp is consistent with previous studies on the role of chaperones in viral replication and pathogenesis (Mayer, 2005; Sullivan and Pipas, 2001). Cellular chaperones have been found to co-purify with replicases and to be required for efficient replication of many classes of viruses (Brown et al., 2005; Glotzer et al., 2000; Hu et al., 2004; Kampmueller and Miller, 2005; Momose et al., 2002; Zylicz et al., 1989) including members of the bromo- (Tomita et al., 2003), tobamo- (Nishikiori et al., 2006), and tombus- (Serva and Nagy, 2006) virus genera. The interaction of Hsc70 with RdRp has been proposed to be necessary for the proper conformational arrangement of the replicase and its assembly at sites of viral replication (Serva and Nagy, 2006). Chaperone-assisted refolding has been shown to activate the polymerase activity and to confer template specificity. For example, *Brome mosaic virus* requires Ydj1, a yeast factor part of the heat shock protein family, for efficient negative strand RNA synthesis (Tomita et al., 2003). In the case of hepadnaviruses, Hsp40/70/90 binding is required for maintaining reverse transcriptase conformation and subsequent initiation of polymerase activity on the viral RNA template (Hu et al., 2002; Stahl et al., 2007). Furthermore, a recent report suggests that cellular dnaJ-like proteins in tobacco interact with *Potato virus Y* capsid protein and are required for efficient potyviral cell-to-cell movement (Hofius et al., 2007).

A subset of Hsc70 is redistributed to membrane and/or nucleus enriched fractions following TuMV infection

We have previously shown the redistribution of PABP2 to nuclear and membrane-associated fractions following TuMV infection (Beauchemin and Laliberté, 2007). In order to assess if the subcellular distribution of cytosolic Hsc70 could be modulated in a similar way in a TuMV infection context, nuclear and membrane fractionation experiments were conducted on mock and TuMV-infected *Brassica perviridis* plants.

Nuclei were purified from mock-inoculated and TuMV-infected leaves as described in Materials and methods. Ten micrograms of protein from the post-nuclear (S12) and purified nuclei (N) fractions were analyzed by immunoblot assay (Fig. 3A). In healthy plants, the bulk of Hsc70 was found in the post-nuclear fraction but was also detected, albeit weakly, in the nuclei fraction.

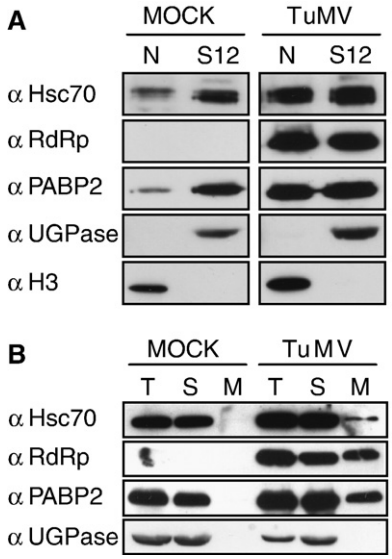

Fig. 3. Subcellular distribution of Hsc70, RdRp, and PABP2 in mock versus TuMV-infected *B. perviridis*. (A) Immunoblot analysis of nuclear and post-nuclear fraction proteins extracted from healthy (mock inoculated) or TuMV-infected plants. Leaves were homogenized and the extract centrifuged at 12,000×*g* through a sucrose cushion to separate the "soluble" fraction (S12) from crude nuclei (N). For each sample, 10 μg of protein was separated by SDS–PAGE. The experiment was repeated three times with different *B. perviridis* extracts and yielded similar results. (B) Immunoblot analysis of soluble and membrane-associated proteins from healthy (mock inoculated) or TuMV-infected *B. perviridis* plants. Total proteins (T) were extracted and soluble proteins (S) separated from membrane-associated proteins (M) by centrifugation at 30,000×*g*. Proteins were separated by SDS–PAGE and analyzed by immunoblotting using mouse/rabbit antibodies directed against Hsc70, RdRp, PABP2, UGPase, and/or histone H3.

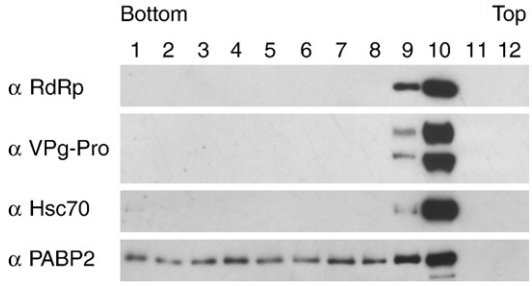

Fig. 4. Characterization of Hsc70 in microsomal fractions through a membrane flotation assay. P30 microsomal fractions were used. Fractions were collected from a step sucrose gradient and proteins in each fraction separated by SDS–PAGE and immunodetected with anti-RdRp, VPg-Pro, Hsc70, and PABP2 antibodies. Fraction 1 corresponds to the bottom and fraction 12 to the top of the gradient. For the anti-VPg-Pro immunoblot, the upper band corresponds to the membrane-associated 6K-VPg-Pro (55 kDa) and lower band to the VPg-Pro (49 kDa) polypeptide. PABP2 and 6K-VPg-Pro have previously been found associated with membrane fractions in flotation assays (Beauchemin and Laliberté, 2007) and are shown as positive controls.

However, when post-nuclear and nuclear fractions from infected plant material were analyzed, a different pattern emerged. Hsc70 was detected in equal amount in both nuclei and post-nuclear fractions (Fig. 3A). This redistribution to the nucleus parallels that observed for PABP in TuMV-infected plants. Relative abundance of Hsc70 was increased in both fractions when compared to mock control, which indicates that Hsc70 protein levels increased as a result of TuMV infection. This is supported by the observation that Hsc70-3-coding mRNA was transcriptionally induced at high levels following TuMV infection (Aparicio et al., 2005). Histone H3 and UDP-glucose pyrophosphorylase (UGPase), which are markers for the nucleus and cytoplasm, respectively, were detected in their respective fractions, indicating the absence of cytoplasmic contamination in the nuclear fraction and the absence of nuclear proteins in the post-nuclear fraction (Fig. 3A). The experiment was repeated three times with different *B. perviridis* extracts and yielded similar results.

Membrane fractionation was also performed on mock-inoculated and TuMV-infected *B. perviridis* leaves 12 days post-infection. Leaves were homogenized, and nuclei, chloroplasts, and cell wall debris were removed by centrifugation at 3700×*g*. Soluble proteins were then separated from membrane-associated proteins by centrifugation at 27,000×*g* and resuspended in same volume to allow quantitative evaluation. Total (T), soluble (S), and membrane-associated (M) proteins were separated by SDS–PAGE and subjected to immunoblot analysis with rabbit sera raised against recombinant forms of RdRp and AtPABP2, as well as serum raised against Hsc70. Hsc70 was absent from membrane-associated fraction and found strictly in the soluble fraction of healthy plants. However, in infected plants, Hsc70 was found in both soluble and membrane-enriched fractions (Fig. 3B). In our experiments, Hsc70 was consistently present in the membrane fraction in TuMV-infected extract and was not detected in the mock extract, this even after prolonged exposure. Again, this membrane association of Hsc70 parallels that of PABP. In both healthy and infected extracts, UGPase was detected only in the soluble and total protein extract fractions, which indicates the absence of cytoplasmic protein contamination in the membrane-enriched fractions.

The presence of Hsc70-3 in P30 fractions of TuMV-infected leaves may result from true membrane association or simply protein aggregation. To distinguish between these two possibilities, a membrane flotation assay was used (Beauchemin and Laliberté, 2007; Zhang et al., 2005). The membrane-enriched fraction (P30) was overlaid with a sucrose step gradient and subjected to centrifugation. Low density membranes and proteins associated with these membranes float to the upper part of the gradient while soluble proteins or aggregated proteins remain at the bottom. As shown in Fig. 4, the RdRp, 6K-VPg-Pro, and PABP2 rose towards the top of the gradient (fractions 9 and 10), indicating their association with membranes. Likewise, Hsc70 was found in fraction 9 and 10, confirming its membrane association.

Interaction of RdRp with Hsc70 and PABP within the membrane-associated fraction was tested by co-immunoprecipitation assay. P30 fraction from *A. thaliana* was solubilized with Triton X-100 and incubated with Protein G Sepharose beads coated with rabbit anti-RdRp, anti-AtPABP2, or pre-immune sera. Following centrifugation, proteins pelleted with the beads were eluted, separated by SDS–PAGE, and subjected to immunoblot analysis. Immunoprecipitation using the anti-TuMV RdRp serum allowed the recovery of Hsc70 and PABP2 (Fig. 5A). No protein was detected in the immunoblot with the pre-immune serum or with the Protein G Sepharose negative controls. No protein was

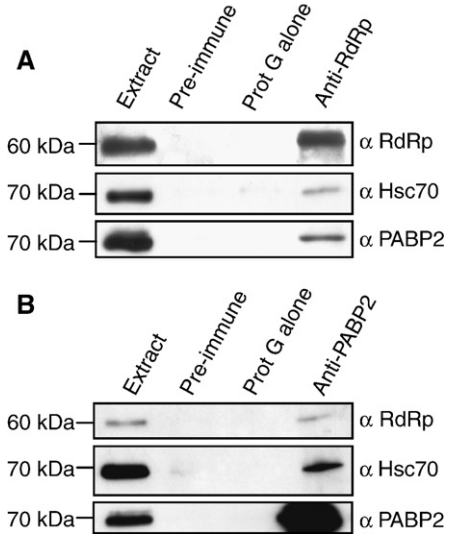

Fig. 5. The RdRp protein is complexed with *A. thaliana* Hsc70 and PABP2 proteins in membrane-enriched fraction of TuMV-infected plants. (A) Immunoprecipitation of Hsc70 and PABP2 with RdRp antibody in membrane-enriched fraction (30,000×*g* pellet) in TuMV-infected *A. thaliana* plants. (B) Immunoprecipitation of RdRp and Hsc70 with PABP2 antibody in membrane-enriched fraction (30,000×*g* pellet) in TuMV-infected *A. thaliana* plants. The immunoprecipitates, total extracts, pre-immune serum, and protein G sepharose controls were subjected to SDS–PAGE and immunoblotted with antibodies against TuMV RdRp, Hsc70, and PABP2. Lane "Extract" indicates the total 30,000×*g* membrane-associated protein extract. Lanes "anti-RdRp" and "anti-PABP2" indicate the immunoprecipitates immobilized onto Sepharose fast Flow protein G beads matrix with the RdRp or PAPB2 antibody. Pre-immune antibodies coupled to protein G sepharose ("pre-immune" lane) and protein G sepharose alone ("Prot G alone" lane) were used as negative controls.

immunoprecipitated when a healthy plant fraction was used (data not shown). Similarly, RdRp and Hsc70-3 were precipitated with the anti-PABP2 serum (Fig. 5B). These experiments indicate that RdRp/Hsc70/PABP2 complexes are formed in the membrane-associated fraction and it also raises the possibility of tripartite interactions between RdRp, PABP2, and Hsc70.

RdRp/Hsc70-3 complex localizes to cytoplasmic vesicles induced by 6K-VPg-Pro

To assess if the RdRp could be responsible for the membrane association of Hsc70-3, RdRp and AtHsc70-3 were fused to the fluorescent protein tags (GFP, mCherry, or DsRed2) and expressed transiently by agroinfiltration in *Nicotiana benthamiana*, a host of TuMV. Proper expression of the fluorescent fusions was assessed by immunoblot analyses using rabbit sera raised against RdRp, Hsc70, or GFP. In each case, a signal corresponding to the expected molecular mass of the analyzed protein was observed, indicating that full-length proteins had been expressed (data not shown).

To facilitate subcellular localization of cytoplasmic and membrane structures, GFP and DsRed2 markers with or without ER targeting signals were co-expressed along with the fluorescent fusion proteins (Beauchemin et al., 2007; Zhang et al., 2005). Fluorescence of GFP-RdRp and Hsc70-3-DsRed2 was observed in the nucleus (excluding nucleolus) and cytoplasm (Figs. 6B and D, respectively). Merging of the fluorescence with that of free DsRed2 or GFP (Figs. 6A and E, respectively) showed co-localization (Figs. 6C and F, respectively). No co-localization was observed when GFP-RdRp was expressed with DsRed2-ER or Hsc70-3 with GFP-ER markers (data not shown). When produced alone, RdRp and Hsc70-3 were thus soluble proteins. The cytoplasmic distribution of Hsc70-3 when fused to GFP is also in agreement with data from Prokhnevsky et al. (2005). Upon co-expression, the distribution of Hsc70-3-DsRed2 (Fig. 6G) and GFP-RdRp (Fig. 6H) remained nuclear and cytoplasmic (Fig. 6I). PABP and RdRp also remained soluble and co-localized mostly to the cytoplasm following co-expression (Figs. 6J to L). Thus, expression of RdRp is not sufficient for redistribution of Hsc70-3 or PABP2 to membranes, indicating that a third partner is likely required.

6K-VPg-Pro induces the formation of cytoplasmic vesicles that harbor the viral replication complex (Léonard et al., 2004; Li et al., 1997; Restrepo-Hartwig and Carrington, 1994; Schaad et al., 1997). Its interaction with the RdRp has been demonstrated for TEV and TVMV (Fellers et al., 1998; Li et al., 1997). We consequently investigated whether expression of 6K-VPg-Pro was responsible for membrane association of RdRp and Hsc70-3.

Upon co-expression of 6K-VPg-Pro-mCherry (Fig. 7A) with fluorescent construct GFP-RdRp (Fig. 7B), most of the merged fluorescence signal was found within cytoplasmic vesicular structures (Fig. 7C), similar to those observed when 6K-VPg-Pro-GFP is expressed alone (Beauchemin et al., 2007). These vesicles were most often perinuclear and typically exceeded in diameter those of 6K-VPg-Pro-GFP, with an average maximum diameter of 16.7 μm (S.E.M.±1.7; $n=8$). On the other hand, the

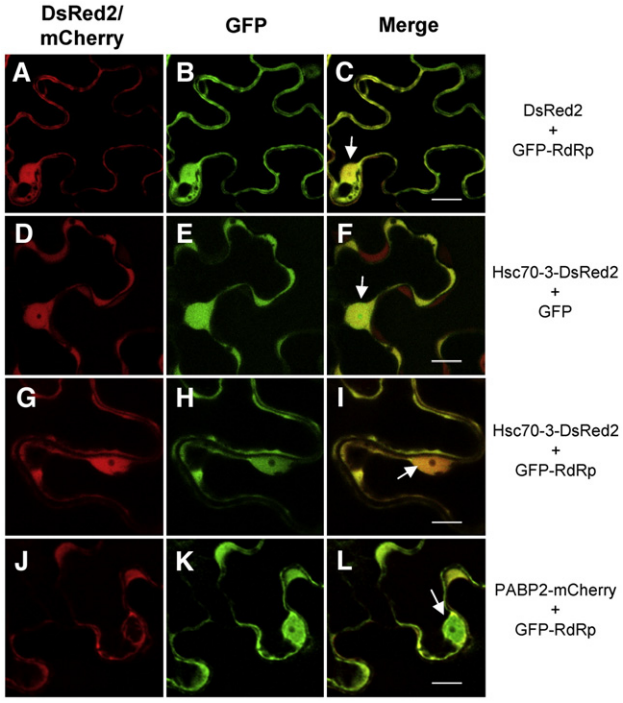

Fig. 6. RdRp/Hsc70-3 and RdRp/PABP2 co-localization *in planta*. Subcellular localization of RdRp, Hsc70-3, and PABP2. *N. benthamiana* leaves were infiltrated with *A. tumefaciens*, and expression of fluorescent proteins was visualized by confocal microscopy 2–4 days later. *A. tumefaciens* suspensions contained binary Ti plasmids encoding DsRed2 and GFP-RdRp (A to C), Hsc70-3-DsRed2 and GFP (D to F), Hsc70-3-DsRed2 and GFP-RdRp (G to I), and GFP-RdRp and PABP2-mCherry (J to L). Scale bar=15 μm. All agroinfiltrations were performed with the P19 inhibitor of silencing as previously described (Beauchemin et al., 2007). Nuclei are indicated with white arrows in the merged panel.

Hsc70-3-DsRed2 fluorescence did not specifically co-localize with the vesicles induced by 6K-VPg-Pro-GFP (Figs. 7D to F).

We then tested if membrane association of Hsc70-3 in infected cells was promoted by its interaction with the RdRp/6K-VPg-Pro complex. First, we looked if expression of 6K-VPg-Pro-ct (Beauchemin et al., 2007), a non-fluorescent form of the viral protein, could induce the formation of cytoplasmic vesicles, within which RdRp would be found. RdRp-GFP, DsRed2-ER, and 6K-VPg-Pro-ct were co-expressed in *N. benthamiana* leaves. DsRed2-ER showed the expected reticulate fluorescent pattern for an ER protein, with the added emergence of a large perinuclear vesicle (Fig. 7G), such vesicle being induced by 6K-VPg-Pro-ctGFP. Similarly to when it was co-expressed with 6K-VPg-Pro-mCherry, RdRp-GFP showed the same fluorescent pattern (compare Fig. 7B with H) and co-localized with the perinuclear vesicle (Fig. 7I). Similar vesicles were observed upon co-infiltration of both GFP-RdRp and Hsc70-3-DsRed2 constructs with 6K-VPg-Pro-ctGFP in *N. benthamiana* leaves. Most of the fluorescence emitted by Hsc70-3 DsRed2 (Fig. 7J) and GFP-RdRp (Fig. 7K) was found within 6K-VPg-Pro induced vesicles, where strong co-localization was observed (Fig. 7L). The size of these cytoplasmic vesicles was similar to those observed when GFP-RdRp and 6K-VPg-Pro-mCherry were co-expressed (14.9 μm: S.E.M.±1.1; $n=7$). Thus, the expression of both RdRp and 6K-VPg-Pro-

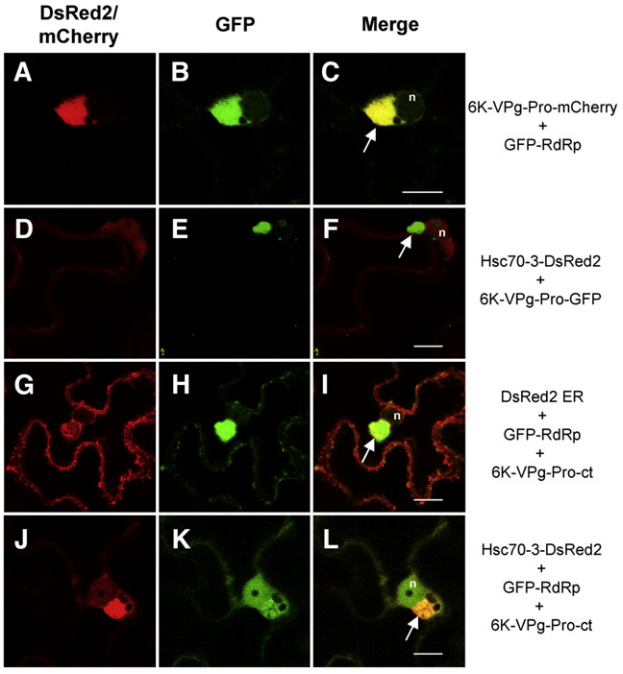

Fig. 7. RdRp and Hsc70-3 are redirected to membranous vesicles when co-expressed with 6K-VPg-Pro. Subcellular localizations of RdRp and Hsc70-3 when co-expressed with 6K-VPg-Pro. *N. benthamiana* leaves were infiltrated with *A. tumefaciens*, and expression of fluorescent proteins was visualized by confocal microscopy 2–4 days later. *A. tumefaciens* suspensions contained binary Ti plasmids encoding 6K-VPg-Pro-mCherry and GFP-RdRp (A to C), Hsc70-3-DsRed2 and 6K-VPg-Pro-GFP (D to F), DsRed2-ER, GFP-RdRp, and non-fluorescent 6K-VPg-Pro-ct (G to I), and Hsc70-3-DsRed2, GFP-RdRp, and non-fluorescent 6K-VPg-Pro-ct (J to L). Scale bar=15 μm. All agroinfiltrations were performed with the P19 inhibitor of silencing as previously described (Beauchemin et al., 2007). Nuclei are indicated with the letter "n" and "6K-VPg-Pro"-induced vesicles with white arrows in the merged panel.

GFP appears to be required to redirect Hsc70-3 to these vesicles. This suggests that Hsc70-3 needs to interact with the RdRp for efficient translocation to 6K-VPg-Pro vesicles.

The interaction of Hsc70-3 with the RdRp and its co-localization with the replicase on membranes suggest that it could be an integral part of the potyvirus replicase complex as seen for other family of plant positive RNA viruses (Nishikiori et al., 2006; Serva and Nagy, 2006; Tomita et al., 2003). Localization data emphasize the role of 6K-VPg-Pro as an important determinant of subcellular redistribution of viral and recruited host components. 6K-VPg-Pro polypeptide alone is sufficient to redirect the RdRp and Hsc70-3 to ER-derived vesicle. This is in addition to the host factors PABP and eIF(iso)4E (Beauchemin et al., 2007; Beauchemin and Laliberté, 2007), which have also been observed to be redistributed in vesicles budding from the ER when co-expressed with 6K-VPg-Pro or to nucleolus when expressed with VPg-Pro. The recruitment of necessary host and viral components to a membrane structure would likely protect the replication machinery from external nucleases and proteases, as seen for instance with for *Brome mosaic virus* (Schwartz et al., 2002) and hepatitis C virus (Aizaki et al., 2004; El-Hage and Luo, 2003) and have positive effects of viral replication/translation. Additionally, it would provide a stable framework for the polymerase and host/virus components to assemble into a functional replication complex.

Conclusion

Identification of host PABP and Hsc70-3 as RdRp-interacting proteins and their targeting to 6K-VPg-Pro putative replication vesicles emphasizes their potential role in replication of TuMV. Hsc70-3 and PABP2 are potentially integral components of the potyvirus replicase complex and assessment of both proteins capacity to regulate the RdRp activity should be pursued. We likely have overlooked many other cellular factors that are part of TuMV replicase complex with the purification strategy used here. Purification and identification of the proteins present within 6K-VPg-Pro-induced vesicles appear as one productive approach that could be employed to characterize the composition of TuMV replicase complex in the future.

Materials and methods

Plant and bacterial expression constructs

The pNTAPi-RdRp *Cauliflower mosaic virus* (CaMV) 35S promoter driven plant expression vector (Fig. 1A) was constructed as follow. RdRp was PCR-amplified from full-length TuMV UK1 cDNA clone p35Tunos (Sanchez et al., 1998) using primers RdRp-GWF and RdRp-GWR (Table S1). The purified PCR product was cloned in pENTR/D-TOPO vector (Invitrogen) and the attL sites within this clone were used to clone the RdRp in the pNTAPi vector (Rohila et al., 2004) with LR clonase (Invitrogen). The control pNTAPi-GFP vector (Fig. 1A) has been described previously (Rohila et al., 2004).

For construction of the vector coding for the N-terminus 6× histidine-T7 tag full-length RdRp fusion protein, TuMV RdRp sequences were PCR-amplified from p35Tunos using primers RdRp-*Bam*HI and RdRp-*Not*I (Table S1). The amplified fragments were digested with *Bam*HI/*Not*I and cloned into similarly digested pET28(a) (Novagen).

For construction of the vector coding for the N-terminus GST fusion of *A. thaliana* Hsc70-3 (At3g09440; GenBank accession no. NM111778) and PABP2 (At4g34110; GenBank accession no. L19418) proteins, sequences were PCR-amplified from validated SSP gold standard full-length ORF clones C104970 and U22035 (Yamada et al., 2003) using primers Hsc70-3F-*Eco*RI and Hsc70-3R-*Eco*RI, and PABP2-*Eco*RI and PABP2-*Not*I (Table S1). The amplified fragments were digested with *Bam*HI/*Not*I or *Eco*RI and cloned into similarly digested pGEX-6P1 (GE Healthcare).

Plasmids for co-localization experiments were constructed as follows. EGFP (Clontech) gene was excised with *Xba*I/*Eco*RI from pGreen/EGFP (Beauchemin et al., 2007) and inserted into similarly digested backbone of pCambia/DsRed2, resulting in plasmids pCambia/EGFP. The cDNA for Hsc70-3 and RdRp were amplified with the RdRpF EGFP-*Sma*I and RdRpR EGFP-*Sal*I primers, or Hsc70-3F DsRed2-*Xba*I and Hsc70-3R DsRed2-*Bam*HI (Table S1) and inserted into the *Sal*I/*Sma*I sites of pCambia/EGFP or *Bam*HI/*Xba*I sites of pGreen/DsRed2. The

resulting plasmids were identified as pGreen/Hsc70-3-DsRed2 and pCambia/GFP-RdRp. 6K-VPg-Pro sequence gene was excised with *Hin*dIII/*Bam*HI from pGreen/6K-VPg-Pro-GFP plasmid and inserted into similarly digested backbone of pCambia/PABP-mCherry, resulting in plasmids pCambia/6K-VPg-Pro-mCherry. The plasmids pGreen/GFP, pCambia/PABP-mCherry, pCambia/DsRed2, pGreen/6K-VPg-Pro-GFP, and pGreen/6K-VPg-Pro-ct have previously been described (Beauchemin et al., 2007; Beauchemin and Laliberté, 2007). All PCR amplifications were performed with *Pfu* Turbo polymerase (Stratagene) and all plasmid constructs verified by sequencing.

Plant material and growth conditions: generation of RdRp-NTAPi transgenic A. thaliana

A. thaliana plants used in this study are all of the Columbia-0 ecotype. Col-0 plants were transformed with the pNTAPi-RdRp or pNTAPi-GFP constructs using a modified version of the floral dipping technique (Martinez-Trujillo et al., 2004). T_1 transformants were sown on a peat based mix and selected with glufosinate-ammonium herbicide (0.00578%). *A. thaliana* NTAPi-RdRp and NTAPi-GFP T_1 lines were evaluated by immunoblot detection of NTAPi-tagged RdRp or GFP in pools of T_2 lines by using anti-RdRp, anti-GFP, and/or anti-Protein A antibodies. Lines were further selected by screening T_2 progenies for glufosinate-ammonium resistance. Only the lines with resistance/sensitivity ratio of approximately 3:1, indicative of a single T-DNA insertion event, were chosen and used in our experiments. All lines used for NTAPi purification were thus homozygous lines at T_3 or T_4 generation with stable expression.

NTAPi purification procedure

Three-week-old NTAPi–RdRp and NTAPi-GFP plants (7.5 g, fresh weight) were ground in liquid nitrogen, thawed in 2 volumes of extraction buffer (50 mM Tris–HCl, pH 7.6, 150 mM NaCl, 10% glycerol, 1 mM DTT, 0.1% IGEPAL, and 1× Complete protease inhibitor; Roche) and centrifuged twice at 30,000×*g* for 20 min. Supernatants were incubated with 400 µl of human IgG sepharose beads (Amersham Bioscience) for 1.5 h at 4 °C with gentle rotation. Beads were washed 3 times with 10 ml of extraction buffer and once with 10 ml of cleavage buffer (50 mM Tris–HCl, pH 7.6, 150 mM NaCl, 10% glycerol, 0.5 mM EDTA, 0.1% IGEPAL, 1 mM DTT, 1 µM E-64 protease). Elution from IgG beads was performed by incubation with 20 µl (200 units) of AcTEV protease (Invitrogen) in 3 ml of cleavage buffer at 10 °C for 2 h with gentle rotation. Column was drained and washed with 1 ml of cleavage buffer. Six milliliters of calmodulin binding buffer (50 mM Tris–HCl, pH 7.6, 150 mM NaCl, 10 mM β-mercaptoethanol, 1 mM magnesium acetate, 1 mM imidazole, 2 mM $CaCl_2$, 0.1% IGEPAL) and 12 µl of 1M $CaCl_2$ was added to the pooled eluates and loaded onto 400 µl of calmodulin affinity resin (Stratagene) and incubated for 1.5 h at 4 °C with gentle rotation. After washing the column three times with 10 ml of calmodulin binding buffer, elution was performed with CBP elution buffer (50 mM Tris–HCl, pH 8.0, 150 mM NaCl, 0.1% IGEPAL, 5 mM EGTA, 10 mM β-mercaptoethanol, and 1 mM imidazole).

Proteins were concentrated using StrataClean Resin (Stratagene) and separated on an SDS–PAGE gel. Protein bands were visualized by immunoblotting using the rabbit anti-calmodulin binding protein epitope tag (Upstate cell signaling solutions) or ProtA mouse monoclonal antibodies (Sigma-Aldrich), silver staining (Silver staining Plus; Bio-Rad) or Bio-Safe Coomassie blue staining (Bio-Rad). The NTAPi purification procedures were repeated independently four times and yielded similar results.

Mass spectrometry analysis

Coomassie or silver stained bands from 1D acrylamide gel were excised and digested with trypsin on a MassPrep robotic workstation (PerkinElmer). Digested peptides were run for an hour on an LC-QToF (Micromass), a tandem MS–MS at Genome Quebec Center at McGill University. Peak identification was carried using Mascot software (Matrix Science).

Mouse monoclonal and rabbit polyclonal antibodies

The primary antibodies were used as follows: anti-PABP2 1:2000; anti-TuMV RdRp 1:1000; mouse monoclonal Anti-Hsp70/Hsc70 1:1000 (Stressgen); rabbit polyclonal anti-Hsp70/Hsc70 (Stressgen) 1:1000; mouse rabbit polyclonal anti-CBP domain (Upstate Biotech) 1:1000; rabbit polyclonal Anti-UGPase (Agrisera) 1:1000; rabbit polyclonal Anti-GFP (Molecular Probes) 1:1000; and goat polyclonal anti-Histone H3 (H3; Santa Cruz Biotechnology) 1:250.

The recombinant clone pET-RdRp in *E. coli* BL21(DE3) cells was used for antibody production as follows. Full-length coding sequence of RdRp polymerase of Qc strain (Nicolas and Laliberté, 1992) was cloned in frame in the pET11d vector (Novagen). The resulting recombinant protein was overproduced in *E. coli* and purified as insoluble inclusion bodies. Inclusion bodies were resuspended in TBS buffer and used for rabbit injection and serum production at McGill University Animal Resources Center.

SDS–PAGE and immunoblotting

Proteins were separated in 8 to 11% SDS gel (Laemmli, 1970), transferred onto nitrocellulose (Bio-Rad) by wet electroblotting, and were reacted with the appropriate antibodies. The antigen–antibody complexes were visualized using a horseradish peroxidase coupled goat anti-rabbit IgG under standard conditions. Complexes were visualized with Super Signal West Pico substrate (Pierce).

Expression and purification recombinant proteins in E. coli

For purification of GST-tagged Hsc70-3, PABP2, or the GST tag itself, a 20 ml overnight culture of *E. coli* BL21 cells containing the recombinant plasmid pGEX6P1-Hsc70-3, pGEX6P1-PABP2, or pGEX6P1 vector alone was used to inoculate 500 ml of LB media containing 75 µg/ml of carbenicillin. Cells were grown at 32 °C to an OD_{600} of 0.6. Protein expression was induced with 0.4 mM of IPTG for 4.5 h for GST-Hsc70-3 and for

2 h at 30 °C for PABP2-GST and GST. Bacterial cells were resuspended in 20 ml of phosphate buffered saline solution (PBS; 4.3 mM Na_2HPO_4, 1.47 mM KH_2PO_4, 137 mM NaCl, 2.7 mM KCl, pH 7.3) supplemented with 1 mM DTT, 40 mg of lysozyme, and 1× complete EDTA-free protease inhibitor. The cells were disrupted by sonication and supplemented with 1% Triton-X-100. Lysate was centrifuged at 30,000×*g* for 30 min at 4 °C. The supernatant was filtered through a 0.45 μm Millex HV PVDF filter (Millipore) and used for affinity purification of either GST-PABP2, GST-Hsc70-3, or GST on glutathione sepharose 4B (GE Healthcare) according to manufacturer's protocol.

For purification of histidine-tagged RdRp of TuMV, a 5 ml overnight culture of *E. coli* BL21(DE3) cells containing the recombinant plasmid pET28(a)-RdRp was used to inoculate 500 ml of LB media containing 50 μg/ml of kanamycin. Cells were grown at 32 °C to an OD_{600} of 0.4 to 0.6. Protein expression was induced with 1 mM of IPTG for 1.5 h at 30 °C. Bacterial cells were resuspended in 5 ml of buffer A (50 mM sodium phosphate buffer pH 8.0, 300 mM NaCl, 5 mM β-mercaptoethanol, 0.1% Tween-20, 10% glycerol, 1× complete EDTA-free protease inhibitor). The cells were disrupted by sonication and the resulting lysate centrifuged at 30,000×*g* for 30 min at 4 °C. The supernatant was used for immobilized metal affinity purification on Talon resin (BD Biosciences). Resin was washed with buffer A supplemented with 10 mM imidazole and proteins eluted with buffer B (20 mM Tris–HCl pH 7.5, 300 mM NaCl, 250 mM imidazole, 2.5 mM DTT).

Concentration of all recombinant proteins produced was measured using a Bradford assay (Bio-Rad) using bovine serum albumin as standard. Protein purity and molecular weight were assessed by Coomassie staining and immunoblot analysis using monoclonal anti-histidine, monoclonal anti-GST, polyclonal anti-RdRp, and/or anti-Hsc70 (data not shown).

RdRp/Hsc70 and RdRp/PABP ELISA-based binding assays

RdRp protein (100 μl of protein at 15 ng μl^{-1} in PBS buffer) was adsorbed to wells of a polystyrene plate (Costar) by incubation at 4 °C for 2 h and wells were blocked with 5% milk PBS solution for 2 h at room temperature. GST-Hsc70-3 or GST-PABP2 proteins were diluted in PBS with 1% milk and 0.1% Tween-20 and incubated for 2 h at 4 °C in the previously coated wells. Detection of retained protein was achieved with a mouse monoclonal (Novagen) or polyclonal (Molecular Probes) anti-GST-tag antibody and horseradish peroxidase-coupled goat anti-mouse or anti-rabbit immunoglobulin (Pierce). Between each incubation, wells were washed four times with PBS supplemented with 0.05% Tween-20. Enzymatic reactions were performed in 100 μl of OPD citrate buffer (50 mM citric acid, 100 mM sodium phosphate dibasic, pH 5.0, 0.5 mg/ml *o*-phenylenediamine dihydrochloride, and 0.1% H_2O_2) and stopped with a solution of 3 M H_2SO_4. Absorbance was measured at 492 nm. The S.E.M. was calculated for three biological replicates from a minimum of two technical replicates.

Subcellular fractionation and membrane flotation assay

Membrane fractionation and membrane flotation assays were performed as previously described on mock inoculated and/or TuMV-infected *B. perviridis* leaves (Beauchemin et al., 2007; Beauchemin and Laliberté, 2007). Nuclear fractionation was performed on the same plant material using CelLytic Plant nuclei isolation/extraction kit (Sigma) according to manufacturer's protocol, and nuclei recovered by pelleting at 12,000×*g* through a 3.2 M sucrose cushion resulting in a soluble fraction (S12) and nuclear pellet (N). Ten micrograms was diluted in 1:5 in SDS loading buffer and subjected to SDS–PAGE and immunoblotting.

In vivo co-immunoprecipitation analyses

For co-immunoprecipitation analyses, 1 g of TuMV-infected or healthy *A. thaliana* tissue was homogenized on ice in 7.5 ml of IP buffer (50 mM Tris–HCl pH 7.5, 50 mM KCl, 200 mM NaCl, 5 mM EDTA, 5% glycerol, and 1× Complete EDTA-free protease inhibitor). Extract was centrifuged twice at 4000×*g* to remove cellular debris and at 30,000×*g* for 20 min. The 30,000×*g* pellet was washed and resuspended in 4 ml of IP buffer supplemented with 1% Triton X-100. After centrifugation, the supernatants were passed through a 0.45 μm MillexHV PVDF filter. For the pull-down assay, 2 ml of the clarified extract was incubated with 40 μl of protein G sepharose 4 Fast flow beads (Amersham Bioscience) previously coupled to 7.5 μl rabbit anti-RdRp, anti-AtPABP2, or pre-immune sera. The matrix beads were washed five times with 1.25 ml of IP buffer. The immunoprecipitated proteins were subsequently released by boiling in 2× SDS Laemmli sample buffer. The protein blot of the immunoprecipitate was performed as described above except that an HRP-coupled monoclonal anti-rabbit IgG specific to Light Chain (Jackson ImmunoResearch) was used to reduce non-specific background.

Agroinfiltration and confocal microscopy

Vectors containing genes for fluorescent and fusion proteins were introduced into *A. tumefaciens* AGL1 by electroporation. Agroinfiltration in *N. benthamiana* and confocal microscope visualization was carried as previously described (Beauchemin et al., 2007). Fluorescence was visualized between 2 and 4 days post-infiltration by confocal microscopy. No notable differences in cellular localization of the fluorescent proteins expressed were observed during this time period with the constructs used. Fluorescence was generally observed in 40% to 60% of the cells in the infiltrated area. Images were collected with a charge-coupled-device camera and treated with Image J (http://rsb.info.nih.gov/ij/) software.

Acknowledgments

We thank Dr. Fernando Ponz for the TuMV clone and Dr. Michael Fromm (University of Nebraska, Lincoln, USA) for pNTAPi and pNTAPi-GFP vectors. We wish to thank Olivier LeGall, Sylvie German, Thierry Michon, and Valérie Nicaise (IBVM, INRA, Bordeaux, France) for helpful discussions and Hélène Sanfaçon (Pacific Agri-Food Research Centre, Summerland, Canada) for critical reading of the manuscript. This work was supported by grants to MGF and JFL from the National

Science and Engineering Research Council of Canada and from the Québec Fonds de la recherche sur la nature et les technologies fund in the form of scholarships.

Appendix A. Supplementary data

Supplementary data associated with this article can be found, in the online version, at doi:10.1016/j.virol.2007.12.014.

References

Aizaki, H., Lee, K.-J., Sung, V.M.H., Ishiko, H., Lai, M.M.C., 2004. Characterization of the hepatitis C virus RNA replication complex associated with lipid rafts. Virology 324, 450–461.

Aparicio, F., Thomas, C.L., Lederer, C., Niu, Y., Wang, D., Maule, A.J., 2005. Virus induction of heat shock protein 70 reflects a general response to protein accumulation in the plant cytosol. Plant Physiol. 138, 529–536.

Audy, P., Palukaitis, P., Slack, S.A., Zaitlin, M., 1994. Replicase-mediated resistance to potato virus Y in transgenic tobacco plants. Mol. Plant-Microb. Interact. 7, 15–22.

Barton, D., O'Donnell, B., Flanegan, J., 2001. 5′ cloverleaf in poliovirus RNA is a *cis*-acting replication element required for negative-strand synthesis. EMBO J. 15, 1439–1448.

Baunoch, D.A., Das, P., Browning, M.E., Hari, V., 1991. A temporal study of the expression of the capsid, cytoplasmic inclusion and nuclear inclusion proteins of *Tobacco etch potyvirus* in infected plants. J. Gen. Virol. 72, 487–492.

Beauchemin, C., Boutet, N., Laliberté, J.-F., 2007. Visualization of the interaction between the precursors of VPg, the viral protein linked to the genome of *Turnip mosaic virus*, and the translation eukaryotic initiation factor iso 4E *in planta*. J. Virol. 81, 775–782.

Beauchemin, C., Laliberté, J.-F., 2007. The poly(A) binding protein is internalized in virus-induced vesicles or redistributed to the nucleolus during *Turnip mosaic virus* infection. J. Virol. 81, 10905–10913.

Brown, G., Rixon, H.W.M., Steel, J., McDonald, T.P., Pitt, A.R., Graham, S., Sugrue, R.J., 2005. Evidence for an association between heat shock protein 70 and the respiratory syncytial virus polymerase complex within lipid-raft membranes during virus infection. Virology 338, 69–80.

Buck, K.W., 1996. Comparison of the replication of positive-stranded RNA viruses of plants and animals. Adv. Virus Res. 47, 159–251.

Craig, E.A., Baxter, B.K., Becker, J., Halladay, J., Ziegelhoffer, T., 1994. Cytosolic hsp70s of *Saccharomyces cerevisae*: roles in protein synthesis, protein translocation, proteolysis and regulation. In: Morimoto, R.I., Tissieres, A., Georgopoulos, C. (Eds.), The biology of heat shock proteins and molecular chaperones. Cold Spring Harbor Laboratory Press, New York, pp. 31–52.

Daros, J.-A., Schaad, M.C., Carrington, J.C., 1999. Functional analysis of the interaction between VPg-proteinase (NIa) and RNA polymerase (NIb) of *Tobacco etch potyvirus*, using conditional and suppressor mutants. J. Virol. 73, 8732–8740.

El-Hage, N., Luo, G., 2003. Replication of hepatitis C virus RNA occurs in a membrane-bound replication complex containing nonstructural viral proteins and RNA. J. Gen. Virol. 84, 2761–2769.

Fauquet, C., Mayo, M., Maniloff, J., Desselberger, U., Ball, L.A., 2005. Virus Taxonomy: VIIIth Report of the International Committee on Taxonomy of Viruses. Elsevier Academic Press, San Diego.

Fellers, J., Wan, J., Hong, Y., Collins, G.B., Hunt, A.G., 1998. *In vitro* interactions between a potyvirus-encoded, genome-linked protein and RNA-dependent RNA polymerase. J. Gen. Virol. 79, 2043–2049.

Glotzer, J.B., Saltik, M., Chiocca, S., Michou, A.-I., Moseley, P., Cotten, M., 2000. Activation of heat-shock response by an adenovirus is essential for virus replication. Nature 407, 207–211.

Guo, D., Rajamaki, M.-L., Saarma, M., Valkonen, J.P.T., 2001. Towards a protein interaction map of potyviruses: protein interaction matrixes of two potyviruses based on the yeast two-hybrid system. J. Gen. Virol. 82, 935–939.

Herold, J., Andino, R., 2001. Poliovirus RNA replication requires genome circularization through a protein–protein bridge. Mol. Cell 7, 581–591.

Hofius, D., Maier, A.T., Dietrich, C., Jungkunz, I., Bornke, F., Maiss, E., Sonnewald, U., 2007. Capsid protein-mediated recruitment of host dnaJ-like proteins is required for *Potato virus Y* infection in tobacco plants. J. Virol. 81, 11870–11880.

Hong, Y., Hunt, A.G., 1996. RNA polymerase activity catalyzed by a potyvirus-encoded RNA-dependent RNA polymerase. Virology 226, 146–151.

Hong, Y., Levay, K., Murphy, J.F., Klein, P.G., Shaw, J.G., Hunt, A.G., 1995. A potyvirus polymerase interacts with the viral coat protein and VPg in yeast cells. Virology 214, 159–166.

Hu, J., Flores, D., Toft, D., Wang, X., Nguyen, D., 2004. Requirement of heat shock protein 90 for human hepatitis B virus reverse transcriptase function. J. Virol. 78, 13122–13131.

Hu, J., Toft, D., Anselmo, D., Wang, X., 2002. *In vitro* reconstitution of functional hepadnavirus reverse transcriptase with cellular chaperone proteins. J. Virol. 76, 269–279.

Jiang, Y., Serviene, E., Gal, J., Panavas, T., Nagy, P.D., 2006. Identification of essential host factors affecting Tombusvirus RNA replication based on the yeast Tet promoters Hughes collection. J. Virol. 80, 7394–7404.

Jones, A.L., Johansen, I.E., Bean, S.J., Bach, I., Maule, A.J., 1998. Specificity of resistance to pea seed-borne mosaic potyvirus in transgenic peas expressing the viral replicase (Nlb) gene. J. Gen. Virol. 79, 3129–3137.

Kampmueller, K.M., Miller, D.J., 2005. The cellular chaperone heat shock protein 90 facilitates flock house virus RNA replication in *Drosophila* cells. J. Virol. 79, 6827–6837.

Kushner, D.B., Lindenbach, B.D., Grdzelishvili, V.Z., Noueiry, A.O., Paul, S.M., Ahlquist, P., 2003. Systematic, genome-wide identification of host genes affecting replication of a positive-strand RNA virus. Proc. Natl. Acad. Sci. U. S. A. 100, 15764–15769.

Laemmli, U., 1970. Cleavage of structural proteins during the assembly of the head of bacteriophage T4. Nature 15, 680–685.

Léonard, S., Viel, C., Beauchemin, C., Daigneault, N., Fortin, M.G., Laliberté, J.-F., 2004. Interaction of VPg-Pro of *Turnip mosaic virus* with the translation initiation factor 4E and the poly(A)-binding protein *in planta*. J. Gen. Virol. 85, 1055–1063.

Li, X.H., Valdez, P., Olvera, R.E., Carrington, J.C., 1997. Functions of the *Tobacco etch virus* RNA polymerase (NIb): subcellular transport and protein–protein interaction with VPg/proteinase (NIa). J. Virol. 71, 1598–1607.

Lin, B., Wang, J., Liu, H., Chen, R., Meyer, Y., Barakat, A., Delseny, M., 2001. Genomic analysis of the Hsp70 superfamily in *Arabidopsis thaliana*. Cell Stress Chaperones 6, 201–208.

Mangus, D., Evans, M., Jacobson, A., 2003. Poly(A)-binding proteins: multifunctional scaffolds for the post-transcriptional control of gene expression. Genome Biol. 4, 1–14.

Martin, M.T., Cervera, M.T., Garcia, J.A., 1995. Properties of the active Plum pox potyvirus RNA polymerase complex in defined glycerol gradient fractions. Virus Res. 37, 127–137.

Martin, M.T., Garcia, J.A., 1991. Plum pox potyvirus RNA replication in a crude membrane fraction from infected *Nicotiana clevelandii* leaves. J. Gen. Virol. 72, 785–790.

Martinez-Trujillo, M., Limones-Briones, V., Cabrera-Ponce, J., Herrera-Estrella, L., 2004. Improving transformation efficiency of *Arabidopsis thaliana* by modifying the floral dip method. Plant Mol. Biol. Rep. 22, 63–70.

Mayer, M., Bukau, B., 2005. Hsp70 chaperones: cellular functions and molecular mechanism. Cell. Mol. Life Sci. 62, 670–684.

Mayer, M.P., 2005. Recruitment of Hsp70 chaperones: a crucial part of viral survival strategies. Rev. Physiol., Biochem. Pharmacol. 153, 1–46.

Momose, F., Naito, T., Yano, K., Sugimoto, S., Morikawa, Y., Nagata, K., 2002. Identification of Hsp90 as a stimulatory host factor involved in influenza virus RNA synthesis. J. Biol. Chem. 277, 45306–45314.

Nicolas, O., Laliberté, J.F., 1992. The complete nucleotide sequence of *Turnip mosaic potyvirus* RNA. J. Gen. Virol. 73, 2785–2793.

Nishikiori, M., Dohi, K., Mori, M., Meshi, T., Naito, S., Ishikawa, M., 2006. Membrane-bound *Tomato mosaic virus* replication proteins participate in RNA synthesis and are associated with host proteins in a pattern distinct from those that are not membrane bound. J. Virol. 80, 8459–8468.

Osman, T.A., Buck, K.W., 1997. The *Tobacco mosaic virus* RNA polymerase complex contains a plant protein related to the RNA-binding subunit of yeast eIF-3. J. Virol. 71, 6075–6082.

Panavas, T., Serviene, E., Brasher, J., Nagy, P.D., 2005. Yeast genome-wide screen reveals dissimilar sets of host genes affecting replication of RNA viruses. Proc. Natl. Acad. Sci. U. S. A. 102, 7326–7331.

Prokhnevsky, A.I., Peremyslov, V.V., Dolja, V.V., 2005. Actin cytoskeleton is involved in targeting of a viral Hsp70 homolog to the cell periphery. J. Virol. 79, 14421–14428.

Quadt, R., Kao, C.C., Browning, K.S., Hershberger, R.P., Ahlquist, P., 1993. Characterization of a host protein associated with *Brome Mosaic Virus* RNA-dependent RNA polymerase. Proc. Natl. Acad. Sci. U. S. A. 90, 1498–1502.

Restrepo-Hartwig, M.A., Carrington, J.C., 1994. The *Tobacco etch potyvirus* 6-kilodalton protein is membrane associated and involved in viral replication. J. Virol. 68, 2388–2397.

Restrepo, M.A., Freed, D.D., Carrington, J.C., 1990. Nuclear transport of plant potyviral proteins. Plant Cell 2, 987–998.

Riedel, D., Lesemann, D.E., Maiß, E., 1998. Ultrastructural localization of nonstructural and coat proteins of 19 potyviruses using antisera to bacterially expressed proteins of plum pox potyvirus. Arch. Virol. 143, 2133–2158.

Rigaut, G., Shevchenko, A., Rutz, B., Wilm, M., Mann, M., Séraphin, B., 1999. A generic protein purification method for protein complex characterization and proteome exploration. Nat. Biotechnol. 17, 1030–1032.

Rohila, J.S., Chen, M., Cerny, R., Fromm, M.E., 2004. Improved tandem affinity purification tag and methods for isolation of protein heterocomplexes from plants. Plant J. 38, 172–181.

Rubio, V., Shen, Y., Saijo, Y., Liu, Y., Gusmaroli, G., Dinesh-Kumar, S.P., Deng, X.W., 2005. An alternative tandem affinity purification strategy applied to *Arabidopsis* protein complex isolation. Plant J. 41, 767–778.

Sanchez, F., Martinez-Herrera, D., Aguilar, I., Ponz, F., 1998. Infectivity of *Turnip mosaic potyvirus* cDNA clones and transcripts on the systemic host *Arabidopsis thaliana* and local lesion hosts. Virus Res. 55, 207–219.

Schaad, M., Jensen, P., Carrington, J., 1997. Formation of plant RNA virus replication complexes on membranes: role of an endoplasmic reticulum-targeted viral protein. EMBO J. 16, 4049–4059.

Schwartz, M., Chen, J., Janda, M., Sullivan, M., den Boon, J., Ahlquist, P., 2002. A positive-strand RNA virus replication complex parallels form and function of retrovirus capsids. Mol. Cell 9, 505–514.

Serva, S., Nagy, P.D., 2006. Proteomics analysis of the Tombusvirus replicase: Hsp70 molecular chaperone is associated with the replicase and enhances viral RNA replication. J. Virol. 80, 2162–2169.

Simon-Mateo, C., Lopez-Moya, J.J., Guo, H.S., Gonzalez, E., Garcia, J.A., 2003. Suppressor activity of potyviral and cucumoviral infections in potyvirus-induced transgene silencing. J. Gen. Virol. 84, 2877–2883.

Stahl, M., Retzlaff, M., Nassal, M., Beck, J., 2007. Chaperone activation of the hepadnaviral reverse transcriptase for template RNA binding is established by the Hsp70 and stimulated by the Hsp90 system. Nucleic Acids Res. 35, 6124–6136.

Sullivan, C.S., Pipas, J.M., 2001. The virus–chaperone connection. Virology 287, 1–8.

Sung, D.Y., Vierling, E., Guy, C.L., 2001. Comprehensive expression profile analysis of the *Arabidopsis* Hsp70 gene family. Plant Physiol. 126, 789–800.

Tomita, Y., Mizuno, T., Diez, J., Naito, S., Ahlquist, P., Ishikawa, M., 2003. Mutation of host dnaJ homolog inhibits *Brome mosaic virus* negative-strand RNA synthesis. J. Virol. 77, 2990–2997.

Wang, X., Ullah, Z., Grumet, R., 2000. Interaction between *Zucchini yellow mosaic potyvirus* RNA-dependent RNA polymerase and host poly(A)-binding protein. Virology 275, 433–443.

Yamada, K., Lim, J., Dale, J.M., Chen, H., Shinn, P., Palm, C.J., Southwick, A.M., Wu, H.C., Kim, C., Nguyen, M., Pham, P., Cheuk, R., Karlin-Newmann, G., Liu, S.X., Lam, B., Sakano, H., Wu, T., Yu, G., Miranda, M., Quach, H.L., Tripp, M., Chang, C.H., Lee, J.M., Toriumi, M., Chan, M.M.H., Tang, C.C., Onodera, C.S., Deng, J.M., Akiyama, K., Ansari, Y., Arakawa, T., Banh, J., Banno, F., Bowser, L., Brooks, S., Carninci, P., Chao, Q., Choy, N., Enju, A., Goldsmith, A.D., Gurjal, M., Hansen, N.F., Hayashizaki, Y., Johnson-Hopson, C., Hsuan, V.W., Iida, K., Karnes, M., Khan, S., Koesema, E., Ishida, J., Jiang, P.X., Jones, T., Kawai, J., Kamiya, A., Meyers, C., Nakajima, M., Narusaka, M., Seki, M., Sakurai, T., Satou, M., Tamse, R., Vaysberg, M., Wallender, E.K., Wong, C., Yamamura, Y., Yuan, S., Shinozaki, K., Davis, R.W., Theologis, A., Ecker, J.R., 2003. Empirical analysis of transcriptional activity in the *Arabidopsis* genome. Science 302, 842–846.

Yamaji, Y., Kobayashi, T., Hamada, K., Sakurai, K., Yoshii, A., Suzuki, M., Namba, S., Hibi, T., 2006. *In vivo* interaction between *Tobacco mosaic virus* RNA-dependent RNA polymerase and host translation elongation factor 1A. Virology 347, 100–108.

Zhang, S.C., Zhang, G., Yang, L., Chisholm, J., Sanfacon, H., 2005. Evidence that insertion of *Tomato ringspot nepovirus* NTB-VPg protein in endoplasmic reticulum membranes is directed by two domains: a C-terminal transmembrane helix and an N-terminal amphipathic helix. J. Virol. 79, 11752–11765.

Zylicz, M., Ang, D., Liberek, K., Georgopoulos, C., 1989. Initiation of lambda DNA replication with purified host- and bacteriophage-encoded proteins: the role of the dnaK, dnaJ and grpE heat shock proteins. EMBO J. 8, 1601–1608.